DESIGN AND HYDRODYNAMIC ASSESSMENT OF A SMALL SEMI-SUBMERSIBLE (SWATH-TYPE) VESSEL

by

Stuart N. Smith,
B.Sc.

This thesis is submitted for the Degree of Doctor of Philosophy in the Department of Naval Architecture and Ocean Engineering, Glasgow University.

March, 1982

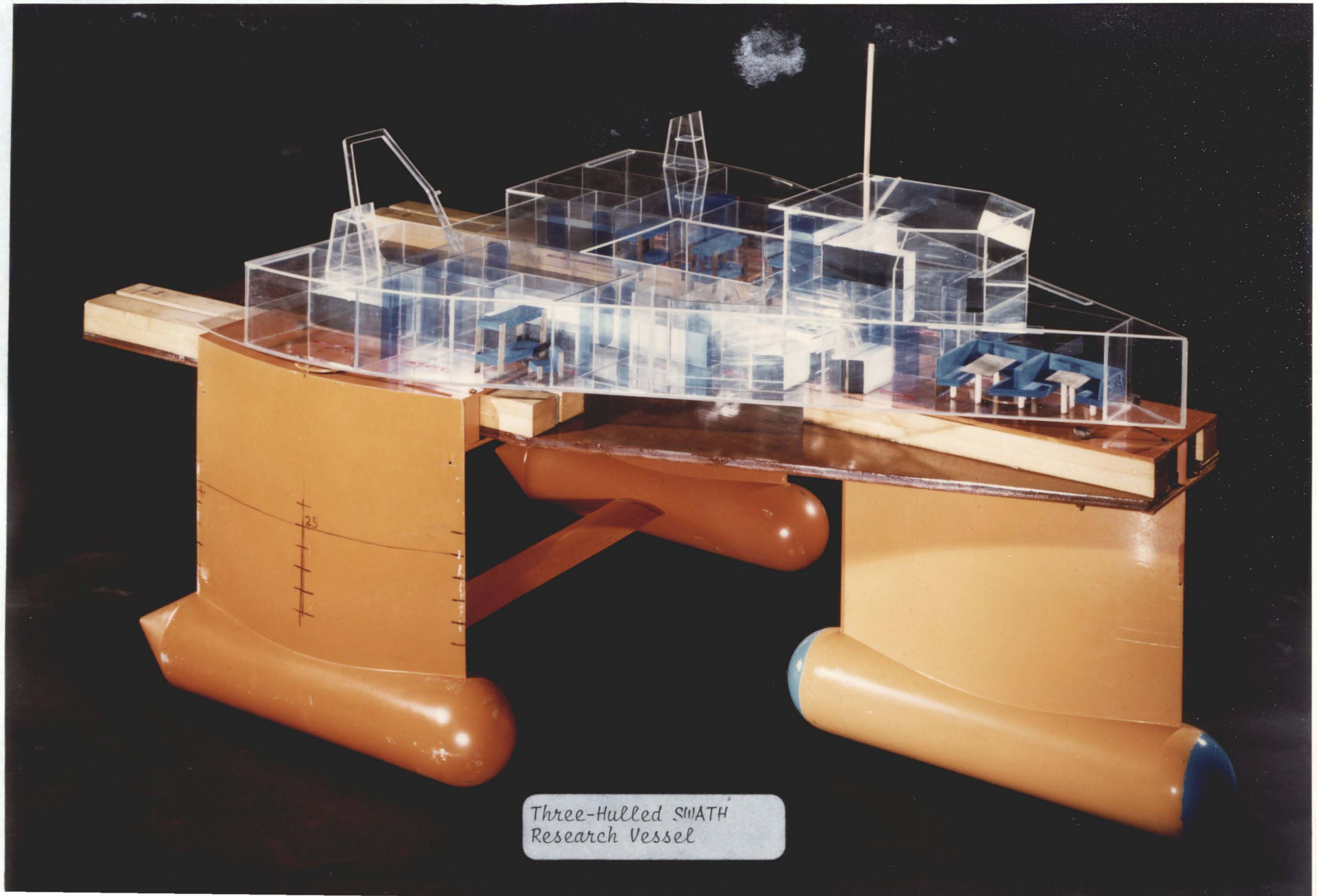
Three-Hulled SWATH
Research Vessel

TABLE OF CONTENTS

TABLE OF CONTENTS, Contd. Page

TABLE OF CONTENTS, Contd. Page

TABLE OF CONTENTS, Contd. Page

TABLE OF CONTENTS, Contd. Page

LIST OF FIGURES

LIST OF FIGURES, Contd. Page

LIST OF FIGURES, Contd. Page

LIST OF TABLES

ACKNOWLEDGEMENTS

The work in this thesis was undertaken in the Department of Naval Architecture and Ocean Engineering at Glasgow University from 1978 - 1981. I would like to thank Professor D. Faulkner, Head of Department, and his staff who made this possible. I am particularly grateful to my supervisor, Mr. N.S. Miller, for his unflagging enthusiasm, encouragement and advice and also for his original suggestion of the small three-hulled semi-submersible.

In addition, I am grateful to all those from many Institutions who spared their time, including Professor R.I. Currie of the Scottish Marine Biological Association, Professor J.A. Allen of the Universities of London and Glasgow Marine Biological Station, Mr. P. Meadows of the Department of Zoology, University of Glasgow, the staff of the Institute of Oceanographic Sciences, the staff at the NERC Research Vessel Bases, various shipbuilders, and others too numerous to mention.

These acknowledgements would not be complete without also mentioning all the research, administrative, secretarial and technical staff who have helped to make my period in the Department such an unforgettable experience. My thanks go to Mr. P. Gallacher for his assistance in performing structural analysis calculations. My indebtedness to Mrs. M. Frieze who typed the manuscript and made order out of chaos will be obvious to anyone who reads the thesis.

The work was sponsored by the Science and Engineering Research Council Marine Technology Directorate.

The frontespiece is by courtesy of the Appleton Laboratory (Slough, Berks).

DECLARATION

Except where reference is made to the work of others this thesis is believed to be original.

* * *

SUMMARY

This thesis studies some of the problems associated with the design and hydrodynamic assessment of SWATH* ships. Although a novel small three-hulled SWATH ship for coastal and inshore, marine-science and engineering research is considered, in particular, the relevance of a large part of the work is not confined to only one vessel. It is of fundamental interest to the advance of SWATH ship technology in general.

A short history of research vessels, and marine-science in relation to them, is given followed by a description and history of SWATH ships. Typical operational requirements for a conventional coastal and inshore vessel are presented and the advantages and disadvantages of adopting a SWATH ship to meet these requirements are outlined.

A brief analysis is made of existing SWATH ships and the choice of configuration and design considerations are discussed. The reasons for the three-hull vessel are presented followed by a description of the proposed design. This includes many traditional naval architecture subjects such as group-weights, equipment, flooding, etc. Stability requirements were considered and revised criteria are proposed. The structural design and analysis from which the steel group-weights are derived is presented as are various other topics such as a simple vibration analysis of the hull-column structure. (A detailed Specification for the vessel is given as a separate enclosure.)

Construction costs based on the specification are presented and operational costs are discussed from which it appears that increased fuel costs would be offset by increased 'research efficiency'. It is possible that the first cost will reduce as experience is gained in building this type of vessel.

---

*Various designers and research workers have used a variety of names, such as 'semi-submersible ship (S^3)", "stable semi-submerged platform (S.S.P.)", "small waterplane-area twin-hull (SWATH) ships" and "semi-submerged catamarans (S.S.C.)", to name a few. Since the acronym "SWATH" has now become widely accepted and is also applicable to the present design it will be used throughout this thesis.

The resistance was investigated both theoretically and experimentally. A wave-resistance program has been developed for a three-hulled SWATH based on potential flow and the thin-ship approximation. The other resistance components were calculated by semi-empirical methods. The experimental resistance was obtained for a total of seven conditions concentrating on speeds in the operational range but also extending up to speeds causing the onset of vertical-plane instability. Wave-resistance theory and measurement showed qualitative agreement but the theory over-estimated the peak wave-resistance by a factor of about two and a half due primarily, it is expected, to the fact that the aft endings of the model hulls were not particularly well suited either to the purpose or to the theory. The correlation between theory and experiment at low speeds suggested that the previously recommended drag coefficient for the endings is too high. The occurrence of boundary-layer separation was briefly investigated in a flow visualisation wind-tunnel and aspects such as blockage correction, cavitation, and turbulence stimulation are touched upon.

The motion response at zero-speed in head and beam seas has been studied and a digital computer program has been developed for head seas which gives good agreement with heave experimental results but not for pitch or the relative motion. The motions were then compared with a conventional monohull and found to be generally lower.

The equations of motion were rewritten to include non-linearities due to viscous damping and column flare and these were solved on an analogue computer. It was found that the viscous damping explained the non-linear behaviour at resonance very well and the fin was identified as being the main cause of this. However, the modelling of the effects of column flare was found to be over-simplified.

A large number of experiments were conducted for various different conditions at a range of wave amplitudes and frequencies. Apart from at resonance it was concluded that even with small and moderate column flares linearity was a good assumption. For large column flare pronounced non-linearities and parasitic motions occurred. The first of these was the so-called 'jump' phenomenon which was attributable to the relative motion of the forward hull/

column and the hardening-spring effect of the flare. A motion resembling beats was also observed. The first parasitic motion was 'parametric' rolling in head seas at half the wave frequency. The theoretical work concentrated on the system dynamics rather than hydrodynamics and the parametric rolling was explained theoretically in terms of the unstable regions in the Mathieu equation. The factors controlling this behaviour were investigated experimentally. In irregular seas in particular, the damping ratio seemed to be of utmost importance and, in fact, rolling only occurred when the damping was low (i.e. in the absence of horizontal bracing). An interesting mechanism whereby, at large wave amplitudes, the jump phenomenon stabilises parametric rolling has been identified.

Beam sea motions were investigated experimentally and it was found that the same condition that admitted rolling in head seas admitted sub-harmonic rolling in beam seas. Although these 'instabilities' are recognised as possible capsize mechanisms the model always remained upright and this would appear to be due to having sufficient GM or area under the GZ curve. The effect, however, is not straightforward and even with zero upright GM_T the model did not capsize under wave action but the sub-harmonic rolling did not occur either.

It should be emphasised that the non-linearities and parasitic motions only occurred when the column flare was large. It is not believed that there is an inherent weakness in the three-hulled design but rather that they could occur for any SWATH configuration with large flare.

Still concentrating on the system dynamics it has been shown that the conventional use of steady-state or regular-wave transfer functions is not necessarily justified for large amplitude motions. A design-wave-group concept has been proposed and used for investigating such behaviour. Since linear theory has been used it is suggested that the results should only be taken as a measure of the uncertainty of the response.

From technical considerations it is concluded that there appears to be no reason why a three-hulled SWATH ship could not be built and operated as a successful research vessel. The work in the

thesis is, however, relevant to other SWATH ships and perhaps also helps to improve the understanding of the behaviour of conventional vessels and semi-submersibles.

NOTATION

a	radius or length of geometrical section
a_o	general wave amplitude
a_i	amplitude of particular wave
a_m	amplitude of largest wave in group
a_a, a_b, a_{ab}	amplitude of wave proceeding or succeeding a_m, or both
a_w	waterplane area per column
am	sectional added mass
A	area or general coefficient
A_{pr}	projected area
A_w	waterplane area
A_w^*	waterplane area at junction with deck-box
AL	aluminium
AM	vessel added mass
b	radius or column breadth
b_i	sectional breadth
bhp	brake horse power
B	damping coefficient, general coefficient, or breadth
BM	distance between centre of buoyancy and metacentre
c	wave celerity, chord length, or forward velocity
c_{am}	sectional added mass coefficient
C	roll restoring moment coefficient or circumference
C_{am}	vessel added mass coefficient
C_D	drag coefficient
C_1	wave damping coefficient or vibration frequency coefficient
C_2	viscous damping coefficient or vibration frequency coefficient
C_ϕ	pitch damping coefficient
$\mathbb{C}$	centreline

D	drag or diameter
D.A.F.S.	Department of Agriculture and Fisheries for Scotland
E	Young's modulus
F	wave exciting force
F_H	horizontal force
F_{am}	added mass force
F_{FK}	Froude-Krylov force
F_v	velocity force
Fn	Froude number
Fn_H	Froude depth number
g	gravitational constant
GM	height from centre of gravity to metacentre
GZ	roll restoring arm
h	depth or wave height
$h_s, h_{1/3}$	significant wave height
$h_{1/10}$	mean height of the one-tenth highest waves
hp	horse-power
I	mass moment of inertia or second moment of waterplane area
I_{AM}	added mass moment of inertia
I_n, J_n	variables in wave resistance calculation
J	three-dimensional added mass reduction factor
k	spring constant
K	wave number
K_z	heave restoring force coefficient
K_ϕ	pitch restoring force coefficient
KB	height of centre of buoyancy above keel
KM	height of metacentre above keel

ℓ	length
L	length
L_{BP}	length between perpendiculars
LCF	longitudinal centre of flotation
LCB	longitudinal centre of buoyancy
m	mass, added mass, area ratio, or defined wave resistance variable
m_o	area under energy spectrum
M	roll exciting moment
M_ϕ	pitch exciting moment
MCTC	moment to change trim one centimetre
n	coefficient for column flare or index for summation
NERC	Natural Environment Research Council
p	pressure
P	parallel hull/column interference factor
PM	Pieron-Moskowitz
qpc	quasi-propulsive-coefficient
Q	magnification factor
r	radius or relative motion amplitude
$r_{1/10}$	mean of one-tenth highest relative bow motion amplitudes
R	radius or resistance
RAO	response amplitude operator
RBM	relative bow motion
RMS	root-mean-square
Rn	Reynolds number
R_d	roughness Reynolds number
R_t	resistance of trip wire

s	column span (depth)
SM	Subjective magnitude
S.M.B.A.	Scottish Marine Biological Association
SW	salt water
$S(\omega)$	spectrum of frequency
S.W.L.	Safe Working Load
t	time or thickness
T	sectional draught or period
TLP	tension-leg-platform
TPC	tonnes per centimetre
u	variable in wave resistance calculation
U	wind velocity
USAF	United States Air Force
V	velocity
VCG	vertical centre of gravity
V_w	wind velocity
W	canal width
x,y,z	general cartesian co-ordinates
x	longitudinal distance
z	heave displacement

Subscripts

FK	Froude-Krylov
H	horizontal
L	longitudinal
T	transverse

Greek Alphabet

α	general parameter or variable in sea spectral formulation
β	general parameter or coefficient in roll equation
γ	damping ratio or peak enhancement factor
γ_ϕ	pitch damping ratio
Δ	mass displacement
∇	volume of displacement
δ	small change, or boundary layer thickness
δ_1, δ_2	stability boundaries
δ, ε	parameters in Mathieu equation
ε	small parameter or error
η	wave profile
θ	roll angle
λ	wave length or roots of equation
ν	kinematic viscosity
ξ	longitudinal co-ordinate
π	3.14159 .....
ρ	density of water
Σ	summation
σ	source strength or cavitation number
τ	natural roll period
ϕ	pitch angle, phase angle, or velocity potential
Ψ	phase angle
Ω	frequency
ω	frequency
ω_e	frequency of encounter
ω_H	heave natural frequency
ω_θ	roll natural frequency
ω_ϕ	pitch natural frequency
ω_m	modal frequency
ω_n	general natural frequency

Notes

(1) Other symbols and subscripts have their standard meaning or are as defined in the text.

(2) A dot superscript represents differentiation with respect to time.

CHAPTER 1

INTRODUCTION

1.1 General

Following extensive development, mostly in the United States and Japan, the SWATH ship has emerged from a background of novel concepts as a serious contender with high development potential[1] for various applications. There are now two SWATH ships afloat, the *S.S.P. Kaimalino*[2] and the *Mesa 80*[3], various small prototypes and manned models, and considerable interest for other craft, including helicopter carriers, offshore transport vessels, passenger vessels and research vessels[4-8]. The large amount of development work conducted has been reviewed by Lamb and Fein[9].

This thesis is centred around a small three-hulled SWATH-type ship (displacement approximately 319t) for use as an inshore and coastal research vessel as illustrated in the frontespiece. The first chapter sets the general scene by describing and discussing various matters such as the immediate background to the project, the development of marine science, research vessels, the SWATH concept, review of meetings, operational requirements, and so on. Thereafter the thesis is laid out in such a way that the work covered in any subject is grouped together rather than in a strictly chronological order. Thus Chapter 2 discusses design considerations, while Chapter 3 gives the reasons for the three-hulled configuration and goes on to describe the design in the state that has been reached including topics such as stability, structural design, flooding, etc. Chapter 4 covers costs, and Chapter 5 is devoted to resistance and propulsion. It will be apparent that some of the contents of Chapter 5 were completed as part of the general design work included in Chapter 3. However, the layout adopted aids continuity. Subsequent chapters deal with motion response in varying degrees of complexity with concluding remarks and recommendations for future work being given in the last chapter. Some additional material is included in appendices.

1.2 Project Background

The immediate background of this project lies in an idea by N.S. Miller to build a small three-hulled semi-submersible (Figs. 1.1 and 1.2) in the University workshops for use in undergraduate naval architecture teaching and for certain research areas, in particular to try and overcome some of the scaling problems inherent in conventional experiment tank testing such as Reynolds number dependent effects on cylinders[10]. (The advantages of this three-hulled concept will be discussed later.)

At about the same time scientists concerned with marine biological research expressed interest in a craft which would allow observation of the top 10m of the sea as well as providing the usual facilities for collecting marine specimens. The anticipated low motion levels and large deck areas were also considered an attractive feature of the proposed design. Interest was shown at an early stage by the Scottish Marine Biological Association (SMBA) at Dunstaffnage, the Institute of Oceanographic Sciences (IOS, Wormley) and various other individuals from the University's Faculty of Science. These groups and individuals were involved in a broad spectrum of work including biological reproduction, ocean circulation, organic degradation, aqua-culture, dermatology, macrobenthos, meiobenthos, phytoplankton, ocean-floor spreading, biochemistry, continental margins, sonar development, geophysics and so on. Discussions were held with these parties (hereafter generically referred to as 'marine scientists'), to try and determine their anticipated requirements for equipment, electrical services, speed, etc. Theirs would be a continuing need and, since the base facilities for operating research vessels already existed at the Millport Marine Biological Station of the Universities of London and Glasgow, the study of a larger design was commenced.

With any novel concept the work involved in producing a workable design will be greater than for a conventional ship because of the scarcity of type-ship data and the lack of established practice. However, this very lack of data can be turned to the advantage of the designer because he then is not constrained by any influence to mirror past practice and is never encouraged to be hide-bound in his

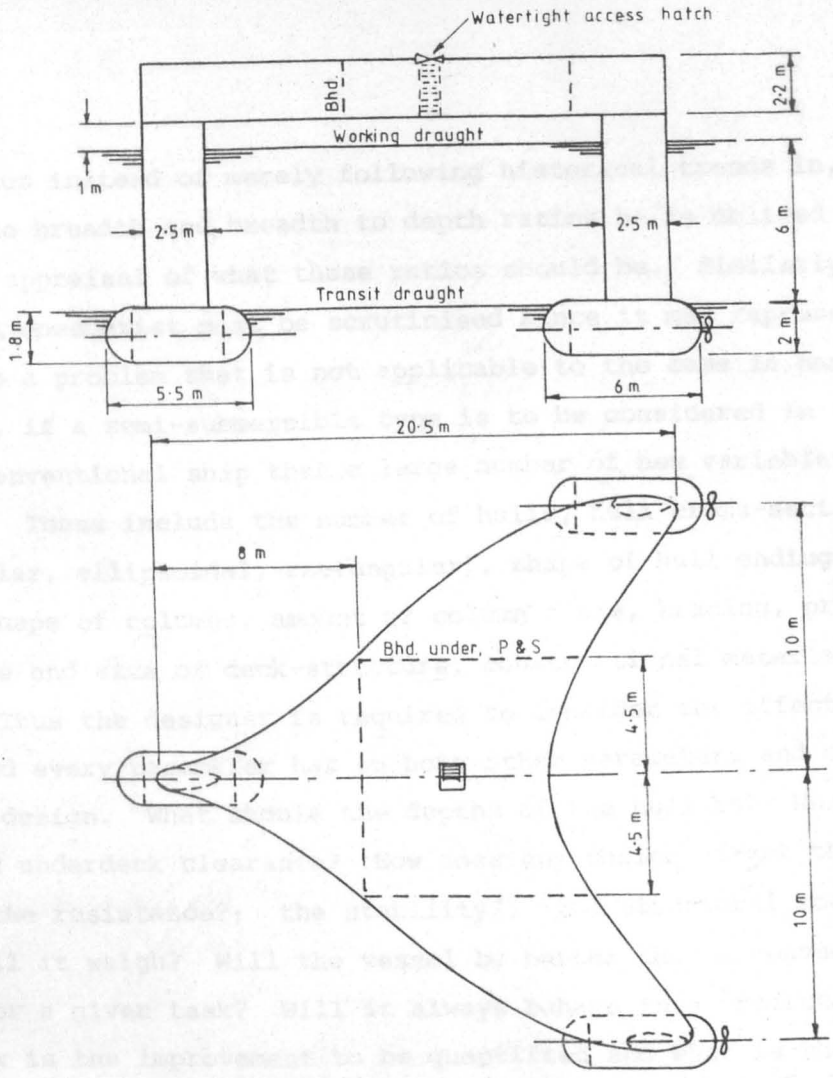

FIG. 1.1. PRELIMINARY SKETCH OF SEMI-SUBMERSIBLE

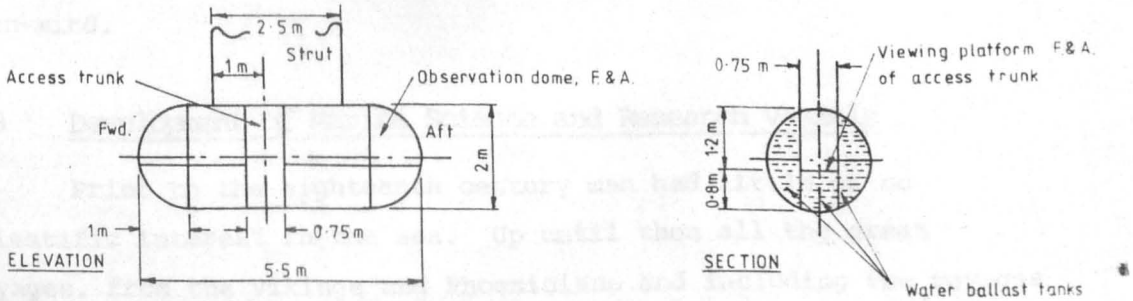

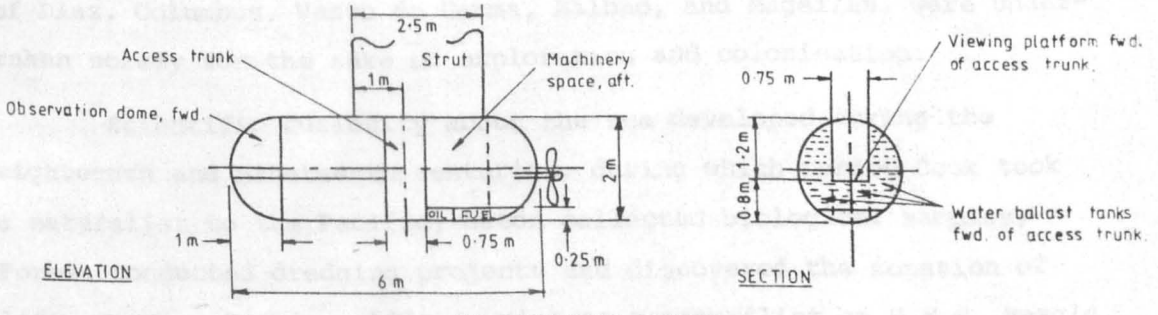

FIG. 1.2. GENERAL ARRANGEMENT OF OBSERVATION CHAMBERS

thinking. Thus instead of merely following historical trends in, say, length to breadth and breadth to depth ratios he is obliged to make a fresh appraisal of what these ratios should be. Similarly, any data that does exist must be scrutinised since it may represent a solution to a problem that is not applicable to the case in hand. For instance, if a semi-submersible type is to be considered in place of a conventional ship then a large number of new variables are created. These include the number of hulls, hull cross-sectional shape (circular, ellipsoidal, rectangular), shape of hull endings, number and shape of columns, amount of column flare, bracing, propulsion, shape and size of deck-structure, constructional material, and so on. Thus the designer is required to consider the effects that each and every parameter has on both other parameters and on the overall design. What should the depths of the hull be? What is the required underdeck clearance? How does any choice affect the motions?; the resistance?; the stability?; the structural loads? How much will it weigh? Will the vessel be better than a conventional one for a given task? Will it always behave in a predictable manner? How is the improvement to be quantified and what is the cost?

These are some of the questions that had to be faced with an open-mind.

1.3 Development of Marine Science and Research Vessels

Prior to the eighteenth century man had little or no scientific interest in the sea. Up until then all the great voyages, from the Vikings and Phoenicians and including the voyages in the late fifteenth and early sixteenth centuries, such as those of Diaz, Columbus, Vasco de Gamma, Balbao, and Magellan, were undertaken solely for the sake of exploration and colonisation.

Scientific curiosity about the sea developed during the eighteenth and nineteenth centuries, during which period Cook took a naturalist to the Pacific, Eaton collected biological samples, Forbes conducted dredging projects and discovered the zonation of life at sea. Darwin, while serving as a naturalist on *H.M.S. Beagle* collected data for his later theories as well as his still-accepted

theory of coral reef and atoll development. Workers such as Maury collected data on winds and currents and the external influence of the desire for a trans-Atlantic cable stimulated interest in ocean floor topography.

The first cruises undertaken solely for scientific marine investigations were those of Thompson in 1869 and 1870 on board *H.M.S. Porcupine*, provided by the Admiralty, following some successful work from *H.M.S. Lightning* in 1868[11]. This led on to the famous vouage of *H.M.S. Challenger* (1872-1876).

Following the *Challenger*, laboratories were set up in Europe and N. America and new techniques and equipment were steadily developed, notably the Nansen bottle and Ekman's current meter. After the First World War the technology existed for the construction of the 'bathysphere' in which Beebe and Barton descended to 930 metres in 1934 opening the way for further deep sea voyages. Similarly, the echo sounder, developed during the Second World War, was quickly adopted by marine scientists and led also to the use of seismic techniques. A notable development from inside marine science was the development of SCUBA gear by Cousteau and Cagran.

Although the most famous voyage, the *Challenger* Expedition, was presumably motivated partly by scientific curiosity, it is probably fair to say that most major developments and much sustaining work have been initiated by external interests or requirements. These include the trans-Atlantic cable already mentioned and, at the present time, man's search for fossil fuels, manganese nodules, the monitoring of radioactive waste, the search for new fishing grounds, marine fouling of offshore structures, etc. These facets of marine science research are directly linked with the present requirements of society and thus the political and economic environment. Because of this environment there is a clearly identifiable need for vessels in which to conduct the work, mostly in home waters, but also on a world-wide basis. These geographical locations together with the varied work mentioned in Section 1.2 require a range of different vessels and different equipment.

The wide variety of different equipment includes trawls, traps, box samplers, corers, sonars, conductivity-temperature-depth

(CTD) probes, water-bottles, current-meters, tide-gauges, air-guns, boomers and sparkers for seismic work, bathythermographs, gravimeters, magnetometers, flourimeters as well as standard laboratory equipment and systems such as satellite navigation and underwater beacons. It is helpful to have some understanding of the equipment, the way it is operated and likely developments in that equipment, because of the influence it has on vessel layout. This can partly be obtained from text books[12] and also from the Cruise Reports of the various users' organisations (e.g. Ref. 13).

Similarly, it is important to be aware of the characteristics of existing vessels[14] and likely future developments. For instance, with the steady, but apparently inexorable, decline of Britain's global interests, it is debatable for how long research efforts in distant waters such as the Pacific and Indian Ocean, however important they may be in their own right, will continue to attract government funding. This will, of course, be influenced by the way in which mineral rights are allocated by the conferences on the International Law of the Sea and is all part of the design environment referred to again in Section 1.6.

The major development area at the present is the replacement of mechanical devices by electrical and the increasing use of computers for both data logging and on-site analysis. Although at present it is possible to envisage the day when water samples, in particular, no longer need be collected it is less easy to conceive the collecting of benthic and pelagic organisms or rock samples being dispensed with. However, the day will undoubtedly come and will herald the disappearance of the conventional, multipurpose, trawler-type research vessel.

Those days have not yet arrived and while *H.M.S. Lightning* (1868) was described[11] as, "... being perhaps the very oldest paddlesteamer in Her Majesty's navy ... and was scarcely seaworthy," present-day research vessels generally have high standards of equipment, accommodation and on-board services. The general rise in these standards is likely to continue.

1.4 The SWATH Concept

The SWATH has been described as an advanced displacement ship[1] and although the concept was born from a general background of high performance craft it can perhaps best be described as a cross between a semi-submersible and a catamaran. The twin-hull SWATH concept is well illustrated by Fig. 1.4, page 12. It consists of a basically rectangular plan-form cross-structure or deck-box joined to submerged slender cylindrical hulls by streamlined struts. (Either one or two per hull.) The hull may, or may not, be joined together by a transverse fin or brace which could accommodate controllable stabilising flaps.

The SWATH offers the following main advantages over a comparable conventional ship:

(a) lower motions and accelerations in most seaways,
(b) large and convenient deck-area and internal volume, and
(c) higher sustained speeds in a seaway.

It is the above characteristics that suggest that SWATHs could be useful for naval applications such as helicopter or VSTOL jet carriers[4,5] while the combination of low motion response, widely separated hulls, and possibly low hydrodynamic noise could make the SWATH host for improved sonar systems, both hull-mounted and towed. Proposed civilian applications include Offshore Personnel Transports[7], passenger vessels[3,8] not to mention research vessels.

The widely separated propellers give rise to good low speed manoeuvrability and station keeping, while the generally regular shapes should be simple to construct and lend themselves to batch production techniques.

The low motions lie at the heart of all semi-submersible design practice and are attributable to a combination of two factors:

(a) the main part of the buoyancy is provided by the submerged hulls which experience relatively small wave-exciting forces because these decrease exponentially with depth below the surface and there is some cancellation between the forces on the different underwater parts, and

(b) the small waterplane-area associated with the columns ensures that the natural frequencies of motions are much lower than a comparable conventional vessel. Since waves with low frequencies (i.e. long wavelengths) occur less frequently, resonant response is seldom encountered.

The general philosophy of design, particularly for small SWATHs is, therefore, to keep the waterplane-area as small as possible within the limitations discussed later.

These advantages must be offset against the disadvantages of:

(a) higher steelweight to displacement ratio, and
(b) increased wetted surface, and therefore, increased frictional resistance component.

Despite the last of the above points, recently developed SWATH designs[9] can have calm water resistance similar to a comparable monohull and will in any case have less speed loss in a seaway. Other factors, such as larger breadth, may be a disadvantage for docking and similarly increased depth could be a disadvantage in confined waters. For research vessels the first two advantages are arguably the most important. The large internal volume will permit more spacious accommodation and it is generally accepted that lower motion levels will not only improve on-board comfort but will also improve the performance of personnel. (It will be shown later than man-power costs are by far the highest proportion of research vessel operating costs and it thus makes economic sense to increase on-board productivity.) Listed in greater detail these advantages would:

(a) enable gear to be handled overboard in higher sea-states;
(b) permit more detailed experiments to be conducted on board;
(c) enable laboratory experiments to be continued in higher sea-states;
(d) improve the efficiency and morale of scientific staff for physiological and psychological reasons due to improved working and living conditions;
(e) permit delicate apparatus to be carried on board with less risk of damage;

(f) produce a greater accuracy in some experiments;

(g) allow better performance for sonar and seismic work (at present seismic data is filtered through hardware costing thousands of pounds to remove the effects of vessel motion);

(h) increase versatility for engineering experiments;

(i) permit a continuously submerged observation chamber;

(j) simplify diver and submersible operations.

On existing research vessels operations are sometimes terminated because of the risk of personnel being washed overboard so the greater height above sea level could be advantageous although at other times it may be a hindrance. In the historical context of developments, it is also more than likely that once low motions are available they will lead to different techniques or processes being adopted for use at sea that at present cannot be considered.

1.5 Short History of SWATH-type Ships

It is an interesting coincidence that, just as the requirement for a trans-Atlantic cable stimulated an interest in ocean-floor topography, so the development of trans-Atlantic telex services stimulated interest in the semi-submersible type ship[15]. A telegraph engineer, F. Creed, proposed a floating boosting station and, during the Second World War, his ideas were considered for use as an aircraft carrier or floating aerodrome. Although he is credited with bringing the concept to the attention of the U.S. Navy in 1943[9] various patented designs apparently already existed, as reported in Refs. 6,16,17. These early designs attempted principally to reduce wave-making resistance, and Creed was probably the first to give consideration to improved seakeeping.

During the fifties and early sixties various studies of novel ship types appeared[17,18,19], and between 1964 and 1966 manned models (*Ficat I* and *II*) were produced[16] for operation at supercritical speeds. Development continued with Leopold[20] and the Dutch[21,22] who launched the 1200 ton twin-hulled, hybrid-catamaran drilling vessel *Duplus*, Fig. 1.3. 1971 saw the launch of the 25 foot prototype *Trisec*[23] and shortly afterwards Lang's work[24,25] led to the construction of the 190 ton *S.S.P. Kaimalino*, Fig. 1.4. This was

arguably the first true full-scale SWATH ship and she first moved under her own power in October 1973[26].

In Japan, following development on a small prototype, *Marine Ace*[3,27] (Fig. 1.5) the first commercial SWATH ship, *Mesa 80*[8,28,29] (Fig. 1.6) was brought into operation.

1.6 The Design Environment

Design has been described as being the optimum solution to the sum of the true needs of the given situation. The design environment for research vessels is such that the designer is likely to find himself in the somewhat invidious position that, firstly, the true needs are not at all clear because of conflicting requirements between different groups, and secondly, he thus does not know what he is trying to optimise.

Various distinguishable groups have an interest in the final vessel, but all from a slightly different viewpoint, and all having different priorities, including first cost, running cost, and workability as illustrated in Fig. 1.7. Thus the design will not only be influenced by the requirements of the users but also by the much broader political and economic climate.

The designer must obtain a balance between these conflicting requirements and will be further hampered by the apparent lack of any useable measure of output. (It is widely accepted that justification for research cannot come solely from economics.) For instance, number of days at sea may be a valid measure of operability, but certainly not of workability. It takes no account of time spent on passage (dependent on vessel speed) on the fact that different vessels (even conventional ones) may take widely differing times on station to conduct the same task (because of differences in motions, whether working over the side or over the stern, etc.). Similarly, minimising passage-time is not particularly helpful if crippling fuel bills prevent the purchase of new equipment.

Faced with this situation the designer should probably try to provide a good basic vessel with spaces and services capable of adaptation to varying needs and with a cruising speed and endurance similar to existing vessels unless he can produce sound arguments for doing otherwise.

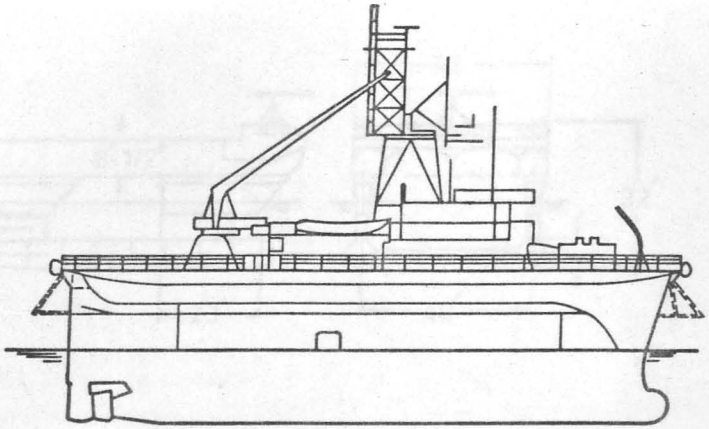

Elevation

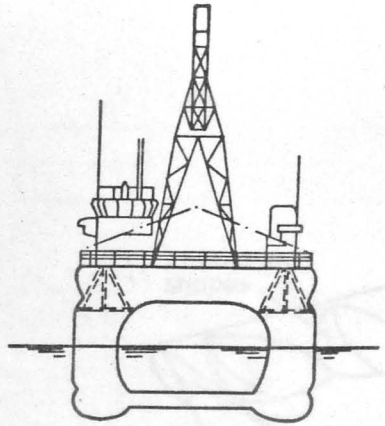

Elevation

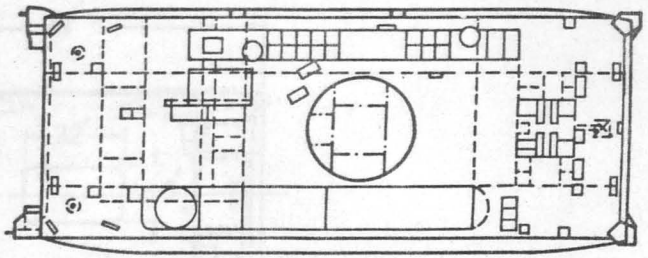

Work deck Plan

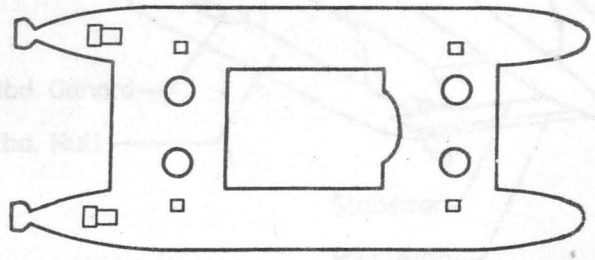

Section

Main Dimensions	154 x 56 x 35 ft.
Maximum Draft	18 ft.
Displacement	1430 tonnes
Well Diameter	23 ft.

Fig. 1·3 "DUPLUS"

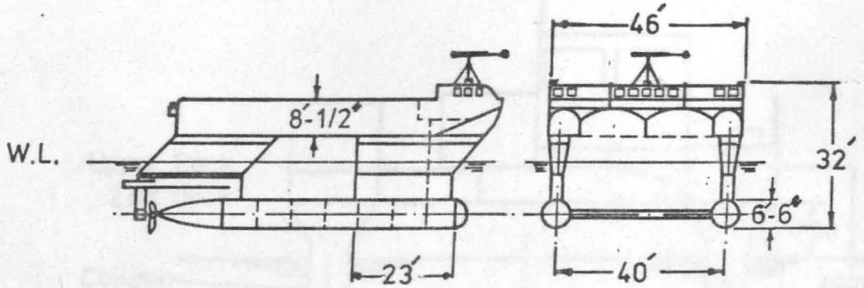

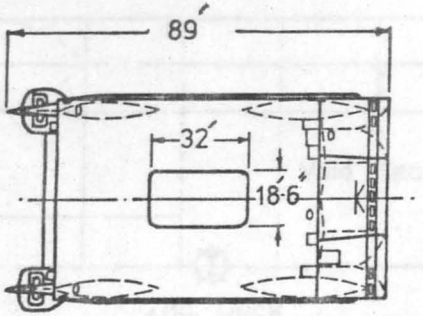

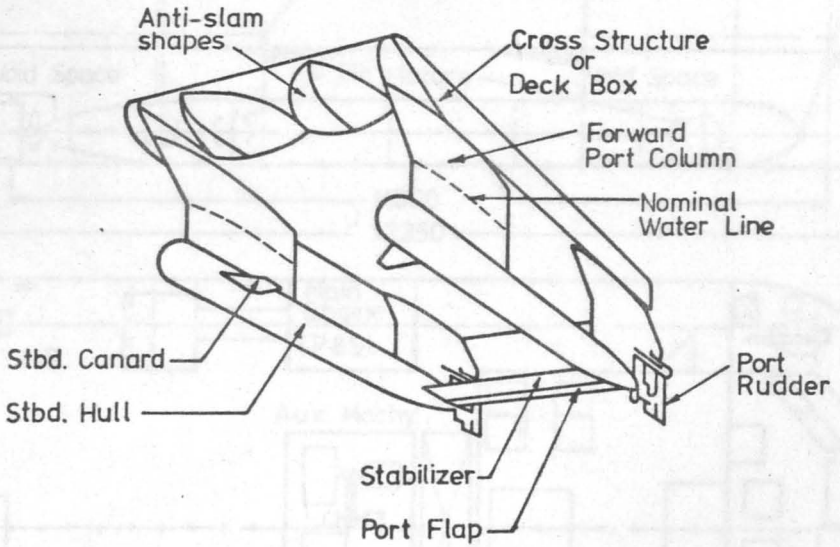

UNDERWATER VIEW

Fig. 1·4 S.S.P. "KAIMALINO"

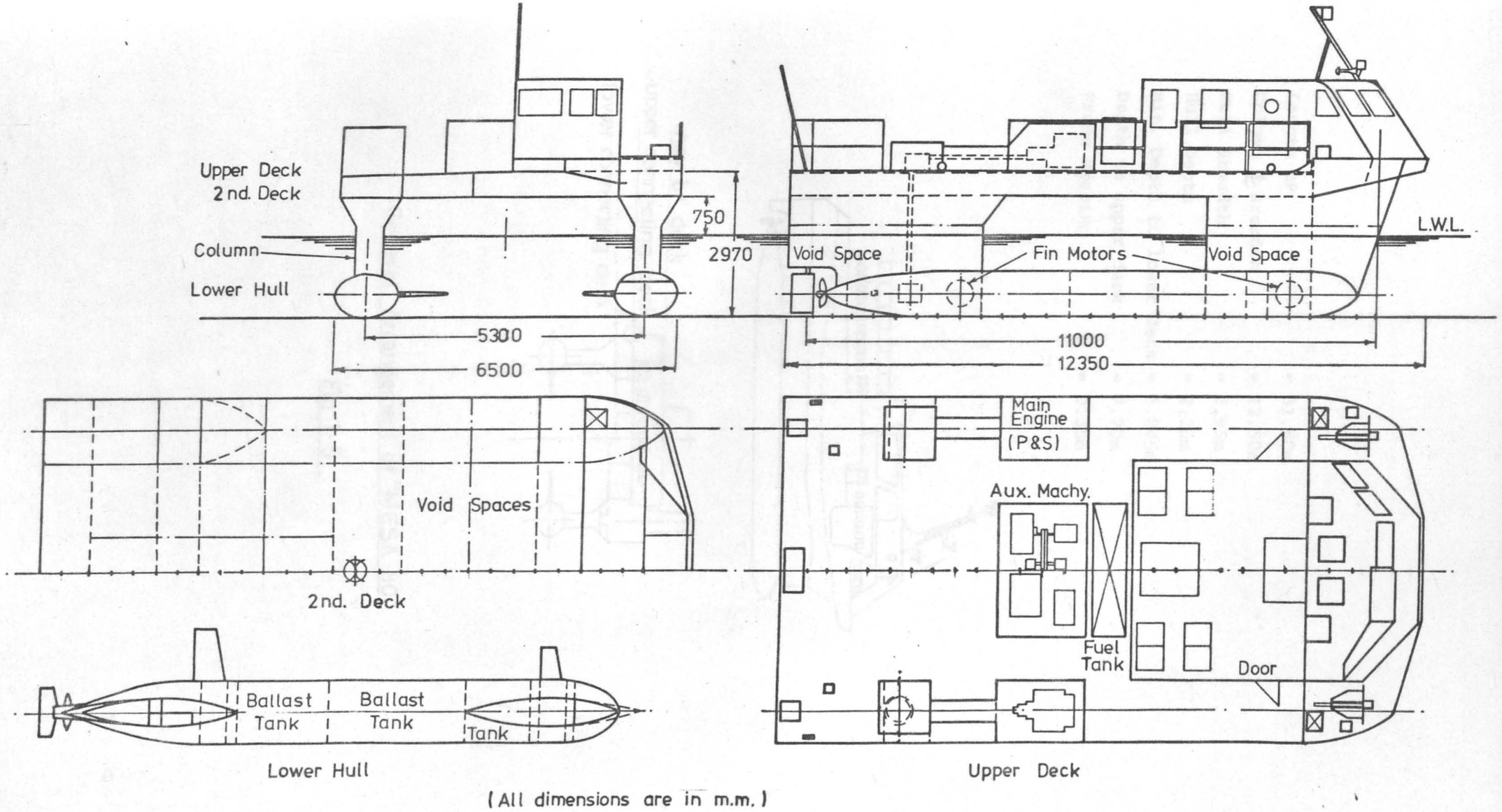

(All dimensions are in m.m.)

Fig. 1-5 General Arrangement of S.S.C. "MARINE ACE"

Length BP	= 31.50m
Column ℄ Breadth	= 13.50m
Hull Breadth	= 2.95m
Hull Depth	= 2.20m
Min. Depth to lower deck	= 5.845m
Depth to upper deck	= 7.70m
Frame Spacing	= 0.35m

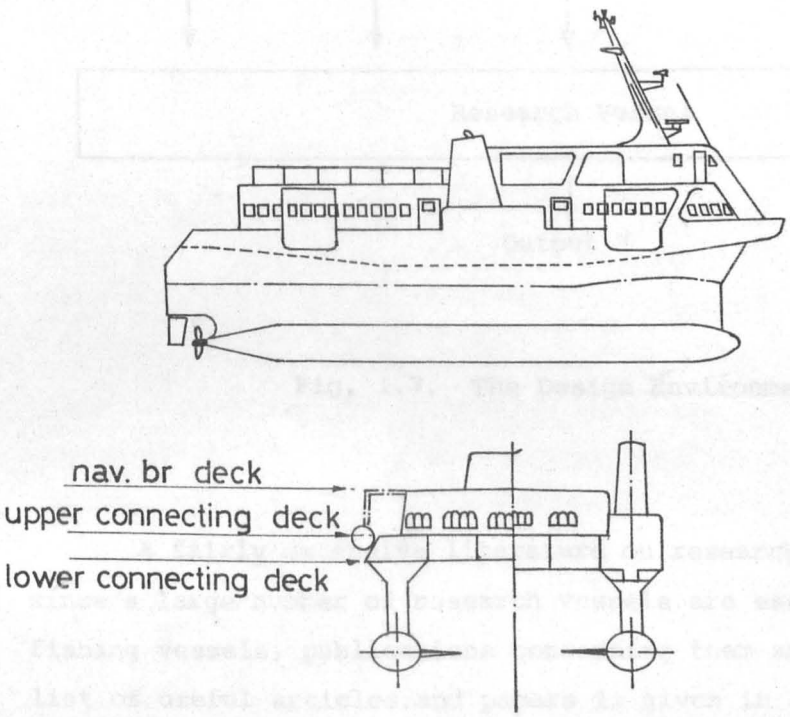

General Arrangement of "MESA 80"

Fig 1·6

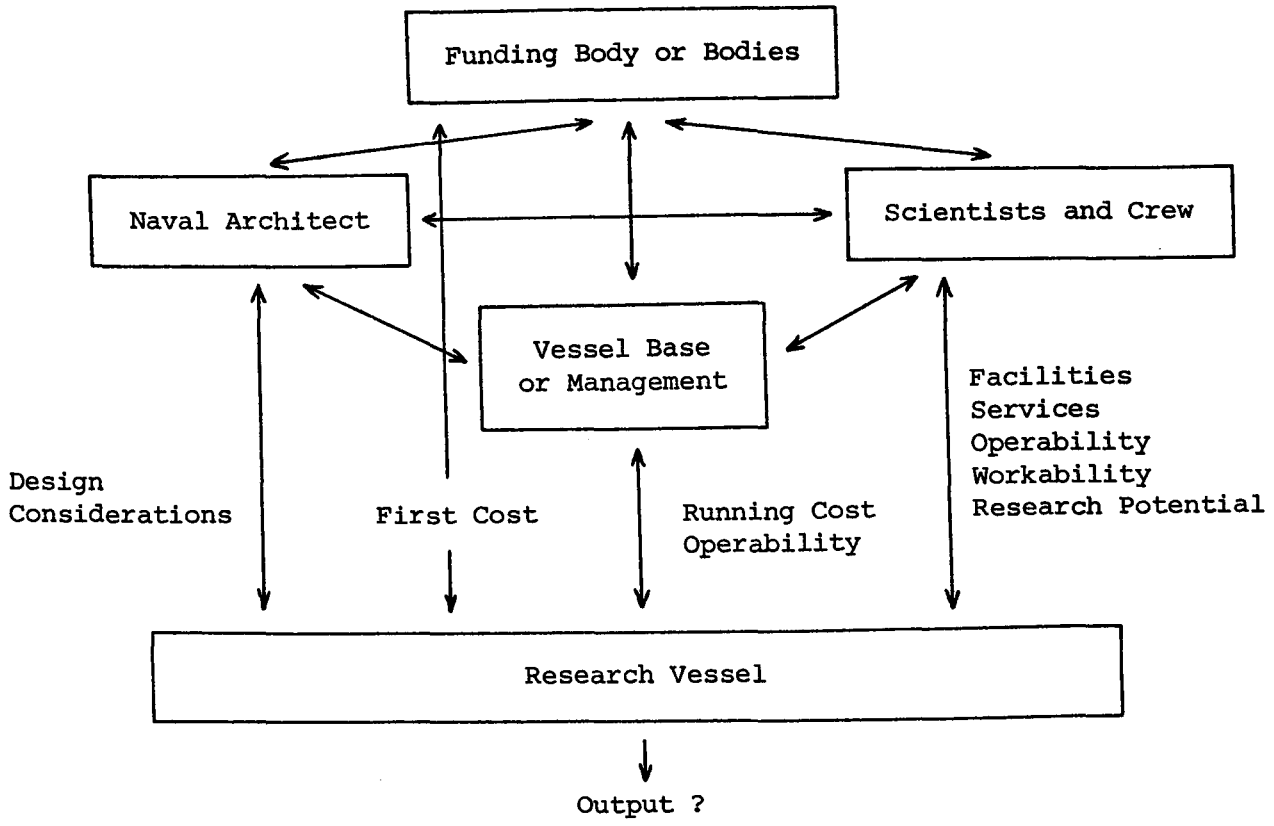

Fig. 1.7. The Design Environment.

A fairly extensive literature on research vessels exists and since a large number of research vessels are essentially adapted fishing vessels, publications concerning them are also relevant. A list of useful articles and papers is given in a Bibliography. This is not exhaustive but is intended to give a general background of the relevant literature.

To obtain some idea of the requirements a number of meetings and seminars were held.

1.7 Review of Meetings

After preliminary meetings with Glasgow University scientists a design study was prepared[30] and was used as the basis for discussion in further meetings at other Universities, research organisations, and the NERC Research Vessel Base. (Appendix A gives a list of the 23 meetings.) This design study generated considerable

interest and some useful comments and criticism. While most agreed on the benefits of low motion-response it should be noted, in the interests of objectivity, that this opinion was not universal. In general, a good view was obtained of the range of interests and type of equipment to be used which then allowed an assessment to be made of likely requirements for winch and crane sizes, electric and hydraulic power, etc. In addition, many items of detail design, such as size and position of sinks and storage racks were discussed, some of which are incorporated in the Specification, (enclosed separately). One of the principle areas of divided opinion concerns the question, particularly relevant, to larger vessels, of whether large multipurpose labs or small specialised ones were better. The majority opinion seems to favour the former.

Two engine manufacturers (Caledonian Engines Ltd. (Caterpillar) and Kelvin Diesels Ltd.) were approached and it was thus determined that there should be no insurmountable problems installing diesel engines in the hulls as proposed.

The above meetings took place throughout the autumn of 1979 and the winter of 1979-80, during which time a second design report was prepared[31]. The *O.W.S. Admiral Beaufort* and the *R.R.S. Challenger*, of the NERC research vessel fleet, were also visited while in harbour. In January 1980 a questionnaire was prepared and circulated, together with two short reports[32,33] to a further 64 potential users (mostly connected with engineering research). Six positive replies were received which, although not an overwhelming number, still indicated that there could be a demand from the engineering community for this type of facility. Further feed-back was obtained from seminars presenting the proposed vessel at Heriot-Watt University and at the Institute of Oceanographic Sciences, a display at the Scottish Marine Biological Association, and by a working trip on the *R.R.S. Challenger*[13].

By this time a fairly wide spectrum of interests had been covered, which led to the formation of the view that the vessel should be for general purposes. Large organisations might benefit from having their own dedicated vessel or if there was a large research vessel fleet then it would be desirable to have specialist

vessels limited to a specific group of tasks but because of the relatively small number of vessels in the British fleet, and the fact that these are used by a number of relatively small organisations and departments with a wide variety of interests, they must be general-purpose.

1.8 Operational Requirements

Since research vessels conduct such a wide variety of work in different scientific disciplines the operational requirements will vary from institution to institution. The main requirements for a conventional general-purpose coastal and inshore vessel may be summarised as follows (not necessarily in order of importance):

(1) Fishing by trawl, lines or traps.

(2) Operation of heavy equipment, such as bottom samplers and dredges.

(3) As a mobile base for diving teams working at a distance from the base laboratory, such that they will be absent overnight or for several nights and where no convenient hotel facilities exist.

(4) As a mobile laboratory for those interested in water chemistry, primary production and other phenomena, the study of which is characterised by the use of an array of laboratory instruments and other apparatus, or the need for sheltered working space and storage space; provision of accommodation as in (3).

(5) Laying and recovery of current meters and other recording instruments.

(6) Work requiring the use of special hydrographic winches and electrical cables.

To the above requirements can be added those arising from engineering research[33], which include:

(7) To be a mobile platform for the attachment and towing of horizontal and vertical cylinders and the logging of data from instrumentation thereon.

(8) To act as a prototype for the collection of data relevant to motion response, wave-induced loads and other structural behaviour characteristics.

(9) To support other engineering activities, including sonar research, submersible handling and anchor testing.

The list of requirements can be determined in a general way from discussion with the potential users and from having a familiarity with their work and equipment. While such discussions are patently essential and can provide much useful information, the Naval Architect should not expect a definitive list. Furthermore, it should be borne in mind that the vessel may outlive several generations of equipment and techniques (especially in view of the rapid progress in micro-electronics, whose full impact on marine science has probably not yet been felt). Thus, while the above may help with technicalities such as electrical power supplies it should be foreseen that various items, even large ones such as extra generators, may need to be installed temporarily on board. Other technical requirements, such as for very accurate navigation arise out of particular projects or techniques and should not necessarily be regarded as part of the vessel's permanent equipment.

CHAPTER 2

SWATH SHIP DESIGN CONSIDERATIONS

The design process is frequently illustrated by the design spiral or more recently it has been modelled by Andrews[34] as a gradually converging conical solid to try and show the various constraints impinging on the vessel, including the design environment as discussed in Section 1.6. The spiralling behaviour of either model reflects the iterative nature of the process and the interaction between different stages. The first constraints on vessel design are those implicit in Archimedes' Law and the requirements for hydrostatic stability. However, consideration of these still leaves a very wide envelope of possible solutions and this chapter discusses further direct naval architecture constraints.

The various configurations (two hulls with two columns, two hulls with four columns, three hulls with three columns) are illustrated in Fig. 2.1. (There could, of course, be others such as two hulls with six columns.) Some of the thinking behind the configurations are explained in the following sections and an attempt is made to deduce the reasons behind various other features.

2.1 Underwater Hulls

The main part of the displacement is provided by the underwater hulls which may have various cross-sectional shapes.

In the *Kaimalino* the underwater hulls have circular sections, whereas those of the *Marine Ace* are elliptical. In general, the circular cross-section provides the minimum wetted surface area per unit cross-section area and is more efficient structurally to withstand the design pressure. The elliptical shape on the other hand provides less hydrodynamic side load and possibly increased damping and added mass against which must be set its increased weight and greater manufacturing expense. Recent developments include the possibility of using contoured hulls[9].

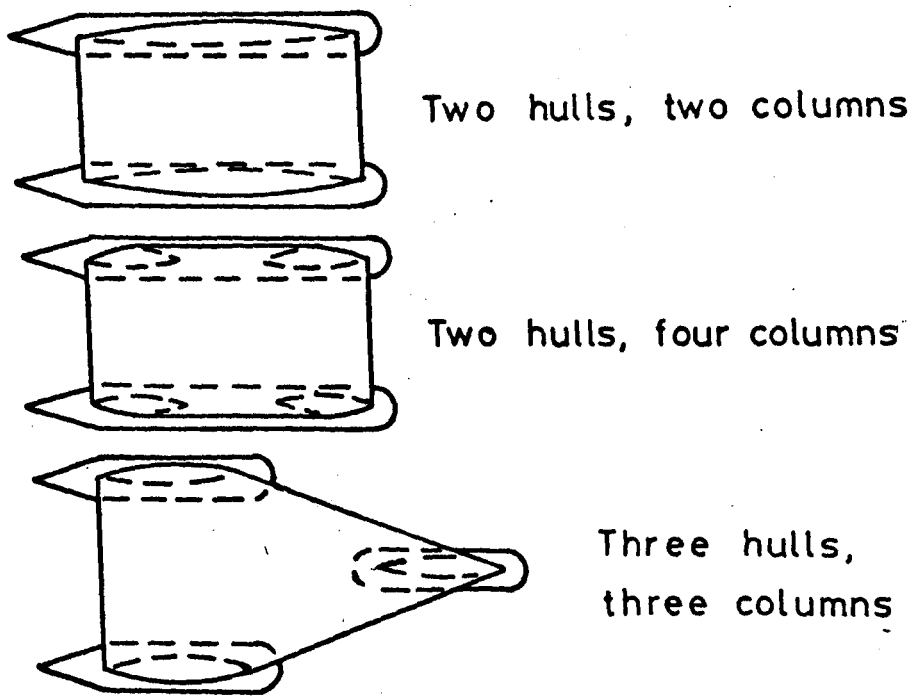

Fig. 2.1. SWATH Ship Configurations.

Rectangular sections have been used on some drilling rigs, but these tend to be heavier, produce greater drag and also have a smaller maximum headroom which will be important for small vessels. They should, however, be cheap to construct, involve a smaller light draft and may give better motion performance under some circumstances.

The forward ending can be either hemispherical or more streamlined. The *Marine Ace* utilises a more streamlined shape, but for the *Kaimalino* it was reported[35] that the minimal reduction in drag did not offset the greater cost and greater weight. For larger vessels this cost penalty would be reduced and a more streamlined shape might be adopted. It is possible that on slower vessels, where the form drag associated with the end shape is a larger proportion of the total drag, due to the vessel's lower wave-making resistance, that the more streamlined shape should be adopted. It is not certain, in any case, that the more streamlined shape would be more expensive if constructed piecewise.

The tailcone should be adequately streamlined to prevent boundary layer separation, (the *Kaimalino* tailcone is 2.5 diameters long if extended to a point[35]), and could, of course, be an oblique cone or even wedge-shaped if these were more convenient for the internal layout.

2.2 Hull Length/Diameter Ratio

The overall hull length is strongly influenced by the column spacing adopted, but inside the envelope of solutions the choice will be affected by various factors.

Increasing the hull length/diameter ratio will tend to reduce the resistance since, although the skin friction will increase with the increased wetted surface area, combination of form drag and wave drag will decrease at a greater rate. The smaller diameter could also improve the inflow to the propeller thus increasing the q.p.c. The increased surface area will result in increased weight for the same scantlings. Since the smaller diameter vessel will be more efficient at resisting the external pressure the scantlings may be reduced, but the net effect is probably a greater steelweight and certainly a greater cost.

2.3 Single Strut or Twin Strut?

From wave-making resistance considerations Chapman[36] suggests that for slow speed SWATHs a single-column per hull should be used (Low Waterplane Catamaran) and as speed is increased two struts per side should be used. This is also mentioned by Lang[35] and is the configuration adopted in the *Duplus* and *Trisec*. For the *S.S.P. Kaimalino* model tests showed that for a one-strut-per-side design the wave drag coefficient would peak at 15 knots while that for the two-strut-per-side peaked at 10 knots. Against this must be set the fact that, for a small vessel (where the minimum column thickness is dictated by access requirements) the large length necessary in a streamlined shape to make the vessel stable in pitch would require more waterplane area. (Adequate GM_L must be provided both to give hydrostatic stability and to avoid dynamic instability.)

Further considerations are:

(a) Hydrodynamic sideforce and platform motion in beam seas will be greater for a one-strut-per-side configuration.

(b) Two-struts-per-side permit a more independent selection of waterplane area, GM_T and GM_L.

(c) Two-struts-per-side designs tend to have less wetted surface area and less structural weight.

In an extensive parametric study McCreight and Stahl[37] show the manner in which the number, shape, and size of columns influence vessel motions. They relate the change in motions to hydrostatic parameters but it seems likely that the motion differences are more due to the resulting changes in the hydrodynamic coefficients.

2.4 Height of Struts

The height of the struts is the sum of the required underdeck clearance and the desired draught. The two are partially coupled, in that increased draught reduces motions and thus affects the clearance required. For certain types of 'life-science' work the working draught may be specified by marine life considerations.

The minimum draught may be dictated by the requirement to maintain propeller immersion or prevent fore-foot emergence at a

certain speed in a certain sea-state while the maximum draught may be limited by the resistance at speed or by harbour and docking facilities. Knowing the motion response for the desired draught or draughts, the clearance will then be set by the requirement to limit slamming to an acceptable level at the speed and sea-state chosen.

This motion response may or may not take into account the beneficial effects of the control surfaces if any and the determination of the clearance is more analogous to a hydrofoil than a large semi-submersible drilling rig. In the large drilling rig the wave frequencies will generally be supercritical (i.e. above the natural frequency of the rig) so that for a first approximation, since the rig is experiencing only small motions the required clearance will be the amplitude of the design wave plus a margin. (In general, the deck structure of the rig will not be designed to withstand wave impacts.) However, SWATH-type vessels will need to operate at subcritical frequencies (for instance in a following-sea) and as a control system will usually be fitted, the vessel will be encouraged to contour waves which otherwise would have contacted the deck structure. A contact occurs when the relative motion between the deck and the sea (probably near the bow) is greater than the underdeck clearance. For a slam to occur it is probably also necessary to exceed a critical relative acceleration and maybe some critical angle[38]. The deck structure, however, must be designed to withstand slamming.

The penalty for increased clearance is, of course, a rise in the VCG which then requires either increased breadth or waterplane area to maintain stability, both being undesirable.

2.5 Strut Cross-section

For stationary vessels, i.e. oil rigs, it is usual to use column cross-sections which are circular, rectangular or rectangular with rounded corners. As the resistance becomes more important due to forward speed a more streamlined shape is used and a twin-strut SWATH ship might have column thickness/chord ratio of approximately 10-15%. This is a compromise between reduced resistance, the need for access to the hulls, longitudinal and transverse stability, and structural weight and cost. The minimum column thickness may be governed by access requirements.

Model tests[25], show the beneficial effects on pitch motions of increasing the cross-sectional area of the forward column. However, this increase appears to cause a worsening in roll and Lang advises treating both these conclusions with caution, but it is surely significant that the *Kaimalino* has enlarged forward columns. He also advocates a large GM_L.

The increased area forward may only be useful to a certain extent. The heave natural frequency is given by

$$\omega_H = \sqrt{\frac{\rho g A_w}{\Delta + AM}} \qquad \ldots\ldots \qquad 2.1$$

Therefore assuming we want to minimise ω_H we also want minimum waterplane area, A_w. Thus if the breadth is considered as fixed, A_w is dictated by static stability requirements (i.e. GM_T and to a certain extent GM_L). For a four column design it is possible to increase the waterplane forward and simultaneously decrease the waterplane aft, thus maintaining constant A_w and adequate transverse stability. There will then be only a small change in ω_H due to the change in added mass.

For a three column design the forward column has only a small effect on the transverse stability, so that any increase in the waterplane area of the forward column cannot be compensated for by a reduction in waterplane area of the aft columns. Thus, any increase in the size of the forward column causes an unavoidable and undesirable increase in the heave natural frequency ω_H and hence the motions. However, increased forward strut cross-sectional area may help reduce the trim in still water at speed; a thinner column with a larger chord apparently does[39]. Similarly, changing the column sizes will alter the relative motion response. Since slamming will tend to occur near the forward end it may be desirable to reduce the relative motion in that region. This is likely to lead to an increase in actual motions and it may be difficult to reconcile the two conflicting desires for low vessel motions and low relative motions.

The option of varying the cross-sectional areas may well be controlled by the less exotic considerations of the vessel's hydrostatics. For instance, the *Marine Ace* has columns of approximately

the same cross-section fore and aft. However, for the *Marine Ace* the main propulsion engines (which are situated on the deck) are further forward than would seem necessary or desirable from a mechanical engineering point of view. This suggests they have been moved forward from consideration of trim, due to LCG being too far aft. In this situation increasing the forward column size would have aggravated the situation. This could be borne out by the position of the hull-nose which is actually underneath the column rather than forward of it as on *Kaimalino*. From structural and cost considerations it would seem to be easier and cheaper to have the nose forward of the column. However, a more likely explanation of the nose position is that in order to install gearboxes and fin control gear the hull had to have as large a diameter as possible (bear in mind that this is a small prototype) and hence for a given displacement, the hull length had to be kept down, while at the same time it was desirable to have the columns spaced as widely as possible to maintain GM_L. This is further borne out by the manner in which the leading edge of the forward strut has a forward rake all the way from the hull centreline instead of from near the LWL as on *Kaimalino*. The only other alternative would have been to move the aft column astern (relative to the hull), but it can be seen that this is virtually impossible because of the need for access to the propulsion gearing system and the aft fin control system. (The position of the nose relative to the column will also affect the wave resistance characteristics.)

2.6 Column Flare

Flaring out the column above the waterline improves the static and damaged stability, provides easier connection between column and deck-box and possibly also deflects spray.

The effect of column flare on motions will be discussed later, but it should be pointed out at this stage that too great a column flare can lead to some unexpected and undesirable results.

On the *Kaimalino* the flare starts below the LWL which one would have thought was undesirable. It is possible to speculate that either the normal operating draught is below the design LWL or that hydrodynamic lift decreases the draught with increasing speed.

2.7 Structural Material

Current shipbuilding practice favours the general use of mild steel with some higher strength steel and aluminium for the upper levels of superstructure and deckhouses. The attraction of aluminium is its lightweight but in practice this benefit is always eroded by the need to provide additional fire-retardant materials. Further, the cost is greater than for steel. Thus while the use of aluminium, particularly for the deck-box, is attractive it was decided at an early stage to limit the design studies to steel primary structure. (The *Kaimalino* and *Mesa 80* both make extensive use of aluminium.)

2.8 Deck-box Bow Shape

Since sufficient underdeck clearance cannot be provided to prevent wave contacts and slamming it is necessary to design the shape of the structure in such a way as to minimise the loads and also sufficiently strong to withstand any resulting load. An investigation for the *Kaimalino*[35] suggested that the best shape was a well faired double bow ('anti-slam shapes', see Fig. 1.4) mounted on a flat surface angled 20° down from the horizontal.

2.9 Control Surfaces - Fins and Rudders

2.9.1 Fins

Experiments by Lang[25] and later in this thesis show that the motions in the pitch/heave mode can be reduced by a fixed fin aft. Similarly, such a fin can increase the speed at which dynamic instabilities occur but it has been shown analytically that beyond a certain size of aft fin the motions will deteriorate again[40]. This is then overcome by adding controllable canard fins forward which can further decrease the motions[25].

As well as providing control the fins increase damping in heave and pitch. The natural heave frequency is lowered by the increase in added mass and the natural pitch frequency is lowered by the increase in mass moment of inertia.

In still water a fixed fin aft will always reduce the speed-induced trim angle. If the bow trims up then the aft fin develops a

positive angle of attack and hence a stern up moment which will reduce the trim angle. If the bow trims down, negative angle of attack at the stern again reduces the trim angle (but in this case increases sinkage of the LCG), however the net effect will still be beneficial. A FIXED fin forward would always tend to increase the trim angle and such a fin would therefore need to be controllable. A possible exception is illustrated by the *Duplus* where the forward fin is given a permanent positive angle of attack while the stern fin has a permanent negative angle of attack. This is a feasible solution if the trim moment is always the same sign (in this case bow down) over the vessel's speed range where trim is a problem.

Stabilisation is possible in heave, pitch and roll. However, for the three column design the forward fins will not be as efficient for roll stabilisation due to their smaller lever from the longitudinal centreline.

The transverse fin could have its performance improved by the addition of controllable flaps on the trailing edge, as in the *Kaimalino*.

2.9.2 | Rudders

Rudders may be considered as optional on SWATH ships. For instance the *Duplus* is steered only by the main engines (possible, since the separation is wide) and extra low-speed manoeuvrability is obtained from the four Voith-Schneider units mounted under the transverse fins.

The *Kaimalino* and *Marine Ace* have rudders in the traditional position astern of the propellers to utilise the increased velocity, and this layout will probably always be adopted when high speed turning and manoeuvring are required.

Other suggestions include rudders mounted as flaps on the trailing edges of the columns or combining the rudder and control fin into one diagonal strut as on Litton Industries, *Trisec* prototype.

Whatever steering system is adopted the two-hull-two-column configuration will have a larger turning radius than a two-hull-four-column. The three-hull-three-column configuration is expected

to lie somewhere between the two. The turning circle will be affected by the use of stabilisers to induce heel.

2.10 Transverse Fin as a Brace

Semi-submersibles are typically fitted with both horizontal and diagonal bracing to serve as structural members. Similarly, on a SWATH ship the transverse brace would help reduce the loads in the deck-box. However, because of the slenderness of the brace and its susceptibility to damage it is felt that the deck-box should be designed to withstand the loads without the brace. However, it may still provide a useful structural function from consideration of fatigue.

For semi-submersibles fatigue-life is a major consideration and similarly the tops of the columns, for instance, of the SWATH may be prone to fatigue cracking. By reducing the maximum stress levels the fatigue-life will be increased so the brace will still be structuraly useful.

For a three-hull design the span of the brace may be about 25% greater than for a twin-hull design thus for the same second moment of area it will be subject to column collapse in compression at a lower load. Similarly, wave-induced forces and lift forces will also cause a greater bending moment at the root.

2.11 Main Machinery and Propulsion

For small and medium SWATH ships the choice is essentially between diesels and gas turbines and the advantages and disadvantages of each are discussed in, for example, Ref. 41 with particular reference to small fast warships.

Typical research vessel requirements for extended periods of station-keeping or low-speed cruising can lead to the usual problems in diesel engines, of valve lacquering and build-up of deposits in inlets and turbo-chargers. For this reason, diesel-electric drive is popular for research vessels although they were rejected for the present case because of the extra weight. Although weight is also critical for conventional semi-submersibles, diesel-electric systems

are common[42,43] partly because of the flexibility this allows in using the generated power for a range of different operations. Steam turbines have been used in research vessels because they have the attraction of quietness but tend to have a higher fuel consumption.

If diesel engines are fitted in the hulls they may require the exhaust diameter to be increased slightly from standard to avoid excessive back-pressure. Similarly, adequate ventilation would be required. A 500 hp diesel requires an air intake of approximately 1100 ft^3/min. The specific air mass flow for gas turbines is higher.

If the main machinery is in the hulls then the length of shafting will be a minimum, otherwise the drive will need to be transmitted down the columns. On the *Kaimalino*, which has gas turbines on deck, there is a chain drive system in the columns while the *Mesa 80* with diesels on deck uses a more conventional Z-drive. In an attempt to avoid problems with wear on the bevel gears this has twin vertical shafts but the extra number of components in either system must increase the noise. Further, sufficient flexible couplings must be included to allow for hull structural deflections.

In semi-submersibles and some ships it is necessary to cut away hull side-structure to remove certain machinery items. For the proposed size of vessel and application it was considered to be desirable to have extraction routes through water-tight portable plates in the decks. As previously discussed (Section 2.5) this places a constraint on the minimum column thickness and it further dictates that the engines should be 'in-line' rather than 'V' configuration. Thus, when the main machinery is installed low down in the hulls the engine dimensions tend to be more important than the actual weight (although the two do tend to be connected).

The operational requirements for towing gear with a large resistance necessitates the use of controllable pitch (or at least dual pitch) propellers.

CHAPTER 3

THE THREE-HULLED SWATH SHIP

The three-hulled SWATH concept was introduced in the first chapter and some of its characteristics were mentioned in the second. This chapter gives the reasons for the three-hulled configuration in more detail and goes on to describe the design in the state that has been reached. Stability, vibrations and other subjects are also included.

3.1 Reasons for Three-Hulled Configuration

As previously stated the waterplane area should be as small as is compatible with stability and access requirements. In the case of the two-hull, one column per hull configuration for the size range being envisaged it became apparent that in order to maintain longitudinal stability the columns would be too thin to be practicable for access, so this option was rejected. A comparison between the two remaining geometries, suitably simplified, Fig. 3.1, was then made as follows.

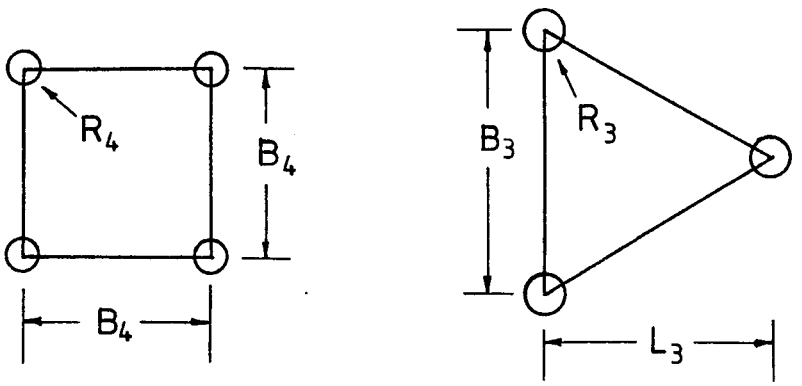

Fig. 3.1. Simplified Configurations.

Both are assumed to have circular section columns (radius R) and the comparison is made on the basis of equal deck area. The four column design is square while the other is an equilateral triangle and it can be shown for either that the second moment of waterplane area (I) is the same about any principal axis. The ratio of dimensions becomes

$$L_3 = 0.87\ B_3, \quad B_4 = 0.66\ B_3 \qquad \ldots\ldots \qquad 3.1$$

where subscripts 3 and 4 refer to the three column and four column geometry respectively.

The waterplane area is set by stability requirements and, for a first approximation, it is required to have the same second moment of waterplane area for either geometry. Considering the transverse case

$$I_4 = I_3 \qquad \ldots\ldots \qquad 3.2$$

$$\rightarrow \frac{1}{4} A_{W_4} B_4^{\,2} = \frac{1}{6} A_{W_3} B_3^{\,2}$$

$$\rightarrow A_{W_4} = A_{W_3}$$

$$R_4 = 0.87\ R_3 \qquad \ldots\ldots \qquad 3.3$$

The column steelweight is related to the circumference C and from above

$$C_4 = 1.16\ C_3 \qquad \ldots\ldots \qquad 3.4$$

i.e. for equal thicknesses the column steelweight is about 16% greater for the four column design. This leads to some increased cost but it is probably negligible since the increased steel is only about 1% of the total lightship weight.

The natural heave frequency, ω_H, is likewise hardly affected by the weight increase and since the waterplane areas are the same the natural heave frequencies are approximately the same.

The first important difference is the waterplane area per column (a_W)

$$a_{W_4} = 0.75\ a_{W_3} \qquad \ldots\ldots \qquad 3.5$$

If the column cross-section is now taken as a parabola (thickness t, chord c) with a thickness to chord ratio of 15% say, we get

$$t_4 = 0.87\ t_3 \qquad \ldots\ldots \qquad 3.6$$

This then means that it will be considerably more difficult to install the engines in the lower hull in a four column design which it is desirable to do both in order to keep the centre of gravity as low as possible and to reduce transmitted vibrations from engines and shafting.

In terms of the centre of gravity if moving the engines to the upper deck resulted in a net shift of 10t upwards through 7m then the lightship VCG would rise by about 0.33m which would result in about a 30% reduction in the lowest GM_T.

Another important difference is the position of the LCF and the LCB. Measuring from the column centre:

$$LCF_4 = 0.5\ B_4, \quad LCF_3 = 0.44\ B_4 \qquad \ldots\ldots \qquad 3.7$$

Since the vessel trims about the LCF anything placed in the aft hull (or when working over the stern) in the three column design produces a smaller trimming moment.

Further, the LCB on the three column design can be more easily positioned by altering the relative displacements of forward and aft hulls.

The three column design offers much better viewing arrangements because an observation compartment may be situated in both the forward and the after ending of the forward hull. Since these observation chambers are separate from the main engines and propellers there should be low transmitted vibrations and less likelihood of aeration from propeller action when manoeuvring.

In a rectangular design the broad underdeck forward has to be carefully shaped to minimise slamming[35] but in the three column design with the forward column flaring out into the apex of the triangular deck slamming should be much less of a problem.

Finally, it has been shown[44,45,46] that wave cancellation between a trimaran's hulls can lead to reduced resistance and it was therefore speculated that this geometry could have potential for high-speed operation.

It can thus be seen that for this size of vessel the three-hull three column geometry appeared to offer several distinct advantages over previous designs.

3.2 Evolution of Design

The starting point for this design study was the sketches of the three-hulled semi-submersible, Figs. 1.1 and 1.2. The first identifiable development from this is shown in Fig. 3.2. However, from the meetings with users (Section 1.7) and preliminary motion response calculations it was determined that the desired size of vessel would have a deck-box area of around 300 m^2. This then led to the General Arrangement given in Fig. 3.3 from the report written at that time[30]. After further development and refinement a model was constructed and tested to determine its motion response and resistance characteristics (see later). This model also had a removeable perspex superstructure to illustrate the layout. The General Arrangement was modified to that given in the second design report[31] by which time the design looked fairly similar to its present state. Subsequently the structure was analysed by hand in some detail (Section 3.8) and sectional steelwork drawings were produced to form part of the Specification that was completed in October 1980, and sent to various shipyards for costing. (The costs are covered in Chapter 4.)

3.3 General Description

The overall concept of the vessel is illustrated in the General Arrangement, Fig. 3.4, and the Machinery Schematic, Fig. 3.5, with main characteristics as in Table I below. A simplified Body Plan and Hydrostatic curves are given in Figs. 3.6 and 3.7 respectively.

It is a steel design (aluminium was rejected as an option because of higher first-cost) with the accommodation and laboratories situated in the deck-box around the working deck, while the forward hull has two observation compartments and could also house a tunnel-thruster. The main engines, remotely controlled from the wheelhouse,

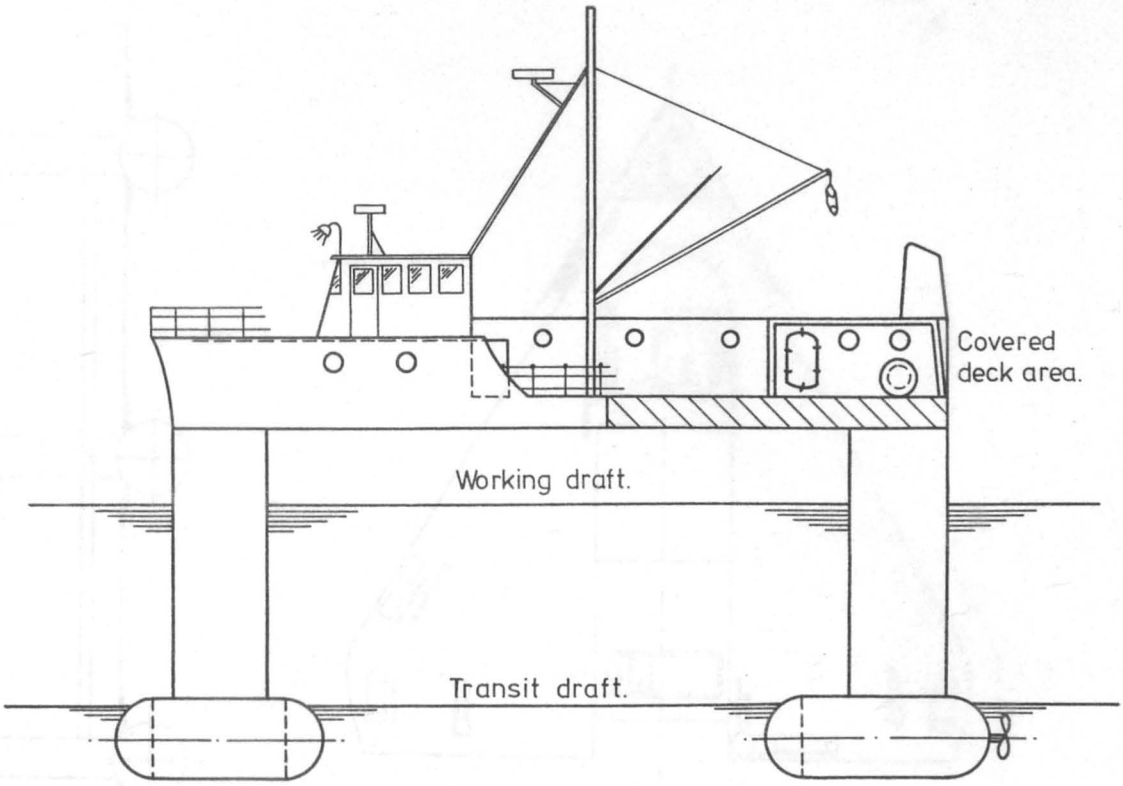

ELEVATION AND SECTION ON "X"–"X"

Principal dimensions.

Deck length 21·0m
Deck breadth 21·0m
Column height 7·0 m
Hull diameter 2·0 m
Laboratory area (approx.) 22m^2
Main deck working area (approx.) 95m^2

Compliment :- 5 Scientists
4 Crew

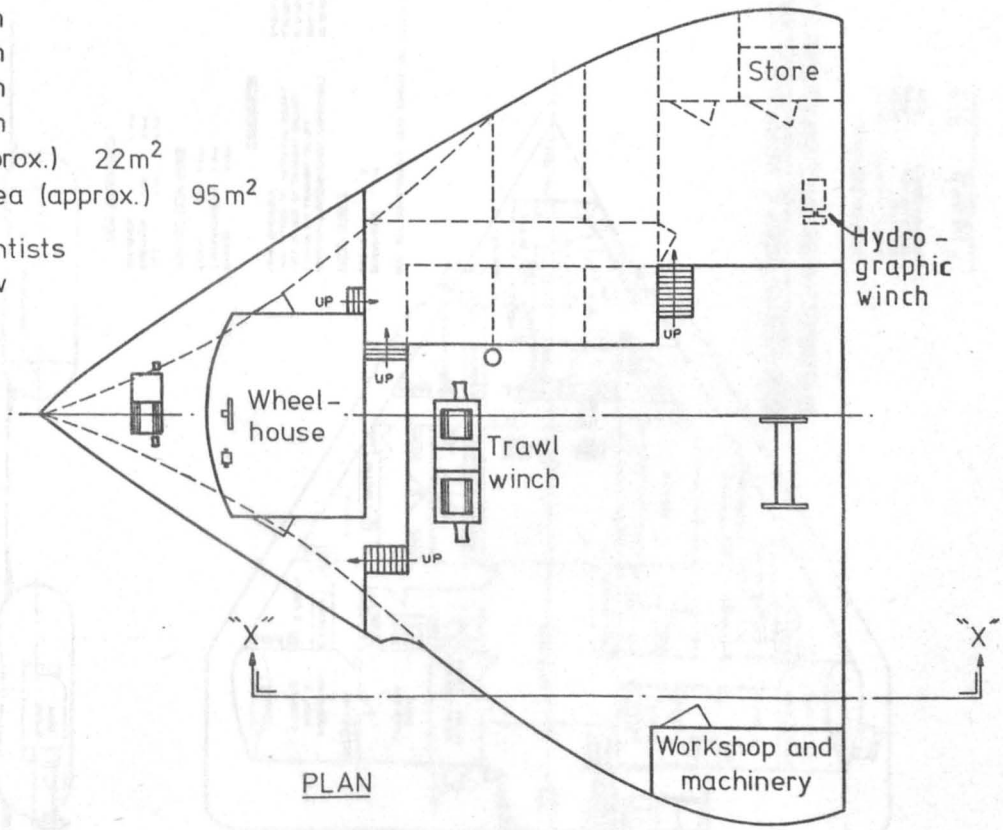

PLAN

PRELIMINARY GENERAL ARRANGEMENT OF SEMI-SUBMERSIBLE FOR LIFE-SCIENCE AND ENGINEERING RESEARCH.

FIGURE 3·2

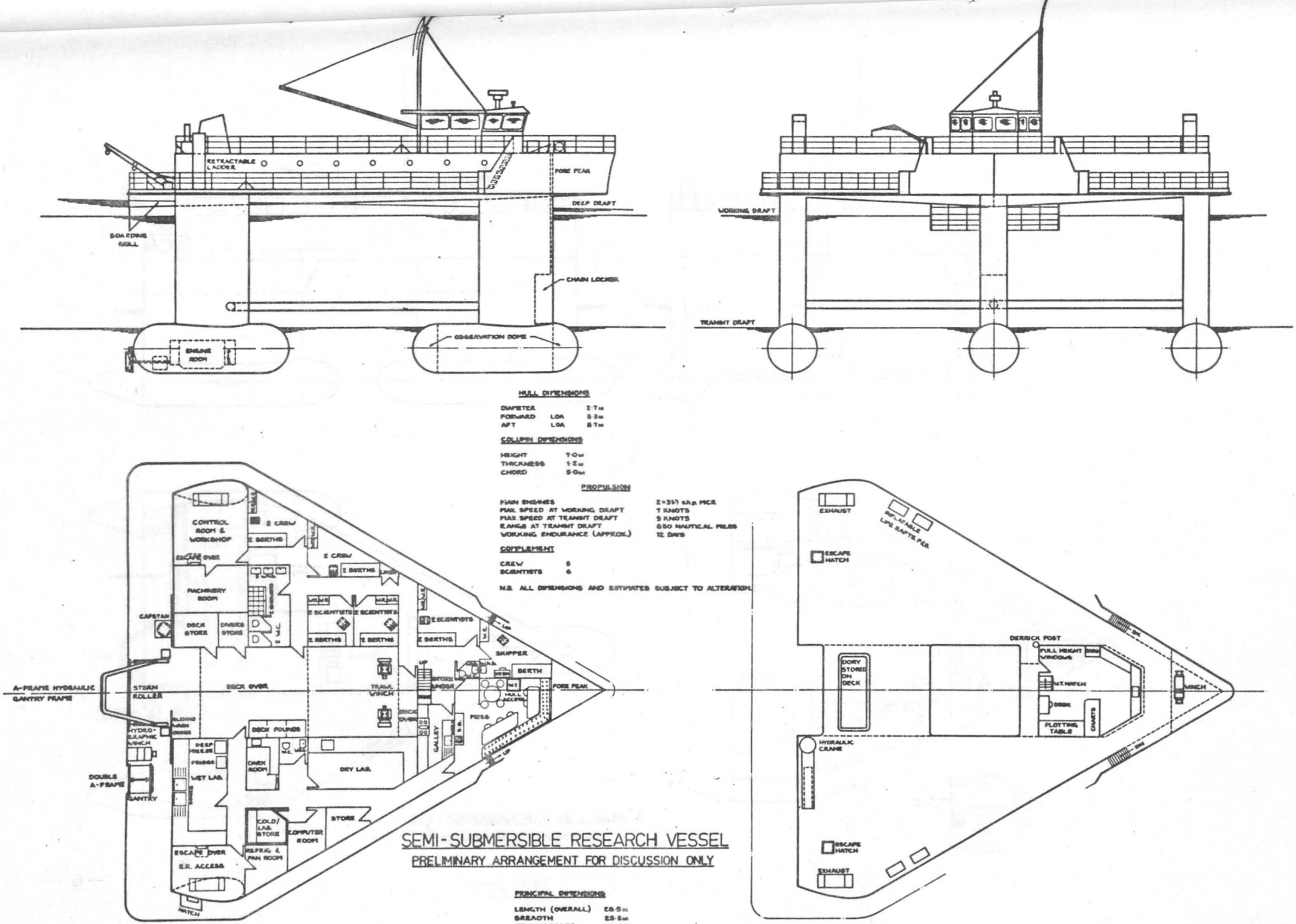

HULL DIMENSIONS

DIAMETER		2·7m
FORWARD	LOA	8·3m
AFT	LOA	8·7m

COLUMN DIMENSIONS

HEIGHT	7·0m
THICKNESS	1·2m
CHORD	5·0m

PROPULSION

MAIN ENGINES	2×351 s.h.p. MCR
MAX. SPEED AT WORKING DRAFT	7 KNOTS
MAX. SPEED AT TRANSIT DRAFT	9 KNOTS
RANGE AT TRANSIT DRAFT	850 NAUTICAL MILES
WORKING ENDURANCE (APPROX.)	12 DAYS

COMPLEMENT

CREW	5
SCIENTISTS	6

N.B. ALL DIMENSIONS AND ESTIMATES SUBJECT TO ALTERATION.

SEMI-SUBMERSIBLE RESEARCH VESSEL

PRELIMINARY ARRANGEMENT FOR DISCUSSION ONLY

PRINCIPAL DIMENSIONS

LENGTH (OVERALL)	28·5m
BREADTH	23·8m
TRANSIT DRAFT	2·6m
WORKING DRAFT	8·7m

Figure 3·3

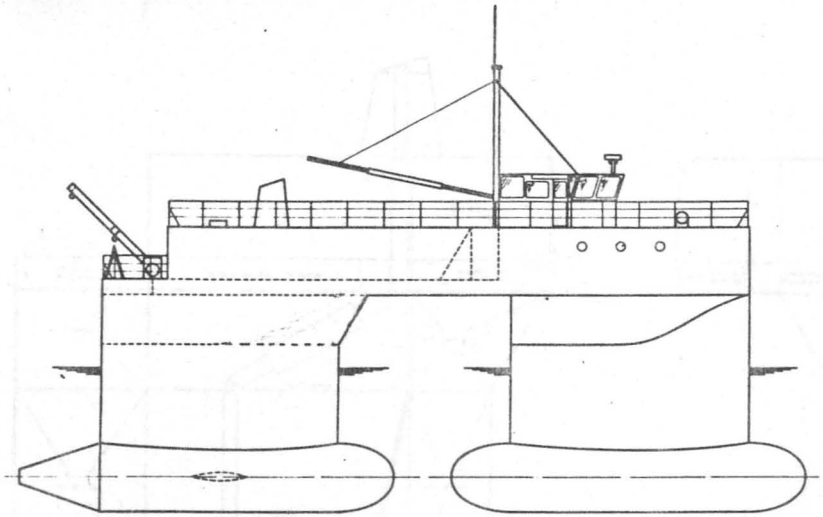

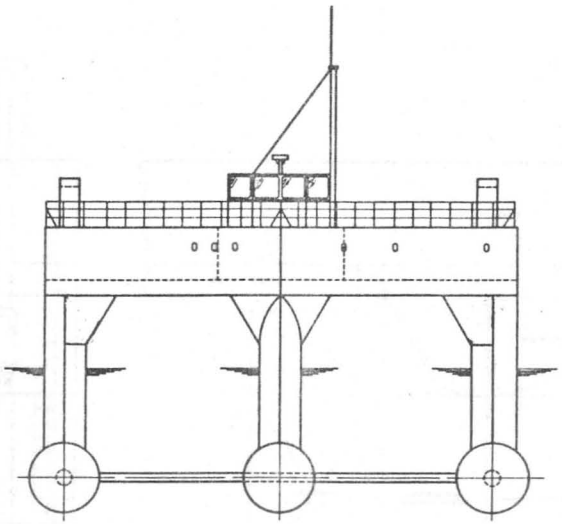

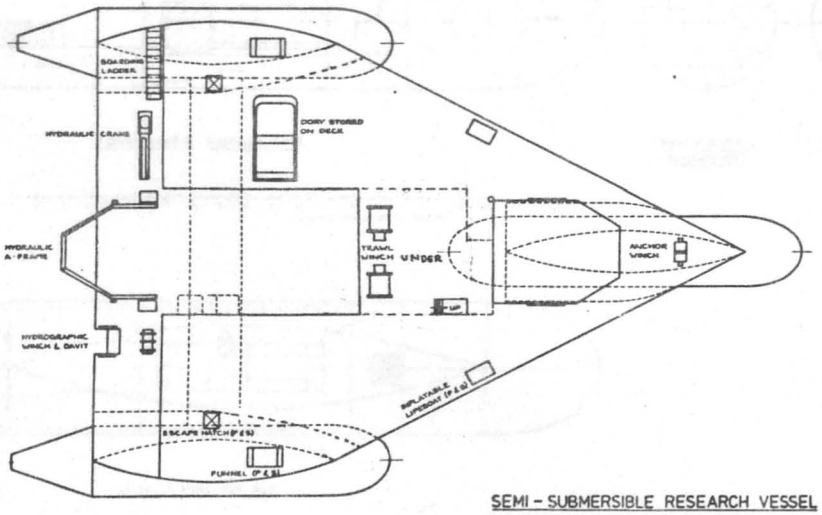

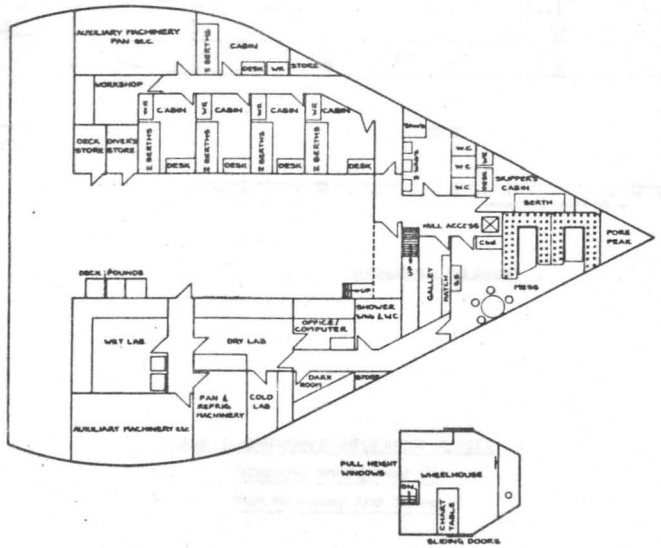

SEMI - SUBMERSIBLE RESEARCH VESSEL

Preliminary General Arrangement

Drawn by S.N. Smith

Traced by A.J. Mc Gowan

Figure 3.4

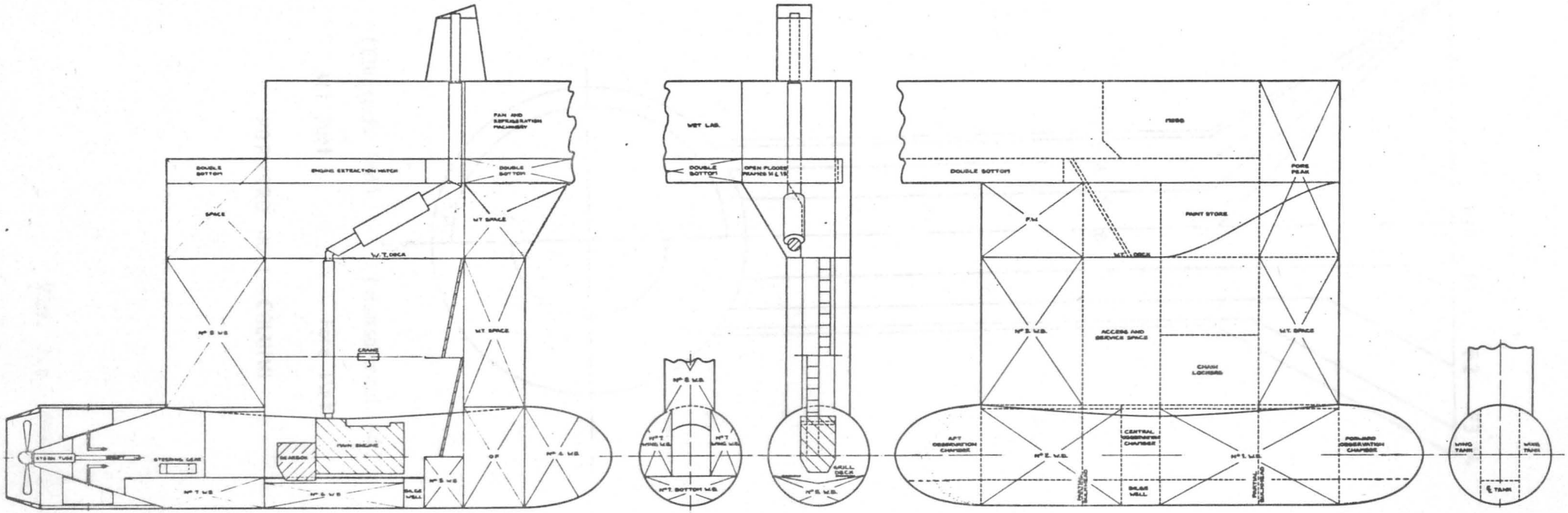

Section on hull ℄ (Looking to port.)

Detail of frame 6. (Looking aft.)

Section on frame 10. (Looking forward.)

Side elevation.

End elevation.

1 2 3 4 5 6 7 8 9 10 11 12 13 14 15 16 17 18 19

Assumed frame spacing 520 mm

32 33 34 35 36 37 38 39 40 41 42 43 44 45 46 47 48 49 50

Assumed frame spacing 520 mm

FORWARD HULL AND COLUMN

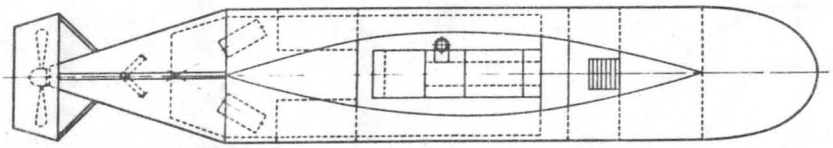

Section on water-tight deck

AFT HULL AND COLUMN

SEMI-SUBMERSIBLE RESEARCH VESSEL

Schematic Arrangement Of

Main Machinery And Tanks.

Drawn by : S.N. Smith.

Traced by A.J. Mc Gowan.

Figure 3.5

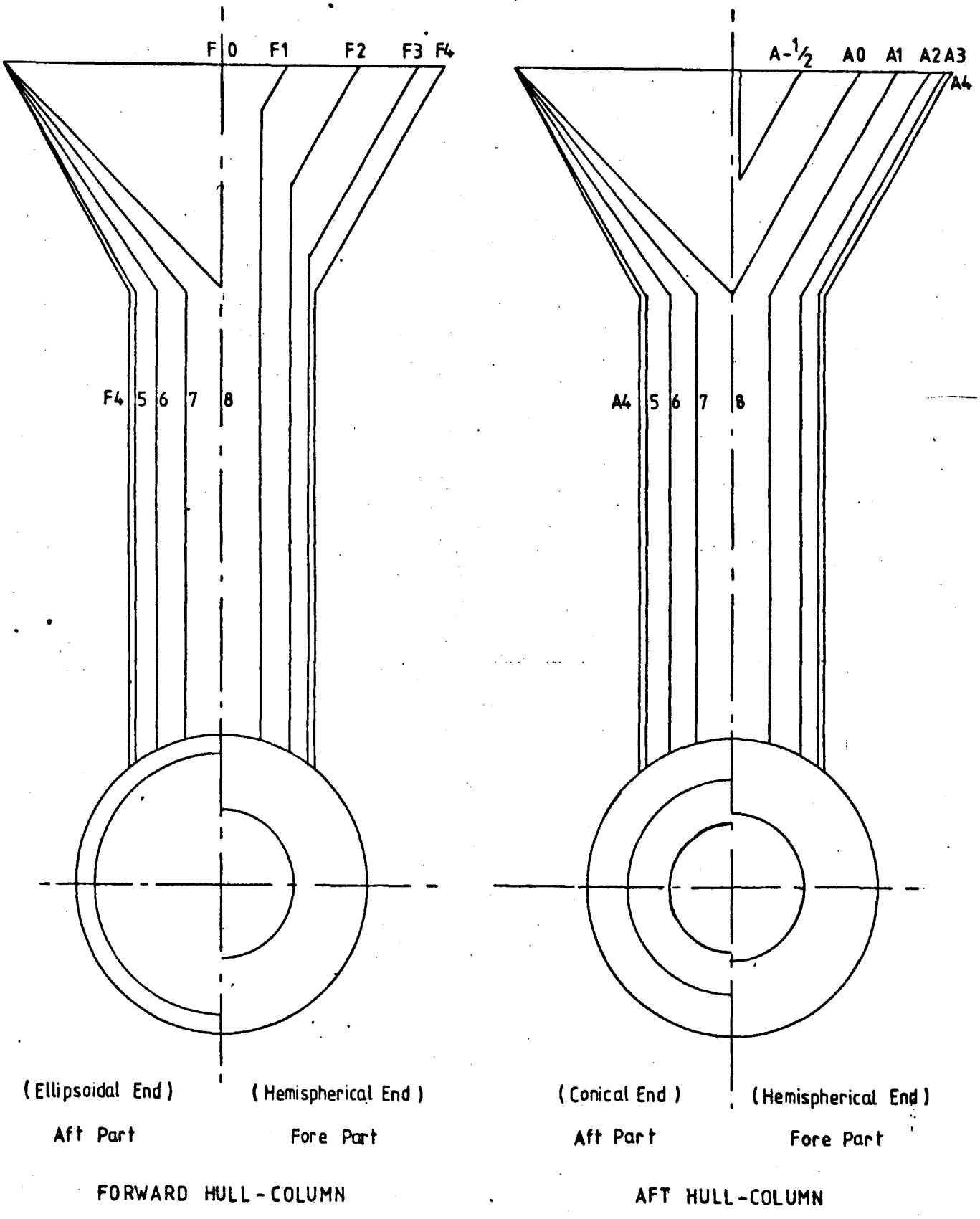

Fig. 3.6. Body Plan from Specification.

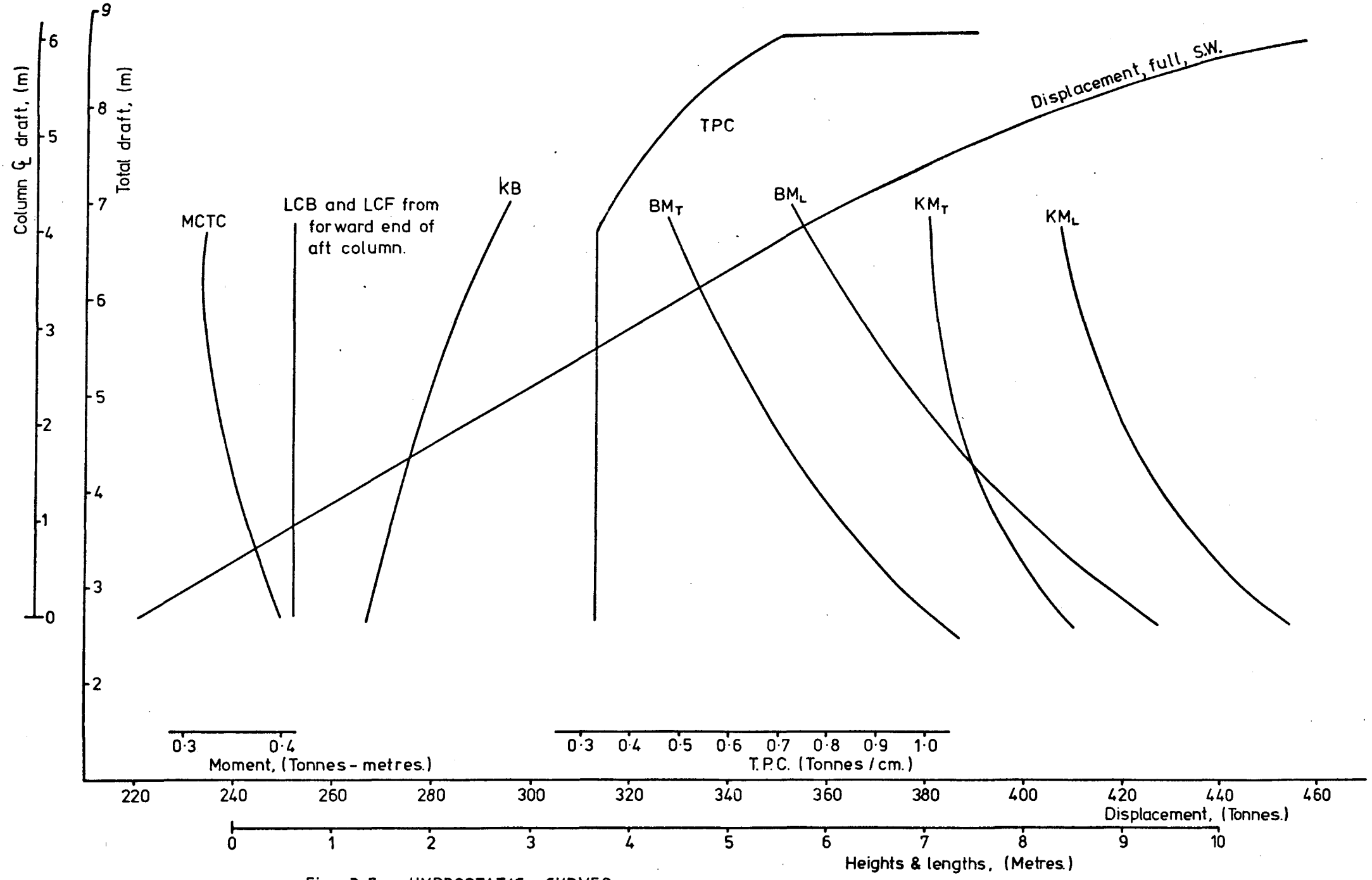

Fig. 3.7 HYDROSTATIC CURVES

Principal Dimensions:	Deck Length	25.5m
	Deck Breadth	18.6m
	Breadth (Ext.)	19.6m
	Draught (Working)	5.7m
	Other Draughts	Variable
Hull Dimensions:	Diameter (Fwd.)	2.7m
	Length (Fwd.)	13.1m
	Diameter (Aft)	2.7m
	Length (Aft)	14.5m
Column Dimensions:	Height	6.0m
	Thickness	1.7m
	Chord	9.4m
Displacement:	At Working Draught	319 tonnes
	Scientific Payload	10 tonnes
Propulsion:	Main Engine	2 × approx. 500 b.h.p.
	Speed (at 2m Column Draught)	9 knots
	Maximum Range	800 nautical miles
	Endurance (Cruise)	14 days (approx.)
Complement:	Crew	5
	Scientists	6
	Students (Day Only)	12

TABLE I. Summary of Main Characteristics.

tanks, and some auxiliary machinery are in the lower hulls or columns. The tops of the columns are flared out for improved static stability and structural strength and the interior of the columns and hulls are sub-divided by watertight decks and bulkheads. The deck-box has a double bottom which not only provides the main structural strength, but also, in conjunction with the top portion of the columns, provides sufficient buoyancy to support the entire vessel in the event of total flooding of all three hulls and lower the portion of the columns. The two aft hulls are connected by a fixed streamlined brace, which could house controllable flaps for roll, heave and pitch stabilisation. A moonpool was not included because of the adverse effect it would have had on the structural strength and, in addition, the pitch motions are very low (see Fig.6.11) so that the increase in motion at the stern is not nearly so great as it would be for a monohull.

3.4 Equipment, Outfit, Groupweights, etc.

To fulfil the operational requirements the items of deck equipment and navigation and communication equipment listed in Tables II and III would be fitted. In general, the emphasis on selection of outfit items would be on lightness with various linings and partitions selected for their noise insulation properties. The various groupweights are given in Table IV. The main tank capacities are given in Table V together with their longitudinal and vertical distribution. Sufficient water-ballast capacity must be installed not only to give the required draught but also to maintain level trim. For this reason it is also desirable to locate heavy consumables such as fuel as near as possible to the LCF.

In the second design report[31] various departure and arrival conditions were calculated. These have not, in general, been updated to take account of the revised structural design (see Section 3.8) except for one condition which was used to ensure that the stability was adequate (Section 3.6). (It is not particularly useful to continue chasing such calculations around the spiral until the structure, which is the largest groupweight, has been checked with a classification society, compliance with other regulations is checked, and firm requirements are established.)

Item	Specification
Main Winch:	2 drums × 650m × 1½" Circumference Warp 1 drum × 500m × 2¼" Circumference Warp 2 Whipping Drums Maximum Pull: 5t on Main Drum 4t on each Smaller Drum
Hydrographic Winch:	1 drum (with Slip Rings) × 250m × 6mm diam. Conductor Cable 1 drum × 250m × 5mm diam. Hydrographic Wire Maximum Pull: 0.5t Variable Speed: 0-2 m/s
Gantry Crane	S.W.L. 6t
Hydrographic Davit	S.W.L. 0.5t
Hydraulic Crane	S.W.L. 1½t at 7m radius
Ship's Derrick	
Net Roller	
Anchor Winches	

TABLE II. Deck Equipment.

Radar
Decca Navigator and Track Plotter
Autopilot
Gyro Compass
Magnetic Compass
Variable Range Echo Sounder with Recorder
Fish-finding Echo Sounder with Headline Transducer
Weather Chart Receiver and Recorder
Log
Chronometer
Radio Telephone
VHF Radio
Watch-keeping Receiver
Emergency Transmitter
Internal Communication System

TABLE III. Navigation and Communication Equipment.

Item	Mass (tonnes)	
Deck-box	91.61	
Columns	35.07	
Hulls	29.64	
Brace	5.18	
(Wheelhouse (AL.)	1.5)	
Sub Total	163.0	
Hull Machinery	12.0	
Other Machinery	8.0	
Outfit and Margin	40.0	
Crew and Effects	1.5	
Oil Fuel	14.0	
Fresh Water	10.0	
Stores	5.0	
Sub Total	253.5	(Corresponding to 1m column draught)
Maximum Water Ballast and Trim Tanks	93.4	
Scientific Payload	10.0	

TABLE IV. Groupweights.

Tank	Mass (t)	VCG (m)	Lever from LCF (m)	Vertical Moment (tm)	Longitudinal Moment (tm) (+ is bow down)
Water Ballast:					
No. 1	16.0	1.2	13.3	19.2	212.9
No. 2	12.5	1.2	8.1	15.0	101.25
No. 3	6.5	4.7	8.0	30.55	52.0
No. 4 P & S	16.0	1.35	0.3	21.6	4.8
					+370.85
No. 5 P & S	5.6	0.8	-2.7	4.48	- 15.12
No. 6 P & S	8.0	0.3	-5.6	2.4	- 44.8
No. 7 P & S	15.8	1.1	-8.6	17.38	-135.88
No. 8 P & S	13.0	4.7	-8.2	61.1	-106.6
	93.4	1.84		171.71	-302.4
					+ 68.45
Fresh Water	10.0	7.4	7.4	74.0	+ 74.0
Fuel	14.0	1.35	-1.38	18.9	- 19.32

TABLE V. Tanks.

Anticipated electric and hydraulic loads are reproduced from the second design report[31] in Table VI.

The general arrangement, outfit, etc., presented here need only be considered as illustrative and could be adapted as desired.

3.5 Laboratory, Accommodation and Deck Areas

A comparison of laboratory, accommodation and deck areas with existing vessels is not inappropriate. Although individual research vessels will seldom be easily comparable because of varying tasks, Table VII gives an idea of the improvements possible with a semi-submersible. (The conventional vessels are from Refs. 47 and 48.)

The 24m ship has a stern deck area of 66 m^2, matched by 60 m^2 in the central well of the SWATH ship which also has another 30 m^2 at the stern.

In addition to having these larger areas, the arrangement of the SWATH is more flexible and is well suited to the addition of temporary accommodation or specialised laboratories by securing containers in the central deck area.

3.6 Intact Stability

For novel ship-types the assessment of stability should be made from a fairly fundamental viewpoint so that some account is taken of the effect that unusual ship geometries have on both the shape of the GZ curve and on the heeling moments. The approach outlined by Sarchin and Goldberg[49] has been adapted for US Navy advanced marine vehicles, including SWATHs by Goldberg and Tucker[50] who foresee no stability problems for SWATHs with regard to beam winds combined with rolling. However, their assumption as to the protection given to watertight closures seem unrealistic for general commercial and civilian standards and it is herein recommended, from a philosophical standpoint, that consideration should be given to the angle of downflooding. The classification society rules for semi-submersibles include the angle of downflooding and it is also essential for SWATHs because, although the deck-box is generally watertight, large openings, even those such as the funnel, may be located near

Item	Passage (kW)	Harbour (kW)
(1) Basic Ship's Load		
Navigation Equipment	4.0	-
Galley	8.0	4.0
Lighting	10.0	5.0
Engine Room Auxiliaries	20.0	5.0
Ventilation	5.0	3.0
Total	47.0	17.0
(2) Laboratory Requirements	10.0	5.0
Diving, Lighting	2.0	-
Total	12.0	5.0
(3) Deck Machinery		
Trawl Winch	40.0	
Crane	8.0	
A-frame	8.0	
Anchor Winch	8.0	
Hydrographic Winch	16.0	
Others	8.0	
Total	88.0	
Maximum Probable	50.0	8.0
Required Capacities		
(a) Full Speed Steaming, Loads (1) & (2) =	59.0 kW	
(b) Slow Speed Trawling, Loads (1) & (2) & (3) =	109.0 kW	
(c) Station Keeping , Loads (1) & (2) & (3) =	109.0 kW	
(d) Harbour Load , Loads (1) & (2) & (3) =	30.0 kW	

TABLE VI. Electric and Hydraulic Loads.

	D.A.F.s *R.V. Clupea*	23m New Construction	SWATH Ship
Length	32m	24m	25.5m
4 scientist cabin	14.5 m^2	-	-
2 scientist cabin	-	5.5 m^2	7.2 m^2
Mess area	16.0 m^2	8.0 m^2	19.0 m^2
Wet Lab.	15.0 m^2	-	15.2 m^2
Dry Lab.	8.5 m^2	-	12.0 m^2
Other Labs. & Offices	-	-	12.0 m^2
Total Labs., etc.	23.5m^2	Lab. + Fish Hold 29.0m^2	39.2 m^2

TABLE VII. Comparison of Three Vessels.

the deck-edge thus permitting extensive flooding at an early stage. This author's suggested revision of the requirements is given in Appendix B.

The GZ curve for the three-hulled SWATH in a deep draught condition, and the wind heeling arm for an 80 knot wind[50] were calculated, Fig. 3.8, and no difficulty was experienced in meeting even the revised criteria. Similarly, an off-centre load of 98.1 kN (from breaking-out an imbedded sampler for instance) did not cause a stability problem.

The sharp rise in GZ after around 15° is caused by immersion of the column flare and the edge of the deck-box, and it is that which gives the good stability characteristics.

3.7 Flooding

To minimise the extent of any flooding the hulls and columns were divided into various watertight spaces and tanks, the largest of which was the engine space, see Fig. 3.5. Flooding of this from an initial light draught would result in a heel angle of about 14°. This prevents any reduction in GM_T although the heel angle could subsequently be reduced by counter-ballasting. When the vessel is at a deeper working draught the heel angle would be smaller.

3.8 Preliminary Structural Design

At various stages during the design process it was necessary to have an estimate of the structural weight, layout and the position of the centre of gravity. As the design became more developed these calculations became more detailed to increase the degree of confidence in the result.

The calculations and procedures adopted will be only briefly described in the following sections because, although they do form an integral and important part of the design process, they are not inherently interesting at the degree of sophistication used. The results hold the main interest and are illustrated by the steel drawings and steel sections in the Specification.

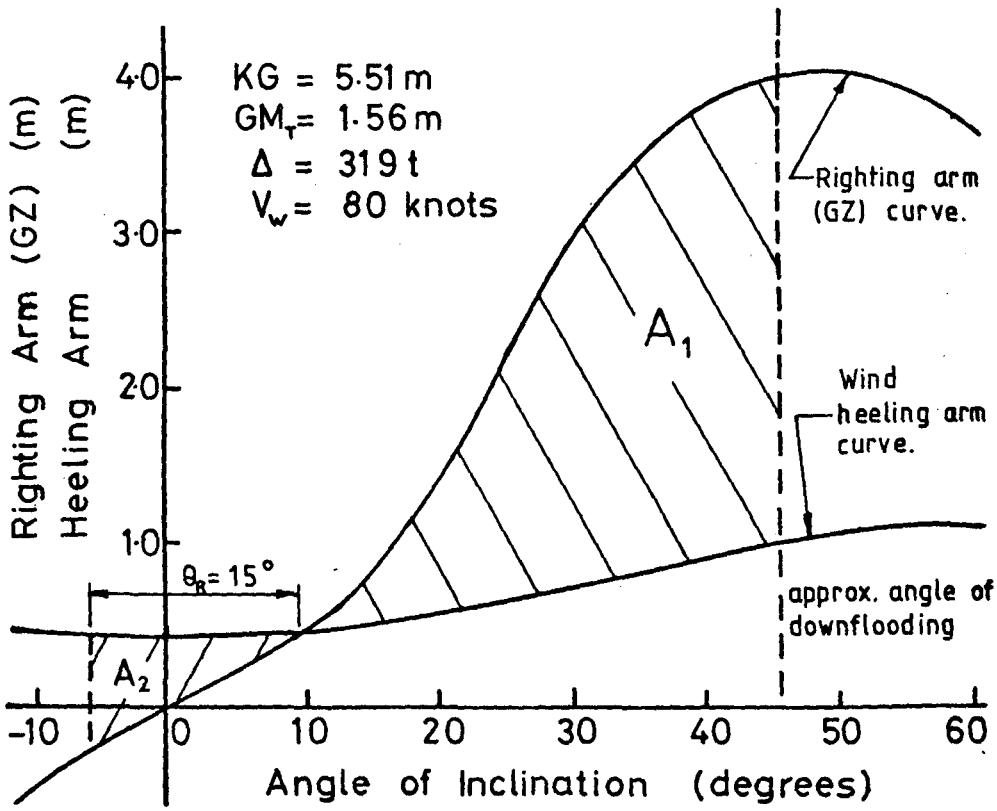

Fig. 3.8. Static Stability Curve.

3.8.1 Initial Design

After an approximate deck area had been determined, preliminary steel drawings were made[31] from which to calculate the steel group-weight and to obtain a quote for the construction cost. In general, these scantlings were derived from consideration of Lloyd's rules for mobile offshore units, ships under 90m, with some extra local strengthening from Fishing Vessel Rules (but it should be noted that these scantlings did not necessarily comply with any classification society rules). The results were checked against the structural densities given in Ref. 51.

In order to simplify the continuity of structure between the main parts, i.e. deck-box, columns and hulls, a constant frame spacing of 520mm was chosen. The main parts are well integrated by connections between the various frames and beams and by continuing plate-floors in the deck-box into bulkheads in the column into bulkheads in the lower hull.

3.8.2 Deck-Box

From experience in the U.S.A. it has been reported[51] that the scantlings are primarily controlled by local loads rather than overall strength considerations.

To derive the preliminary scantlings the deck-box was assumed to be a floating vessel in its own right and guidance was then taken from the various Lloyd's rules. The group-weight thus obtained (Table VIII) was believed to be a reasonable estimate and included various components not shown on the drawings current at that time.

ITEM	MASS (t)
(1) Deck-box	80.0
(2) Columns	32.6
(3) Hulls	41.5
(4) Wheelhouse	2.7
(5) Brace	4.0

TABLE VIII. Preliminary Steelweights.

In general, the plates in the deck-box are minimum thickness permitted, but heavier plates are used in three places in acknowledgement of Fishing Vessel Rules:

(1) in way of A-frame at stern,
(2) in way of trawl winch, and
(3) on the bottom of the deck-box bow.

The double-bottom between the aft columns is heavily strengthened with plate floors in order to resist the forces from the columns and to act as foundations for machinery. Elsewhere, struts are fitted and there is a watertight girder on each side in addition to the centre-line girder. The structure at the bow is reinforced by extra half-height girders and plate floors. Extra support for the upper deck in the forward part is provided by centre-line pillars.

3.8.3 Columns

The column scantlings were derived using the Rules for watertight bulkheads since the external pressure constitutes one of the principal loads. The flare at the top of the columns is necessary because of the high bending moment at the junction with the deck-box. (It also serves to increase the statical stability and can have a large effect on vessel motions.)

3.8.4 Hulls

The hulls were designed from first principles as pressure vessels using interframe collapse as the criterion of failure. Since the frame spacing was essentially already decided and the shell thickness was basically a minimum plus corrosion allowance, the ring-frame scantlings were easily determined.

Because of the large number of bulkheads the ring-frame scantlings are very light and it would probably be more economical to use longitudinal stringers instead.

The hull endings were also designed as unstiffened pressure vessels.

3.8.5 Wheelhouse

The wheelhouse is in aluminium to reduce the topside weight.

3.8.6 Brace

The overall brace dimensions are such that sufficient lift can be generated to counteract any dynamic trim moment. The scantlings were chosen rather arbitrarily to be approximately the same as in the columns, pending a more detailed analysis.

3.8.7 Cathodic Protection

The purpose of any preservation or maintenance programme is to prevent or delay deterioriation of the system and thus ensure its continuing operability. Further, with an approved system of corrosion control installed in a ship's hull, Lloyd's rules, for instance, permit an initial reduction in thickness of 10% or 5% (depending on the item) subject to certain provisos. A substantial weight saving can therefore be achieved.

The application and design of cathodic protection, as well as details such as current density requirements and corrosion rates, are given in, for example, Ref. 52, which was used during the preparation of the Specification.

3.9 Structural Analysis and Redesign

For the preparation of the steel drawings and steel sections, as reproduced in the Specification, a more detailed analysis and redesign of the structure was carried out. (As stated in the acknowledgments this was considerably facilitated by the assistance of Mr. P. Gallagher who performed many of the structural calculations.)

The five cases considered are outlined in the Specification but, in general, it was found that the most critical areas were in way of the tops of the aft columns and at the mid-span of the deck-box.

For a conventional semi-submersible in beam seas the greatest transverse splitting force and hence highest bending moment in the deck-box results from a wave with length equal to twice the transverse column spacing. Similarly, for SWATHs the maximum loading occurs in beam seas and is greatest when stationary[3,40]. However, because of diffraction effects, it is at a wavelength slightly greater than twice the spacing[35]. The horizontal forces are an

order of magnitude greater than the vertical forces and following various investigations it has been suggested that for early feasibility studies a uniformly distributed horizontal force, corresponding to half of the ship displacement at the centre of the lower hull can be used[51,35]. In an unbraced two columns per hull design this gives $F_H = 0.25\ g\Delta$ per column. The internal forces and bending moments can then be calculated using a free-free-beam approach[40].

In this study a strip theory approach with design wave of length twice the column spacing was used, i.e. λ=33.8m (see Fig. 3.9). (The validity of this is questionable because of the above mentioned diffraction effects. The column length perpendicular to the wave crest is 0.28 times the wavelength which is slightly greater than the usual criterion for neglecting diffraction that it should be less than 0.2 times the wavelength.)

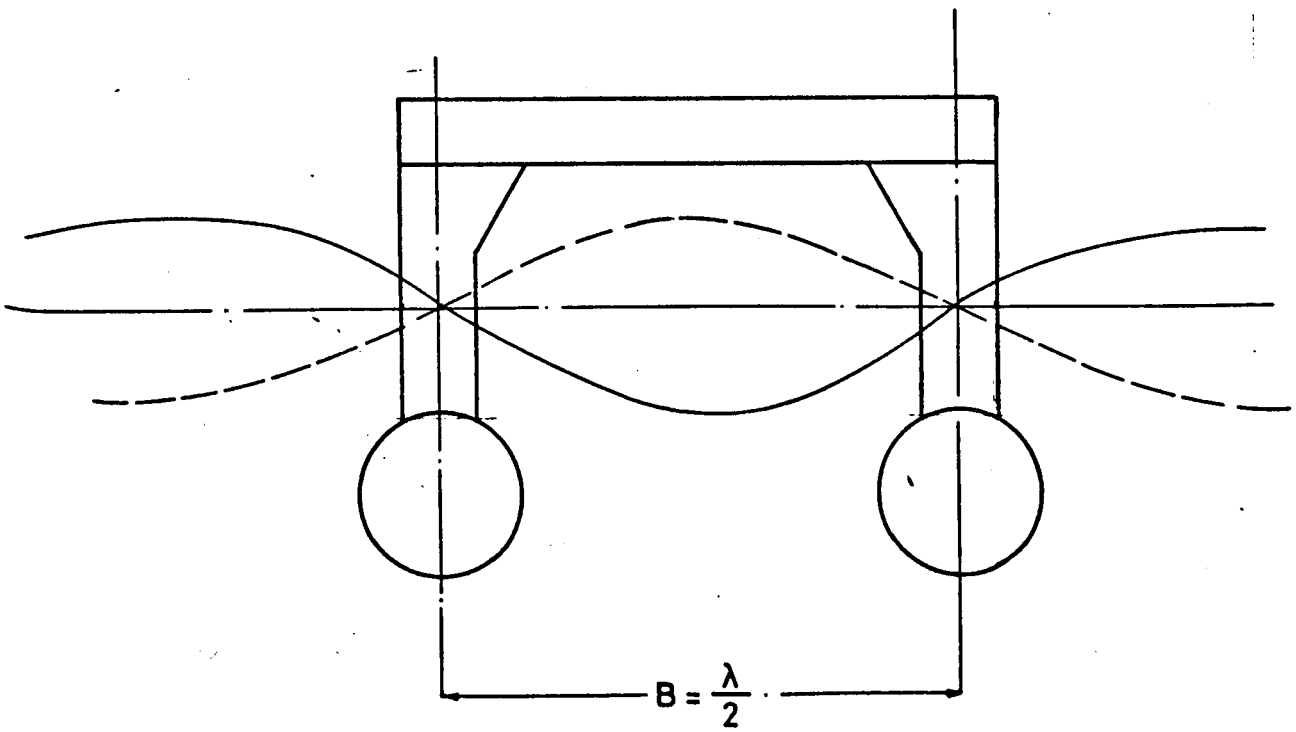

Fig. 3.9. Design Wave.

A wave height of $h = 0.607\sqrt{\lambda}$ was chosen, giving $a_o = 1.75$m. (This is the metric equivalent of the widely used $h = 1.1\sqrt{\lambda}$[53] and is quite severe at lengths less than about 50m. In order to use a strip theory approach the columns and hulls were idealised as in Fig. 3.10.

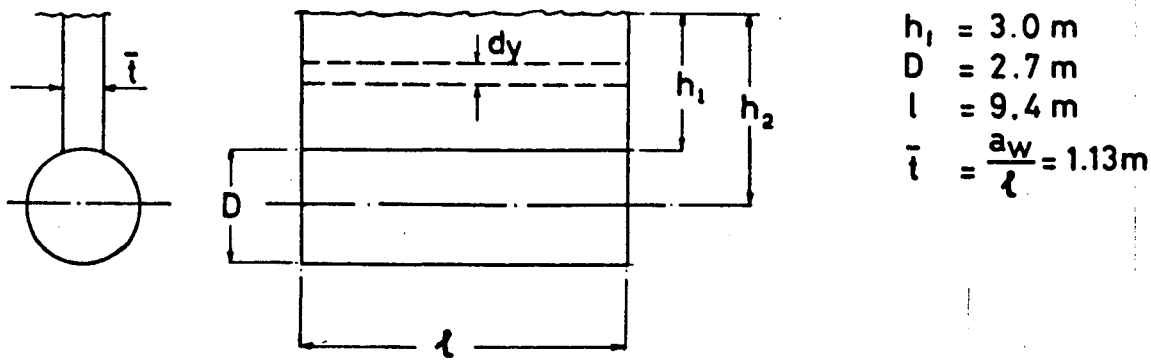

Fig. 3.10. Idealisation of Hull/Column.

The total force is taken as consisting of added-mass, Froude-Krylov (or pressure) and velocity components.

For strip dy on the column the added-mass

$$m_L = \tfrac{1}{4}\rho\pi\ell^2 \qquad \ldots\ldots \qquad 3.8$$

Similarly, for the hull in isolation

$$m_L = \rho\pi R^2\ell \qquad \ldots\ldots \qquad 3.9$$

The horizontal acceleration in the wave is given by

$$kga_o\, e^{ky} \sin k(x-ct) \qquad \ldots\ldots \qquad 3.10$$

Therefore, on the column, neglecting the reduction in added-mass caused by the presence of the free-surface, the added-mass component is given by

$$F_{am} = \int_o^{-h_1} \tfrac{1}{4}\rho\pi\ell^2\, kga_o\, e^{ky} \sin k(x-ct)\, dy \qquad \ldots\ldots \qquad 3.11$$

$$= \tfrac{1}{4}\rho\pi\ell^2\, ga_o\, (1-e^{-kh_1}) \sin k(x-ct) \qquad \ldots\ldots \qquad 3.12$$

Similarly, on the hull, taking the acceleration at the centre-line and neglecting the presence of the column

$$F_{am} = \tfrac{1}{4}\rho\pi R^2\ell\, kga_o\, e^{-kh_2} \sin k(x-ct) \qquad \ldots\ldots \qquad 3.13$$

The pressure component on the column is neglected as being small, while on the hull the pressure force will be the same as the acceleration force. The sum of the added-mass and pressure forces is, therefore

$$F_{am+FK} = \rho\pi g a_o \sin k(x-ct) \left\{\tfrac{1}{4}\ell^2 \left(1-e^{-kh_1}\right) + 2r^2\ell k\, e^{-kh_2}\right\} \ldots \quad 3.14$$

An allowance for viscous effects was made by including a velocity force of the form

$$dF_v = \tfrac{1}{2}\rho C_D \ell a_o^2 gk\, e^{2ky} \cos k(x-ct) \left|\cos k(x-ct)\right| dy \quad \ldots \quad 3.15$$

The above gave rise to a horizontal splitting/compressive wave force of 900 kN which, for determining the bending moment in the deck-box, was assumed to act at half-draught. (This force is slightly greater than that corresponding to the previously mentioned 0.25 Δ.) The force was considered in conjunction with various gravity loads as outlined in the Specification and some steps were taken along the road to ensuring that the maximum permissible stresses given in the Specification (from sources such as Lloyd's rules and BS 5500) were not exceeded. The cross-structure and its junction with the columns were designed using these loads but neglecting the strength added by the brace. The brace is therefore redundant, structurally, although it does serve to improve the fatigue life of the structure by reducing stress levels. The deck-box was treated as a free-free beam and, at the mid-span, the total forces and moments were taken as being evenly distributed over 20 frame spaces. At the top of the columns the forces and moments were distributed between the two main transverse bulkheads.

A certain amount of high strength steel was desirable at the mid-span of the deck-box and the column tops to maintain a low structural weight. Elsewhere the plate thicknesses are generally the minimum permitted by classification society rules, although in certain areas, such as the underside of the deck-box bow and in way of the trawl winch and crane, heavier scantlings have been used because of the high local loads. The structure has not been approved by any authority, but is thought to be realistic, and is illustrated

by the various sections and drawings in the Specification. The scantlings shown include reduced corrosion allowances, (cathodic protection would be fitted) and gave rise to the steelweights and densities in Table IX.

Item	Steelweight (tonnes)	Structural Density (kg/m^3)	(lb/ft^3)
Deck-box	91.61	111	6.93
Columns	35.07	156	9.74
Hulls	29.64	161	10.05
Brace	5.18	912	56.93
{Wheelhouse (AL.)}	1.5}	-	-
TOTAL	161.5	130	8.14

TABLE IX. Steelweights and Densities.

The overall structural density is remarkably close to that given for the *Duplus* in Ref. 51, but higher than all other vessels considered therein. For this particular design the deck-box configuration is not a particularly efficient structure, due to the well-deck, but since the *Duplus* has strengthening for navigation in ice it is felt that this estimate is sufficiently accurate for design purposes and hydrodynamic assessment. The agreement obtained between the method used and the structural density method gives confidence in the use of the latter for computerised design models [54].

3.10 Noise

The designer of research vessels is primarily interested in two principal areas of noise, namely, noise levels in accommodation and working spaces, and hydrodynamic noise around the hull.

The latter is of particular interest for naval vessels because of their requirements both to avoid detection and to use passive listening sonars. It is a large subject in its own right and will not be further considered here, except to say that because research

vessels may make extensive use of sonar techniques the possibilities of low hydrodynamic noise and low aeration offered by SWATH hulls could be of increasing practical significance.

The growing use of lightweight, highspeed machinery and generally increased machinery loadings has led to increased noise levels on board ship. The designer is concerned with keeping these to an acceptable level.

In accommodation spaces structure-borne noise from machinery and propellers is the principal source and these are generally combatted by the use of resilient mountings to isolate vibrating machinery and the proper installation of acoustical absorbents. Ref. 55 gives two procedures for estimating sound levels as well as information on different measuring systems, noise sources, regulations, arrangement of acoustically treated cabins, etc. The development of a noise control specification for a research vessel is given in Ref. 56, while detailed data on, for instance, sound transmission losses for different constructions of partitions, and noise reduction coefficients for different materials can be found in texts[57].

In general, successful noise control lies in the isolation of sources and the specification and proper use of adequate absorbing materials, as well as details such as flexible pipe hangers, low noise-making fans, etc., some of which are included in the vessel Specification.

3.11 Vibration

For conventional ships it is common to calculate the frequencies of the different modes of hull vibration. However, for a SWATH ship it was felt to be particularly appropriate to calculate the frequencies of the hull-column assembly and of the transverse brace. The purpose of this being to ensure that these two frequencies did not coincide either with each other or with a wave encounter frequency which would be extremely serious. For a vessel proceeding at 10 knots in head seas with wavelength of 10m, for example, the encounter frequency is ω_e = 5.7 rads/sec.

For a cantilever beam with uniform mass along the length and a concentrated mass at the end, Fig. 3.11, the lowest fixed base (infinitely stiff) natural frequency can be calculated from

$$\omega_\infty = \sqrt{\frac{3EI}{(M+0.25m\ell)\ \ell^3}} \quad \text{rads/sec.} \qquad \ldots\ldots \qquad 3.16$$

where E = Young's Modulus

I = Moment of Inertia

M = concentrated mass

m = mass per unit length

ℓ = length.

This will be evaluated in the next section.

3.11.1 Lumped-Mass Approach for Hull-Column Vibration

For the hull-column assembly it is possible to use a lumped-mass approach, based on Dunkerley's equation and energy principles, such as has been used for deckhouse eigenvalue analysis[58]. The structure is modelled as a cantilever beam on a flexible base, Fig. 3.12, with lumped-masses along its length, Fig. 3.13, and constant piecewise section properties. The lowest fixed base natural frequency, including bending and shear effects, is then given by Eq. 3.17

$$\omega_\infty = \sqrt{\frac{1}{\sum_{i=j}^{N} M_i \sum_{j=1}^{i} \frac{(\ell_i-\ell_{j-1})^3 - (\ell_i-\ell_j)^3}{E_j I_j} + \frac{\ell_j-\ell_{j-1}}{As_j\ G_j}}} \quad \text{rads/sec.} \qquad \ldots\ldots \qquad 3.17$$

where As_j = shear area

G_j = shear modulus.

Once the fixed base natural frequency has been calculated it must be corrected to account for the flexibility of the base support structure to produce an estimate of the actual frequency of the structure

$$\omega_e = \sqrt{\frac{1}{\frac{1}{\omega_\infty^2} + \frac{1}{\omega_\theta^2} + \frac{1}{\omega_v^2}}} \quad \text{rads/sec.} \qquad \ldots\ldots \qquad 3.18$$

where $\omega_\theta = \sqrt{\frac{K_\theta}{I_m}}$ rads/sec.

$\omega_v = \sqrt{\frac{k_v}{M}}$ rads/sec.

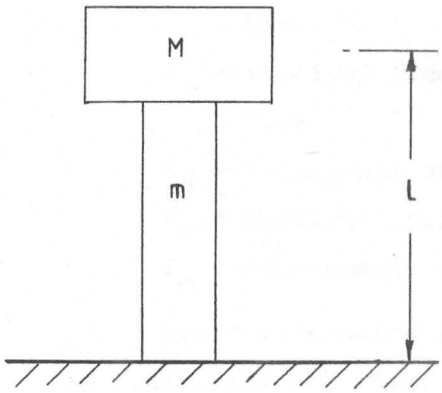

SIMPLE MODEL

Fig. 3·11

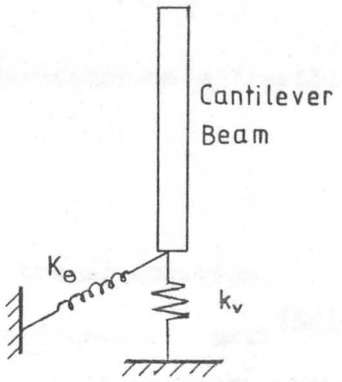

FLEXIBLE BASE

Fig. 3·12

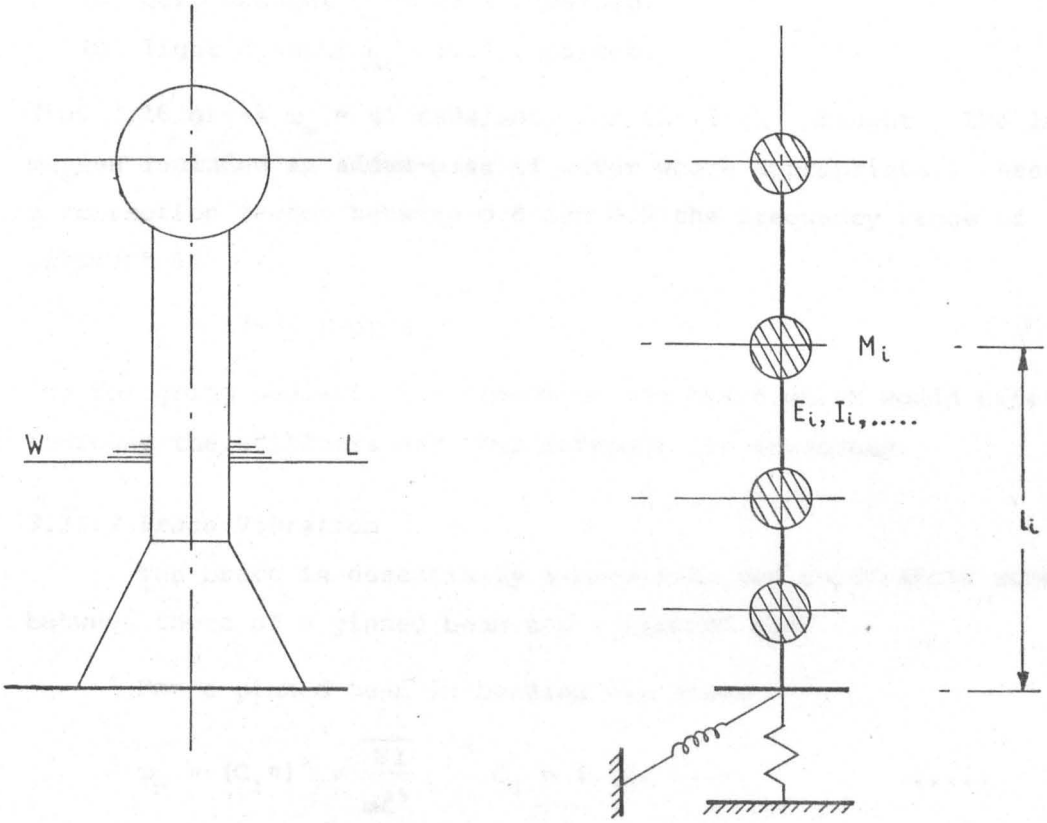

HULL & COLUMN MODELED AS LUMPED - MASS BEAM

Fig. 3·13

ω_θ = rotational frequency of a rigid structure on a flexible base

ω_v = vertical frequency of a rigid structure on a flexible base

K_θ = rotational stiffness of base

k_v = vertical stiffness of base

I_m = mass moment of inertia about centre of rotation.

The contribution from the vertical stiffness if small[58]. The rotational stiffness could be computed, but it has been shown[59] that the actual frequency can be as low as 0.6 times the fixed base frequency.

Eq. 3.17 was evaluated for a deep draught and a light draught condition on an Apple microcomputer giving the following fixed base natural frequencies:

(a) deep draught ω_∞ = 29.1 rads/sec.

(b) light draught ω_∞ = 37.8 rads/sec.

(Eq. 3.16 gives ω_∞ = 41 rads/sec. for the light draught. The lumped-masses included an added-mass of water where appropriate.) Assuming a correction factor between 0.6 and 0.9 the frequency range of interest is:

ω_e = 17-34 rads/sec.

The foregoing neglects the effect of the brace which would effectively increase the stiffness and thus increase the frequency.

3.11.2 Brace Vibration

The brace is essentially a beam with end constraints somewhere between those of a pinned beam and a clamped beam.

For a pinned beam in bending vibration

$$\omega_n = (C_1\pi)^2 \sqrt{\frac{EI}{m\ell^4}} \qquad C_1 = 1, 2, \ldots\ldots \qquad \ldots\ldots \qquad 3.19$$

and for a beam with both ends clamped

$$\omega_n = 2\pi C_2 \sqrt{\frac{EI}{m\ell^4}} \qquad C_2 = 3.56, 9.82, 19.2, \ldots\ldots \qquad 3.20$$

Evaluating Eqs. 3.19 and 3.20 (with added-mass included) gives the brace's lowest frequency range as

$$\omega_B = 8\text{-}18 \text{ rads/sec.}$$

3.11.3 Discussion

The error analysis of Ref. 58 shows that the frequencies calculated will always be lower than the true values. It is therefore apparent that the hull-column frequency and brace frequency will not coincide and further, the structure is not likely to resonate at wave frequencies although higher modes could still be excited by machinery.

It should be noted that increasing the plating thickness on the brace for instance only produces a small change in the lowest frequency. If k is some constant, then

$$\omega_n = k \sqrt{\frac{EI}{M\ell^3}} \qquad \ldots\ldots \qquad 3.21$$

where M = brace mass and added-mass

$= m\ell + am$

$= m\ell(1+k_2)$

and in this case $k_2 = 10$.

The plating makes the greatest contribution to the moment of inertia and for a double parabola

$$I = 0.267\, t_p c t^2 \qquad \ldots\ldots \qquad 3.22$$

where t_p = plating thickness

t = overall thickness

c = chord.

Then

$$\omega^* \simeq k \sqrt{\frac{EI\,\frac{t^*}{tp}}{m\ell(\frac{t^*}{tp} + k_2)\,\ell^3}} \qquad \ldots\ldots \qquad 3.23$$

where t^* = new plating thickness

$$\omega^* = \omega \sqrt{\frac{\frac{t^*}{tp}(1+k_2)}{\frac{t^*}{tp} + k_2}} \qquad \ldots\ldots \qquad 3.24$$

Therefore, if the plate thickness is doubled $\omega^* = 1.35\ \omega$ which is only a fairly small change for such a large change in thickness.

CHAPTER 4

CONSTRUCTION AND OPERATING COSTS

For a commercial operation the *raisôn d'etre* of any vessel, maybe as part of a larger system, is to make a profit, where

Profit = Revenue - Costs

This can be conveniently quantified for cargo ships by evaluating, for instance, the capital recovery factor or the profit per tonne of cargo deadweight. However, for a research vessel the concept of 'revenue' is virtually meaningless since the monetary value of the output or product cannot be assessed. Furthermore, it is not obvious how the 'output' varies with the 'input'.

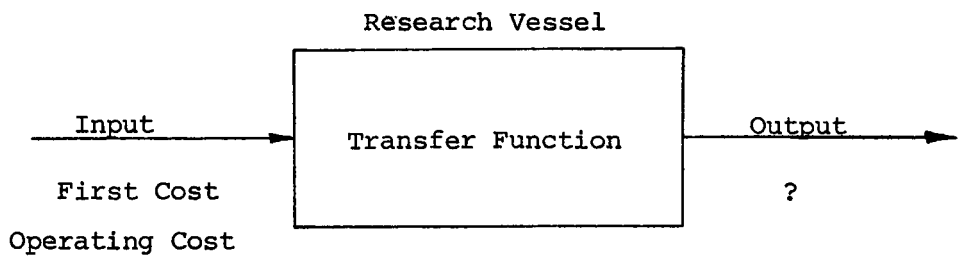

Fig. 4.1. Research Vessel as a Transfer Function.

4.1 Steelwork Cost

The preliminary steel drawings[31] and a derived component list, giving about 163t (net) of steel, were sent out (in March, 1979) for an initial costing to two shipyards, both of which were equipped with building docks in which this type of ship might be most efficiently constructed. The two shipbuilders quoted as follows on the basis of the information supplied:

Shipbuilder A - price at March, 1979: £385,000
ex works, ex VAT

Shipbuilder B - price at March, 1979: £169,170

The quotation of Shipbuilder B does not allow for 2.7t of aluminium, but otherwise they are for the same work and are equivalent to about £2400/t and £1050/t respectively. It will be seen that quotation A is over 100% greater than B. This was partly expected because the scantlings were much lighter than those normally used by A which, therefore, obliged them to do the work completely by hand rather than using their panel assembly line.

In general, the total steel cost will be greater than a conventional vessel. The actual increase should not be in direct proportion to the steelweight since in the SWATH ship, particularly in the deck-box, there are very few curved members, which means that the man-hours per tonne of steel will be reduced.

4.2 Machinery Cost

The required propulsion power is between 1½ and 2 times that of a conventional ship of similar length and speed. Therefore, on the basis of using two engines instead of one the first cost will approximately double. (The August, 1979 price for one 520 h.p. marine diesel with transmission was approximately £25,000.) On a comparison with a conventional vessel having similar laboratories and accommodation the powering difference will be reduced.

Other machinery costs will vary directly with the services supplied and can, therefore, be said to be the same as a conventional vessel, with the exception of items such as ballast pumps. It was thus expected that the machinery cost would not be significantly greater than for a conventional vessel.

4.3 Total First Cost

It was anticipated that the first cost of a SWATH vessel should be only slightly greater than the 'comparable' conventional ship. This increased cost is due to the greater steelweight and greater propulsion requirements apart from which the costs vary with

services, outfit provided, and the standard required. For instance, for a medium size ship it has been suggested[60] that the SWATH would only cost 10% more than an equivalent displacement monohull.

With the optimism generated it became imperative to obtain an accurate first cost. To enable this to be done a detailed specification incorporating all the desired design features was prepared. This was completed in October, 1980, and the following budget prices were obtained:

Shipbuilder B	£2,000,000
Shipbuilder C	£1,650,000

These prices were somewhat higher than anticipated. For 'cheap' limited role naval designs Brown and Andrew[61] suggest that the hull structure may be about 20% of the total ship cost, propulsion 23%, electric 22%, ship system 19%, and various smaller components. Obviously this will vary from case to case but it is reasonable to envisage the proportions being approximately the same (excluding weapons) for a SWATH research vessel as for a basic warship. The SWATH price will include a fabricated steel cost of about £200,000 (160t net at £1250/t), main engines (with gearboxes, propellers, associated equipment and Lloyd's requirements) at about £130,000 and computing equipment at £40,000, all suggesting a total ship cost of around £1 million.

Cost savings could be achieved by measures such as reducing the quantity of insulation and less stringent specification of lightweight items, although this may adversely affect the payload or stability. Similarly, reducing the number of watertight bulkheads would save the cost of the bulkhead itself and also reduce the outfit costs involved in providing watertight penetrations for cables, pipes, and ventilation.

4.4 Operating Costs

Any comparison of operating costs is difficult to make because of the scarcity of published data. However, some of the costs for a small 23m long wooden vessel, the *R.V. Calanus*, owned by the S.M.B.A. are available[62].

This data is plotted in Fig. 4.2 for two consecutive years. Although the absolute values are not directly relevant because of the difference in size, the age of the vessel, etc., it is noticeable that Salaries and Wages, excluding scientific and technical staff, account for well over 50% of the Total Running Costs, while Fuels and Oil amount to less than 10%.

If 10 scientific staff at a salary of, say, £10,000 per annum are notionally attached to the research vessel the running costs are more than doubled and the fuel becomes an even smaller percentage. Similarly, for an establishment such as Glasgow University, staff costs (excluding staff, librarians, etc.) were over 56% of the total expenditure of £41 million[63] while for a container ship in 1975[64] manning and fuel were 7.5% and 26.5% respectively of the ship operating cost. This merely illustrates that while fuel savings can considerably reduce the costs for a commercial operation the same is not necessarily the case for a research organisation if the true costs are considered.

Other operating costs include consumable items such as disposable coring barrels, Decca hire charges, etc. A disposable coring barrel may cost £40 and be used at the rate of one every 3 hours. The NERC fleet Decca hire charges are about £700 for 6 months and the *Discovery* alone has 27 chart folios for which the hire charges are about £800 per month. The port charges at Barry (NERC Research Vessel Base) are £150 per entry and departure, plus a further £50 for the pilot. In geological research the cost of 'mud' alone for a borehole can be over £12,000 (or £200/day) or more typically, £6000 per hole. These costs give some perspective to the situation but will not be further considered.

As previously mentioned there is no useable measure of the 'output' of a research vessel, but it is reasonable to assume that lower motions will raise this output thus increasing a notional 'research efficiency'. For instance, conventional vessel motions can be such that when using a box-sampler several 'casts' are required before an adequate sample is obtained. The lower motions of a SWATH could reduce this number thus increasing the 'research efficiency' from this point of view, as well as facilitating other onboard tasks such as chemical analysis as discussed in Chapter 1.

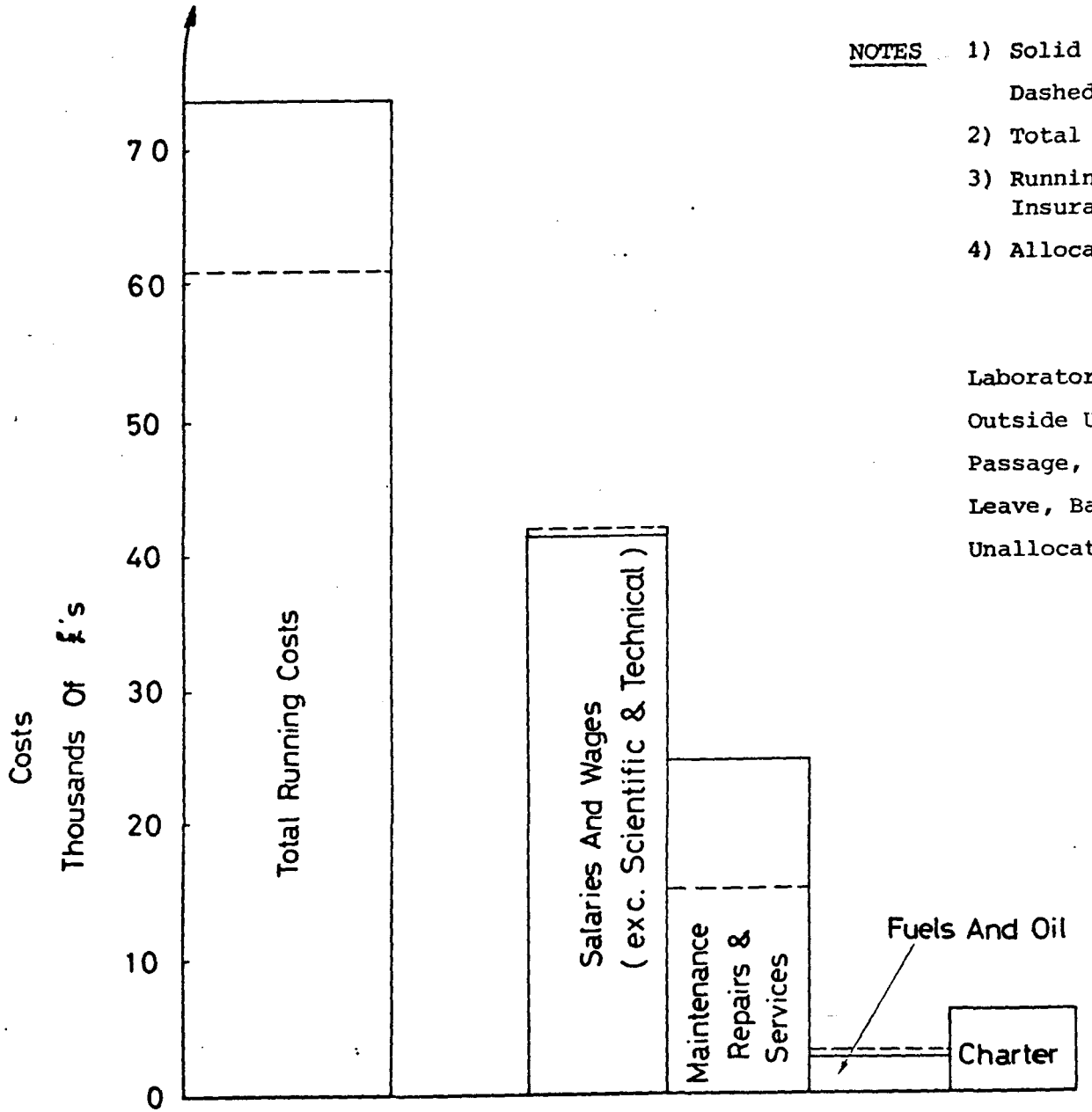

NOTES
1) Solid Lines - 1978-79
Dashed Lines - 1977-78
2) Total Crew = 7
3) Running Cost is exclusive of Overheads, Insurance, Port Charges, etc.
4) Allocation of Time (Days)

	1977-78	1978-79
Laboratory Research Projects	106	94
Outside Users	55	39
Passage, Refit, etc.	36	50
Leave, Bad Weather, etc.	168	-
Unallocated	-	57
	365	240

Fig. 4.2 Running Costs For R.V 'Calanus'

It was also mentioned in Chapter 1 that calm water resistance of SWATH ships may be 1.5-2.0 times that of a comparable monohull, although recent designs tend to reduce the difference[9]. In order to make a comparison, an annual fuel bill for the SWATH of £20,000 can be assumed from Fig. 4.2. (This makes generous allowance for increased utilisation of the vessel as well as higher resistance.) For the worst powering situation this represents an additional cost over the conventional vessel of £10,000. If the vessel is at sea with four scientists for 250 days then, using a rate of £100 per man day, this represents an investment of £100,000. Now if the research efficiency is 1/10 greater, due to fewer lost days and higher output, then the increased fuel cost is exactly offset. If the research efficiency is 1/5 greater then

$$\text{net annual saving} = 1/5 \times £100{,}000 - £10{,}000$$
$$= £10{,}000.$$

This annual saving can be reduced to its present worth as follows:

Years	Interest Rate %	SPWF*	Present Worth
5	15	3.353	£33,530
10	15	5.014	£50,140
15	15	5.852	£58,520
20	15	6.235	£62,350
25	15	6.468	£64,680

*Series Present Worth Factor

TABLE X. Present Worth of Annual Saving.

Thus it would seem that, in terms of this rough analysis, the increased operating cost could be justified in purely economic terms because of the assumed increase in research efficiency.

Furthermore, it should be remembered that the vessel is also intended to conduct certain engineering experiments which do not produce conclusive or reliable results in a normal test-tank, and such tank-time costs in the order of £500-£2,000 per day.

4.5 Comparison with Charter

This thesis is not particularly concerned with economics but it is, nevertheless, interesting to include the data on charter rates that has been gathered.

On a large drill-ship the basic charter rate could be £10,000/day, with a further £1000/day for mud. Data for another two vessels that have been used for research are as follows:

(a) *M.V. Whitethorn* (1500t)

Basic charter rate	:	£2,300/day
Extras (approx.)	:	£ 500/day
Average working fuel consumption	:	3.5t/day @ £140-£200/t

(b) *M.V. Sperus* (1000t)

Average total rate	:	£2000/day
(inclusive of most items except scientific personnel and user-supplied equipment)		

The above are larger than the proposed vessel. The basic charter rate for an antiquated 30m LOA vessel for a 12 hour day with a 4 man crew, but exclusive of fuel, lubricating oil, and charterers food was £325/day at December, 1979 prices. On a long-term charter this rate would be less but even so, allowing for inflation to 1981 prices, a total bill of £1 million could still accumulate in about 10 years of 250 operating days.

In view of this data the first cost is not too unreasonable, while as shown in Section 4.4 the increased operating costs should be directly offset by higher research efficiency.

CHAPTER 5

RESISTANCE AND PROPULSION

This chapter is devoted to the resistance and propulsion characteristics of the three-hulled SWATH. Some of the contents were completed as part of the general design work in Chapter 3, but other parts such as the high-speed tests, flow visualisation, and wave resistance calculations are of wider interest.

5.1 Model and Experiment

A model was constructed in which the length over the columns was adjustable, Fig. 5.1, and which had a removable streamline brace (or fin) between the two aft columns, Fig. 5.2. It was tested in the towing tank (76m × 4.6m × 2.4m) by towing from the leading edge of the aft columns just clear of the still-waterline using the standard ship resistance dynamometer in which the model is generally free to sink and trim, Fig. 5.3. The towing point was thus close to both the LCG and VCG. Two sets of tests were conducted with several different conditions, Table XI, the first of which were primarily to determine the propulsion requirements. The second set investigated some uncertainties associated with the hull-endings and also the effect of column separation and included speeds up to the onset of vertical-plane instability which was significantly higher than the proposed design speed. As part of the investigation into the hull-endings, experiments were conducted in an air flow-visualisation tunnel.

5.2 Results

The results from the first set of experiments, Conditions R1 and R2, together with the low and medium speed results from the second set are given in Fig. 5.4 to a base of model speed and chord Froude number. (A blockage correction was not made because the use of conventional formula suggested that it was negligible, see Appendix C.) For Condition R1 the trim was quite noticeable (see

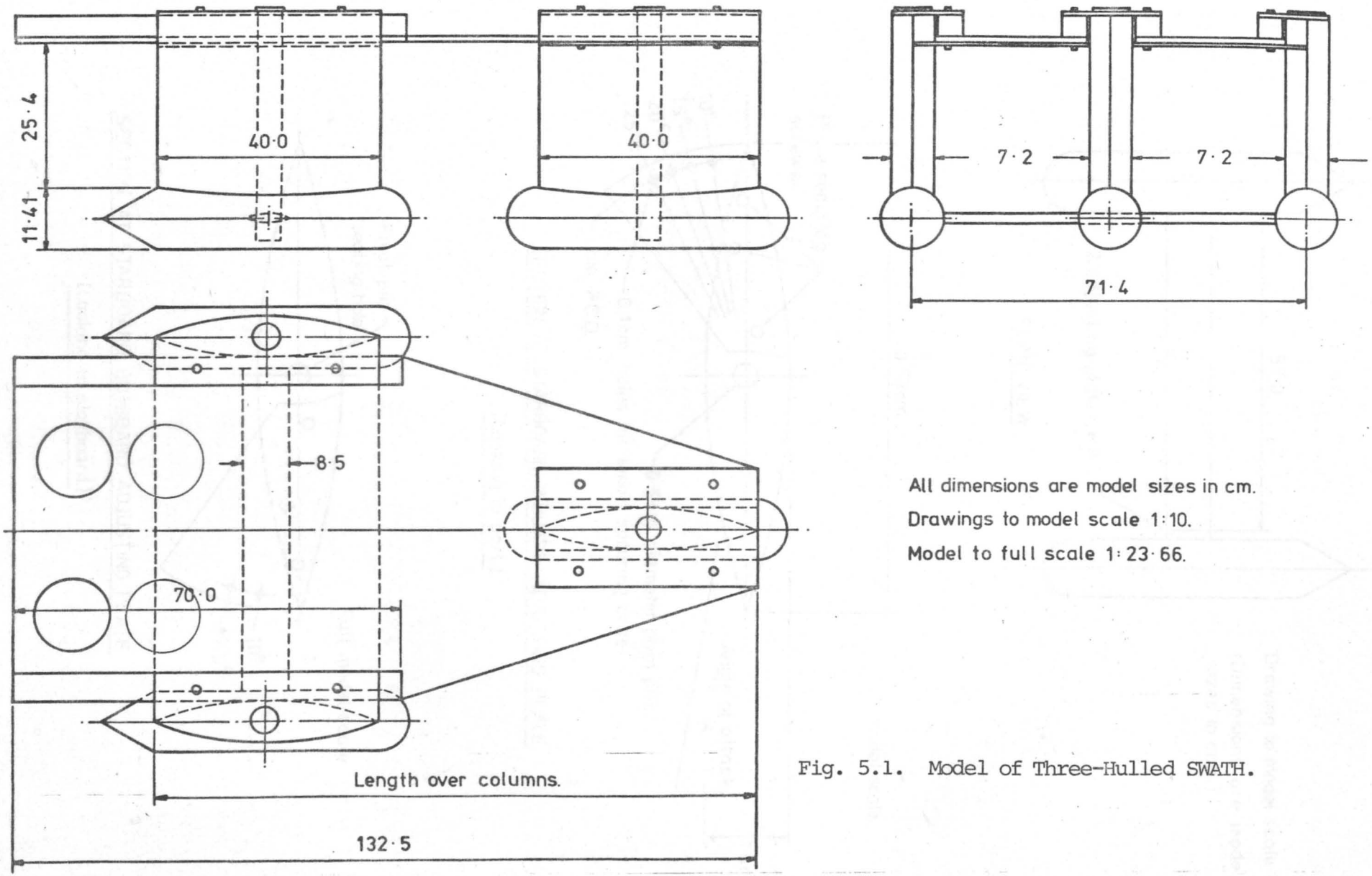

All dimensions are model sizes in cm.
Drawings to model scale 1:10.
Model to full scale 1:23·66.

Fig. 5.1. Model of Three-Hulled SWATH.

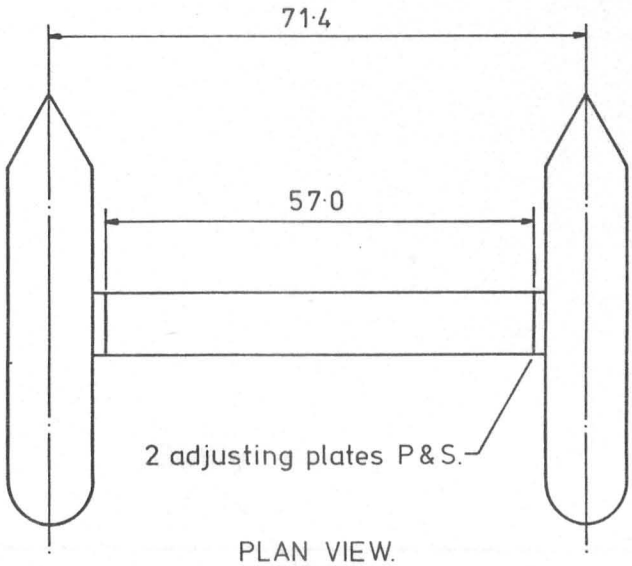

PLAN VIEW.

Drawing to model scale 1:10

(Dimensions are model sizes in cms.)

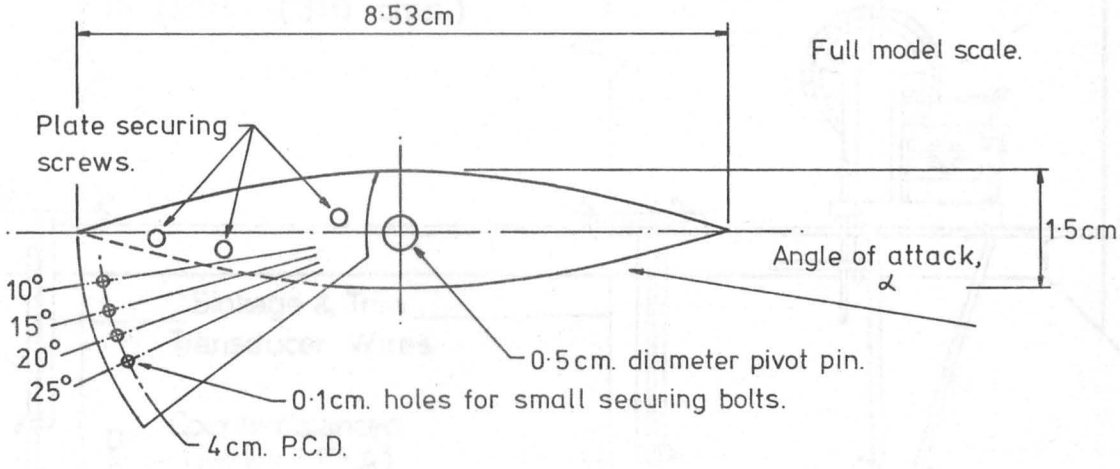

SECTION AT STARBOARD INBOARD ADJUSTING PLATE.

(Looking to port.)

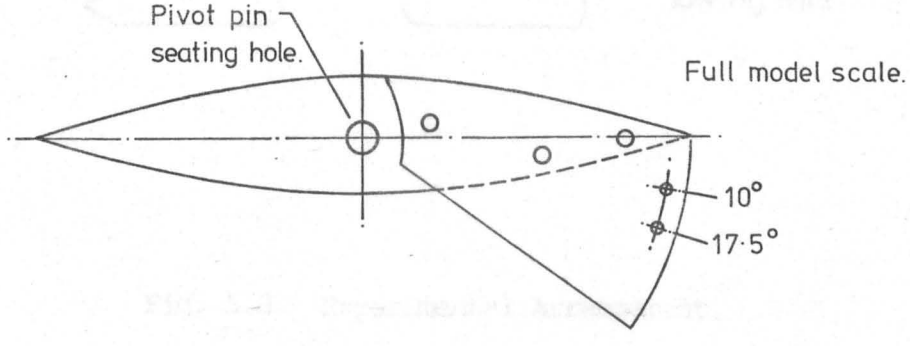

SECTION AT STARBOARD OUTBOARD ADJUSTING PLATE.

(Looking to starboard.)

THREE HULLED SEMI-SUBMERSIBLE SHIP, FIN & ADJUSTING MECHANISM

FIG. 5·2

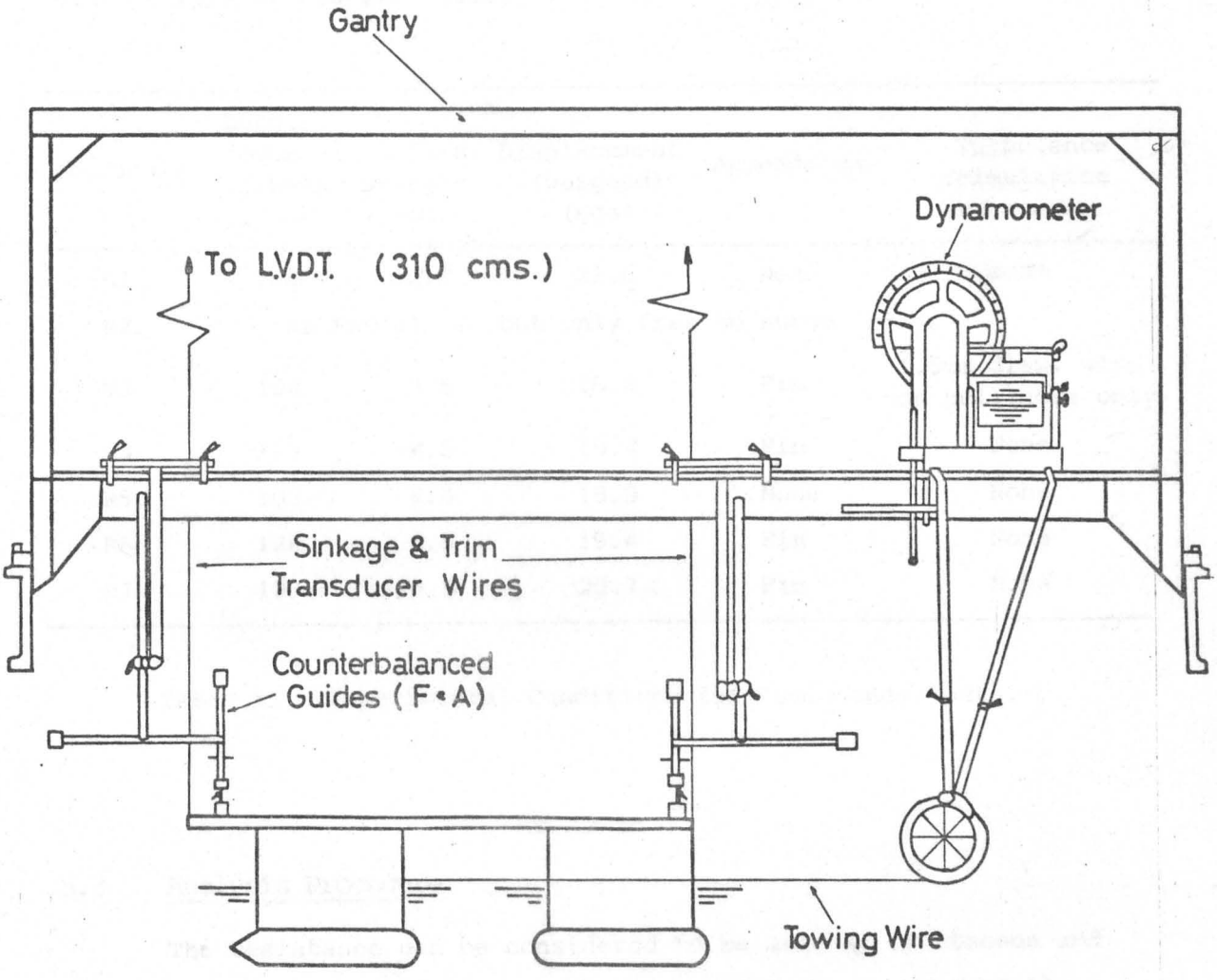

Fig. 5.3. Experimental Arrangement.

Section 5.6), therefore to try and ensure that reliable results were being obtained the towing apparatus was modified in such a way that trim was prevented and sinkage limited, giving Condition R2. While the fact that no appreciable difference can be seen between R1 and R2 gives confidence in the results it does not entirely confirm their reliability since it is possible that both towing arrangements introduced errors of the same size.

Condition	Length over Columns (cm)	Column Draught (cm)	Displacement (weighed) (kgs)	Appendages	Turbulence Stimulation
R1	108	12.7	21.6	None	None
R2	As for R1 - but only free to surge				
R3	108	8.5	19.4	Fin	1.5mm diam. wire on hull nose only
R4	108	8.5	19.4	Fin	None
R5	108	8.4	18.9	None	None
R6	128	8.5	19.4	Fin	None
R7	103	10.8	20.7	Fin	None

TABLE XI. Experimental Conditions for Resistance Tests.

5.3 Analysis Procedure

The resistance can be considered to be made up of viscous and residuary components where the residuary resistance is essentially wave-making (but also spray drag at higher speeds) and the viscous or profile resistance consists of frictional and form sub-components. It is common practice to relate these last two sub-components by a form factor which is assumed to be constant over the speed range. However, for this model such an approach is inappropriate because the drag of the rather blunt endings is strongly dependent on Reynolds number (R_n). (Such scale effects have also been investigated for full-form ships[65].) Furthermore, it is uncertain what

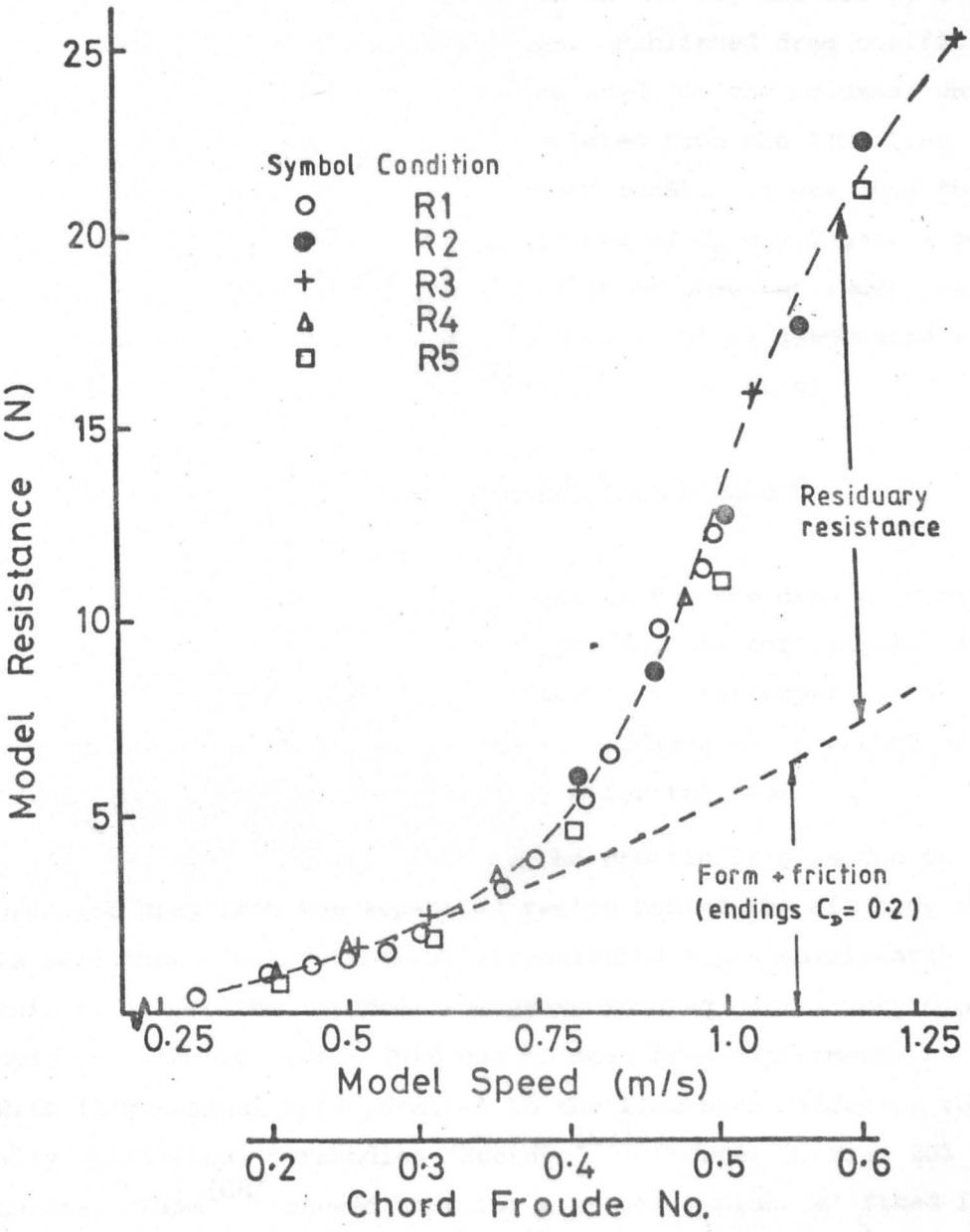

Fig. 5.4. Model Resistance Results.

value to use for the endings drag coefficient. The other viscous sub-components were therefore calculated in the way set out by Grekoussis and Miller[66] for semi-submersibles. Published drag coefficients (Hoerner[67] Chapter 6, Fig. 2) were used for the columns, while the hull frictional resistance was calculated from the ITTC line (which is slightly higher than the Schoenherr line). It was thus found that a value for the endings drag coefficient of $C_D = 0.2$ gave a good fit to the low-speed data. This appears to be somewhat lower than previous recommendations[66]. The uncertainties associated with the hull-endings are discussed in the following section.

5.4 Hull-Ending Profile Drag, Flow Visualisation and Turbulence Stimulation

A large collection of data exists for the drag of bodies of revolution such as spheres and ellipsoids, see for example Ref. 67. However, this is not directly applicable to the experimental analysis, particularly at low Reynolds numbers, because the presence of the cylindrical hulls can significantly alter the flow.

The greatest proportion of the profile drag is due to the pressure drag from the separated region behind the aft body and it is well-known that sufficient streamlining can significantly reduce this drag. On the forebody the pressure drag can be very close to zero or even negative. This can be seen from experiments on cylinders with longitudinal axis parallel to the flow with different rotationally symmetrical forebodies (Hoerner[67] Chapter 3, Fig. 20) and from theory. Zahm[68] showed that for a sphere radius 'a' fixed in a uniform stream of inviscid fluid that the zonal pressure drag was given by

$$D = \int p \, dydz = \pi a^2 \sin^2\phi \, (1-\tfrac{9}{8} \sin^2\phi) \, p_n \qquad \ldots\ldots \qquad 5.1$$

for a nose cap whose polar angle is ϕ, where p_n is the stagnation or nose pressure and a zone is that part of the sphere's surface bounded by two planes normal to the direction of flow. Evaluation of this expression for $\phi = \pi/2$ gives

$$D/p_n = - 0.39 \, a^2 \qquad \ldots\ldots \qquad 5.2$$

The negative sign indicates that the 'drag' is upstream on the front half. (Equally it is downstream on the rear half thus giving a

resultant of zero drag in an inviscid fluid; d'Alembert's paradox.) For the real case the flow over the forebody, especially above the critical R_n is similar to that in inviscid fluid but at the afterbody there can be a large region of separated flow.

Flow-visualisation experiments in an air tunnel illustrated the separated region around the blunt stern endings but showed attached flow for longer endings, Fig. 5.5, as already discussed in Section 2.1. (The streak-lines were obtained by injecting smoke into the tunnel through several nozzles and illuminating this with a sheet laser-beam, hence obtaining an essentially two-dimensional view of the flow. The results were originally photographed but the exposure time in relation to the air speed was such that the photographs were poor quality and are therefore reproduced here as sketches.)

These experiments also showed that a separation bubble occurred at trim angles ('angle of attack') of around 5°. The Reynolds number, using hull diameter, was $R_n \simeq 2 \times 10^4$ which for a sphere is sub-critical and the same order of magnitude as in the resistance experiments. The usual flow patterns around cylinders perpendicular to the flow exhibit a similar separation on the forebody at sub-critical Reynolds numbers, but at post-critical Reynolds numbers this occurs on the afterbody. Thus the separation bubble would not be expected in the full-scale.

Further to the above while elliptical noses might appear to give a lower profile drag on the model scale this probably would not be significant on the full-scale because of this Reynolds number effect. This is partly why Lang used hemispherical ends on the *Kaimalino*[24]. He also suggested they would be cheaper which may be true for the 6" thick acryllic domes he used but is not necessarily true for steel endings which could be constructed piecewise. Nor do hemispheres necessarily give the lowest wave resistance.

Because of the cylindrical hull the flow becomes reattached after separating on the forebody, thus forming the bubble, and downstream of this point the boundary layer will be turbulent, even without stimulators, thus justifying the use of a turbulent friction line.

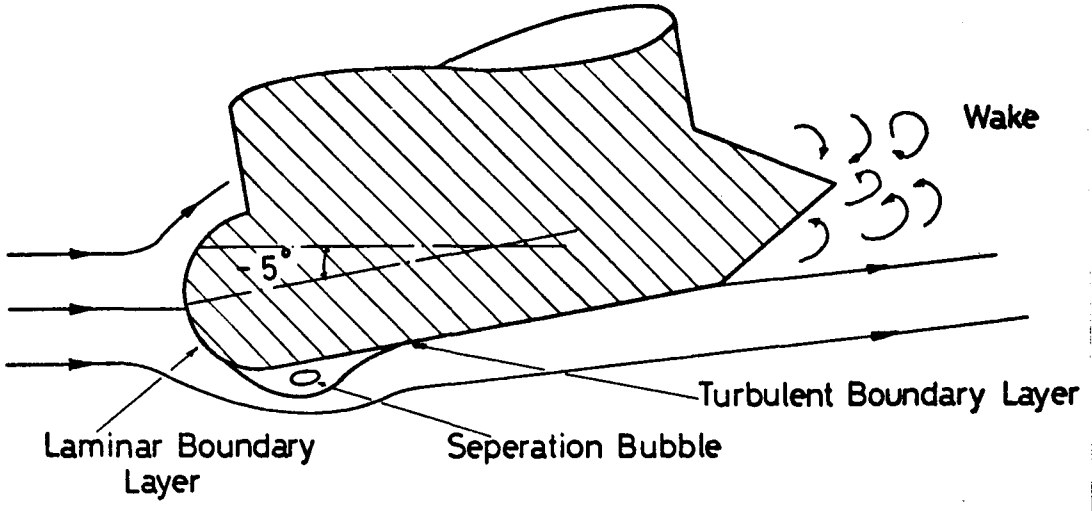

(a) Hemispherical Nose And Blunt Aft Ending

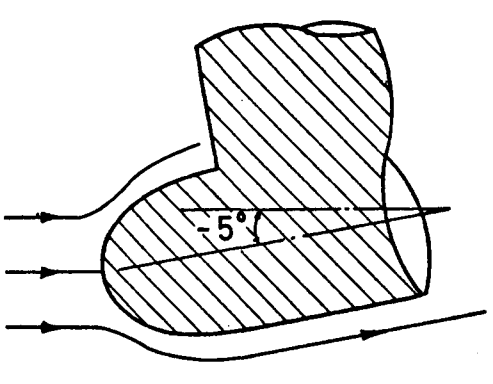

(b) Ellipsoidal Nose
(Half Length = 1.7 × Radius)

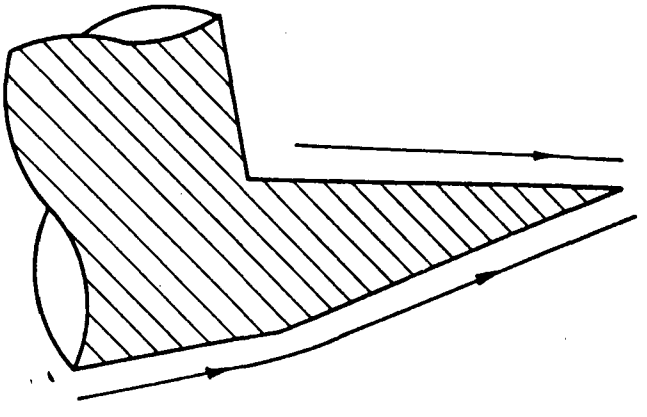

(c) Extended Tail Cone
(2.5 Diameters Long)

These sketches were made from photographs with speed of flow such that Rn ≃ 2×10^4 based on hull diameter.

Fig. 5.5. Flow Past a SWATH Hull/Column.

To try and model the full-scale flow, turbulence stimulators were fitted on the hull noses. These consisted of a ring of 1.5mm diameter wire at a polar angle of 45°, (see Fig. 5.6). This is Condition R3 in Fig. 5.3.

To obtain turbulent flow it is necessary for the local roughness Reynolds number ($R_d = u_d d/\nu$) to exceed a critical value, (u_d is the local boundary layer velocity at stimulator diameter, d, for wires). Fages Criterion[69] is often used, i.e. critical $R_d = 400$ but later work by Preston[70] suggested a value of 600. Other authors such as Tani[71] suggest a critical R_d between 600 and 830, but in recent work by McCarthy et al.[72] the value of 600 is endorsed and that is therefore taken here.

For a flat plate the velocity in a laminar boundary layer can be approximated with considerable accuracy by the well-known and simply applied Pohlhausen expression, i.e.

$$\frac{u}{U_\infty} = 2(y/\delta) - 2(y/\delta)^3 + (y/\delta)^4 \qquad \ldots\ldots \qquad 5.3$$

For the spherical forebody this is not particularly appropriate but we can, however, use a similar expression for the ideal potential velocity distribution from Schlichting[73]

$$\frac{u}{U_\infty} = \tfrac{3}{2}\left(\frac{x}{R}\right) f_1' - \tfrac{1}{2}\left(\frac{x}{R}\right)^3 (g_3' + h_3') + \frac{8}{30}\left(\frac{x}{R}\right)^5 (g_5' + h_5' + \frac{10}{3}(k_5' + j_5' + q_5')) \qquad \ldots\ldots \qquad 5.4$$

The coefficients are the functional coefficients of the Blasius series and are tabulated against η in Ref. 73, where

$$\eta = \frac{Y}{R}\sqrt{\frac{U_\infty R}{\nu}} \qquad \ldots\ldots \qquad 5.5$$

This has been evaluated for the case of $\phi = 45°$ and is shown in Fig. 5.6. With the 1.5mm diameter trip wire for the critical $R_d = 600$ a speed of $u_d = 0.45$ m/s is required and from Fig. 5.6 this is reached when the free stream velocity is about 0.4 m/s.

Conventionally when using turbulence stimulators it is usual to assume that the deficit in resistance due to laminar flow on the leading edge is offset by the trip self-drag. The self-drag of the

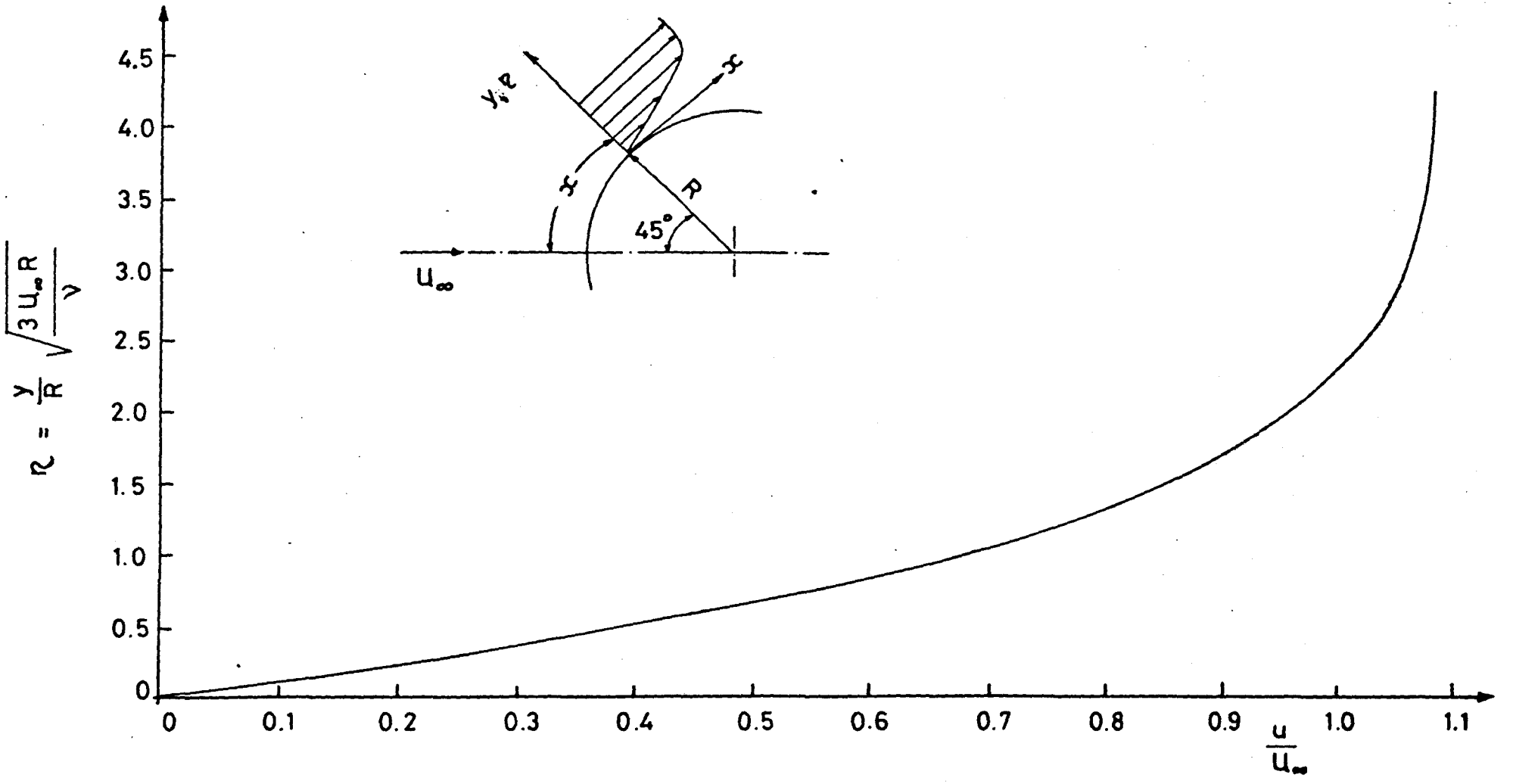

Fig. 5.6. Velocity Distribution around Sphere, $\phi = 45°$.

trip in the direction of the free stream velocity can be found from an equation with the general form

$$R_t = \tfrac{1}{2} \rho C_{Dt} A_{pr} V^2 \sin\phi \quad \ldots\ldots \quad 5.6$$

Hughes and Allan[74] present experimental drag coefficients as a function of Reynolds number. For the velocity they use the root mean square value within the laminar boundary layer (estimated from flat plate theory) up to the thickness of the diameter of the wire. However, McCarthy et al. recommend the simpler procedure of using a constant value of drag coefficient of $C_{Dt} = 0.75$ together with the velocity in the laminar boundary layer at the height of the trip wire diameter. This procedure was used herein and it was calculated that the model resistance results should be reduced by around 2% at speeds less than 1 m/s. This was done before plotting Condition R3 onto Fig. 5.4. Condition R4 is the same without the trip-wires. The whole exercise is rather inconclusive in a numerate sense but it can, however, easily be concluded that for these resistance experiments it is desirable to have the model sufficiently large for the endings Reynolds number to be above the critical value.

The concept of the virtual origin of turbulence has been discussed[71] and could be quite important when the drag of the trip-wires is large. It seems to be straightforward to use for a slender ship, but when the curvature is large as on a spherical ending, it is unclear how this should be positioned. For this case the effect of the virtual origin seemed to be negligible.

5.5 Viscous Resistance Interference Effects

In the case of tandem circular cylinders interference is a very important effect[66] but for streamlined columns with realistic separation ratios it is unimportant as far as viscous resistance is concerned[67]. Viscous interference effects between widely spaced parallel streamlined columns will also be negligible.

The case of column-hull interference is similar to wing-body interference and to wing-tip tanks in aerodynamics. The hull tends to act as an end-plane or ground-board causing the flow over the column

to be largely two-dimensional, thus justifying the use of two-dimensional drag coefficients. The presence of columns over the hull will reduce the hull wetted surface but if the total surface area for a cylinder is used then the parasitic interference drag, which will occur in the angles between the columns and the hulls, is at least acknowledged.

5.6 Sinkage and Trim

The sinkage and trim results from Condition R1 are given in Fig. 5.7. By equating the moment of the resistance components and towing force to the hydrostatic restoring moment the trim angle due to the towing arrangement was calculated and found to be directly responsible for around 50% of the total trim angle. Similarly, it must also have effected the sinkage. For a self-propelled model, or for the full-scale ship, this moment would be in the opposite direction. In addition, as mentioned in a previous section, any effects from separation near the bow would probably not be present for the full-scale. It is not therefore appropriate to use such results either to scale directly to full-size or to compare with theoretical or semi-empirical calculations. (A theoretical approach has been developed in Ref. 39.)

5.7 Full-Scale Powering

To obtain the full-scale powering estimate the residual resistance was extrapolated in the usual manner. For the viscous resistance a full-scale endings drag coefficient of less than $C_D = 0.1$ should be obtainable but here the values of $C_D = 0.1$ and 0.2 were used. A resistance augment of 8% was allowed and quasi-propulsive coefficients of 0.7 and 0.75, thus corresponding to an overall propulsion coefficient between 0.65 and 0.7 as determined by Yeh and Neal[75]. These calculations, Fig. 5.8, show that for a ship speed of 9 knots two engines of around 500 bhp should be required.

In addition to the conservative calculation of endings viscous drag, it will be shown later that the wave-making resistance could also be decreased, thus decreasing the required engine power. Other uncertainties include the change of wetted surface with speed.

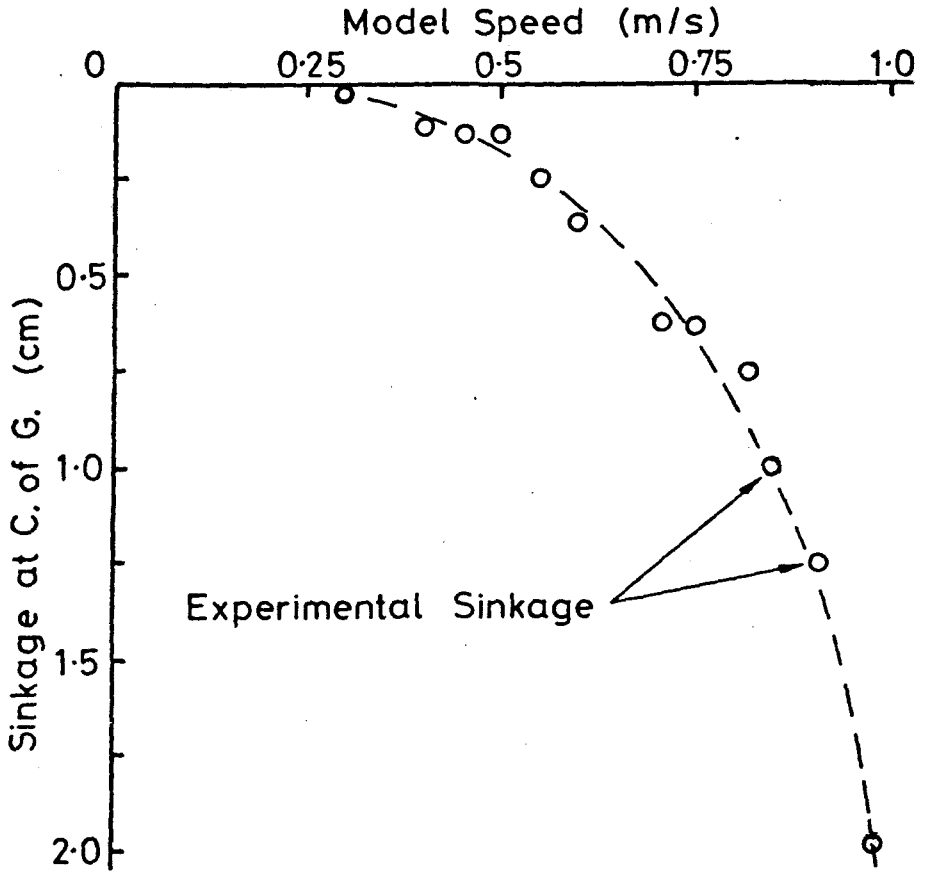

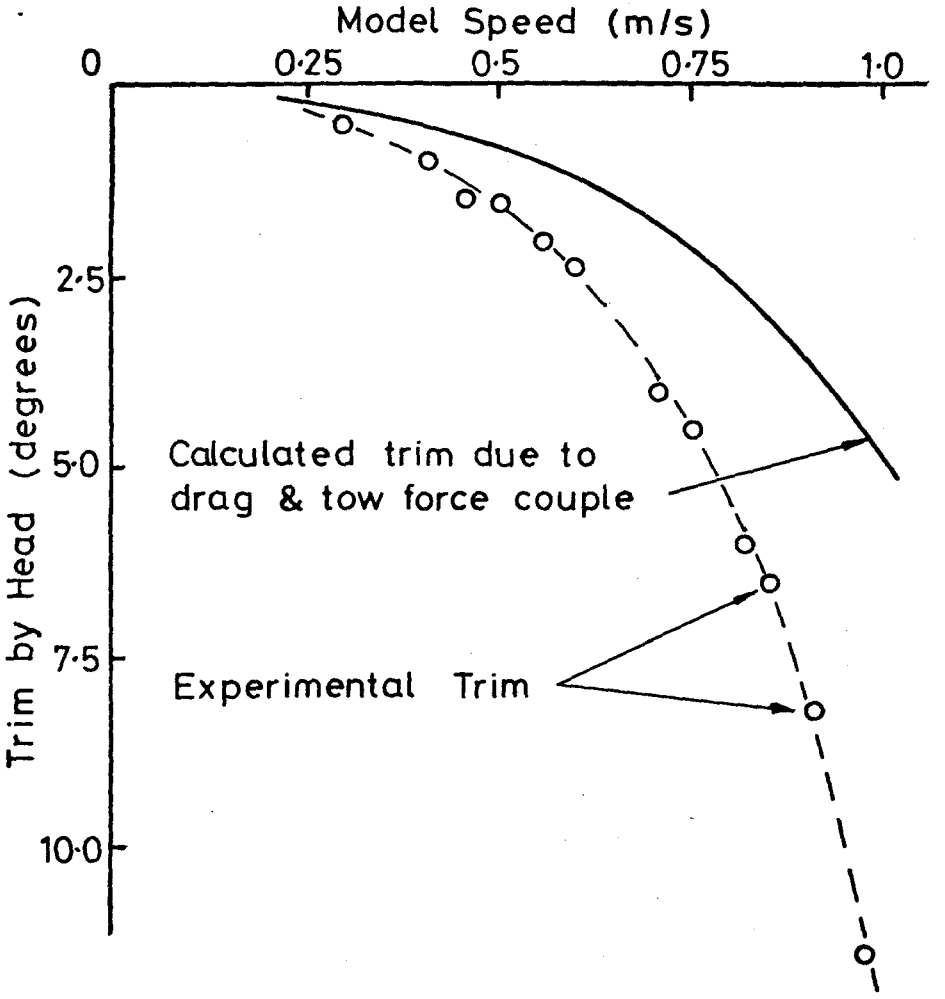

Fig. 5.7. Sinkage and Trim (Condition 1).

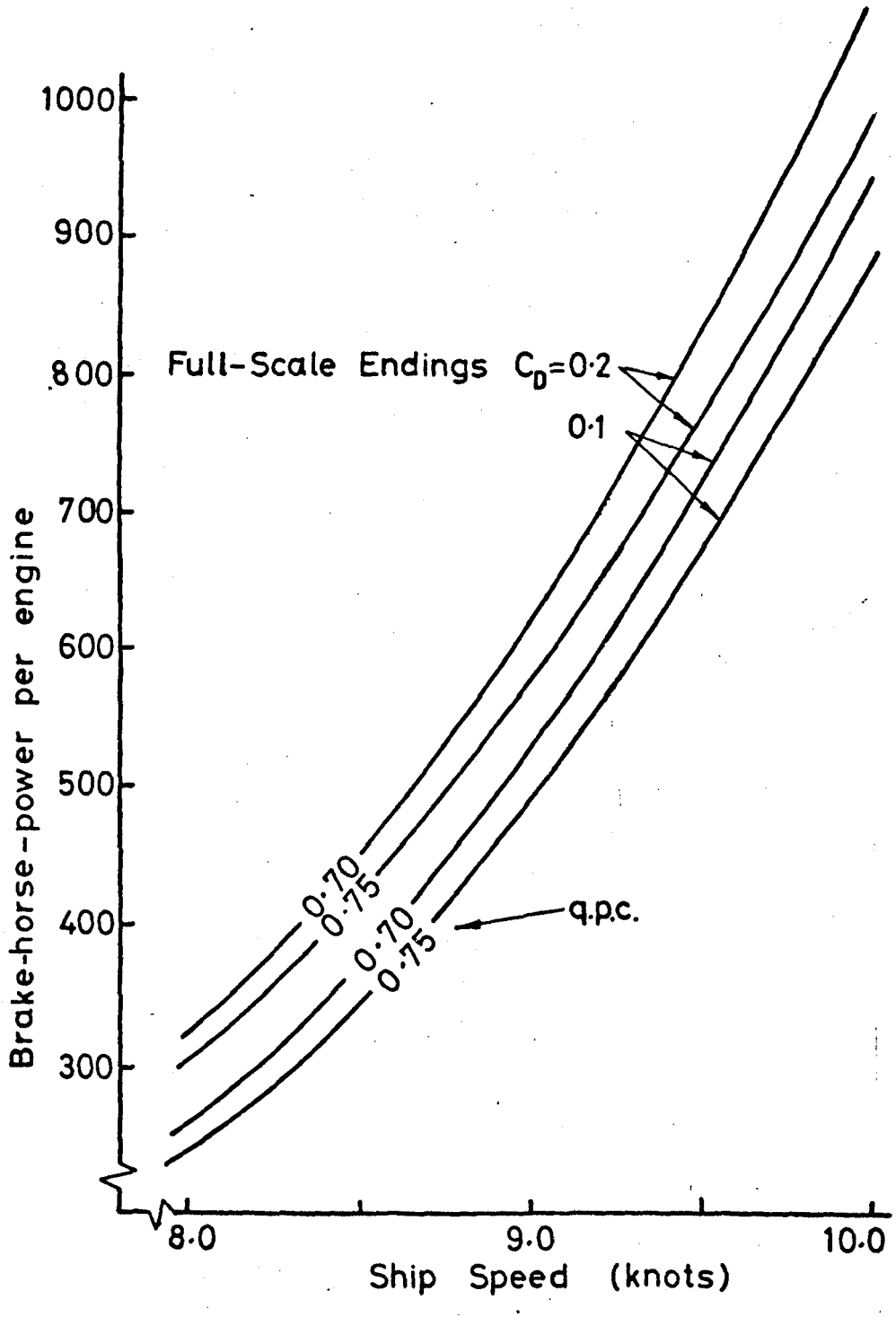

Fig. 5.8. Full-Scale Powering Estimate.

5.8 Higher Speed Tests

These tests were conducted for several variations in column-spacing, draught, and appendages as in Table XI. The results, Fig. 5.9, illustrate the expected peak and trough[36,76] in the resistance curve between a chord Froude number of $F_n = 0.6 - 0.7$ depending to a certain extent on the column separation.

For Condition R3 the speed was increased until the onset of vertical plane instability[40], characterised by a porpoising motion. At these higher speeds well-developed spray-sheets were present[77], and in the absence of any spray rails or discontinuities on the outside of the model, the sheet extended several centimetres above deck-level.

Condition R5 has no transverse fin and shows a remarkably lower resistance above $F_n = 0.8$. It can be speculated that this is not only due to resistance of the fin in isolation, but the effect it has, combined with the towing arrangement, on the model attitude.

Condition R7, at a deeper draught, and small separation, has a high resistance at the first peak followed by a correspondingly deeper trough.

5.9 Wave Resistance

A SWATH ship may be very slender, and Chapman[36] has shown that this combined with the relatively simple shapes which can be defined analytically allows the wave resistance to be calculated by a comparatively straightforward method. The basic method was adapted to make it suitable for the three-hull configuration. A complete description of the theory is given in Appendix D but an outline is useful at this point.

As shown by Lunde[78] the wave-making resistance of a source distribution $\sigma(x,y,z)$ with the linearised free-surface condition is given by

$$R = 16\pi\rho K^2 \int_0^\infty (I^2 + J^2) \cosh^2 u \, du \qquad \ldots\ldots \quad 5.7$$

where K is the wave number, and

$$I + iJ = \iint \sigma\{\exp iK(x \cosh u + y \sinh u \cosh u) + Kz \cosh^2 u\} \, dS \qquad \ldots\ldots \quad 5.8$$

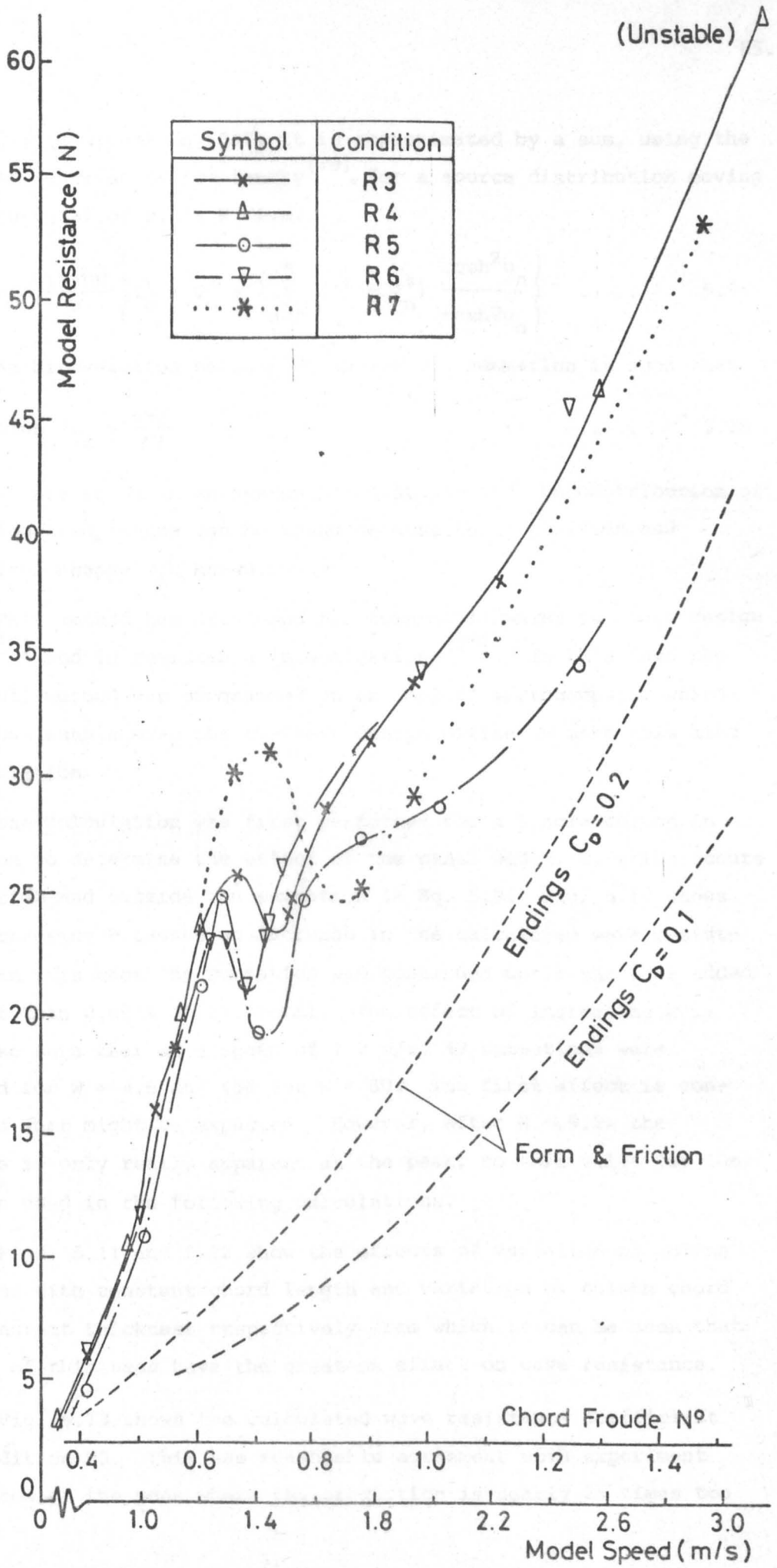

Fig. 5.9. Higher Speed Resistance Results.

In order to evaluate Eq. 5.7, it is approximated by a sum, using the expression derived by Srettensky[79] for a source distribution moving in a deep canal of width W, i.e.

$$R = \frac{16\pi^2\rho K}{W}\left\{I_o^2 + J_o^2 + 2\sum_{n=1}^{\infty}(I_n^2 + J_n^2)\frac{\cosh^2 u_n}{\cosh 2u_n}\right\} \quad \ldots\ldots \quad 5.9$$

which can be evaluated because u_n inside the summation is such that

$$\sinh 2u_n = \frac{4\pi n}{KW} \quad \ldots\ldots \quad 5.10$$

I_n and J_n are an infinite system of constants and the contribution of the various components can be found because their position and geometrical shapes are known.

This method has been used for twin-hull SWATHs in other design studies[6] and in resistance investigations[80]. In this case the three-hull method was programmed on an 'Apple' microcomputer which would thus enable even the smallest design office to make this kind of calculation.

The calculation was first performed for a single column in isolation to determine the effect of the canal width, W, which occurs both inside and outside the summation in Eq. 5.9. Fig. 5.10 shows that increasing W causes an increase in the calculated wave resistance. In this case the summation was continued until the term added was less than 0.001% of the total. The effect of increasing W is then also such that at a speed of 1.2 m/s, 49 summations were required for W = 4.6 and 458 for W = 50. The first effect is contrary to what might be expected. However, after W = 9.2m the increase is only really apparent at the peak, so this value (or 10m) has been used in the following calculations.

Figs. 5.11 and 5.12 show the effects of variation of column thickness with constant chord length and variation of column chord with constant thickness respectively from which it can be seen that changes of thickness have the greatest effect on wave resistance.

Fig. 5.13 shows the calculated wave resistance coefficient for Condition R5. This has reasonable agreement with experiment apart from at the peak where the prediction is nearly 2½ times too

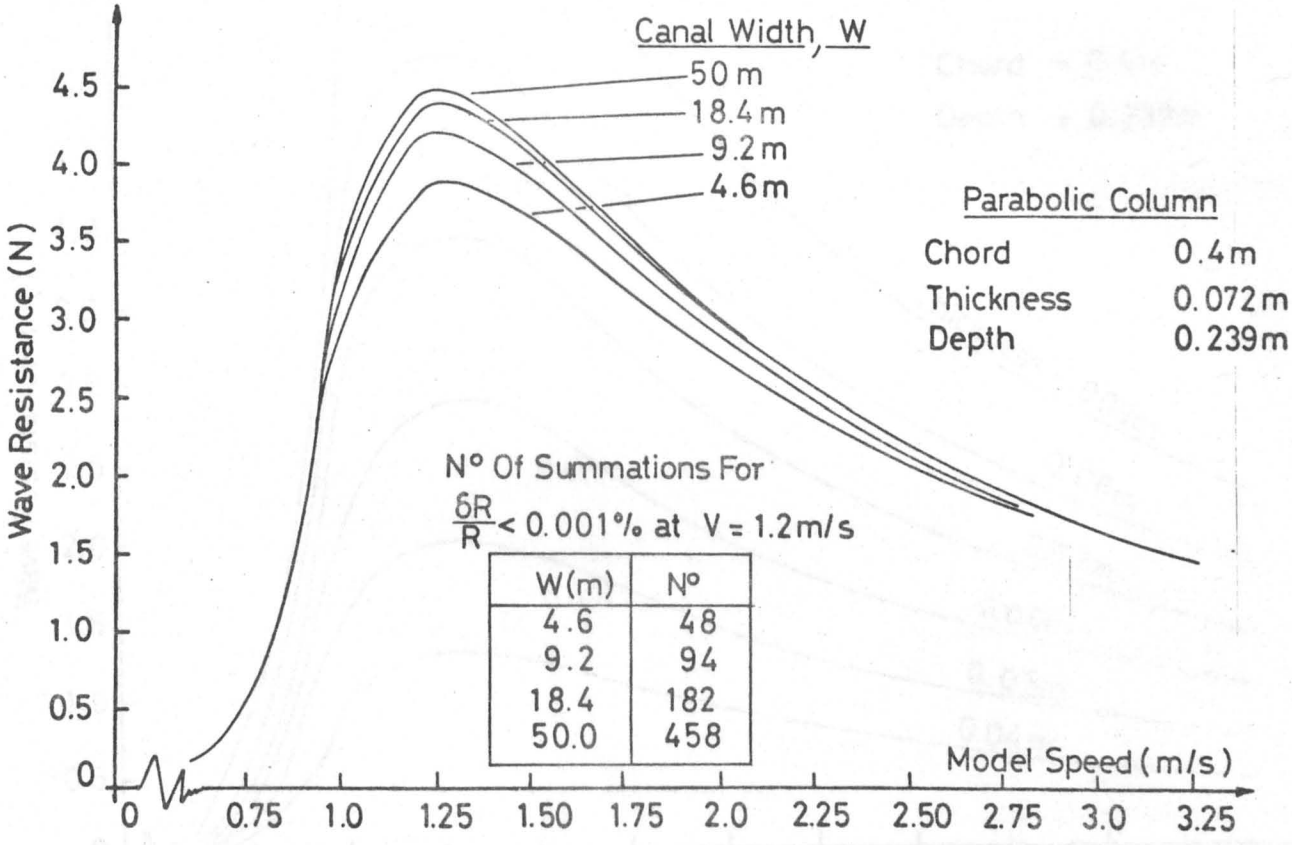

Fig. 5.10. Effect of Canal Width on Calculated Column Wave Resistance.

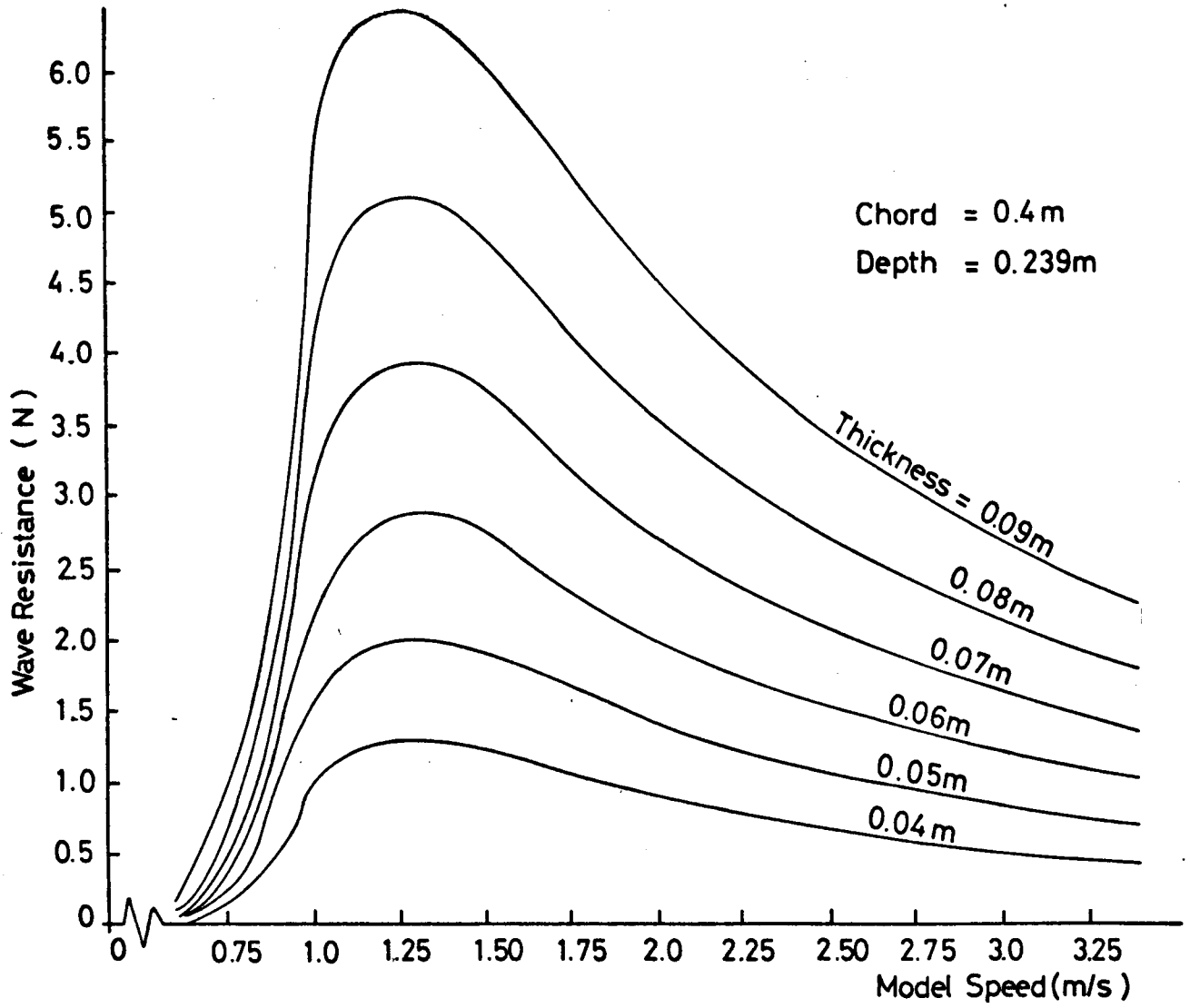

Fig. 5.11. Effect of Column Thickness on Calculated Wave Resistance.

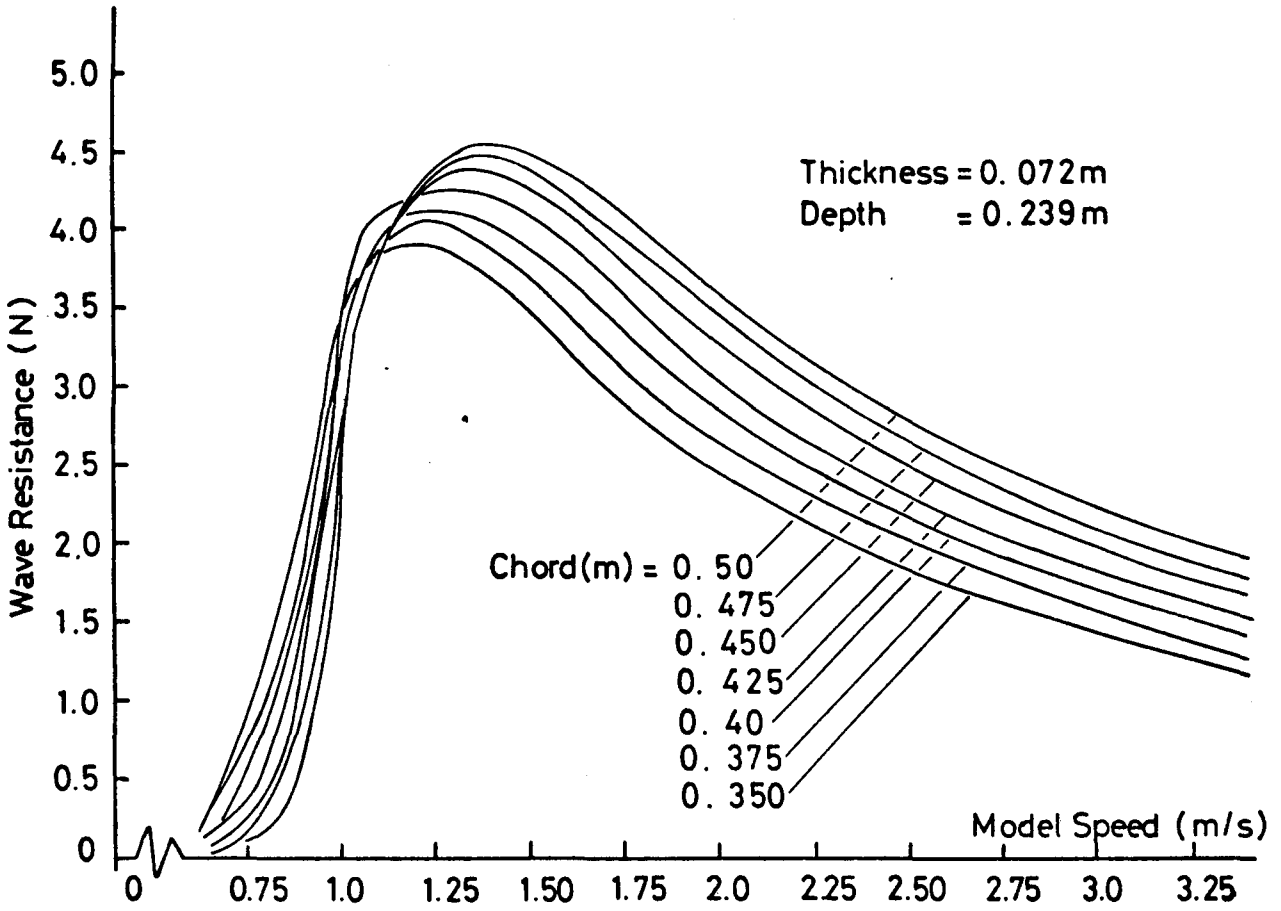

Fig. 5.12. Effect of Column Chord on Calculated Wave Resistance.

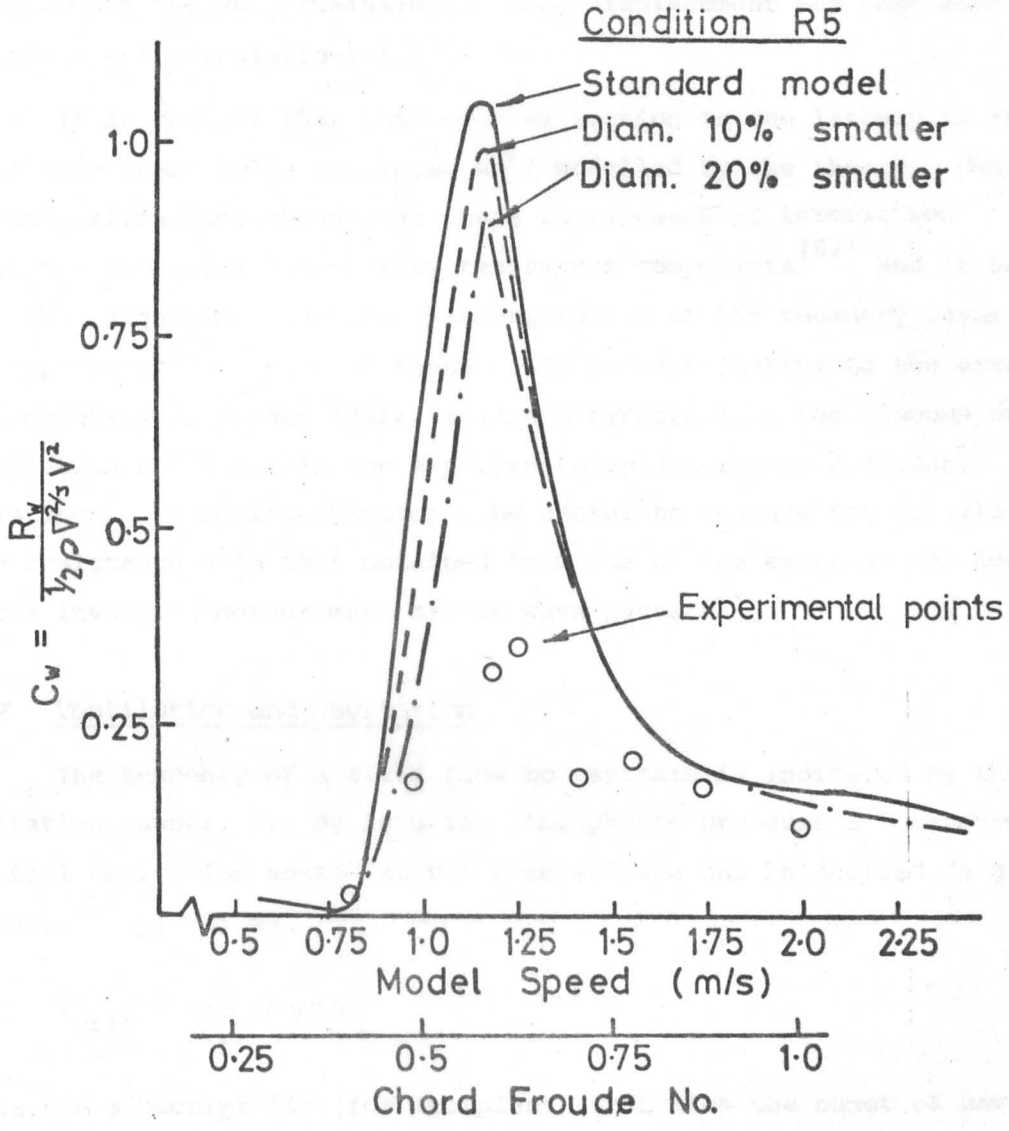

Fig. 5.13. Effect of Hull Diameter on Calculated Wave Resistance for Condition R5.

large even when a factor of 0.6, such as used by Inui[81] was applied to the contribution of the stern endings. This graph also shows that adoption of more slender forward hulls, for instance, could reduce the wave resistance. (The displacement was kept constant for the calculations.)

It is thought that this over-estimation is due largely to the relatively short hulls not being well modelled by the theory. Other investigations have shown that there is evidence of interaction between viscous and wave-making resistance components[82] and it has also been suggested that the characteristics of the boundary layer are important[83]. Both of these could be contributing to the error. As previously discussed there is some uncertainty in the viscous drag calculation and hence in the experimentally determined residuary resistance. It would, therefore, be useful to compare the calculated wave resistance with that obtained from one of the experimental techniques involving measurement of the wave pattern.

5.10 Ventilation and Cavitation

The tendency of a fluid flow to cavitate is indicated by the cavitation number, σ. By ignoring atmospheric pressure a "standard critical cavitation speed" at the free surface can be derived (e.g. Hoerner[67] p10-5) as

$$V_{crit} = \frac{22}{\sqrt{\sigma_i}} \text{ (knots)}$$

where the subscript 'i' (for incipient) indicates the onset of cavitation. He suggests that for a sphere at supercritical Reynolds number $\sigma_i \simeq 1.8$ thus giving $V_{crit} = 20$ knots. Other authors[84,85] indicate that $\sigma_i \simeq 0.5$ giving $V_{crit} = 38$ knots. Since the critical speed will increase with increasing depth it is apparent that cavitation is unlikely to be a problem for most vessels. If further investigation of the higher speed cases showed cavitation to be a likely problem then a more streamlined ending could be adopted.

Similar data from the same sources shows that ventilation is unlikely to be important except in cases of very high speed.

5.11 Discussion

Chapman[36] has made some conclusions about the choice of columns and column separation from a wave-resistance point of view, and suggests that for slow speed SWATHs a single column per hull should be used and that as speed is increased two struts per side becomes more favourable. However, as already discussed this is not necessarily compatible with other requirements such as maintaining adequate longitudinal GM and having sufficient thickness for access. Sobolewski[80] has found that the Chapman technique adequately predicts the Froude numbers at which the wave-making drag humps occur as well as the change in hump location with change in tandem strut spacing. Furthermore, changing the strut spacing could alter the total resistance by ±10 - 15%. However, for this case it can be seen from Fig. 5.4 that in the design speed-range (chord Fn ≈ 0.4 - 0.5) the total resistance is not sensitive to changes in the longitudinal column separation. It is, therefore, more important to minimise the resistance of the individual components. For trimarans, Narita[45] reached virtually the same conclusion, namely, that it was more promising to use optimised hull forms rather than to use ones with a high wave-making level and trying to obtain favourable interference effects. However, in other designs the interference effects may be more important as evidenced by the contoured lower hulls in SWATH 8[9].

In the present three-hulled design the geometry of the aft hull/columns is largely dictated by other requirements but the forward hull/column could be adapted. Figures 5.11 and 5.12 show, not unexpectedly, that increasing column thickness generally causes a greater increase in wave-resistance than increasing the column chord, so the first step in reducing the resistance could be to use a more slender forward column. Similarly, Fig. 5.13 illustrates that a lower resistance would be obtainable by increasing the L/D ratio of the forward hull which is also quite a feasible proposition. Although the theory over-estimates the peak wave-resistance by a factor of about 2½ there is no reason to doubt the trends in the Figures.

It is expected that for a model with more slender hulls better agreement would be obtained between theory and experiment, but to confirm this it would be useful to compare the theoretical wave-resistance with that obtained from an experimental technique involving measurement of the wave pattern.

The inter-related problems of estimating the form component, turbulence stimulation, and extrapolating to full-scale have been investigated and discussed and it can only be suggested that for resistance work the model should be sufficiently large to achieve a Reynolds number above about $R_n = 3 \times 10^5$, based on hull diameter, for the operating range.

From the above it is apparent that the design could be altered to reduce the resistance. Such action would reduce the operating costs and would, therefore, further improve the comparison with the monohull research vessel in Chapter 4.

CHAPTER 6

MOTION RESPONSE

6.1 General Introduction

In motion predictions the linear frequency domain description has proved to be quite successful for both conventional ships (except perhaps in roll) and also semi-submersibles. In particular, it is usual to assume that when the response can be taken as linear the statistical description of a vessel's motion in irregular seas can be obtained from linear superposition of the responses in regular waves following the well-known 1953 paper of St. Denis and Pierson[86]. It has been shown that even in quite rough weather good agreement is obtained between full-scale measurements of statistical averages, such as significant heave and calculations from linear theory[87]. However, in the case of ship roll, non-linearities cannot be ignored and linearisation is necessary if the traditional frequency domain approach is to be used[88]. Similarly, for large amplitude heave and pitch motions non-linearities may need to be taken into account[89,90,91].

The motion response of SWATH ships has been the subject of several papers. Lee and Curphey in a major work[40] have developed a five degree-of-freedom strip theory program in which weak non-linearities from viscous drag and forward speed viscous lift are treated by the widely used equilinearisation method. They used the coupled equations of motion and for evaluation of the sectional added mass and damping coefficients they used the Frank close-fit method and consequently the program uses a significant amount of computer time. To reduce this, Dalzell[92] has developed a simplified method of computing the sectional coefficients at zero-speed in head seas. This work is reportedly being extended[9]. Extensive parametric studies have also been conducted[37].

In general, both the above methods give good correlation between theory and experiment for heave at low speeds, but not necessarily for pitch. At higher speeds in head seas, (high frequency of encounter), Lee and Curphey[40] report good agreement for pitch but

at lower speeds it has been shown[9] that the pitch motion can be over-predicted by a factor of nearly two for quite a large range of frequencies. The inclusion of a correction for surge forces has resulted in improved agreement[9]. Low speed roll correlation is also a problem which is being worked on[9]. Similarly, the relative bow motion (RBM) in head seas has shown lack of agreement particularly at low speeds. This has reportedly been improved but it has not been reported how this improvement has been achieved. It could be from theoretical considerations or by using semi-empirical correction factors to different terms.

For this study the first requirement was to determine the motion response for the vessel during the design stage so that it could be determined whether or not the motions were lower than those of an equivalent monohull and, if not, how the vessel would have to be altered to achieve this. To that end a program was written based on the synthesis procedure used for semi-submersibles by Oo and Miller[93]. This used constant added mass coefficients and the damping ratio obtained from motion decay tests (at the natural frequency) or based on past experience. An example from this program is given in an early report[30] for heave response since, as mentioned by Lee and Curphey[40] the dominant contribution to vertical displacement of the ship within a practical range of wavelengths is from the heave motion at resonant frequency. It became apparent at that stage that frequency-dependent effects were more important than for a conventional semi-submersible because of the relatively greater waterplane area and the closer proximity of the hulls to the free-surface. A second program was therefore written which incorporated frequency-dependent sectional added mass coefficients and uncoupled equations of motion and, as will be shown later, gave good agreement with experimental heave motions. By this time a model of the design had been built and was then tested for a variety of different conditions to determine the absolute motions, the RBM and how these were affected by certain parameters. The linear theory, experiments, and the subsequent processing of the results form the main part of this chapter, but it is convenient to introduce the other parts of the motion response work at this point although they are included in different chapters.

The first version of the second program still used the experimentally determined damping ratio which is of critical importance in the resonant region. Damping coefficients can be calculated from potential flow theory (and were later included in the program) but as discussed by Lee and Curphey[40] this ignores viscous effects which can contribute about 50% of the total damping, depending on the motion amplitude. While it is undoubtedly very difficult to improve the purely theoretical evaluation of these effects, it seemed that there was adequate scope for semi-empirical improvements which would provide good engineering solutions. It was felt that this could be best achieved by the use of an analogue computer and although this operates in the time domain, frequency domain response amplitude operators as a function of wave amplitude could be obtained.

Equations of motion were patched on the analogue to investigate both viscous damping and the effect of change in heave restoring force due to column flare. This produced plausible looking results which were reported along with some interesting results for large amplitude heave motions[94] which arose from considering recent work on wave groups and the complete solution to the equation of motion, i.e. including transients. This will be described in Chapter 10. To verify the simulations, a further experimental series was commenced in which the model was tested in a wide range of wave frequencies and amplitudes with and without bracing and with different amounts of column flare. During these experiments the 'jump' phenomenon (recognised for non-linear spring systems) occurred and it was also discovered that severe rolling in head seas at half the wave frequency, as described by the Mathieu equation and sometimes called parametric rolling, could occur. At this point it seemed more appropriate to utilise the time and experimental resources available to investigate these motions, which had not been reported in the literature, rather than trying to improve the theoretical calculation of the linear or weakly non-linear motions. (The improvements could be achieved by, for instance, including horizontal forces and coupling between the modes of motion which as previously mentioned appears to be the subject of considerable research in the U.S.A.) The experimental programme was therefore considerably extended to

include variations in some of the parameters that were thought might be important, such as GM and damping. The results are given fully in subsequent chapters but during the experiments the occurrence of 'beats' and sub-harmonic rolling in beam seas was also investigated. These types of motion have previously been reported as a possible capsize mechanism for ships[95,96] and are also known for tension-leg-platforms (TLPs)[97,98]. They have not previously been reported for SWATH ships and despite the association with capsizing this never seemed imminent in head or beam seas. In fact, even with zero upright transverse GM the model would not capsize under the action of beam waves.

The above refers entirely to zero-speed head and beam sea motions. Although not investigated here it is worth bearing in mind that in following seas certain undesirable features, such as deck-box bow immersion have been noted[9]. The severity of these motions have not been reported in the open literature. Similarly, it is not yet known to what extent these are being investigated although it has been suggested that 'control can reduce these problems'[9].

The effects of forward speed are not investigated herein either, but it is recognised that increasing forward speed in head seas generally decreases motions although there does come a point when vertical plane instability will set in if adequate stabilisation is not provided. The required size of stabilising fins and the beneficial effects these have on forward speed motions can be determined using the methods of Lee and Curphey[40]. To study the active control of motions in detail it is necessary to consider the non-linearities associated with the active controller, namely, clipping and rate limiting as well as those due to viscous effects. This has been investigated by Livingston and Newman[99] who have developed a model which uses transfer functions obtained by theory or experiment then adds the effects of the further non-linearities and control laws to obtain modified transfer functions by iteration. These modified transfer functions are then solved for 15 wave frequencies of random height and phase transposed into the time domain.

We shall now revert from discussion of these developments to consider the zero-speed, head seas motion response and the comparison of the SWATH design's motions with those of a monohull.

6.2 Co-ordinate System

Motions of points in the vessel taken as a rigid body are defined on the basis of a heave component z (positive upwards) and a pitch component ϕ (positive for bow displaced upwards). A general point along the length has co-ordinate ξ or, for the i^{th} strip, x_i, and the origin is taken at the LCG.

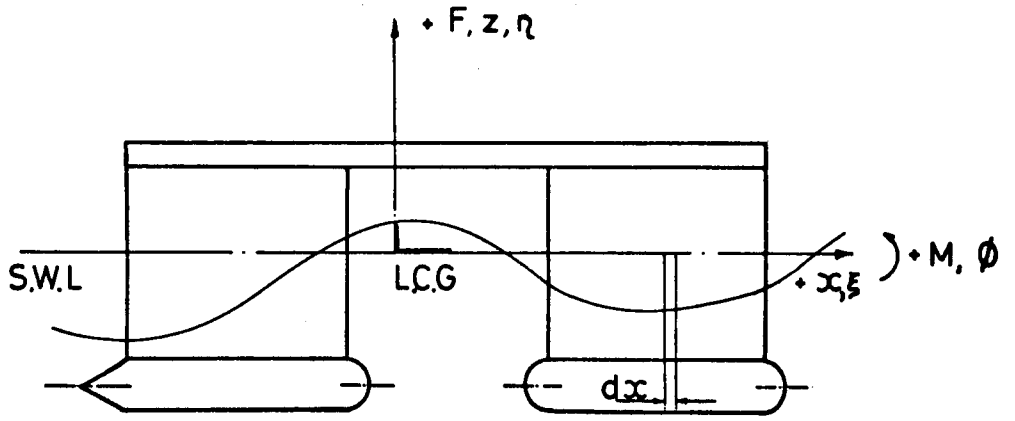

Fig. 6.1. Co-ordinate System for Heaving and Pitching.

The wave profile at any point is given by

$$\eta_\xi = a_o \cos K(\xi - ct) \quad \ldots\ldots \quad 6.1$$

and the heave and pitch motions are given by

$$z = z_o \cos(\omega t + \Psi_1) \quad \ldots\ldots \quad 6.2$$

$$\phi = \phi_o \cos(\omega t + \Psi_2) \quad \ldots\ldots \quad 6.3$$

where Ψ_1 and Ψ_2 are the phase angles between the force and heave and between moment and pitch respectively.

6.3 Equations of Motion

Throughout this chapter only uncoupled, linear single degree-of-freedom, motions are considered. In the heave case the solution is required to the well-known equation

$$(\Delta+AM)\ddot{z} + C_1\dot{z} + K_z z = F\cos\omega t \qquad \ldots\ldots \quad 6.4$$

where $K_z = \rho g A_w$

(Herein the right-hand side is referred to as the exciting force.) The complete solution consists of a particular integral plus a complementary function and takes the form

$$z = \{Ae^{\lambda_1 t} + Be^{\lambda_2 t}\} + \frac{F/K_z \cos(\omega t-\phi)}{\sqrt{\{1 - (\frac{\omega}{\omega_H})^2\}^2 + 4\gamma^2(\frac{\omega}{\omega_H})^2}} \qquad \ldots \quad 6.5$$

where $\phi = \tan^{-1}\dfrac{2\gamma\,\frac{\omega}{\omega_H}}{1 - (\frac{\omega}{\omega_H})^2}$ and $\omega_H = \sqrt{\dfrac{K_z}{\Delta+AM}}$

A and B are constants depending on the initial conditions while λ_1 and λ_2 are the roots of the characteristic equation

$$\lambda^2 + 2\gamma\omega_H\lambda + \omega_H^2 = 0$$

The first term in Eq. 6.5 (the transient part) is the term for the damped free vibration while the second term is for the forced vibration and represents the steady-state solution. The steady-state solution is the theoretical equivalent of the regular wave response and is the part usually considered, i.e.

$$z_o = \frac{F/K_z}{\sqrt{\{1 - (\frac{\omega}{\omega_H})^2\}^2 + 4\gamma^2(\frac{\omega}{\omega_H})^2}} \qquad \ldots\ldots \quad 6.6$$

In other words, it is generally considered that the transients are negligible which is an essential assumption for applying the linear theory of superposition[86]. (The importance of including the transient part, particularly for large amplitude motions is discussed in Chapter 10.)

Similarly, the linear equation for pitch is

$$(I+I_{AM})\ddot{\phi} + C_\phi\dot{\phi} + K_\phi\phi = M_\phi\cos\omega t \qquad \ldots\ldots \quad 6.7$$

where $K_\phi = \rho g \nabla GM_L$

with solution

$$\phi_o = \frac{M_\phi / K_\phi}{\sqrt{\left\{1 - \left(\frac{\omega}{\omega_\phi}\right)^2\right\}^2 + 4\gamma_\phi^2 \left(\frac{\omega}{\omega_\phi}\right)^2}} \qquad \ldots\ldots \quad 6.8$$

where $\omega_\phi = \sqrt{\frac{\rho g \nabla GM_L}{I+I_{AM}}}$

6.4 Exciting Forces and Moments

The usual strip theory assumptions are made that, (1) the flow adjacent to thin vertical slices of the body is two-dimensional (i.e. fore and aft force components are neglected but the added mass coefficients are multiplied by a reduction factor to allow for three-dimensional flow), and (2) the resulting forces can be summed over the length of the body to give the total forces. The Froude-Krylov hypothesis is also assumed to apply (viz. the motions of the body do not alter particle motions in the wave, although the particle motions influence the motions of the body).

The moments are obtained by multiplying the vertical sectional forces by the lever from the LCG and summing over the length of the body.

For calculating extreme motions and loads on semi-submersibles, much attention has been paid to calculating forces from higher order wave theories (such as Stokes' 3rd and 5th order) but this work uses small amplitude linear wave theory since this generally allows the use of spectral analysis and is also convenient for investigating the system dynamics.

For head seas the wave length is generally long in comparison with the characteristic breadth of the structure and the force is then assumed to be made up of two components:

(1) Variation of the water pressure on the structure due to the passage of the wave; herein called the Froude-Krylov component, but sometimes called the pressure component.

(2) Force due to the product of particle acceleration in the wave and the added mass associated with the structure, (herein called the added mass component).

The forces due to particle velocity effects are assumed to be negligible in comparison with the above components, although this may not be so at certain frequencies.

6.4.1 Added Mass Component

The vertical added mass component per unit length on the i^{th} strip is

$$dF_{am} = -\tfrac{1}{2}\rho\pi T_i^2 c_{am} JKg\, a_o e^{-Kh_i} \sin K(x_i - ct) \quad ..... \quad 6.9$$

where c_{am} is the frequency dependent added mass coefficient for the appropriate partially immersed bulbous cylinder with draught T_i and the depth, h_i, is taken as that of the centreline of the cylindrical portion of the hull. (As previously mentioned Lee and Curphey[40] use the Frank-Close-Fit method for calculation of added mass and damping. which is quite time-consuming, but Dalzell[92] has developed a simplified method which considerably reduces the computation time required.) In this work coefficients from published data[100], e.g. Fig. 6.2, are used augmented by results for the fin from a version of the Frank-Close-Fit program being developed in the department[101].

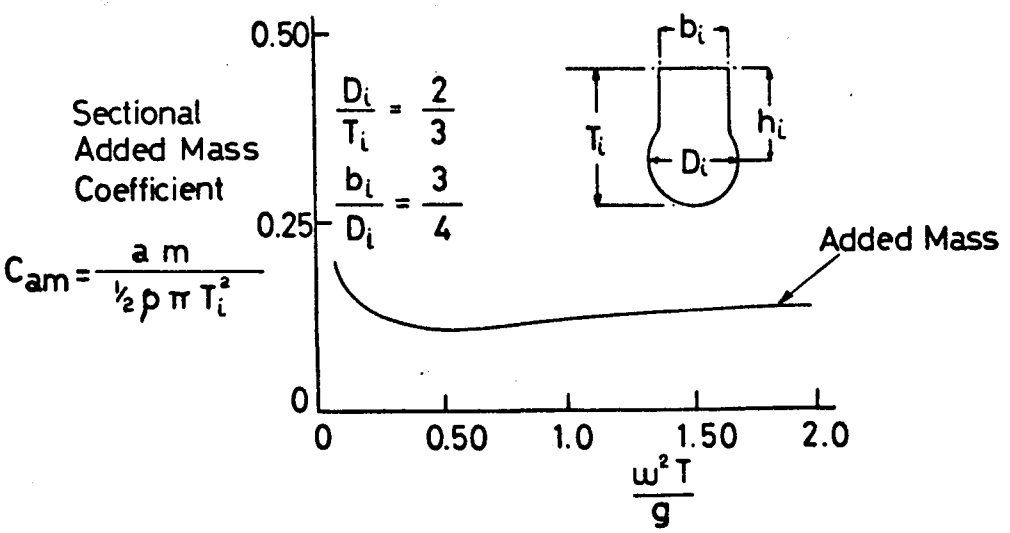

Fig. 6.2. Typical Sectional Added Mass and Damping Coefficients[100].

6.4.2 Added Mass Reduction Factor

The added mass around the two-dimensional transverse sections has to be corrected to compensate for the three-dimensional nature of the actual flow, especially around the endings. To do this Lewis'[102] reduction factors have been used as in Fig. 6.3 adapted from Saunders[103].

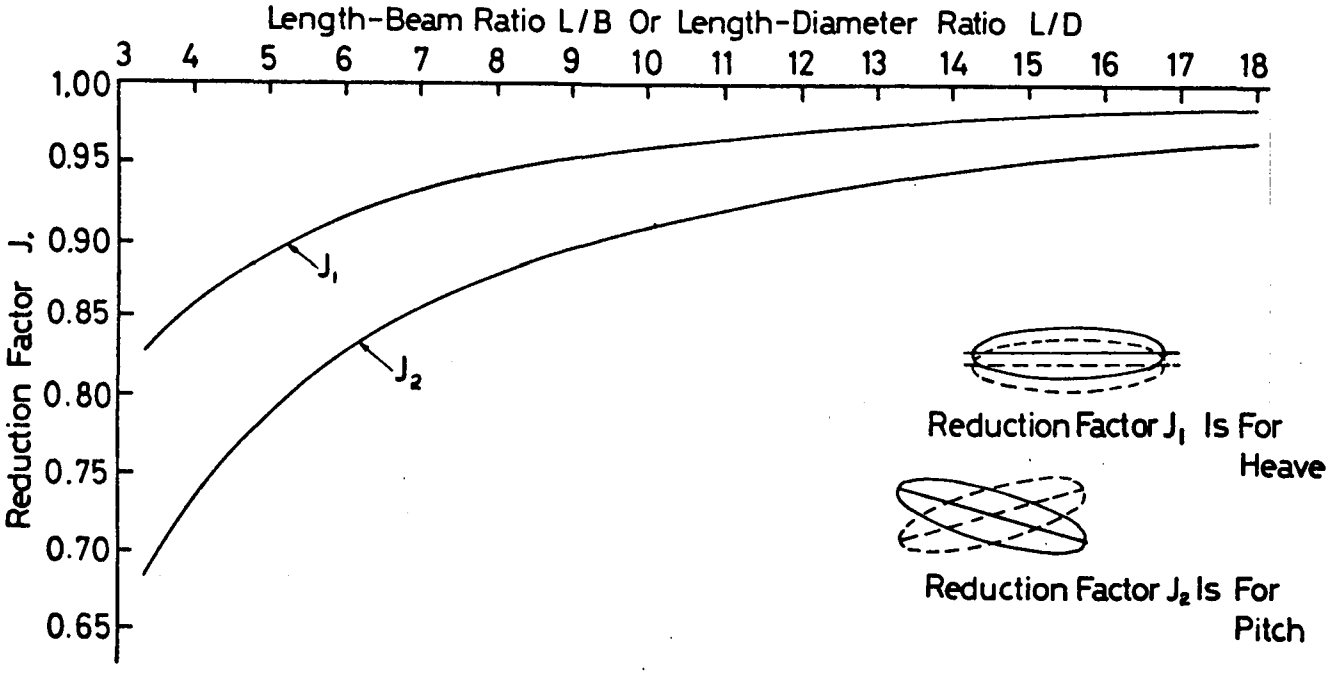

Fig. 6.3. Added Mass Reduction Factors[103].

Since the length-diameter ratio in this case is around 4.0 the reduction factor, J, especially for pitch, is quite large, about 0.75, and there is thus considerable uncertainty in the total added mass even when sectional coefficients are obtained by highly sophisticated methods such as the Frank-Close-Fit method.

6.4.3 Froude-Krylov Component

The procedure used is similar to that explained by Oo and Miller for semi-submersibles[93]. For a submerged circular cylindrical section, radius R_i, the vertical Froude-Krylov component per unit length is

$$dF_{FK} = - \Pi\rho g \, a_o K \, R_i^2 \, e^{-Kh_i} \sin K(x_i - ct) \quad \ldots\ldots \quad 6.10$$

and if there is a column present at this i^{th} section, an additional term is included to take account of this

$$dF_{FKc} = \rho g\, a_o\, b_i\, e^{-Kh_z} \sin K(x_i - ct) \quad \ldots\ldots \quad 6.11$$

where h_z is the depth of the column and b_i is the sectional breadth.

6.4.4 Integration

For circular cylinders with longitudinal symmetry about midships relatively simple expressions can be obtained when the force components are integrated over the length. However, in this case the integrated expressions became very cumbersome and in addition the added mass bore little resemblance to the experimental value. As previously stated the added mass data from Frank[100] was then used, and since this entailed different sections having different added mass coefficients which were not simple to relate analytically it became necessary to use numerical integration.

6.4.5 Damping

The value of damping used in Eqs. 6.3 and 6.5 is only of particular importance around resonance. Thus although theoretical sectional damping coefficients (based on potential flow) were available[100] the factor initially used was determined from heave decay tests on the model and thus included a viscous effect averaged over cycles of different amplitude.

6.5 Relative Motion

The relative motion is a function of heave, pitch, wave profile and the phase angles between them as discussed in various textbooks, e.g. Ref. 96. Thus referring back to Fig. 6.1, for zero forward speed, the vertical displacement at a distance ξ is

$$z_\xi = z + \xi\phi \quad \ldots\ldots \quad 6.12$$

then substituting Eqs. 6.2 and 6.3

$$z_\xi = z_o \cos(\omega t + \Psi_1) + \xi\, \phi_o \cos(\omega t + \Psi_2) \quad \ldots\ldots \quad 6.13$$

$$= z_{\xi_o} \cos(\omega t + \Psi_3) \quad \ldots\ldots \quad 6.14$$

where $Z_{\xi_o} = \sqrt{Z_o^2 + (\xi \phi_o)^2 + 2Z_o \xi \phi_o \cos(\Psi_1 - \Psi_2)}$ 6.15

and $$\tan \Psi_3 = \frac{Z_o \sin\Psi_1 + \xi \phi_o \sin\Psi_2}{Z_o \cos\Psi_1 + \xi \phi_o \cos\Psi_2}$$ 6.16

The relative motion is then given by

$$\begin{aligned} r_\xi &= Z_\xi - \eta_\xi \\ &= Z_{\xi_o} \cos(\omega t + \Psi_3) - a_o \cos K(\xi - ct) \\ &= r_{\xi_o} \cos(\omega t + \Psi_4) \end{aligned}$$ 6.18

where $r_{\xi_o} = \sqrt{Z_{\xi_o}^2 + a_o^2 - 2Z_{\xi_o} a_o \cos(K\xi - \Psi_3)}$ 6.19

and $$\tan \Psi_4 = \frac{a_o \sin(K\xi) - Z_{\xi_o} \sin\Psi_3}{a_o \cos(K\xi) - Z_{\xi_o} \cos\Psi_3}$$ 6.20

Now Ψ_1 and Ψ_2 are the phase angles between wave motion and body motion for heave and pitch respectively and can be expressed as

$$\Psi_1 = \Psi_a + \Psi_b$$ 6.21

where Ψ_a is the lag between wave and exciting force
Ψ_b is the lag between exciting force and motion

$$\Psi_b = \tan^{-1} \left\{ \frac{2\gamma_H \frac{\omega}{\omega_H}}{1 - \left(\frac{\omega}{\omega_H}\right)^2} \right\}$$ 6.22

Similarly

$$\Psi_2 = \Psi_c + \Psi_d$$ 6.23

where $\Psi_d = \tan^{-1} \left\{ \frac{2\gamma_\phi \frac{\omega}{\omega_\phi}}{1 - \left(\frac{\omega}{\omega_\phi}\right)^2} \right\}$

6.6 Experimental Arrangement

The model was moored approximately half-way down the tank by slack, elasticated, transverse mooring lines attached just above the still-water-line. The motions were measured by displacement transducers at the bow and at the aft end of the deck structure placed equidistant from the LCG. The signals from these were amplified and then fed to pen-recorders via a summer/differencer. The relative bow motion was measured by a wave-probe which was attached 8cm outboard of the forward perpendicular. The wave-probe for measuring the wave amplitude was located on a bridge upstream of the model.

6.7 Experiments and Results

As stated in the introduction the purpose of this first set of experiments was essentially to produce the data to verify that the motions would be lower and more comfortable than an 'equivalent' monohull in the expected areas of operation. As in the resistance experiments the longitudinal column separation was adjustable which therefore allowed the natural pitch frequency to be changed considerably for constant heave natural frequency. In addition, the removal of the brace caused a considerable change in added mass and damping. The model was tested in head seas at zero Froude number for six different conditions, see Table XII. The height of the centre of gravity for these conditions was obtained from inclining experiments and the transverse GM corresponds to a full-scale value of about 1m or greater. The variations in GM_T at constant draught but different separations are due to the necessary redistribution of ballast weights between forward and aft hulls which gave different heights of the vertical centre of gravity. The longitudinal GM is 2.5 times greater since a large GM_L is recommended by Lang and Higdon[25] to provide less trim change with speed. The central position of the ballast in the columns corresponds to a certain extent with centres of mass in the full-scale and as can be seen from Fig. 5.1 large holes were cut in the overhanging aft structure to help achieve a realistic mass moment of inertia.

The results for the six conditions are presented in Figs. 6.4, 6.5 and 6.6 for heave, pitch and relative bow motion respectively. Curves have been drawn for ease of visualisation.

Condition	Appendages	Displacement (weighed) (kgs)	Column Draught (cm)	Length over Columns (cm)	GM_T (cm)	GM_L (cm)	Natural Frequencies (rads/sec)	
							Heave	Pitch
1	Fin	22.1	12.8	108	4.0	11.0	3.75	2.24
2	Fin	22.1	12.8	118	4.4	19.8	3.75	2.98
3	Fin	22.1	12.8	128	4.9	29.9	3.75	3.16
4	Fin	23.2	15.0	108	4.8	11.0	3.54	2.32
5	None	21.6	12.7	108	4.0	11.0	4.15	2.32
6	None	21.6	12.7	118	4.6	20.1	4.20	2.91

TABLE XII. Experimental Conditions for Motion Tests.

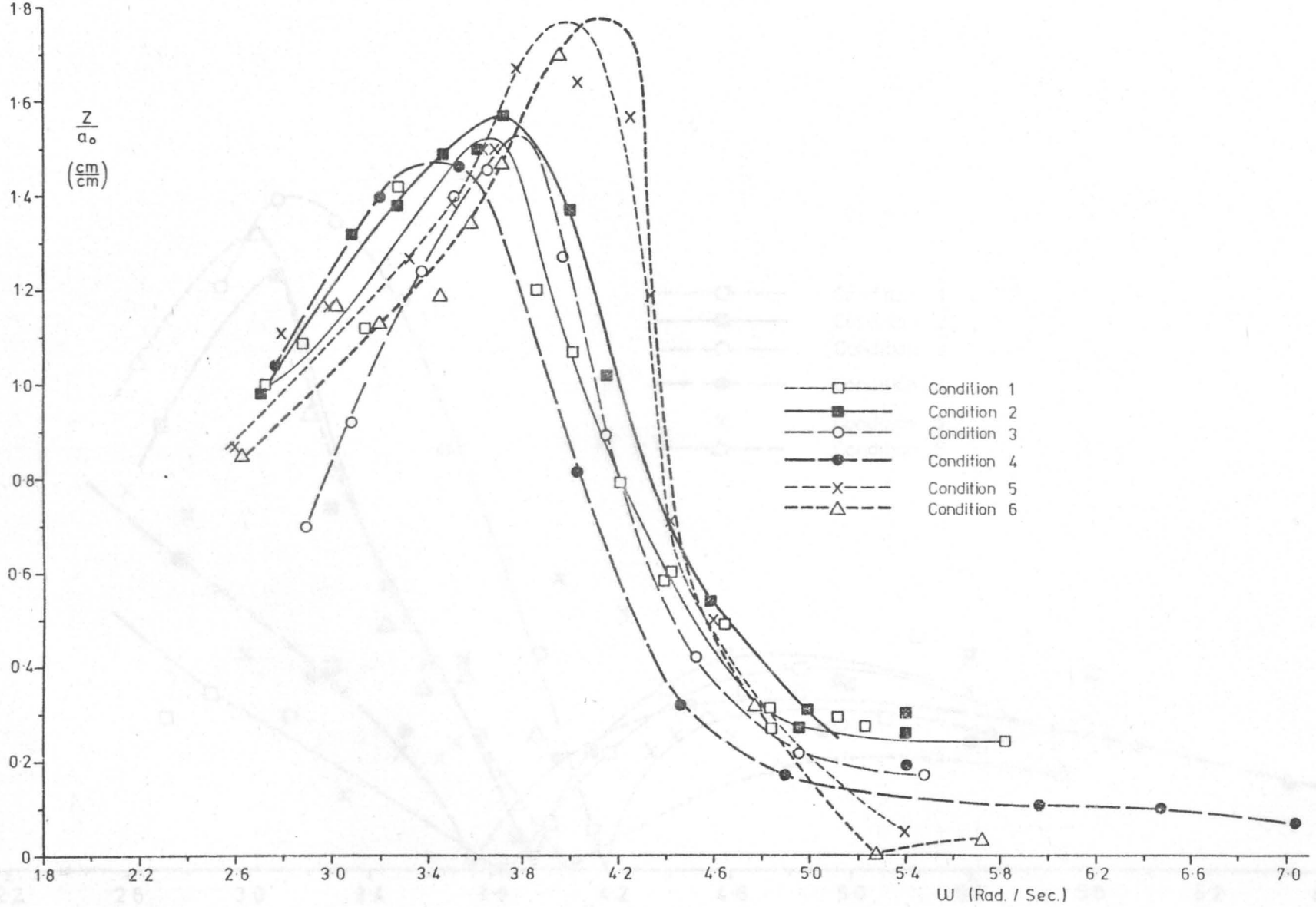

Fig. 6.4 Heave Response (Frequency Domain)

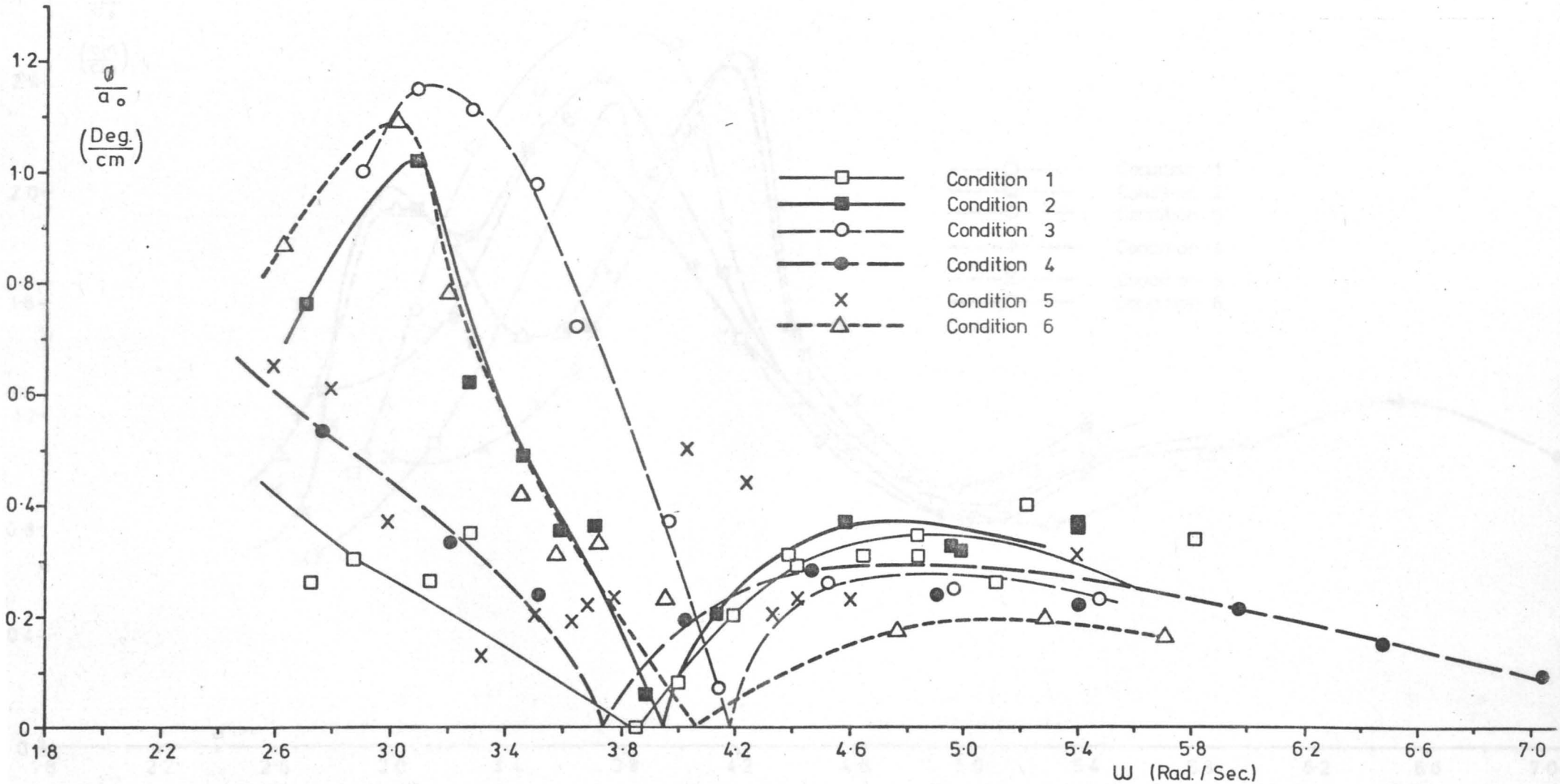

Fig. 6.5 Pitch Response (Frequency Domain)

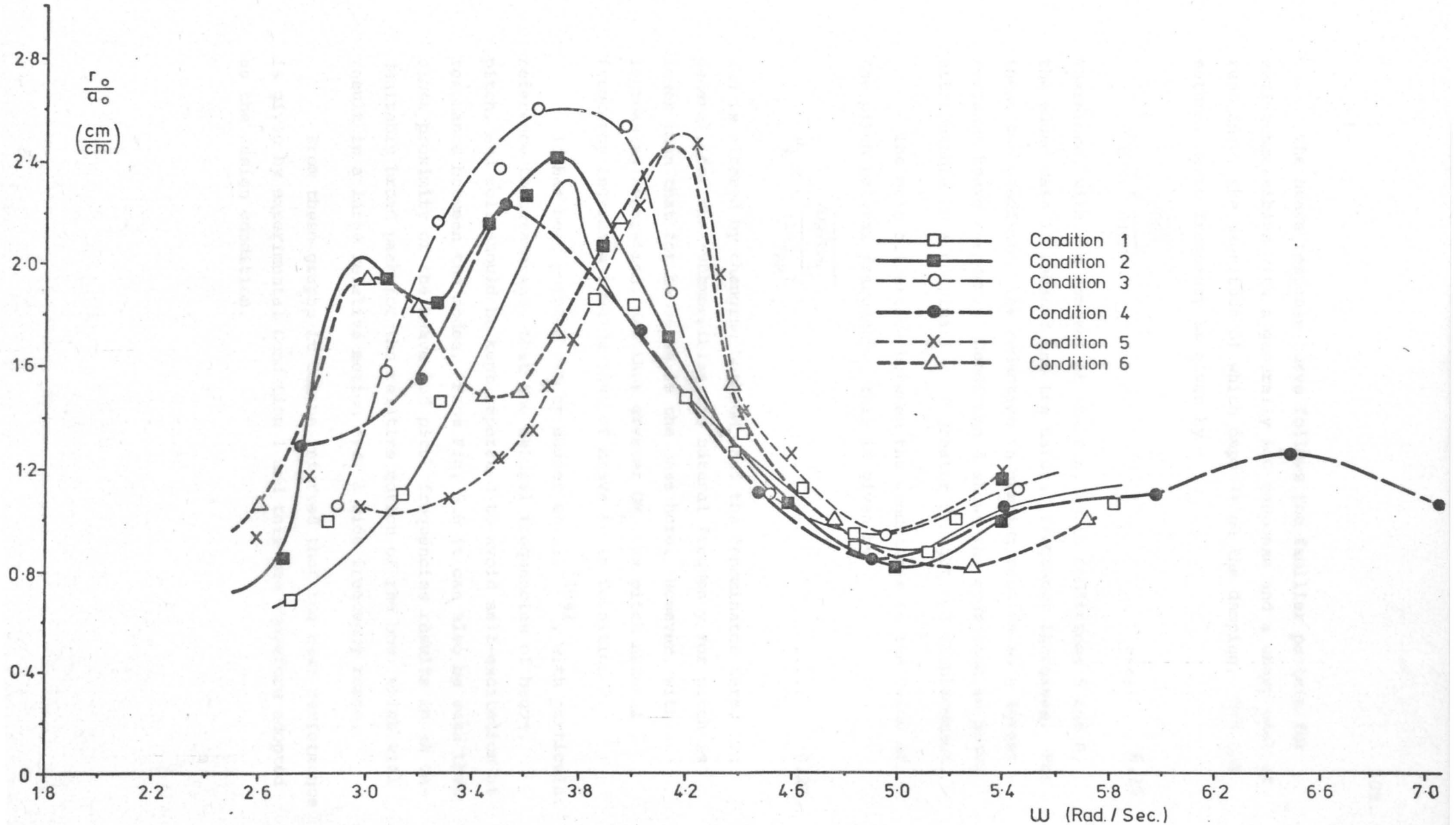

Fig. 6.6 Relative Motion of Bow (Frequency Domain)

The heave response curve follows the familiar pattern for semi-submersibles with a generally low response and a sharp peak at resonance, the magnitude of which depends on the damping. Now the natural heave frequency is given by

$$\omega_H = \sqrt{\frac{\rho g A_w}{\Delta + AM}} \qquad \ldots\ldots \qquad 6.25$$

Therefore, with the removal of the fin, as in Conditions 5 and 6, the added mass is reduced and the natural frequency increases. For these two conditions the reduction in damping results in a larger resonant heave response. Condition 4 shows the reduction in heave attributable to a combination of greater draught and displacement.

The main difference between the conditions is the value of the pitch natural frequency. This is given by

$$\omega_\phi = \sqrt{\frac{\rho g \nabla GM_L}{(I + I_{AM})}} \qquad \ldots\ldots \qquad 6.26$$

and is altered by changing both GM_L and the denominator term. In general, for semi-submersibles the natural frequency for pitch is lower than that for heave as is the case here. However, with increasing separation, and thus greater GM_L the pitch natural frequency increases towards that of heave as in Condition 3.

It has been pointed out by Hadler et al.[104], with particular reference to catamarans, that the natural frequencies of heave, pitch, and roll should be kept separated to avoid self-excitation at resonance between the modes. From Fig. 6.6 it can also be seen that close proximity of the heave and pitch frequencies results in an undesirably broad peak for the relative motion of the bow, which will result in a large relative motion over a wide frequency range.

From these graphs it can be inferred that the best performance is given by experimental Condition 1 and this was therefore adopted as the design condition.

6.8 Comparison between Theory and Experiment

Fig. 6.7 shows the comparison for heave motions in Conditions 1 and 5, between linear theory, using the experimental damping coefficients, and the experiment results. Generally good agreement is obtained. The main discrepancies are near the 'zero' in the response curve around 4.6 rads/sec especially for Condition 1. From consideration of the experimental results later in this thesis the discrepancy can be attributed to neglect of velocity forces on the bracing.

The prediction of both pitch response and relative bow motion is shown in Fig. 6.8. Comparison of these curves with the relevant data from Figs. 6.5 and 6.6 is not particularly favourable. The pitch at the resonant peak is over-predicted by a factor of about 2.5 which is roughly the same as the over-prediction reported in the literature as discussed in Section 6.1. (The work being conducted elsewhere to improve these predictions has already been discussed in Section 6.1.) This error in pitch is obviously carried over into the relative bow motion calculations. These are sensitive to the phase angles and it may be necessary to include surge motions as well as pitching moments from horizontal forces and coupling between the modes of motion.

6.9 Sea Spectra (JONSWAP)

In order to compare the motion response of different vessels it is necessary to have information on the conditions in which the vessels will operate. This is also useful in determining certain dimensions, such as the underdeck clearance in this case, or the height of the bow for satisfactory seakeeping in conventional ships, when previous practice does not give adequate guidance. For that reason, as has been done elsewhere [105,106] a family of 24 mean JONSWAP spectra [107] for wind speeds up to 19.0 m/s and for fetch lengths of 50, 100, and 200 km were used, i.e. in terms of $\frac{1}{2}a_o^2$

$$S(\omega) = \alpha \frac{g^2}{\omega^5} \exp\left\{-1.25\left(\frac{\omega_m}{\omega}\right)^4\right\} \gamma^{\exp\left[\frac{-(\omega-\omega_m)^2}{2\sigma^2 \omega_m^2}\right]} \quad \ldots\ldots \quad 6.27$$

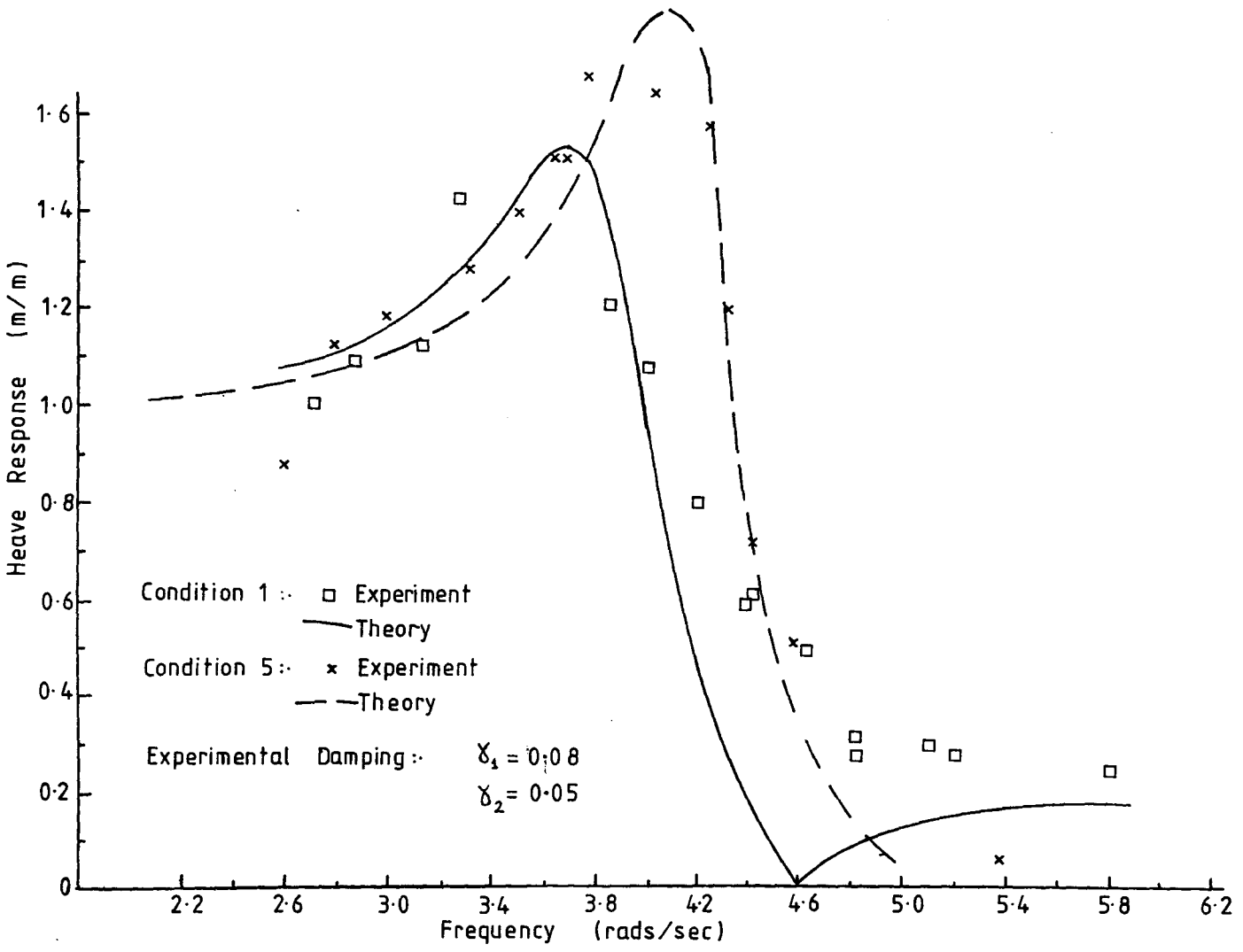

Fig. 6.7 Heave Response: Theory and Experiment

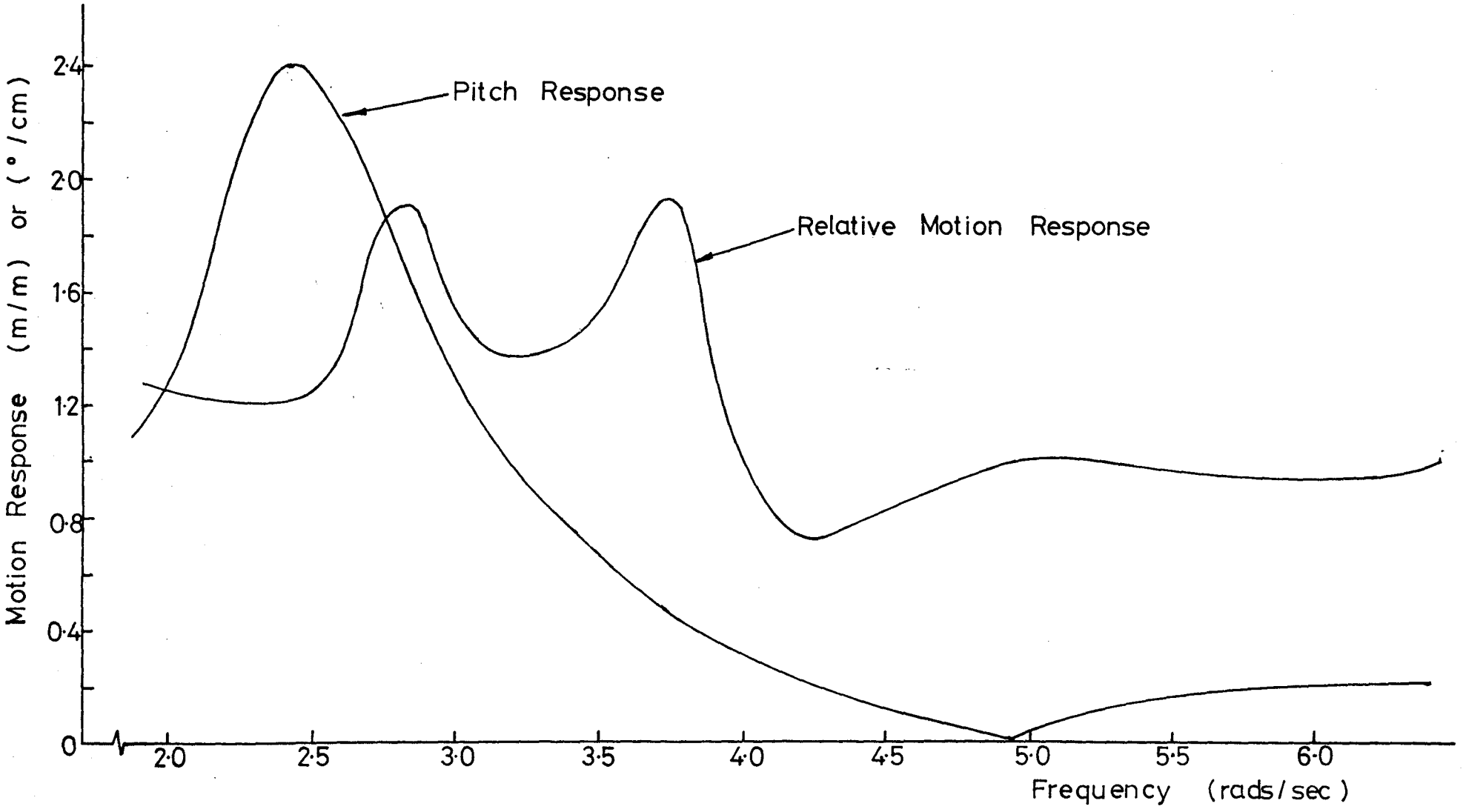

Fig. 6.8 Pitch and Relative Motion of Bow: Theory

where $\gamma = 3.30$ 6.28

$$\sigma = \begin{cases} \sigma_a = 0.07 \text{ for } \omega \leq \omega_m \\ \sigma_b = 0.09 \text{ for } \omega > \omega_m \end{cases} \quad \text{.....} \quad 6.29$$

$$\left.\begin{aligned} \alpha &= 0.076\ (\bar{X})^{-0.22} \\ \omega_m &= 2\pi\ 3.5\ \frac{g}{u}\ (\bar{X})^{-0.33} \end{aligned}\right\} \quad \bar{X} = \frac{gX}{u^2} \quad \begin{aligned} X &= \text{fetch length (m)} \\ u &= \text{wind speed (m/s)} \end{aligned} \quad \text{.....} \quad 6.30$$

The significant wave height and the mean height of the one-tenth highest waves are then given by

$$h_{1/3} = 4\sqrt{m_o} \quad \text{.....} \quad 6.31$$

$$h_{1/10} = 5.1\sqrt{m_o} \quad \text{.....} \quad 6.32$$

where m_o is the area under the energy spectrum.

Table XIII shows the significant wave height for the family and since such a vessel might be used around the Hebrides the percentage exceedance of the wind speeds at S. Uist[108] is also included.

6.10 Underdeck Clearance

Sufficient underdeck clearance is required to prevent an unacceptable number of contacts with the waves on the under-side of the deck. The required clearance can be judged by equating some function of the relative motion to the underdeck clearance. (It should be noted that a water contact does not necessarily imply a slam.)

The relative motion response curve for Condition 1 was scaled to full size and the mean of the tenth highest relative bow motion amplitudes was calculated for the spectral family, Fig. 6.9. The design underdeck clearance for the working condition was 3m so that for a 200 km fetch $r_{1/10} > 3$m for approximately 15% of the time (all seasons) and for a 100 km fetch $r_{1/10} > 3$m for about 1% of the time (all seasons). A map of the Hebrides will show that in the Minches, for example, there are only a few areas where the fetch can be as high as 200 km for prevailing west and south-westerly winds. An underdeck clearance of 3m was therefore taken as acceptable for the working condition.

Wind Speed m/s	% Exceedance at S. Uist (all seasons)	Significant Wave Height (m) 50 km Fetch	100 km Fetch	200 km Fetch
0.0	97.75	-	-	-
1.0	91.5	-	-	-
2.6	82.25	-	-	-
4.4	63.5	0.26	0.79	1.29
7.0	33.75	0.75	1.31	2.04
10.0	17.25	1.17	1.88	2.86
12.6	6.00	1.50	2.36	3.57
15.7	2.00	1.88	2.90	4.34
19.0	0.25	2.28	3.48	5.22

TABLE XIII. Significant Wave Height for Spectral Family and the Wind Climate at South Uist.

6.11 Comparison with a Monohull

The heave and pitch responses, for Condition 1, were scaled to full-size and, on the assumption of linearity, were compared with data for a monohull. The use of zero-speed responses is quite logical because many critical research vessel operations are conducted while stationary. (The actual monohull data used was for an 86m research vessel[109], which had a demonstrably low response scaled to 30m. The response may not be obtainable in a realistic design of a 30m vessel and is certainly lower than experimental results from a conventional transom-sterned trawler.) When the heave and pitch response amplitude operators are scaled to full-size it can be seen that the SWATH heave response is lower up to a wavelength of about 90m and that the SWATH pitch is lower to an even longer wavelength. More usefully the significant heave and pitch in the spectral family were calculated. The heave results, Fig. 6.10, show that for 50 and 100 km fetch lengths the significant heave is always less for the SWATH and at frequently occurring wind speeds it is approximately half. When the fetch length is 200 km the crossing point is at a wind speed of about 10 m/s or about $h_{1/3}$ = 2.8m. These figures represent the transition between Beaufort 5 and 6 or Sea-state 5. At S. Uist, 10 m/s

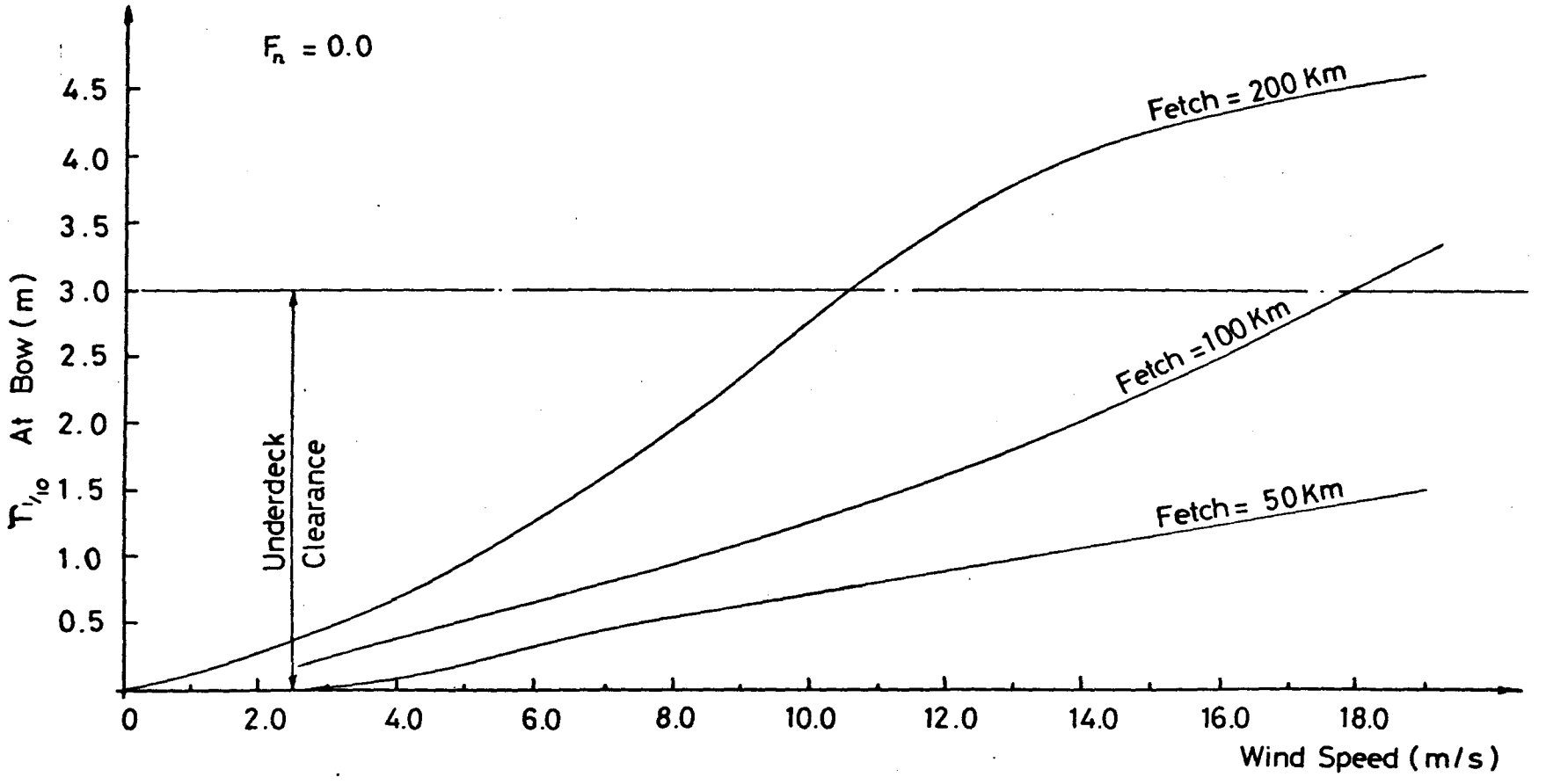

Fig. 6.9. Mean of Tenth Highest Relative Bow Motion Amplitudes in JONSWAP Spectra.

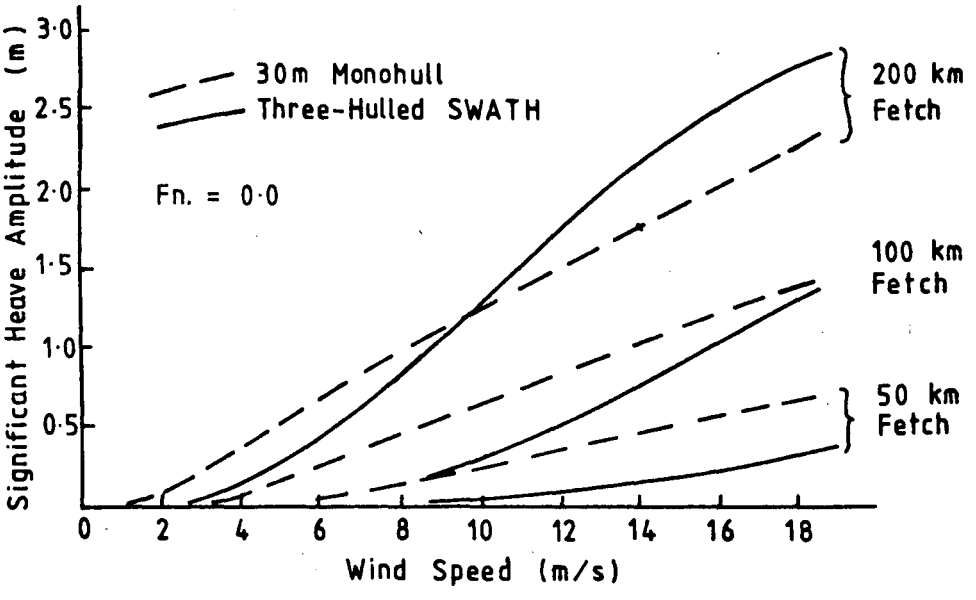

Fig. 6.10 Significant Heave Motion Comparison

winds are only exceeded about 17% of the time. Thus, bearing in mind previous comments on fetch lengths and the optimistic nature of the monohull data it can be said that the SWATH heave motions are generally lower than an equivalent monohull.

The pitch comparison, Fig. 6.11, is even more favourable since it can be seen that the significant pitch is roughly one-third that of the monohull, or less.

6.12 Subjective Motion

The previous section made a comparison between the SWATH and the monohull on the basis of amplitudes of motion displacement, however, it is generally accepted that ride comfort is more affected by accelerations.

Based on the work of Shoenberger[110], Lloyd and Andrew[111] used the concept of 'Subjective Magnitude' (SM) to compare ship motions. This essentially recognised that, subjectively, the magnitude of motion is a function of acceleration and frequency. Thus two motions which have different accelerations and frequencies but felt the same (to Shoenberger's USAF personnel) have the same subjective magnitude. Brown and Marshall[112] expressed the SM in terms of m_4 (the variance of absolute acceleration) and m_6 (the rate of change of m_4), i.e.

$$SM = \left[3.087 + 1.392\left(\log_e \frac{1}{2\pi}\sqrt{\frac{m_6}{m_4}}\right)^2\right] m_4^{0.715} \quad \ldots\ldots \quad 6.33$$

and used the results for ships between 50m and 90m LBP. Other papers have also used the technique, e.g. Refs. 113 and 87. It is possible to use different weighting factors to take account of personnel location and also express limits for different exposure periods. However, here it is simply assumed that Eq. 6.33 will apply and the SM is then calculated for midships only (i.e. heave) for the case with 200 km fetch and $h_{1/3}$ = 2.86m, Table XIV, from which it can be seen that the SWATH has a lower SM.

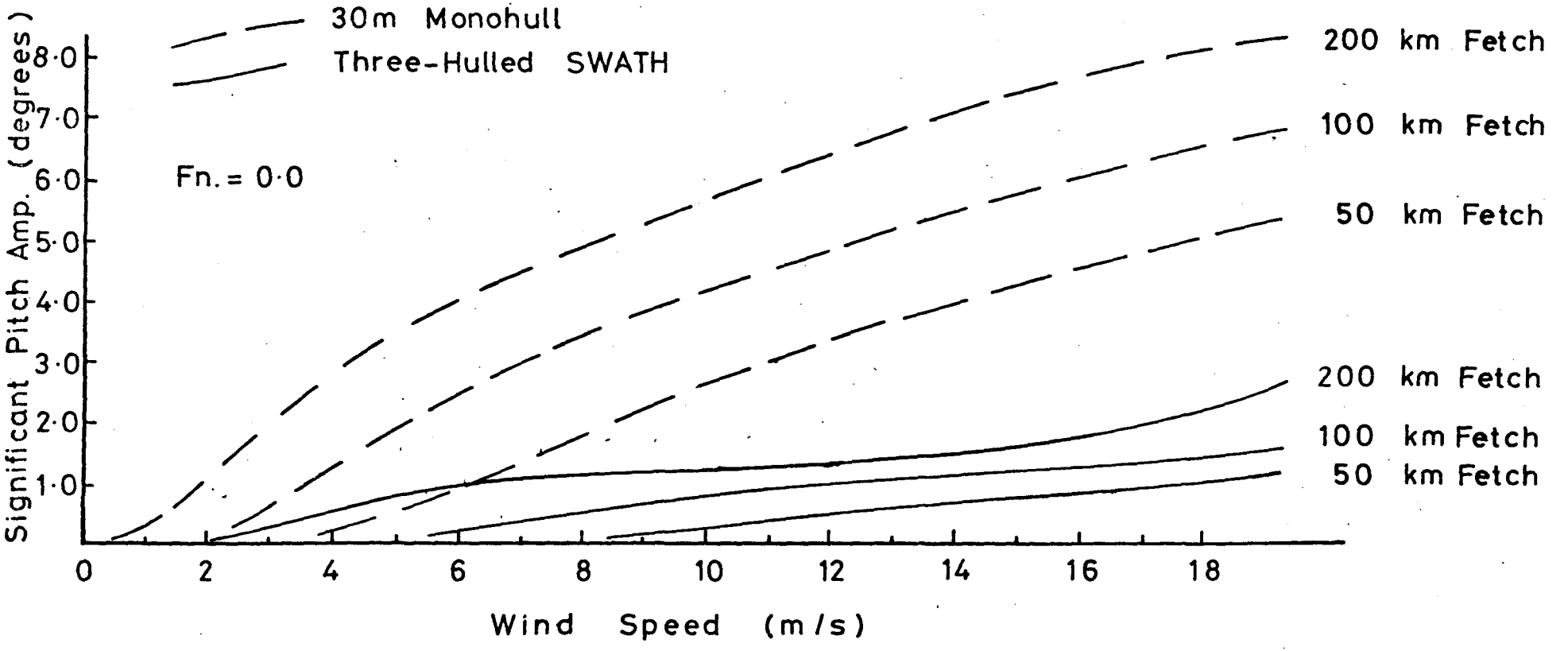

Fig. 6.11 Significant Pitch Motion Comparison

	Subjective Magnitude
SWATH	2.2
Monohull	3.0

TABLE XIV. Subjective Motion.

6.13 Discussion

The comparisons above have shown that, at zero speed, the absolute heave motions of the SWATH ship in commonly occurring seas is less than that of an equivalent monohull and that the pitch motions were considerably lower for all the seas considered. Furthermore, when the motions were compared using the subjective magnitude technique the SWATH heave would be more comfortable than the monohull, (essentially because most of the contribution to the significant heave came from lower frequency components).

It should also be noted that the SWATH shows further benefits with forward speed. Increasing forward speed in head seas will lead to a reduction in SWATH motions[114] but generally causes an increase for monohull motions[114,115]. This is basically due to the lower natural frequency of the SWATH ship so that as speed increases the frequencies of encounter are above resonance and the magnification factor drops. Also, it is quite feasible to reduce heave, pitch, and roll motions on a SWATH by active control whereas for conventional ships stabilisation is only usually considered for roll. For the *Kaimalino* it has been reported that the active control system becomes effective at speeds as low as 5 knots[2].

CHAPTER 7

HEAVE AND PITCH MOTIONS - SOME NON-LINEAR EFFECTS

7.1 Introduction

Much work has been reported in the literature on the effects of non-linearities. These can be conveniently divided into those which merely modify linear behaviour and those which cause a marked variation from the expected behaviour. The former type include the effects of viscosity, calculating forces in the displaced position, and higher-order wave theories. The second type of non-linearity has been investigated for ships, particularly with respect to severe rolling, and includes the 'jump' phenomenon due to the shape of the GZ curve and parametric rolling in head seas. Various of these 'parasitic' motions have also been identified for tension-leg platforms.

In this study viscous effects, which are known to be important at resonance[40] were first investigated, both theoretically on an analogue computer and experimentally. Subsequently the effect of column flare was investigated and from the experimental side it was found that when the flare was increased sufficiently certain marked non-linearities occurred. These included both the 'jump' phenomenon and 'beats', which will be discussed in this chapter, and rolling in head seas, which will be discussed in Chapter 8.

7.2 Viscous Damping and Analogue Computer Simulation

In Chapter 6 the damping was considered in the customary form as a linear function of velocity. It can, however, be more realistically expressed in a binomial form where the linear part is attributable to wave-making and can be calculated from potential-flow theory, while the quadratic part is due to viscous effects. The equation of motion can then be written as

$$(\Delta+AM)\ddot{z} + C_1\dot{z} + C_2\,\dot{z}|\dot{z}| + K_z z = F \sin \omega t \qquad \ldots\ldots \qquad 7.1$$

In this chapter the wave-making damping was calculated using avail-

able data from Frank's method[100] with additional data[101] as for the added mass calculation. The viscous damping cannot be conveniently calculated from theory but the quadratic coefficient can be rewritten as

$$C_2 = \tfrac{1}{2} \rho C_D A_{pr} \quad \ldots\ldots \quad 7.2$$

Equation 7.2 was substituted into 7.1 and patched on an analogue computer. The exciting force was calculated digitally as before. A patch diagram of the simulation is shown in Fig. 7.1. (This diagram includes a loop for non-linear heave restoring force considered later.)

7.3 Experimental Results and Discussion

The model was tested at the resonant frequency for Condition 1 and at the same frequency for Condition 5. Figure 7.2 shows that at resonance with the brace the heave response-amplitude-operator (RAO) drops from about 1.8 to 1.2 with increasing wave amplitude. (The wave amplitude is taken as half the crest to trough height.) The results from the simulation drawn on the same graph show that a value of $C_D = 0.55$ in Eqs. 7.1 and 7.2 gives a reasonable fit to the data. The maximum horizontal-plane area was used for A_{pr} since as discussed in Chapter 5 the greatest contribution to the drag comes from the form sub-component. If the skin-friction had been more important the wetted-surface area could have been used. By analogy with data from circular cylinders in an enclosed channel[116] it might have been expected that the drag coefficient would be amplitude-dependent since at constant frequency change in motion amplitude corresponds to a change in Keulegan-Carpenter number. However, this appears not to be the case (or if it is then it is masked by other effects) probably because the term arises largely from the brace which is essentially a flat plate. The experimental damping ratio was $\gamma = 0.08$ with the brace and $\gamma = 0.05$ without. From potential-flow theory for Condition 1 (i.e. with the brace) a value approximately corresponding to $\gamma = 0.05$ was obtained. The length to breadth ratio of the brace gives rise to a drag coefficient, deeply submerged in unidirectional flow, of about $C_D = 1.35$. Thus, assuming this is applicable the brace accounts for about 70% of the viscous damping and hence the

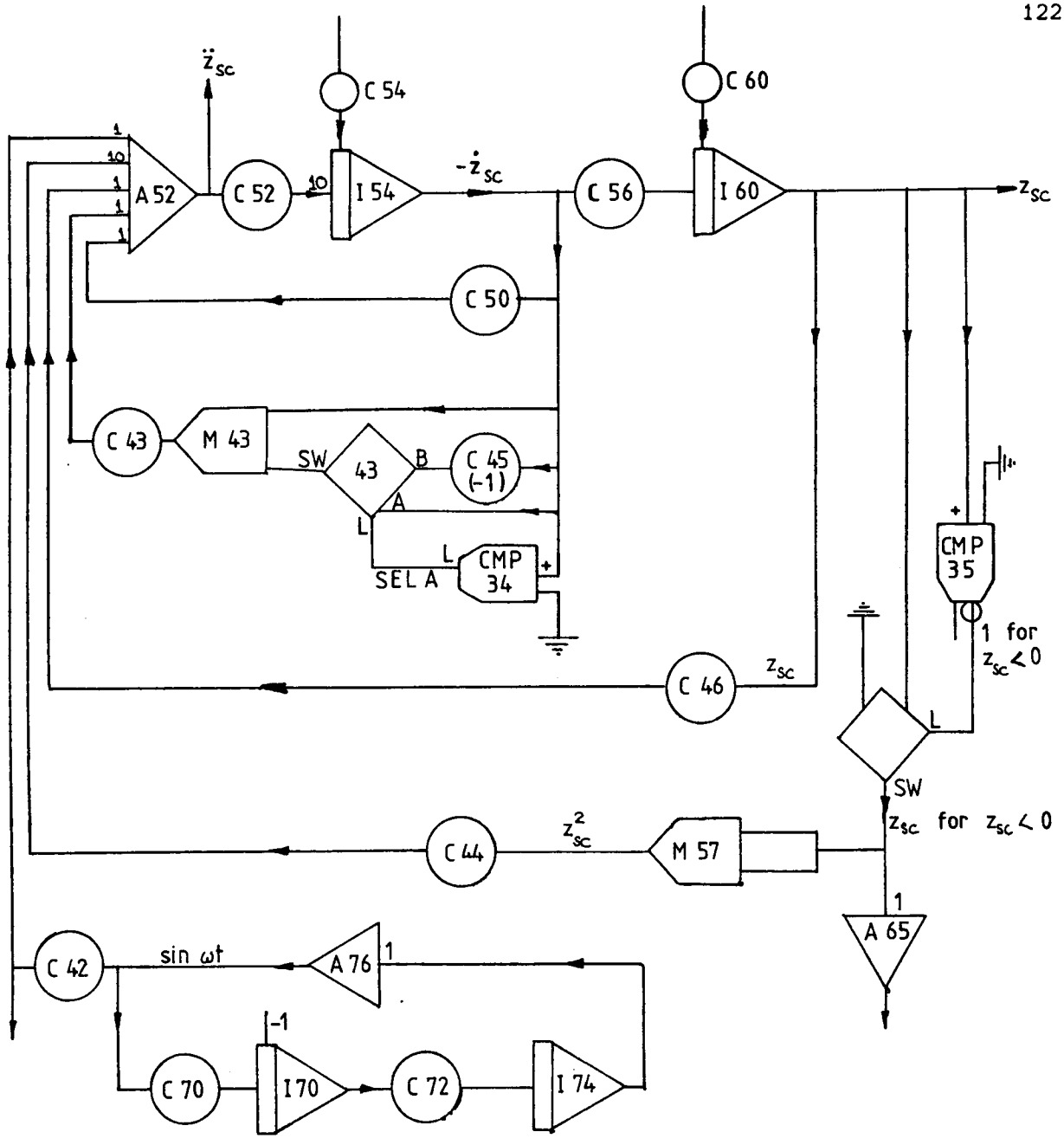

$$m' \ddot{z} + c_1 \dot{z} + c_2 \dot{z}|\dot{z}| + kz + \delta^* kn z^2 = F \sin \omega t$$

Fig. 7.1 Analogue Patch Diagram

non-linearity at resonance. It could thus be expected that removing the brace could considerably reduce the non-linearity. Figure 7.2 shows that this is indeed the case over most of the amplitude range although no longer strictly at resonance. The experimental error at small wave amplitudes could be quite large but even so the lower response at less than 3cm wave amplitude without the brace is not satisfactorily explained.

Further experiments were conducted at different frequencies and wave amplitudes to determine the importance of non-linearities. Results are given for heave, pitch, and relative bow motion for Condition 1 at 5 different frequencies, Figs. 7.3 - 7.7, and are most noticeable for their linearity. However, Fig. 7.4 shows a slight increase in RAO with wave amplitude which is attributable to velocity forces in the region where the sum of the other force components is small.

Figures 7.8 and 7.9 give results for Condition 5, (i.e. Condition 1 without the brace). The slight downward trend in response with increasing wave amplitude in Fig. 7.8 brings the heave response down to the Condition 1 value in Fig. 7.7. Figure 7.9 shows no rise in response comparable to Fig. 7.4. This, in conjunction with the data in Fig. 7.2 shows that the bracing can have an effect on vessel motions. (In a previous study for semi-submersibles Forsyth and Miller[117] suggested that in head seas bracing had negligible net effect on the heave response but their experimental data only went down to $\omega/\omega_H \simeq 1.9$.) Figure 7.10 shows the results that accompany the Condition 5 heave results of Fig. 7.2.

7.4 Effect of Column Flare

Flaring the columns above the still-water-line improves the static stability and the structural strength, and it has also been implied[6] that it decreases the motions. It is generally recognised, from examination of the steady-state solution for forced vibrations of a linear single-degree-of-freedom system, i.e. Eq. 6.6, that at sub-resonant frequencies the response is largely controlled by the spring constant (which in this case is $\rho g A_w$). Increasing this will tend to decrease the motion, (although it will also affect the

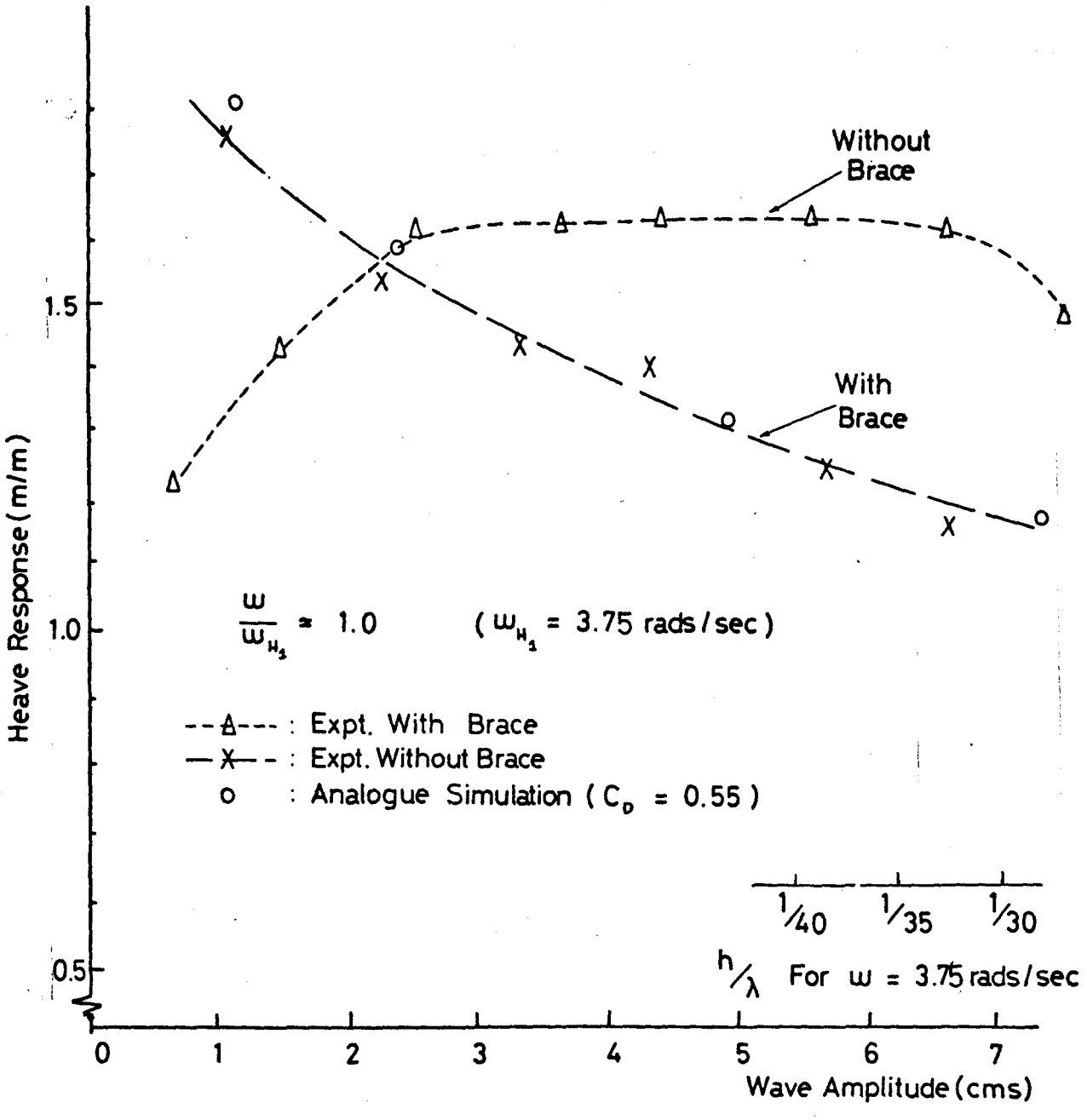

Fig. 7.2. Resonant Heave Response.

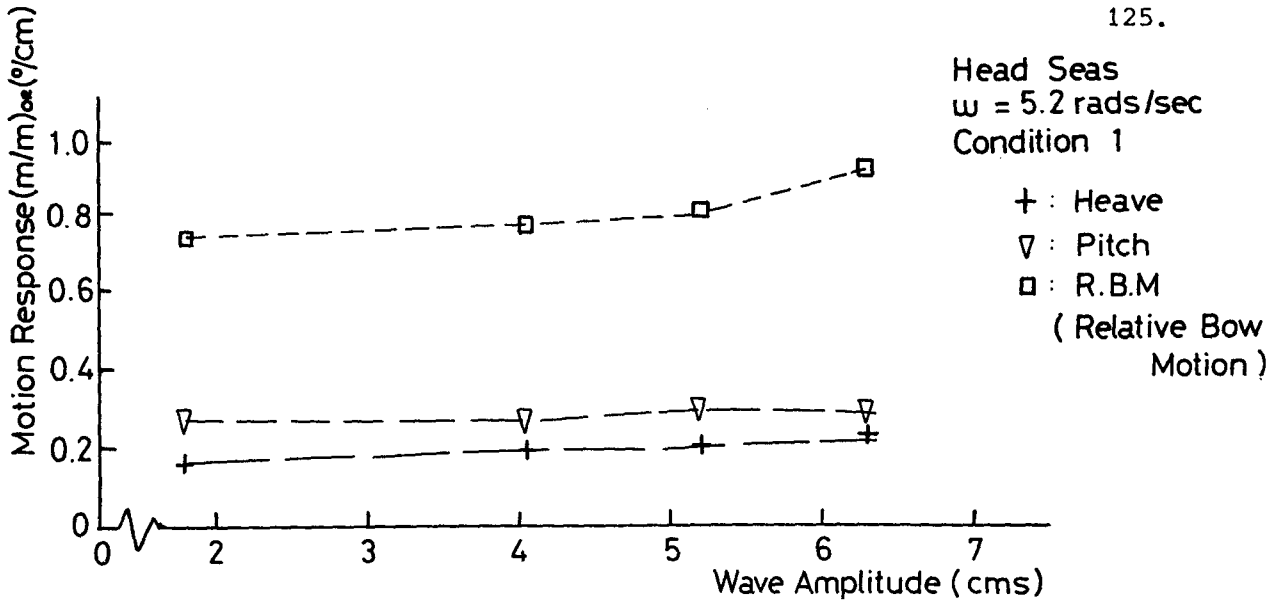

Fig. 7.3. Head Sea Motion Response.

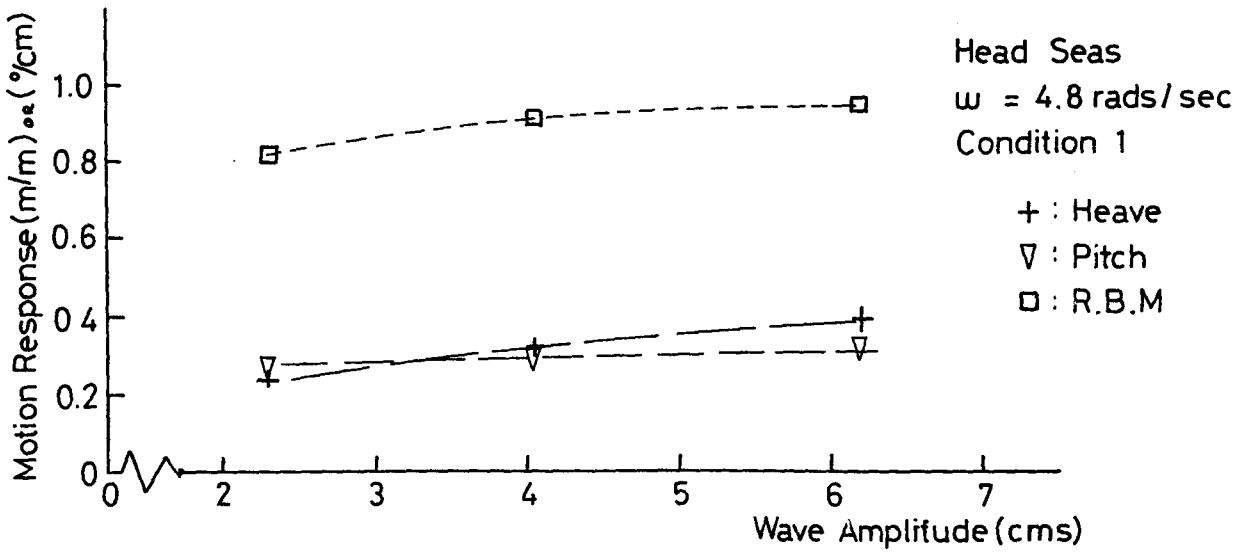

Fig. 7.4. Head Sea Motion Response.

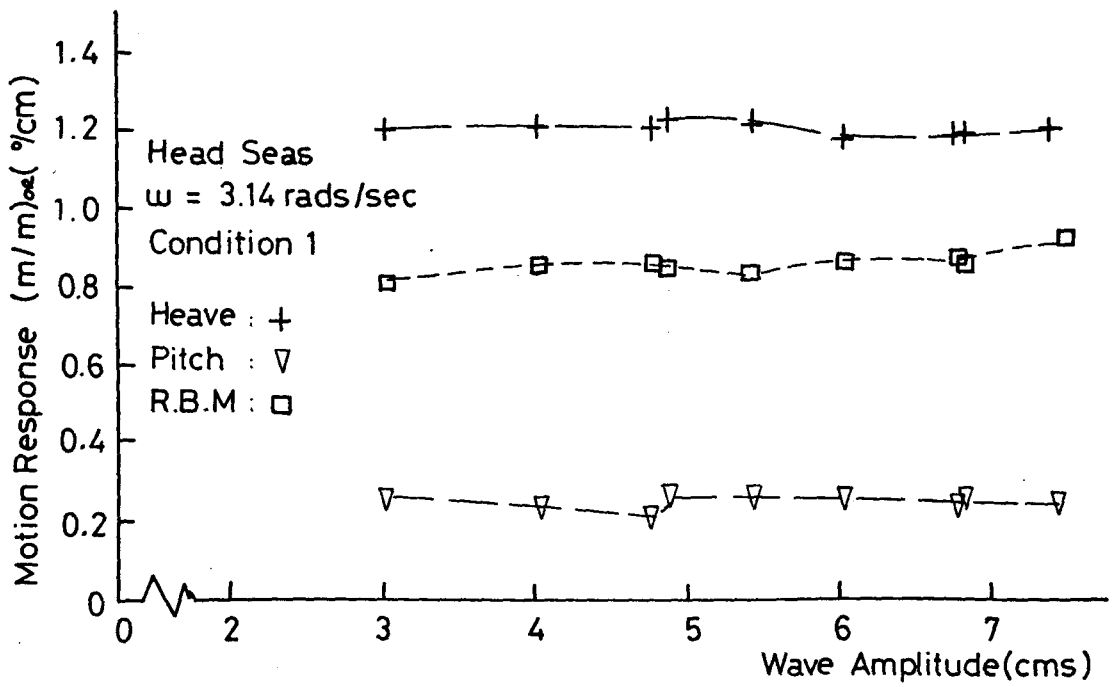

Fig. 7.5. Head Sea Motion Response.

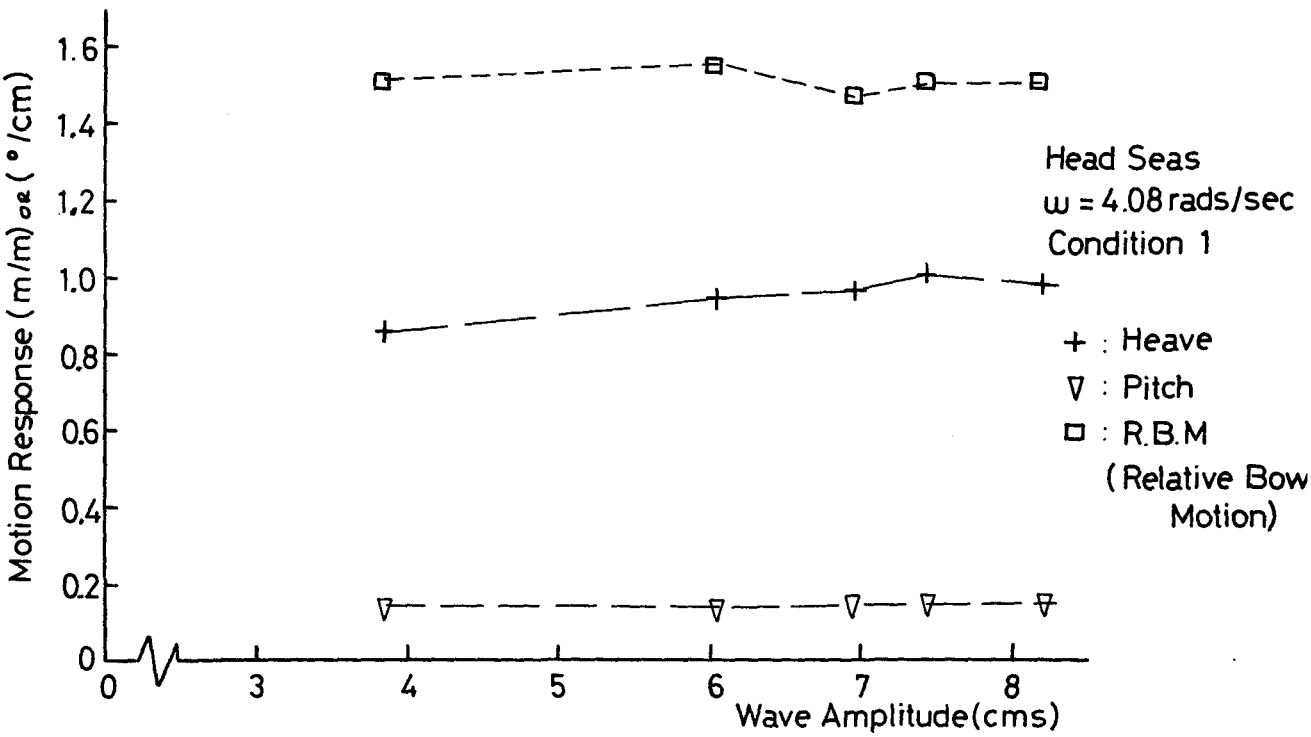

Fig. 7.6. Head Sea Motion Response.

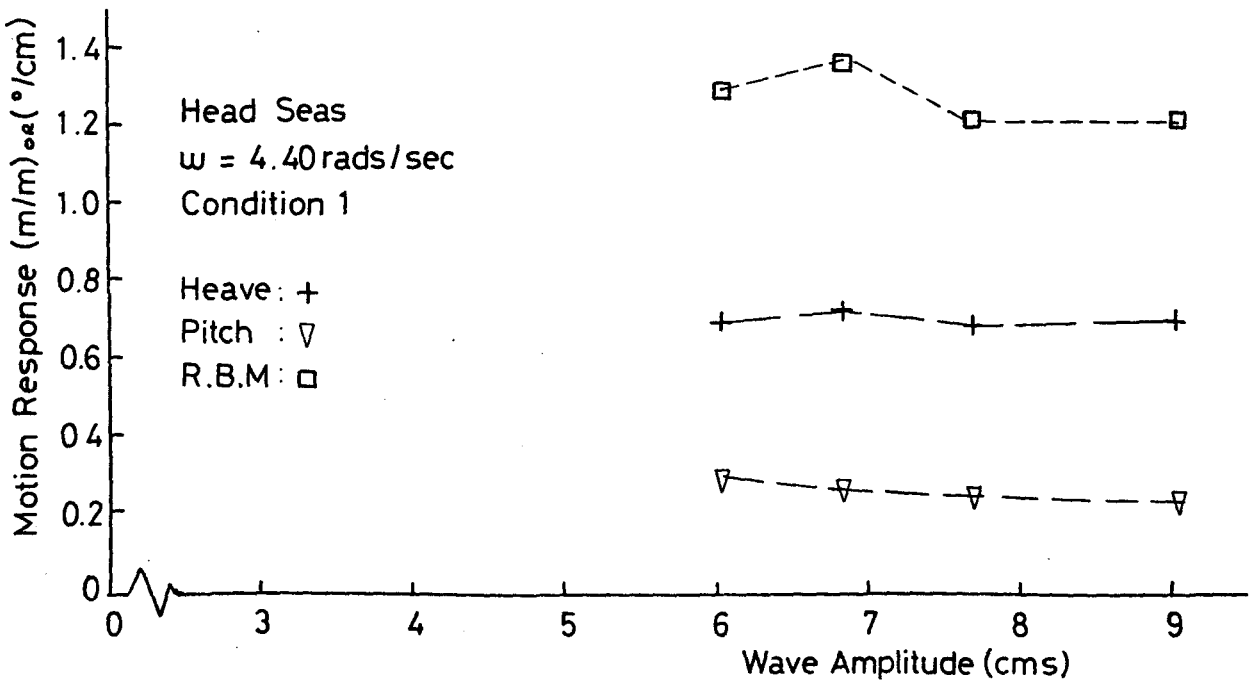

Fig. 7.7. Head Sea Motion Response.

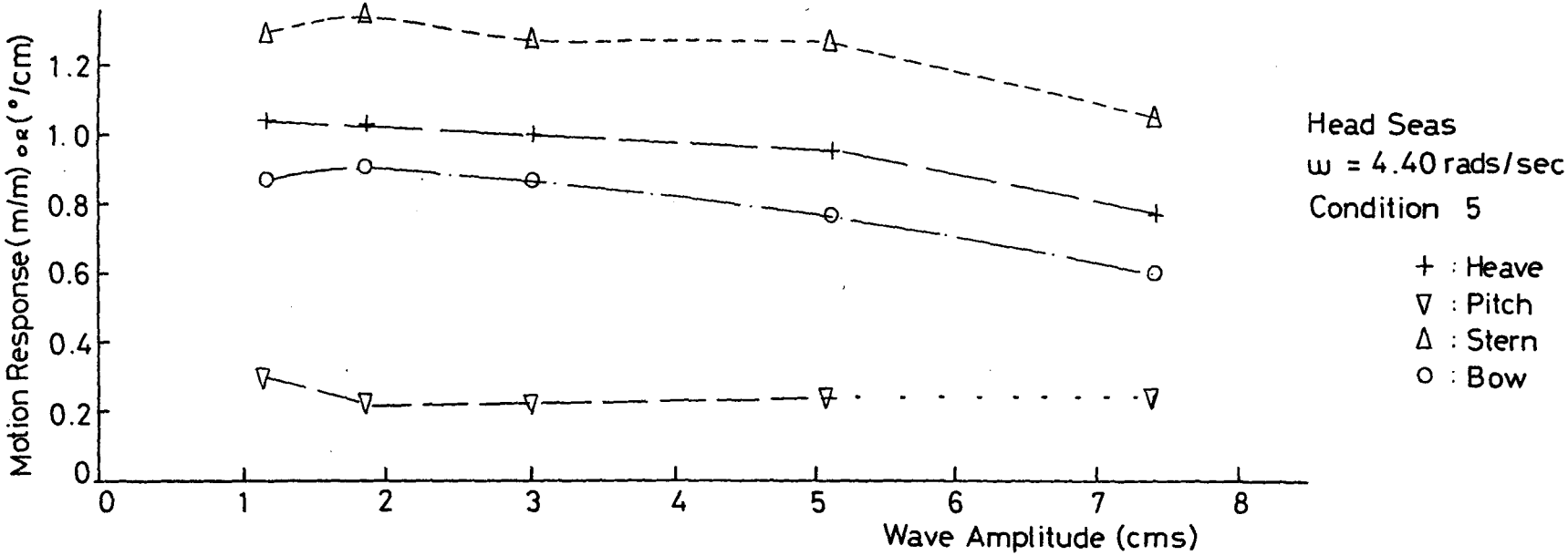

Fig. 7.8. Head Sea Motion Response.

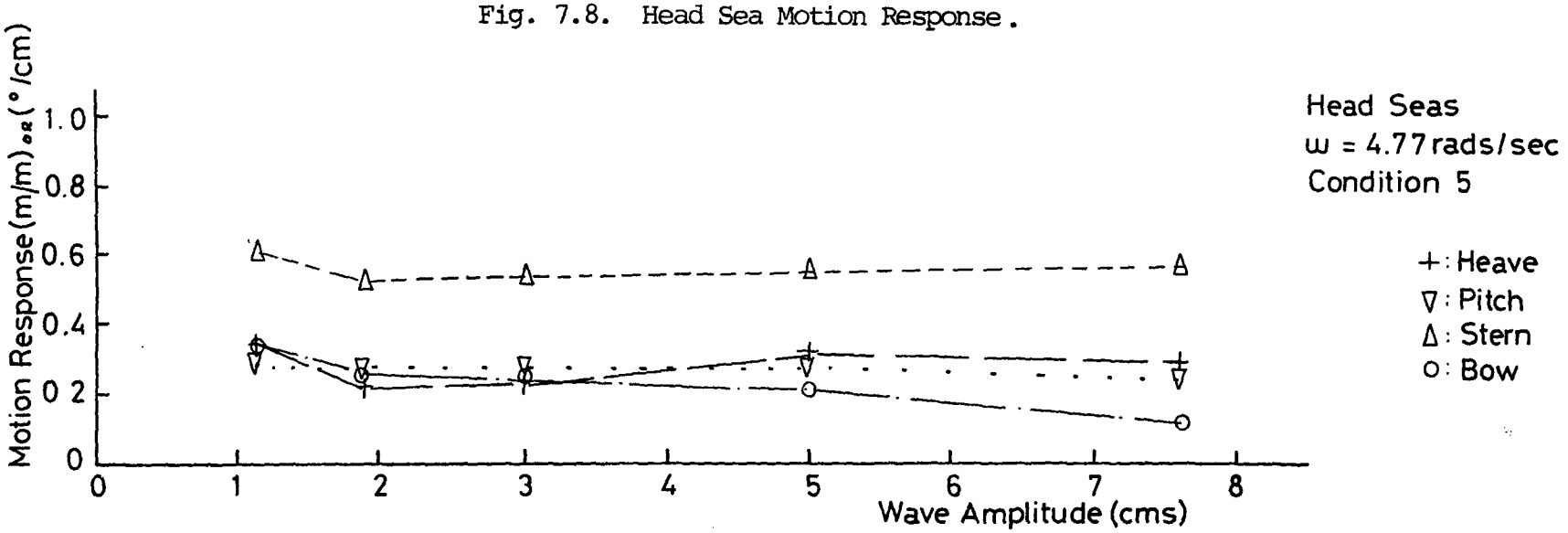

Fig. 7.9. Head Sea Motion Response.

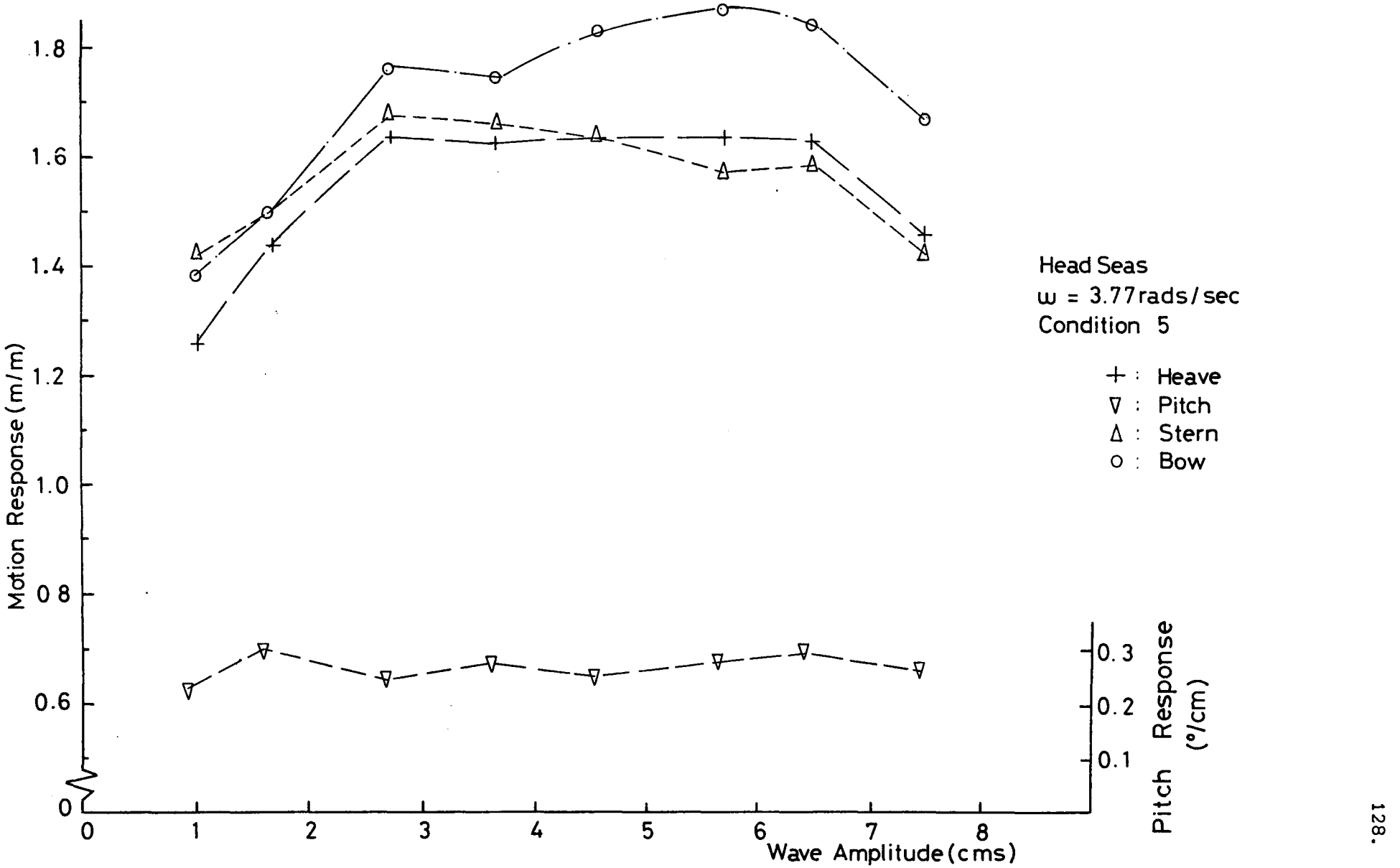

Fig. 7.10. Head Sea Motion Response.

natural frequency). To investigate this effect using the analogue computer it was assumed that the column flare only contributed to the heave restoring force and only when the vessel heaved downwards. Thus the equation of motion was patched as

$$(\Delta+AM)\ddot{z} + C_1\dot{z} + K_z z + \delta^* K_z nz^2 = F \sin \omega t \quad \ldots\ldots \quad 7.3$$

where $\delta^* = 0$ for $z \geqslant 0$ and $\delta^* = -1$ for $z < 0$.
The factor, n, gives the desired ratio for A_w^*/A_w where A_w is the waterplane area at the still-water-line and A_w^* is the waterplane area at the junction between column and deck. (For $A_w^*/A_w = 2$, $n = 8.33$; for $A_w^*/A_w = 3$, $n = 16.66$.) All other values were maintained as before. This was included in an internal report[118] and typical curves are shown in Fig. 7.11. The reduction in heave response with increasing column flare looks quite plausible but was not borne out by subsequent experiments. Similarly, the decrease in response-amplitude-operator with increased wave amplitude seemed quite reasonable.

7.5 Experimental Results

To investigate the answers from the simulation, flare was added to the model columns. These were very light polystyrene 'wedges', (the mass to double the waterplane area was about 0.07 kg or 0.32% of the displacement) so neither the displacement nor the height of the centre of gravity were significantly altered. The 'wedges' were symmetrical fore and aft with the shape as defined by the body-plans, Fig. 7.12.

Head sea experiments were conducted for a number of different conditions involving different permutations of column flare, fin and GM. The column separation, draught, and displacement are essentially as in Conditions 1 or 5, in Table XII, and other details are as given in Table XV.

For Condition 7 the results at three frequencies are given in Figs. 7.13, 7.14 and 7.15. Comparing Figs. 7.14 and 7.2 no real heave reduction is apparent and certainly not of the size predicted by the simulation, Fig. 7.11.

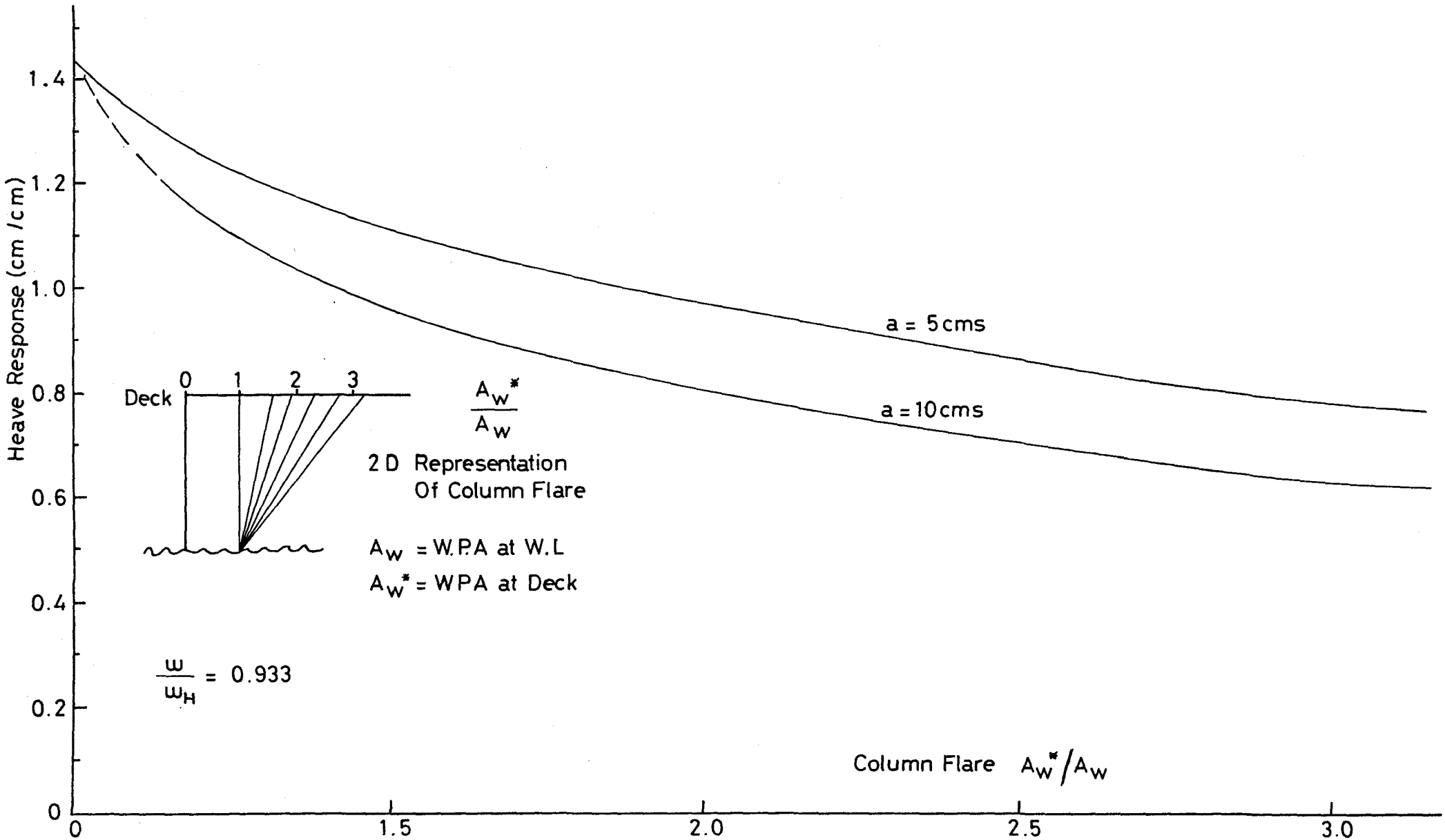

Fig. 7.11. Heave Response: Simulated Effect of Column Flare.

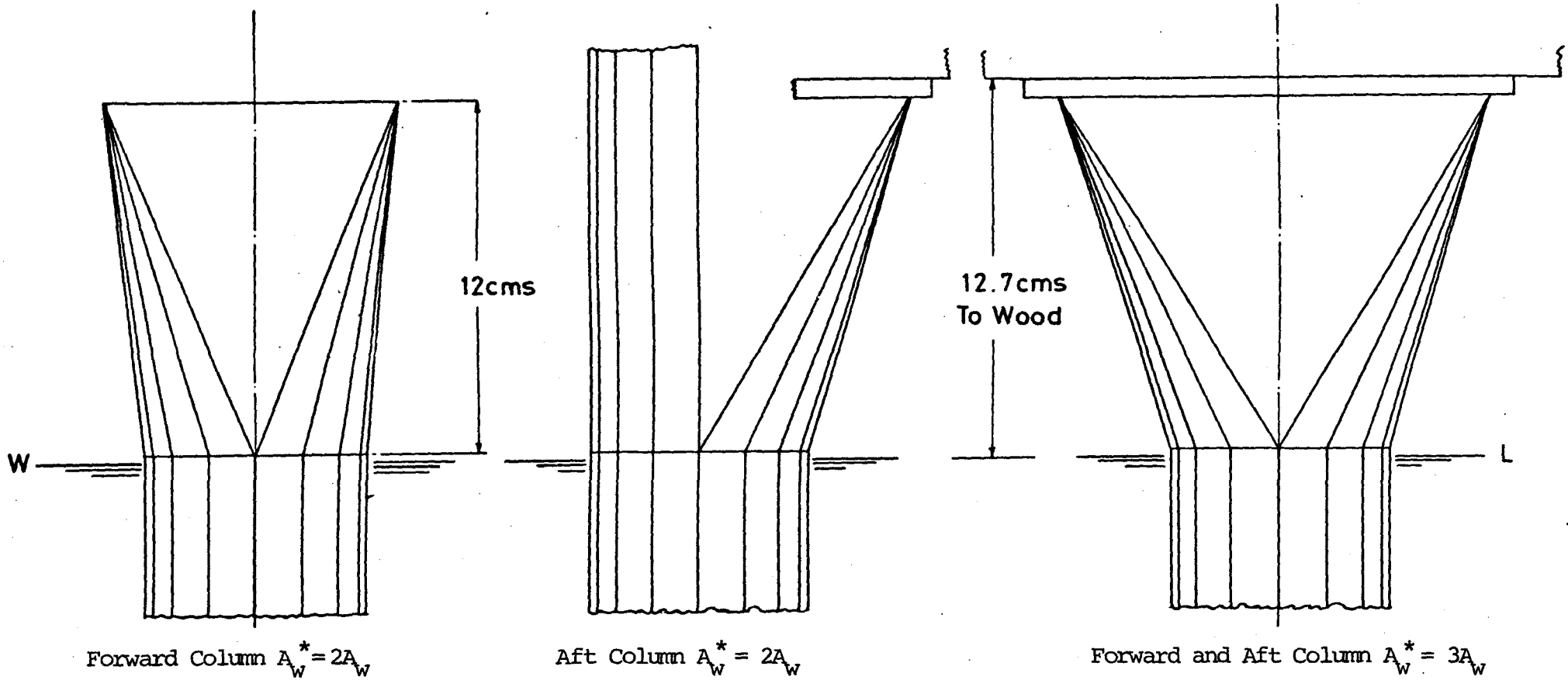

Fig. 7.12. Body Plans for Column Flare used in Motion Tests.

Condition	Appendages	Upright GM_T (cms)	Column Flare, $\frac{A_W^*}{A_W}$		Approximate 'Resonant' Frequencies	
			Forward	Aft	Heave (rads/sec)	Roll (rads/sec)
7	Brace	4.0	2	2	3.95	1.86
8	Brace	4.0	3	2	4.00	1.86
9	None	4.0	3	3	4.20	1.90
10	Brace	4.0	3	3	4.23	2.00
11	Brace	1.7	3	3	4.23	1.82
12	None	4.0	3	3	4.49	1.89
13	Brace	1.7	-	-	3.75	1.20
14	Brace	1.7	3	2	4.00	1.80

TABLE XV. Flared Column and Other Conditions

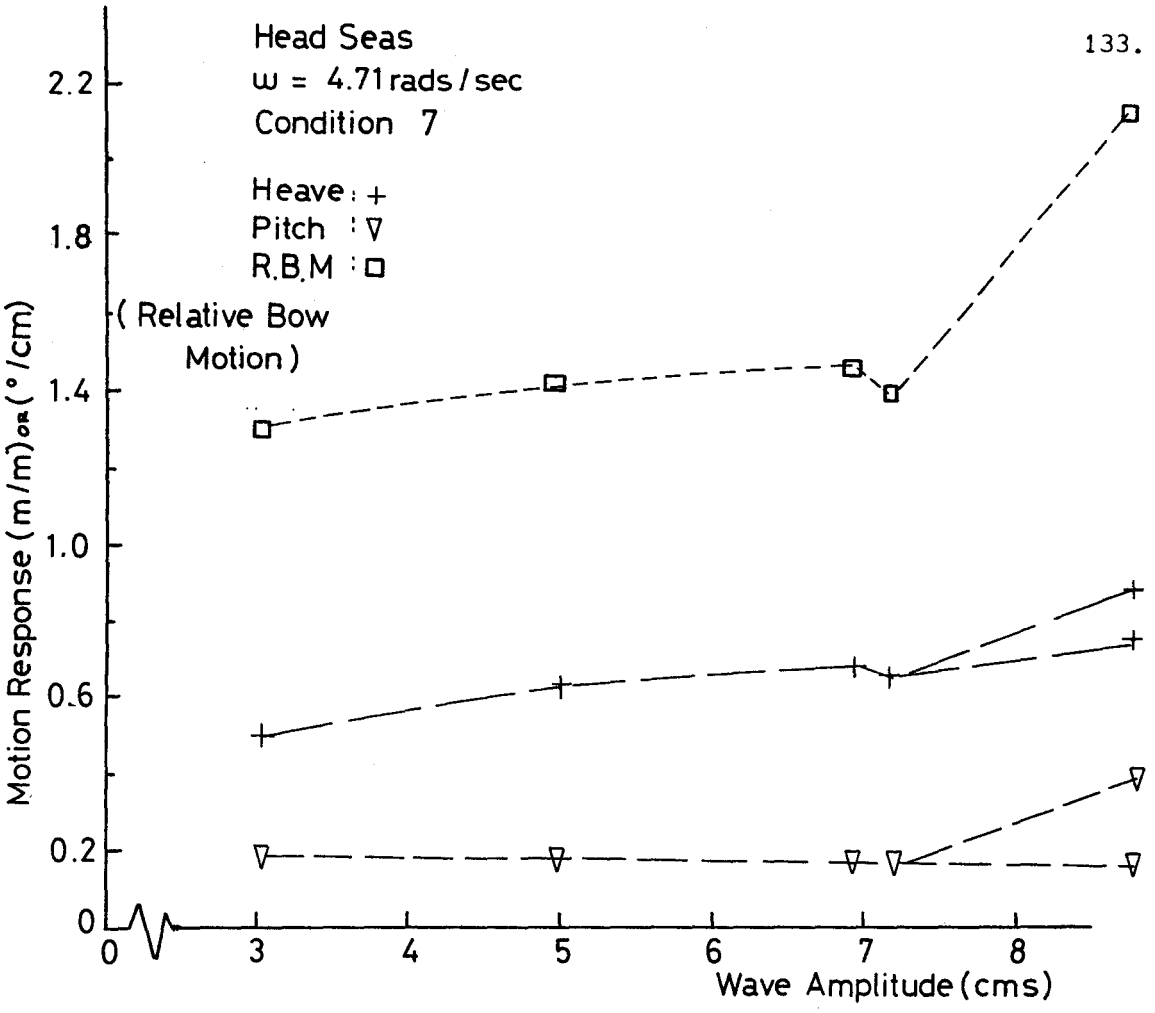

Fig. 7.13. Head Sea Motion Response.

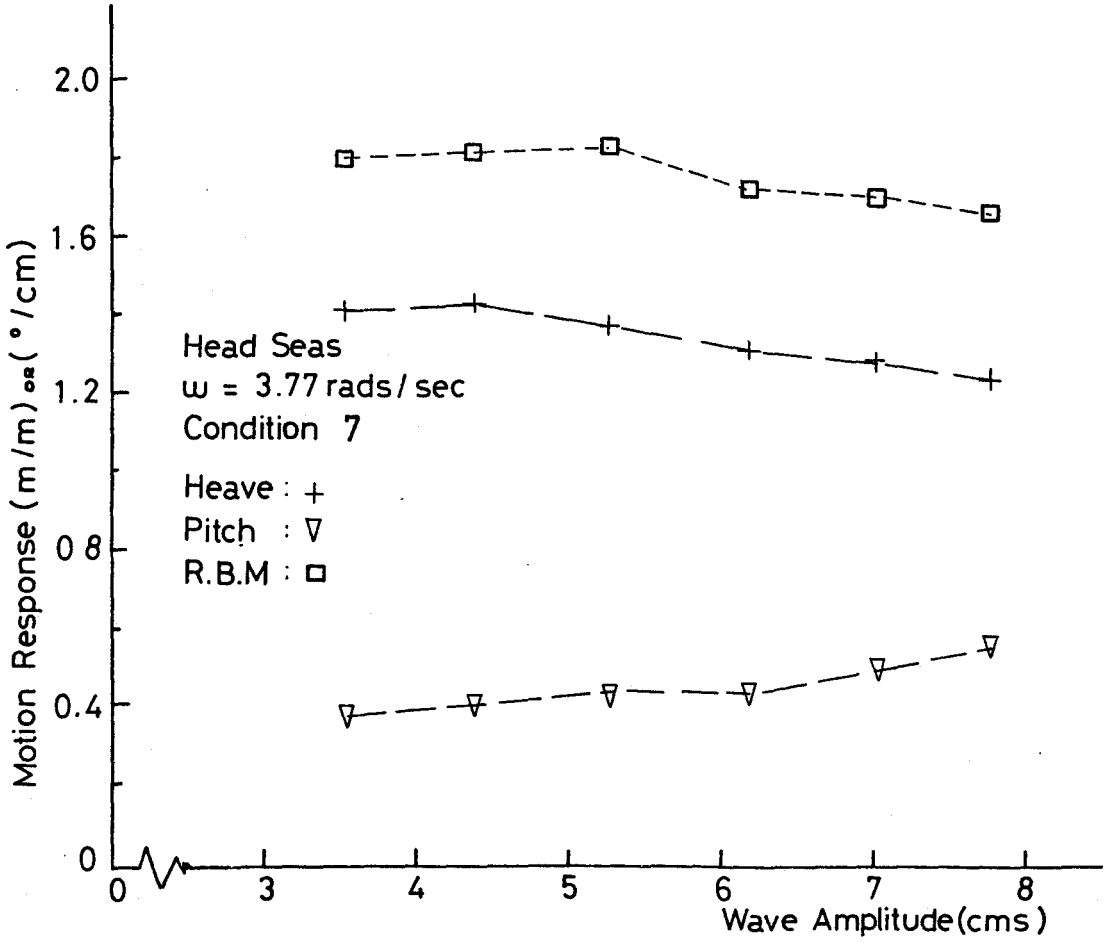

Fig. 7.14. Head Sea Motion Response.

Comparing Figs. 7.15 and 7.5 although there is a heave reduction of around 8% the pitch motions increase by about 30% as does the relative bow motion, which can hardly be called an improvement.

The column flare was further increased on the forward column to give Condition 8 (i.e. Aft $A_w^* = 2A_w$, Fwd $A_w^* = 3A_w$). Some experimental results are given in Figs. 7.16 - 7.24 for a range of frequencies. Immediately noticeable for this Condition is the fact that there is a marked departure from the expected behaviour in Figs. 7.16 and 7.20. This is the 'jump' phenomenon which is a characteristic of mass-non-linear spring systems. The response of such a system with damping and a hardening spring, as is the case here, is illustrated in Fig. 7.25. Strictly speaking, resonance is not possible for such a system but Table XV still includes a 'natural' frequency based on decay tests. From Fig. 7.16 it can be seen that there is an abrupt change in the heave, pitch and relative motion responses at a wave amplitude around 7cm. However, the actual value is not clear-cut because there is a band of amplitude about 0.5cms wide in which either solution seems to be able to exist in a well-defined and enduring manner in any one experimental run. Figure 7.20 again shows the jump (although no actual overlap of solutions in this case) and includes also the motion at the bow and stern. From both Figs. 7.16 and 7.20 before the jump the pitch is very small and since in both cases the relative bow motion response is about twice the heave response then it can be concluded that the bow motion is approximately 180° out of phase with the wave crest. This is borne out by visual observation and results in a considerable increase in waterplane-area for the forward column during the cycle. This is the equivalent of a hardening-spring and it can therefore be hypothesised that the jump actually occurs for the forward column thus affecting all the other motions.

Above the 'natural' frequency the column flare does not cause any decrease in heave motions as can be seen from comparing Figs. 7.17 and 7.3, and Figs. 7.18 and 7.2. Even before the occurrence of the jump the heave in Fig. 7.20 is larger than the corresponding values in Fig. 7.7 and after the jump the heave is nearly 50% greater than it would have been without flare. A sharp rise is evident in Fig. 7.22 and comparison of Fig. 7.23 with 7.6 suggests that the jump has occurred here as well.

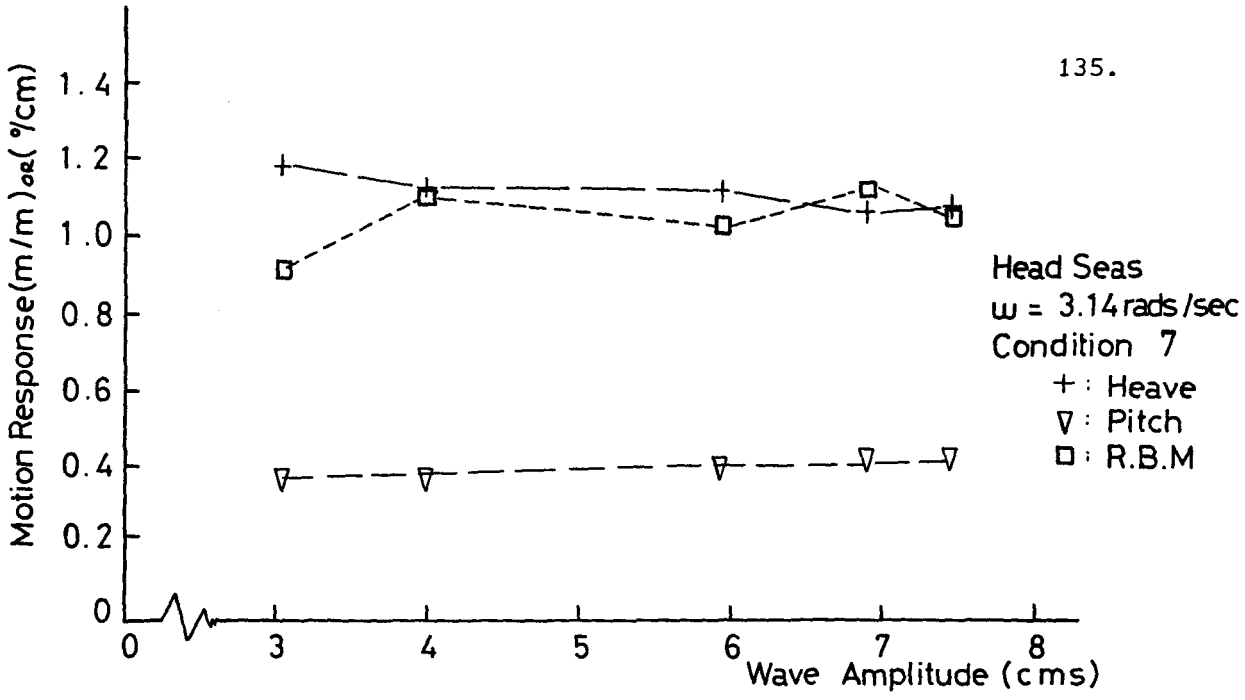

Fig. 7.15. Head Sea Motion Response.

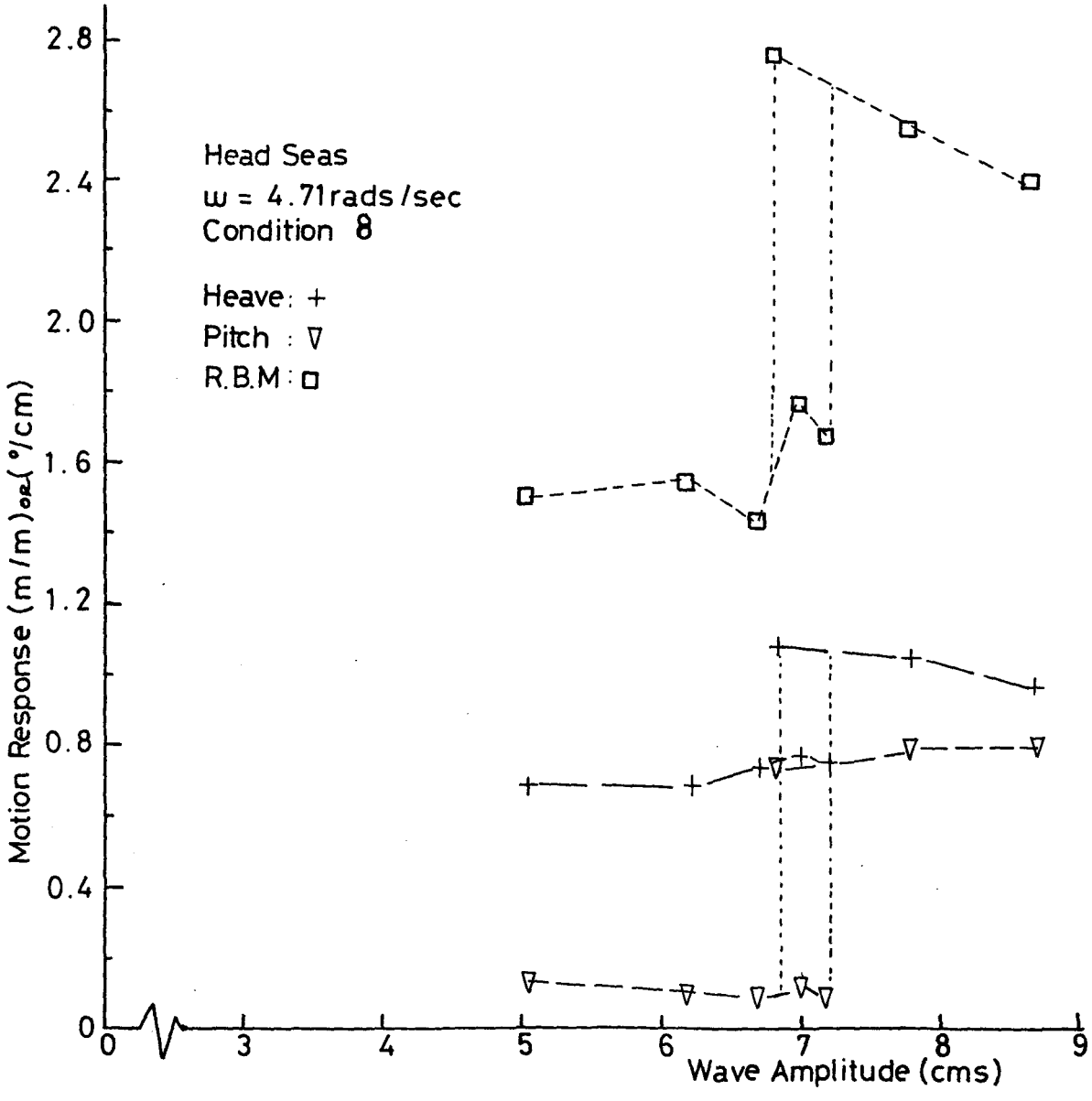

Fig. 7.16. Head Sea Motion Response.

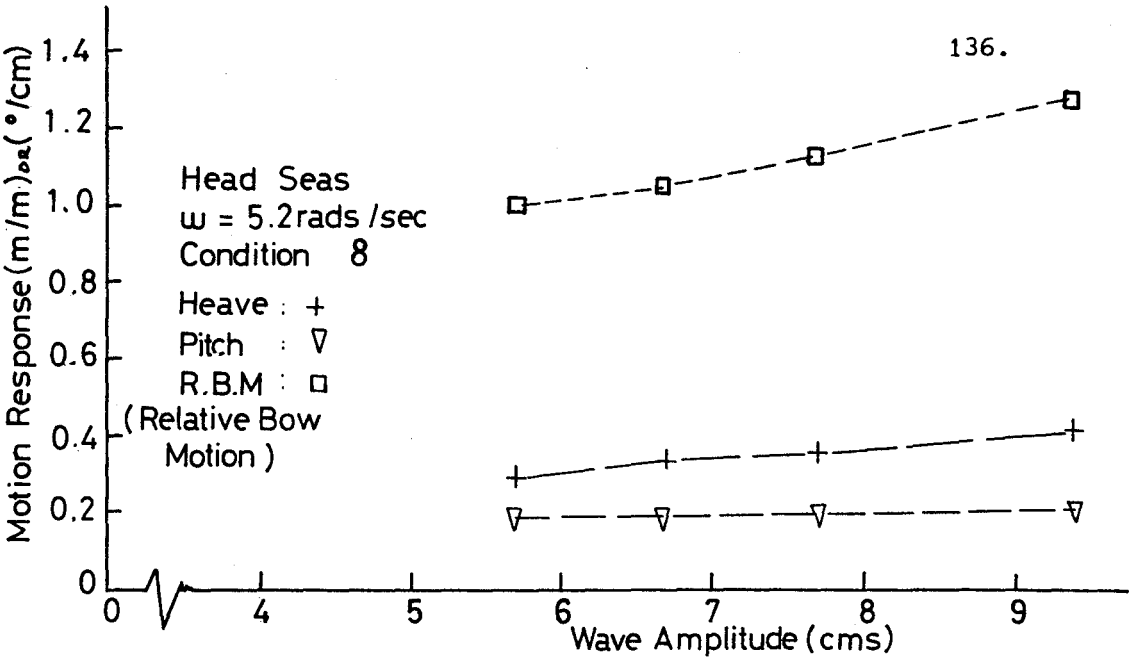

Fig. 7.17. Head Sea Motion Response.

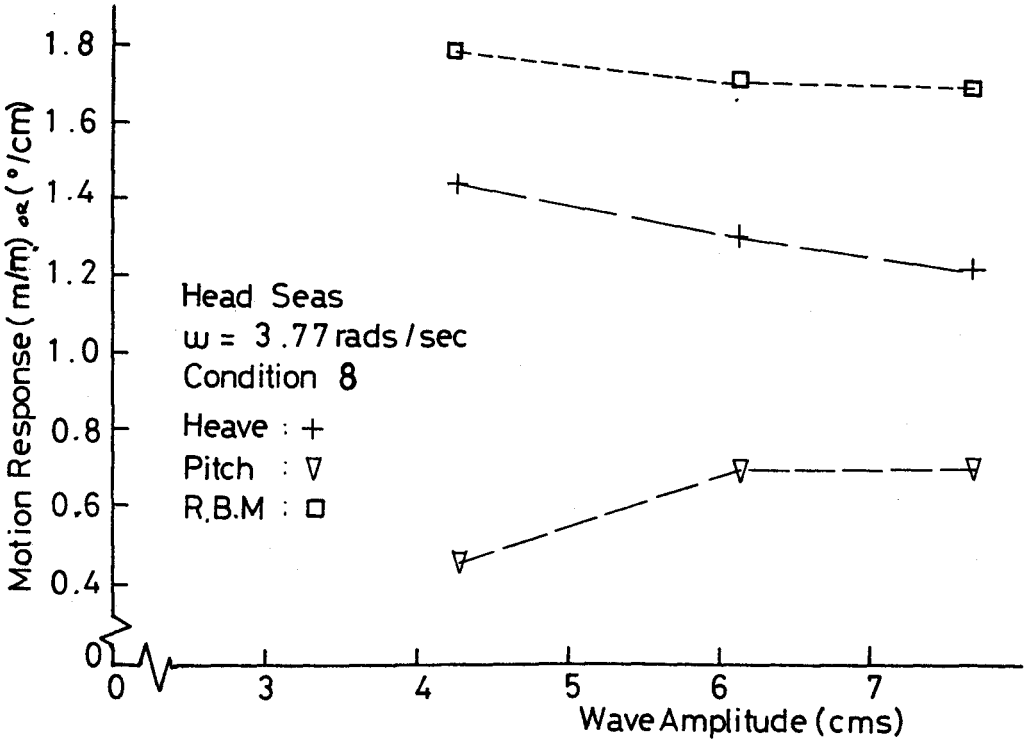

Fig. 7.18. Head Sea Motion Response.

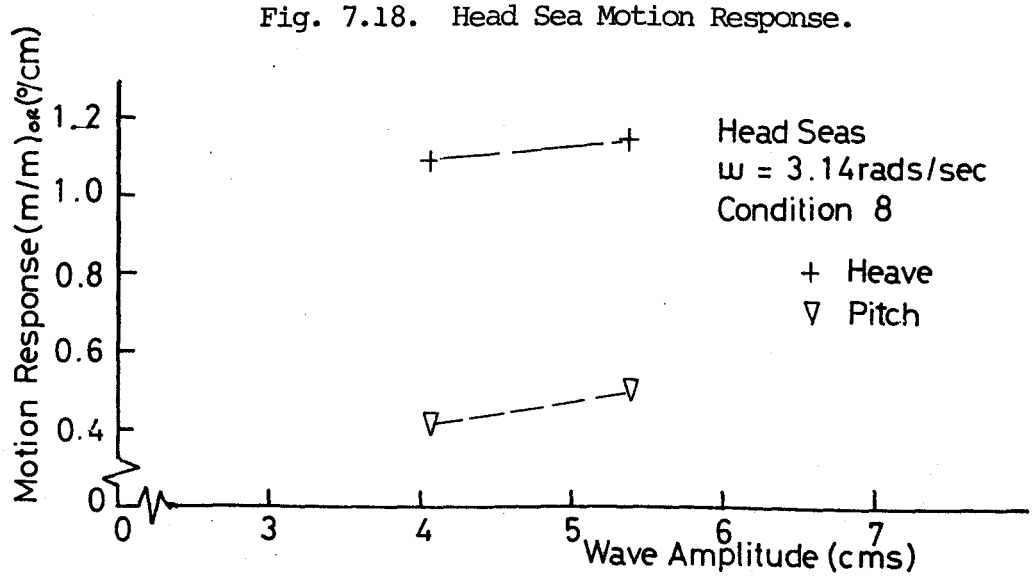

Fig. 7.19. Head Sea Motion Response.

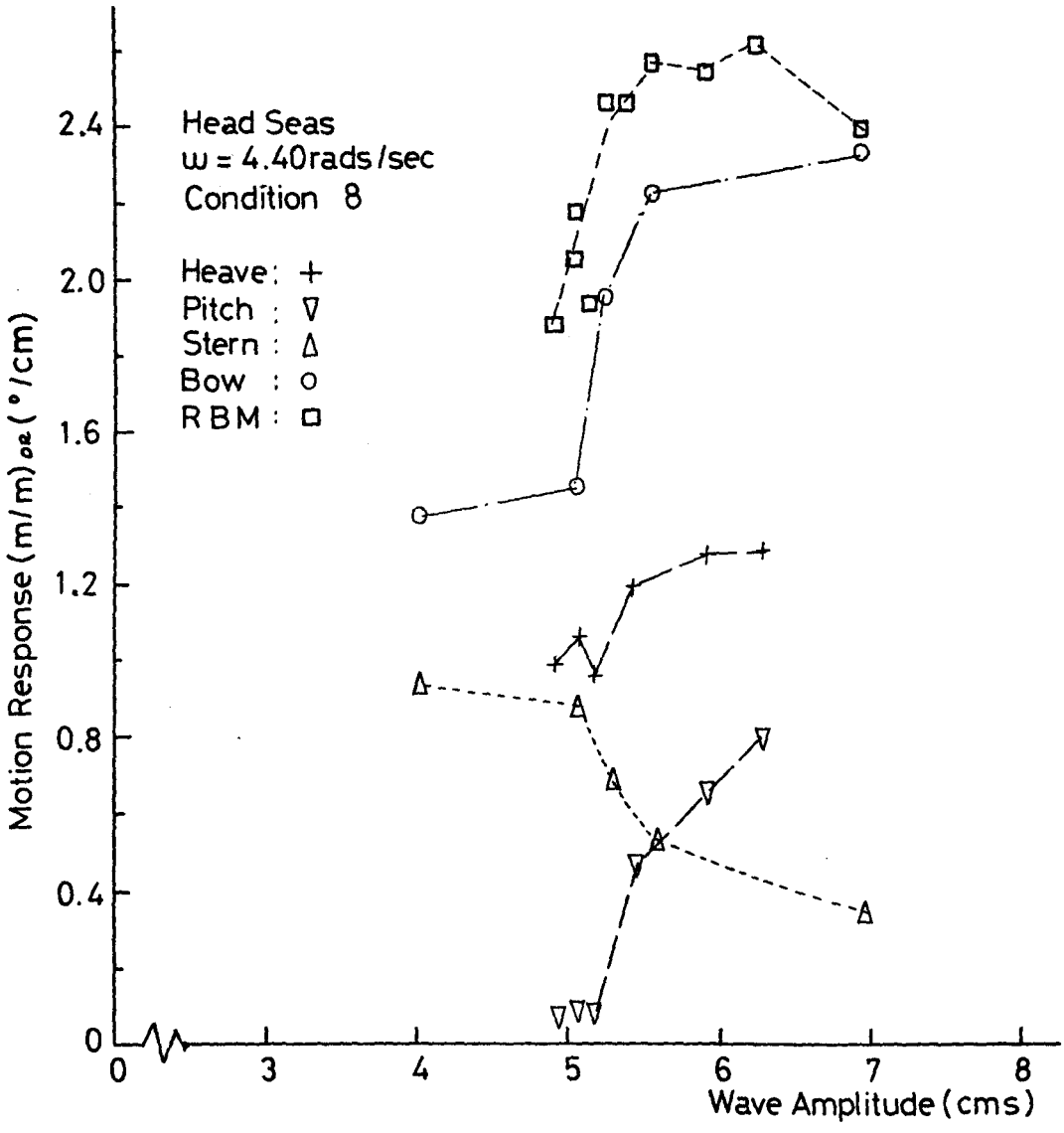

Fig. 7.20. Head Sea Motion Response.

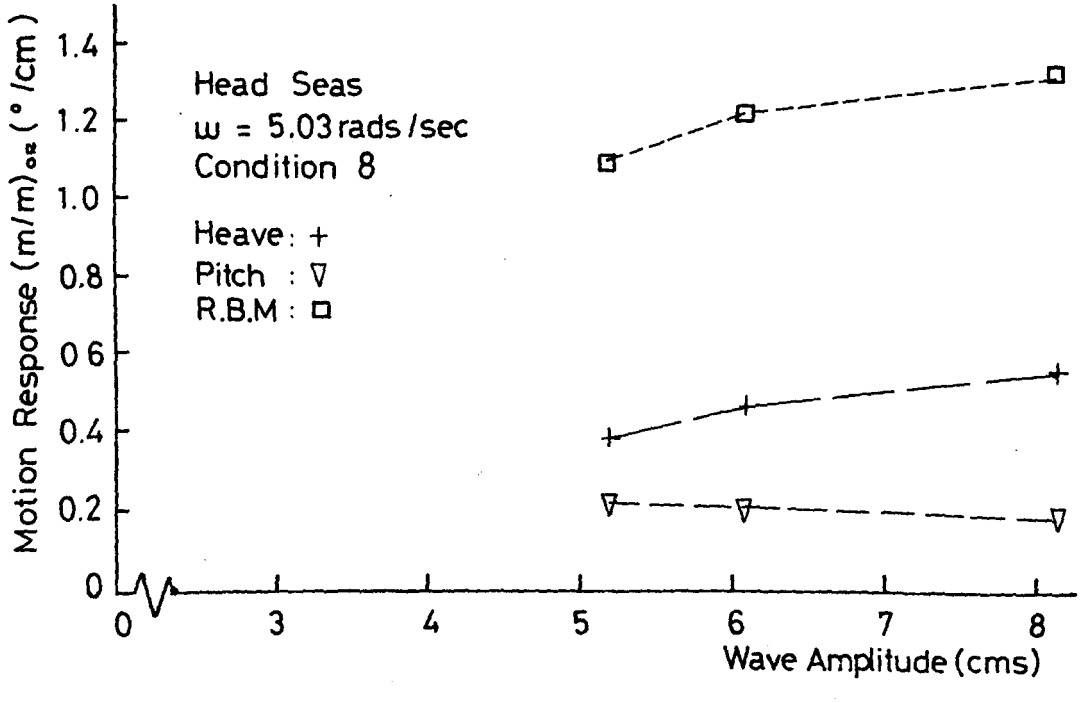

Fig. 7.21. Head Sea Motion Response.

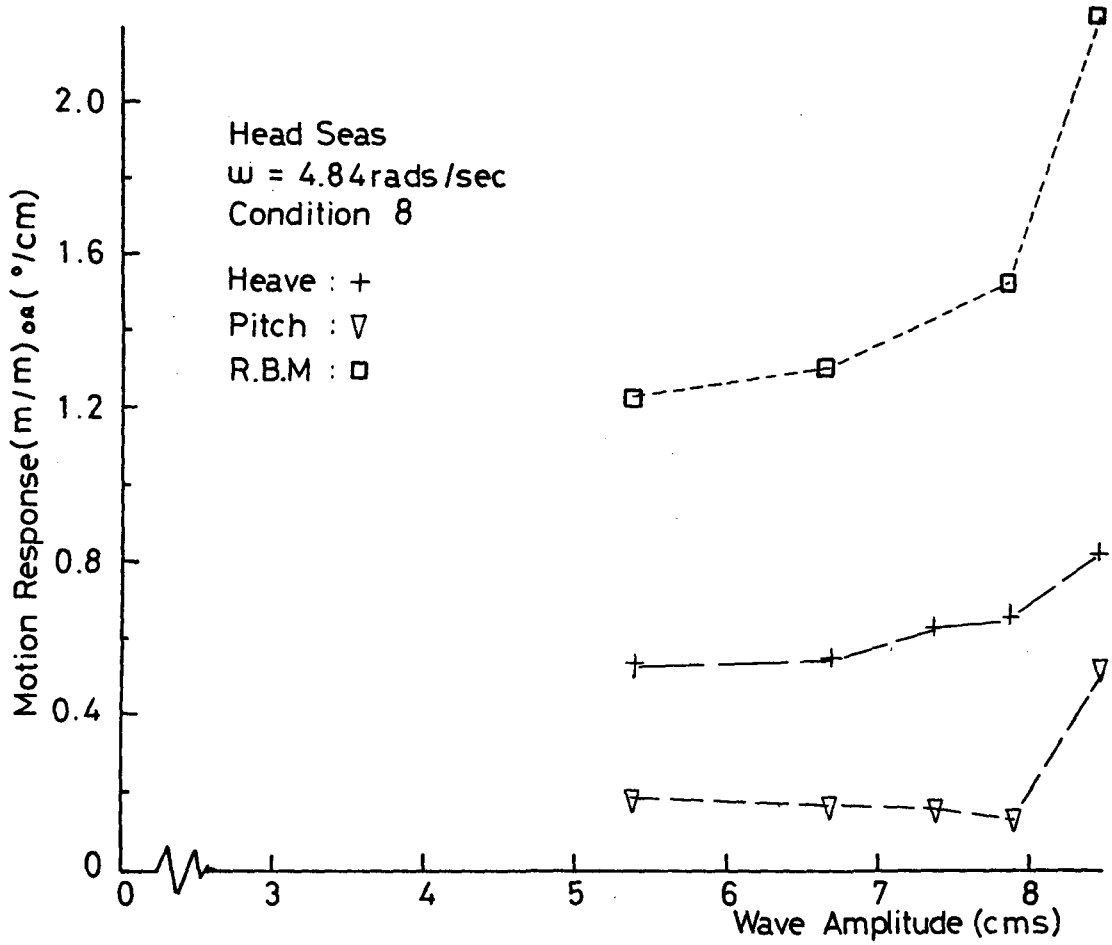

Fig. 7.22. Head Sea Motion Response.

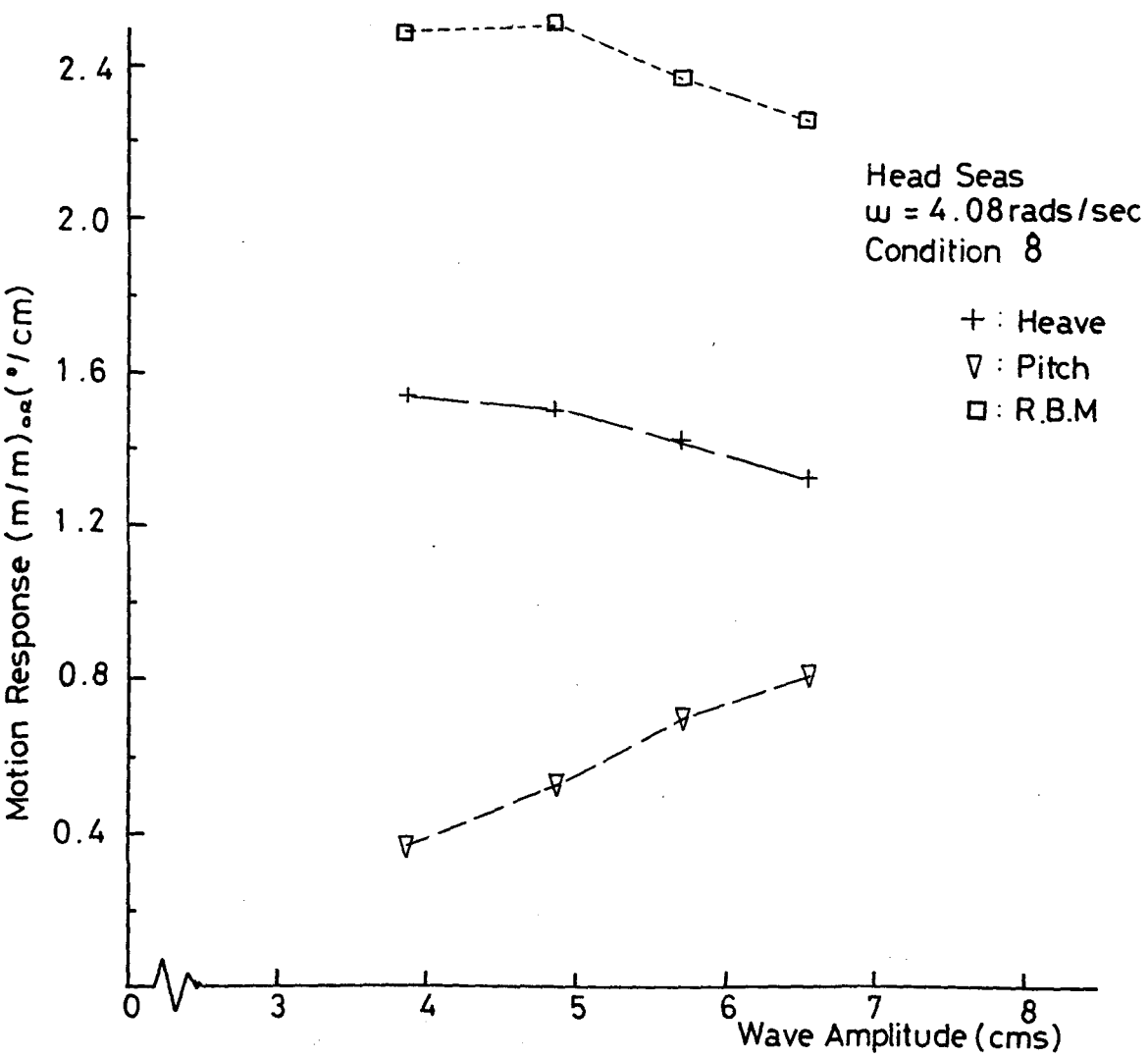

Fig. 7.23. Head Sea Motion Response.

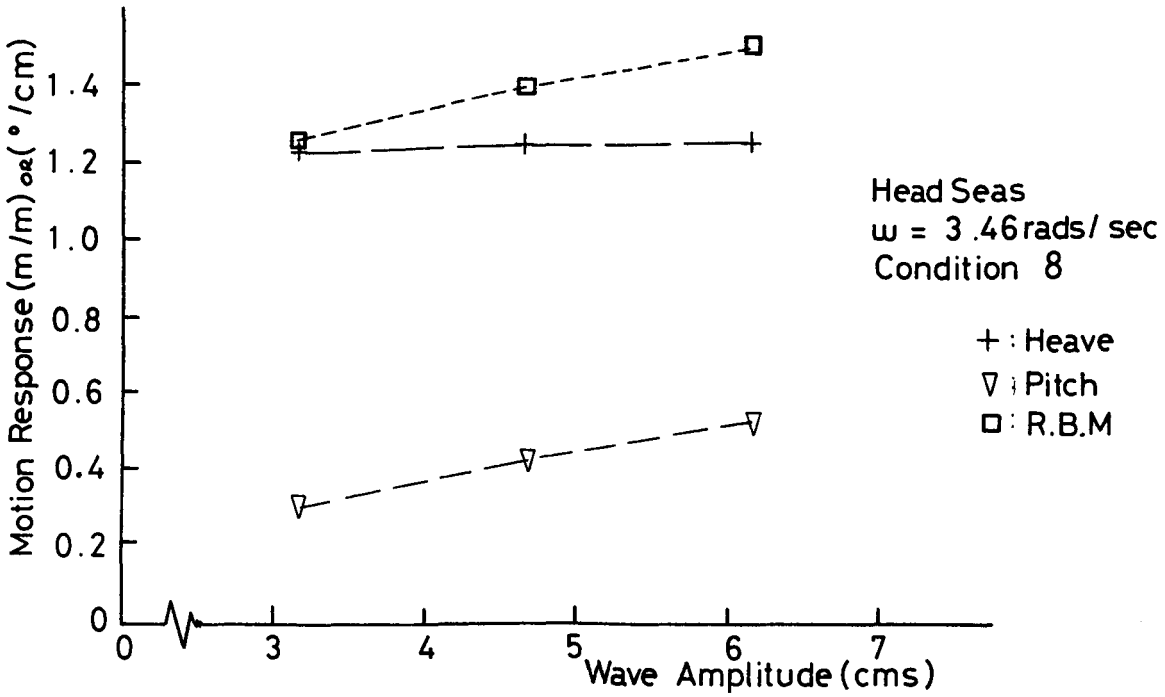

Fig. 7.24. Head Sea Motion Response.

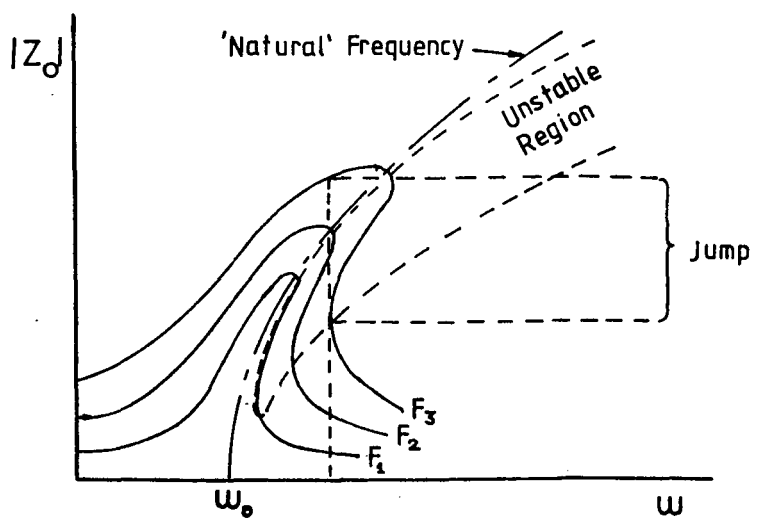

Fig. 7.25. Response for Damped Mass Hardening-Spring System.

At lower frequencies it can be seen from comparing Figs. 7.19 and 7.5 that with the flare a small heave reduction of around 8% occurs. However, this is not as great as suggested by the simulation, Fig. 7.11, and, in addition, the experimental results suggest an increase in response-amplitude-operator with increasing wave amplitude rather than a decrease. In Condition 9, which is Condition 8 without the brace the jump phenomenon also appeared. However, in this case, because of the lower damping, the responses were even larger as can be seen from comparing Figs. 7.26 and 7.20. Even more interestingly there was a wave amplitude at which the 'stern' exhibited a 'beating' motion. It has been shown above that in Condition 8 there existed a thin band of wave amplitudes for which two experimental solutions could exist which were both 'stable' in the sense that they persisted all during the course of a long test. A probable explanation for the beating motion is that it represents the stern (in this case) moving from one solution to another.

7.6 Discussion

The foregoing results show that the linear response approximation is generally valid. At resonance the presence of the brace seems to cause a reduction in response-amplitude-operator with increasing wave amplitude which is attributable to viscous effects. This has been modelled on an analogue computer. At other frequencies the bracing can also have a minor effect. (For conventional semi-submersibles in which only a small proportion of the hulls are covered by columns the behaviour at the corresponding frequencies may be affected by the hulls and not just the bracing. This may cause the effect of the bracing to seem less significant.)

The main exception to the above generalities is the occurrence of the jump phenomenon which can cause a dramatic change in motion response. To predict such motions it is necessary to have an accurate prediction of the relative motions, especially at the bow in this case. As shown in Chapter 6 this has not been achieved here but work reportedly being conducted elsewhere may enable it to be done.

The jump phenomenon is of course well-known and is conveniently illustrated theoretically by the Duffing type of equation considered

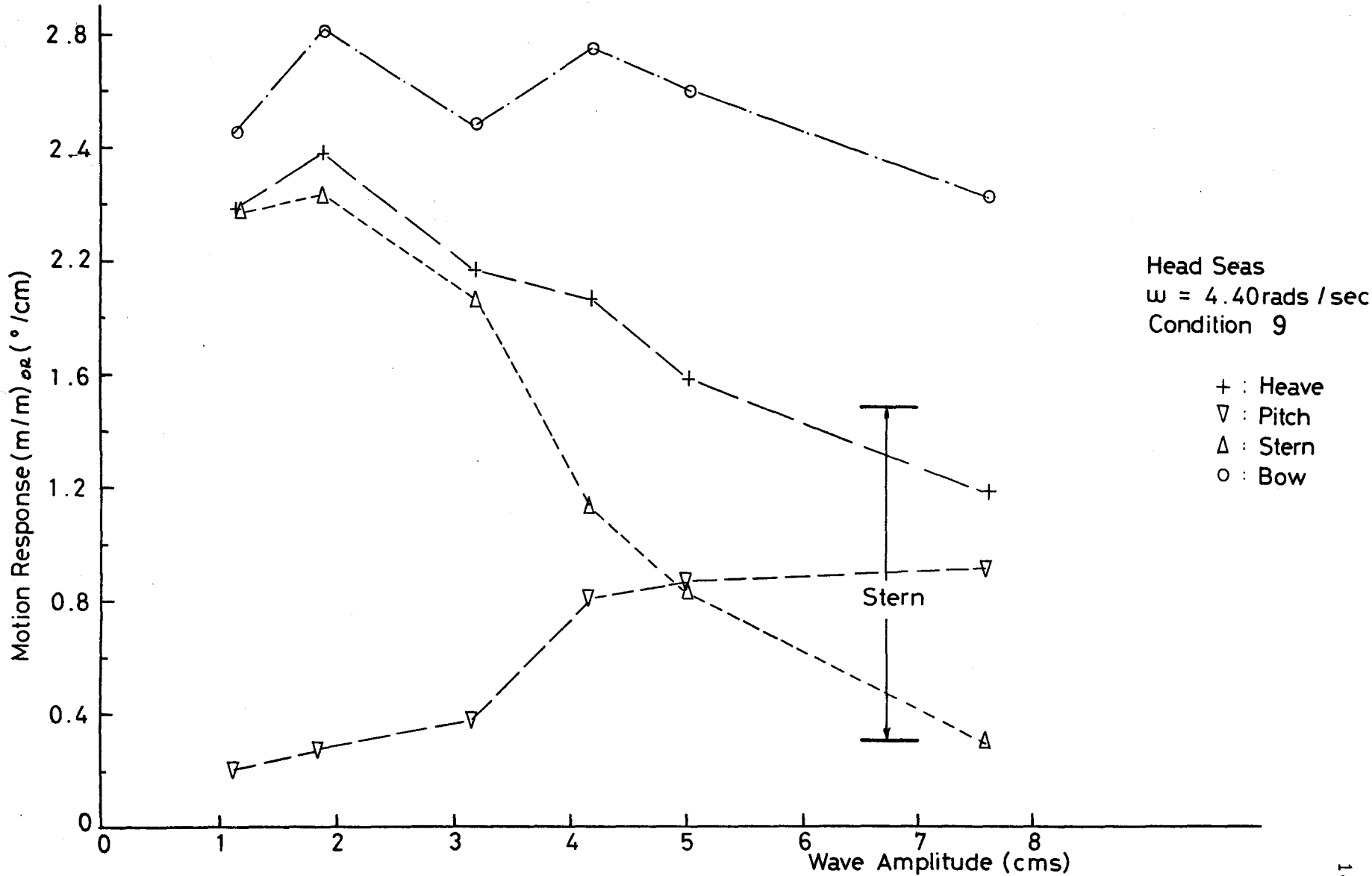

Fig. 7.26. Head Sea Motion Response.

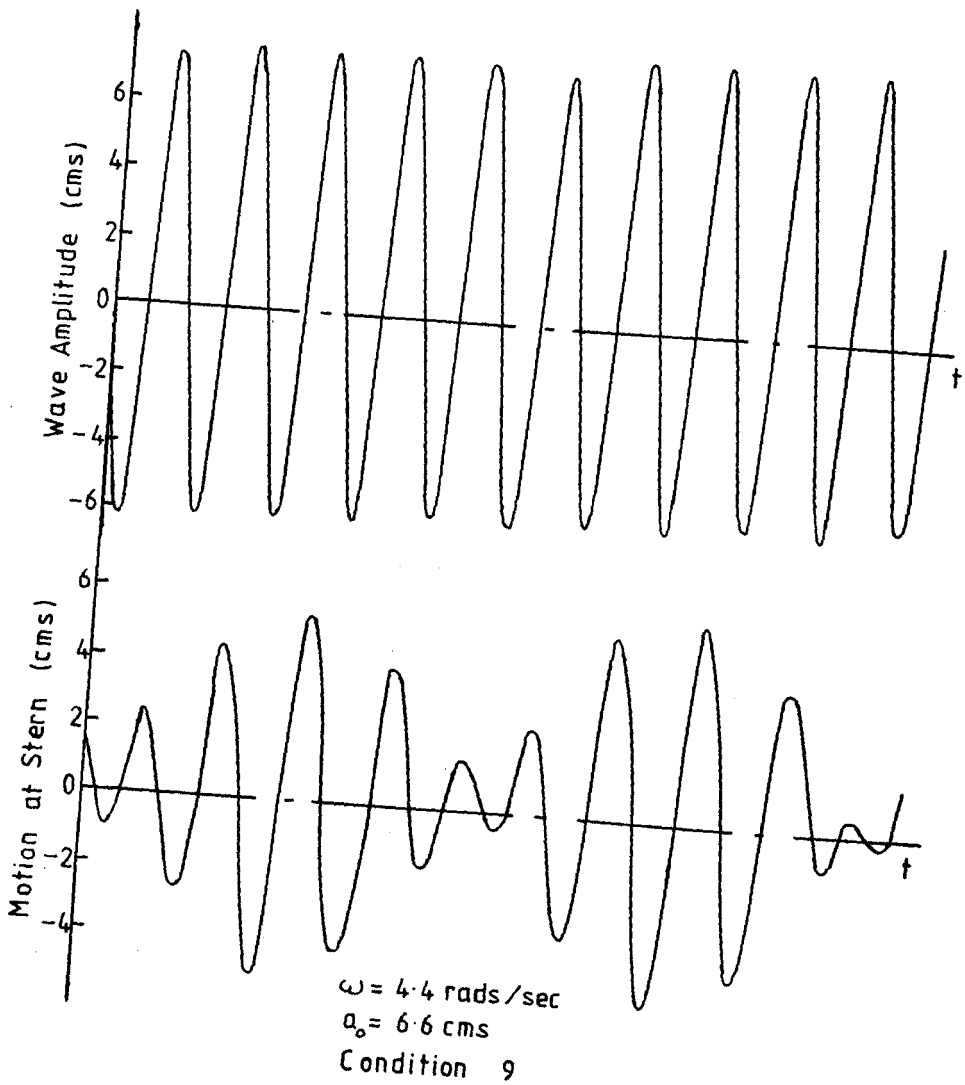

Fig. 7.27 Time History of 'Stern' Motion Showing 'Beats' in Regular Head Sea

in many vibration texts; see for example Meirovitch[119]. Equation 7.3 is considered with a cubic rather than a square term and is re-arranged to give the following form for a perturbation analysis

$$\ddot{z} + \omega_n^2 z = \varepsilon[-2\gamma\ \omega_n \dot{z} - \omega_n^2\ (\alpha z + \beta z^3) + F^*\ \cos\ \Omega t] \quad \ldots\ldots \quad 7.4$$

in which ω_n is the natural frequency of the linearised system, Ω is the driving frequency, (made equal to ω_n during the analysis), α and β are given parameters, ε is small, F^* is the exciting force per unit mass plus added mass and is now also non-linear. This is solved in the above-mentioned texts and the solution to the zero-order approximation is

$$[\omega_o^2\ (1 + \tfrac{3}{4}\varepsilon\beta z_o^2) - \omega^2]^2 + (2\varepsilon\gamma\omega_o^2)^2 = \left(\frac{\varepsilon F^*}{z_o}\right)^2 \quad \ldots\ldots \quad 7.5$$

where ω_o can be identified as the undamped natural frequency of the associated linear system, i.e. $\beta=0$. This can then be used to plot $|z_o|$ against ω as illustrated in Fig. 7.25.

The response of such a system in irregular seas would be very complex to analyse mathematically. For the simpler case of two harmonic forcing functions with distinct frequencies ω_1 and ω_2 the response of a mass-non-linear spring system consists of harmonic components with frequencies in the form of integer multiples of ω_1 and ω_2 as well as linear combinations of ω_1 and ω_2, (the type of harmonics depending on the nature of the non-linear term).

CHAPTER 8

ROLL MOTION IN HEAD SEAS

8.1 Introduction

For conventional vessels it has been recognised that operation in a group of large following waves can result in a large rolling motion and capsizing after a few cycles. This unstable rolling, sometimes referred to as 'low-cycle resonance', 'auto-parametrically-induced rolling' or 'parametric rolling' occurs at half the wave encounter frequency and is similar to the unstable motion described by the Mathieu equation. The phenomenon has been known for sometime. For instance, Grim[120] found that at certain frequencies of encounter unstable roll oscillations could occur because of the periodic variation of restoring moment. Paulling and Rosenberg[121] examined the stability of ships in a calm sea and showed the existence of non-linear coupling which could result in unstable roll motions. This led onto various studies of capsizing[95,122]. (There has also recently been an interest in unstable and parasitic motions for Tension-Leg Platforms (TLPs)[123-125].) The Mathieu equation is covered by Maths and vibrations texts, e.g. Ref. 119.

Since the phenomenon is usually associated with following seas for free floating vessels it was not anticipated before the experiments.

8.2 Equation of Motion

For head seas there is no exciting moment and the standard roll equation, e.g. Ref. 96, can be written as

$$(I+I_{AM})\ddot{\theta} + B\dot{\theta} + C(t)\theta = 0 \qquad \ldots\ldots \qquad 8.1$$

in which the third term, the hydrostatic restoring moment, is written as a function of time. As the wave passes along the length of the ship this restoring moment varies due to a combination of the instantaneous water-line and also the heave and pitch motions of the ship.

For linear theory the hydrostatic roll restoring moment is a constant and is simply

$$C = \rho g \nabla GM_T \quad \ldots\ldots \quad 8.2$$

However, to allow for the above effects Eq. 8.2 can be written as [124]

$$C(t) = \rho g(\nabla+\delta\nabla)(GM_T + \delta GM_T) \quad \ldots\ldots \quad 8.3$$

Since $\delta\nabla$ and δGM_T are small compared with ∇ and GM_T

$$C(t) = \rho g \nabla GM_T + \rho g \nabla \delta GM_T + \rho g \delta \nabla GM_T \quad \ldots\ldots \quad 8.4$$

where $\delta\nabla$ and δGM_T are the fluctuations in ∇ and GM_T due to the passage of the waves and the vessels heave and pitch motions. It can be assumed that the sum of the fluctuations is harmonic and Eq. 8.4 can then be written as

$$C(t) = \rho g \nabla GM_T (1 - \beta \cos \omega t) \quad \ldots\ldots \quad 8.5$$

where β is some function of wave amplitude. C(t) is expanded in Eqs. 8.3 and 8.4 with the inclusion of the $\delta\nabla$ term to indicate that balancing the ship on the wave by some means is not a satisfactory way of evaluating β. This is particularly true in the present case since, as will be shown, the phenomenon occurs in the vicinity of heave resonance with correspondingly large vertical motions.

Substituting Eq. 8.5 into 8.1 and neglecting damping gives

$$(I+I_{AM})\ddot{\theta} + \rho g \nabla GM_T (1 - \beta\cos \omega t)\theta = 0 \quad \ldots\ldots \quad 8.6$$

Putting $\frac{2\pi}{T} = \omega$ and rearranging then gives

$$\ddot{\theta} + \frac{\rho g \nabla GM_T}{I + I_{AM}} (1 - \beta \cos \frac{2\pi t}{T})\theta = 0$$

$$\ddot{\theta} + (\frac{2\pi}{\tau})^2 (1 - \beta \cos \frac{2\pi t}{T})\theta = 0$$

where τ is the natural roll period.

Changing the time variable to $t^* = \frac{\pi t}{T}$ gives

$$\frac{d^2\theta}{dt^{*2}} + \left(\frac{2\pi}{\tau \frac{\pi}{T}}\right)^2 (1 - \beta \cos 2t^*)\theta = 0$$

$$\frac{d^2\theta}{dt^{*2}} + \{(\frac{2T}{\tau})^2 - \beta (\frac{2T}{\tau})^2 \cos 2t^*\}\theta = 0 \quad \ldots\ldots \quad 8.7$$

This compares with the standard form of Mathieu's equation (see for example Meirovitch[119]), i.e.

$$\ddot{x} + (\delta + 2\varepsilon \cos 2t)x = 0 \qquad \ldots\ldots \qquad 8.8$$

where in this case

$$\delta = \left(\frac{2T}{\tau}\right)^2 = 4\left(\frac{T}{\tau}\right)^2 \qquad \ldots\ldots \qquad 8.9$$

$$\varepsilon = -2\beta\left(\frac{T}{\tau}\right)^2 \qquad \ldots\ldots \qquad 8.10$$

The interest lies in the stability characteristics of the system which can be plotted conveniently in the (δ,ε) parameter plane (Strutt diagram). The plane can be divided into regions of stability and instability by boundary curves and in this case we are interested in the principal instability region, i.e. the region terminating at $\delta=1$, $\varepsilon=0$. Meirovitch[119] obtains the equations of the boundary curves by Lindstedt's perturbation method as

$$\delta_1 \simeq 1 - \varepsilon - \tfrac{1}{8}\varepsilon^2 \qquad \ldots\ldots \qquad 8.11$$

$$\delta_2 \simeq 1 + \varepsilon - \tfrac{1}{8}\varepsilon^2 \qquad \ldots\ldots \qquad 8.12$$

8.3 Experimental Results

This unstable rolling at half the wave frequency occurred for Condition 10, i.e. $A_w^* = 3A_w$ (see Table XV) for which the natural roll frequency was found to be $\omega_\theta = 2.0$ rads/sec from roll decay tests. Experiments were conducted over a range of wave amplitudes and frequencies to determine the regions of stability and instability. The experimental set-up was as previously, but it should be noted that the unstable motions still occurred with variations in the mooring geometry and, indeed, in the absence of any moorings.

At this stage the value of β (in Eqs. 8.6, 8.7 and 8.10) has not been calculated theoretically, but, as previously discussed it should be possible to do so when the prediction of the relative bow motion is improved. However, it was found that to fit the Strutt diagram Eq. 8.10 had to be written as

$$\varepsilon = 0.75\, a_o \left(\frac{\omega_\theta}{\omega}\right)^2 \qquad \ldots\ldots \qquad 8.13$$

to give a reasonable fit for $\delta<1$. The experimental results together

with the boundary curves, (Eqs. 8.11 and 8.12) are given in Fig. 8.1. For $\delta>1$ it can be seen that the chosen function for ε does not fit the data because stable trials lie in the unstable region. It is not particularly surprising that a different function is required and indeed it may only be coincidence that the same ε function gives agreement for different values of δ at $\delta<1$. However, for $\delta>1$ there is insufficient experimental data to determine ε as a function of a_o.

For most of the trials in Fig. 8.1 the response of the bow and stern and, where applicable, the roll amplitude are shown in Figs. 8.2 - 8.6. From these Figures it can be seen that, for a given frequency, when the low wave amplitude results are stable, the inception of rolling at a higher amplitude causes a noticeable change in the motion of bow and stern. The frequencies at which the rolling stops at high wave amplitudes are particularly interesting. It can be seen that when the motion of the bow becomes very large the rolling stops. In other words when the 'jump' phenomenon occurs the motions at the stern are affected in such a way that the fluctuation of C(t) in Eq. 8.1 becomes insufficiently large to cause the roll motion.

Two frequencies were repeated for Condition 11, i.e. lower GM, (Figs. 8.7 and 8.8). Comparing Fig. 8.7 with 8.4 it appears that with the lower GM the roll motion, especially at small wave amplitudes, is larger. However, the jump phenomenon occurs for both Conditions at about the same wave amplitude. Contrary to the above, from Figs. 8.8 and 8.6, the Condition with higher GM gives larger rolling motion. The results in the stable region are, however, similar as would be expected.

Changing the GM affects both the roll natural frequency, (and hence δ and ε) and also the roll restoring moment. Clearly, the net effect is complicated and because of this it is difficult to make meaningful conclusions from the available data about the effect of GM in isolation.

One frequency was repeated for Condition 12, i.e. standard GM, but no fin and hence lower damping. The results in Fig. 8.9 were obtained from which it can be seen that the roll motion is significantly larger than the corresponding results in Fig. 8.8. (The maximum RAO without the fin is three times greater than that with the fin,

and at other wave amplitudes it can be twice as great.) In the case of zero damping the theoretical response goes to infinity in the unstable region. It can also be seen that the unstable rolling commences at a lower wave amplitude, without the fin but this is attributable to the change in the natural frequency affecting the values of δ and ε. (Damping also has a small direct effect on the position of the stability boundaries[119].)

It should be noted that starting from rest these unstable roll motions typically take 10 - 12 wave cycles to build-up to a large amplitude, e.g. Fig. 8.10 for Condition 10. The question then arises whether or not these instabilities will be manifest in irregular seas.

8.4 Roll Response in Irregular Head Seas

Three pre-recorded Pierson-Moskowitz type spectra, with a model scale significant wave height of h_s = 5.2 cms, 10.5 cms and 15.8 cms, for the complete run, corresponding approximately to sea-states 3, 5 and 6 in the full-scale were used. (The most severe sea had one wave amplitude over 15 cms in a run lasting about 20 minutes.) For Condition 12 intermittent rolling occurred in the two largest of these spectra as illustrated in Fig. 8.11 for the largest one. However, when the fin was fitted, i.e. Condition 10, no rolling whatsoever was observed which appears to be due to the effect of damping. The seas used were random, but if there was more wave-grouping present it is still possible that parametric rolling could occur for other conditions.

8.5 Discussion

Further discussion of unstable rolling is given at the end of the next chapter.

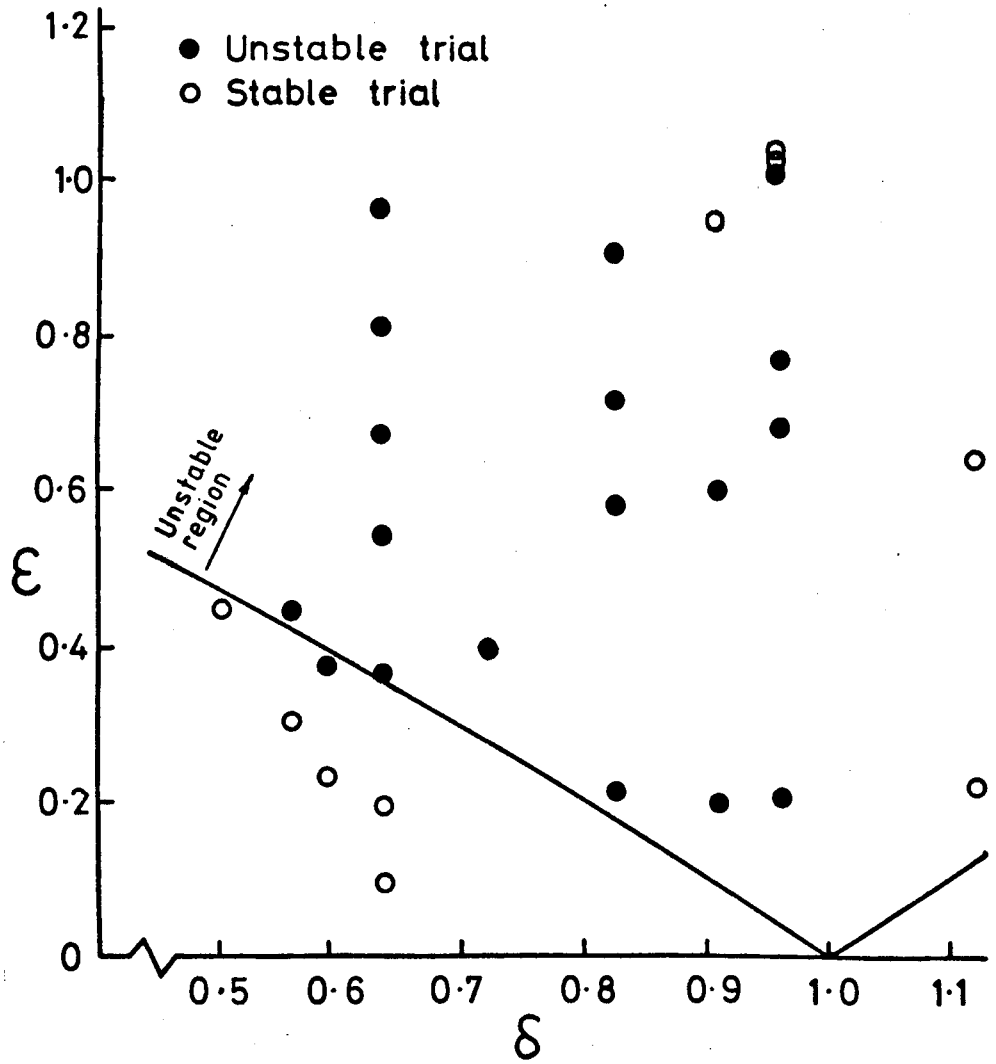

Fig. 8.1. Roll Motion in Head Seas:
Stability Characteristics Fitted to (δ,ε) Plane

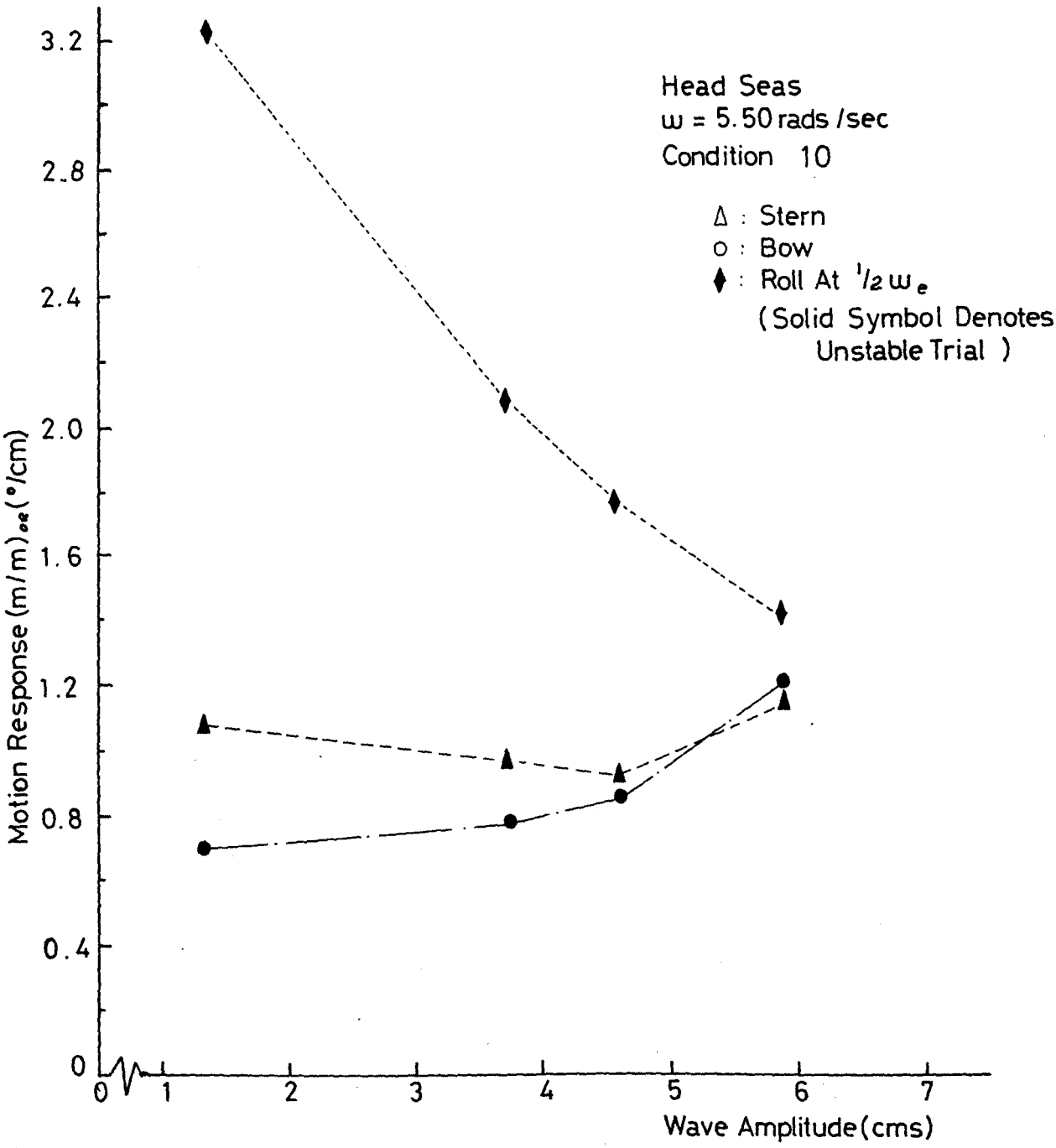

Fig. 8.2. Head Sea Motion Response.

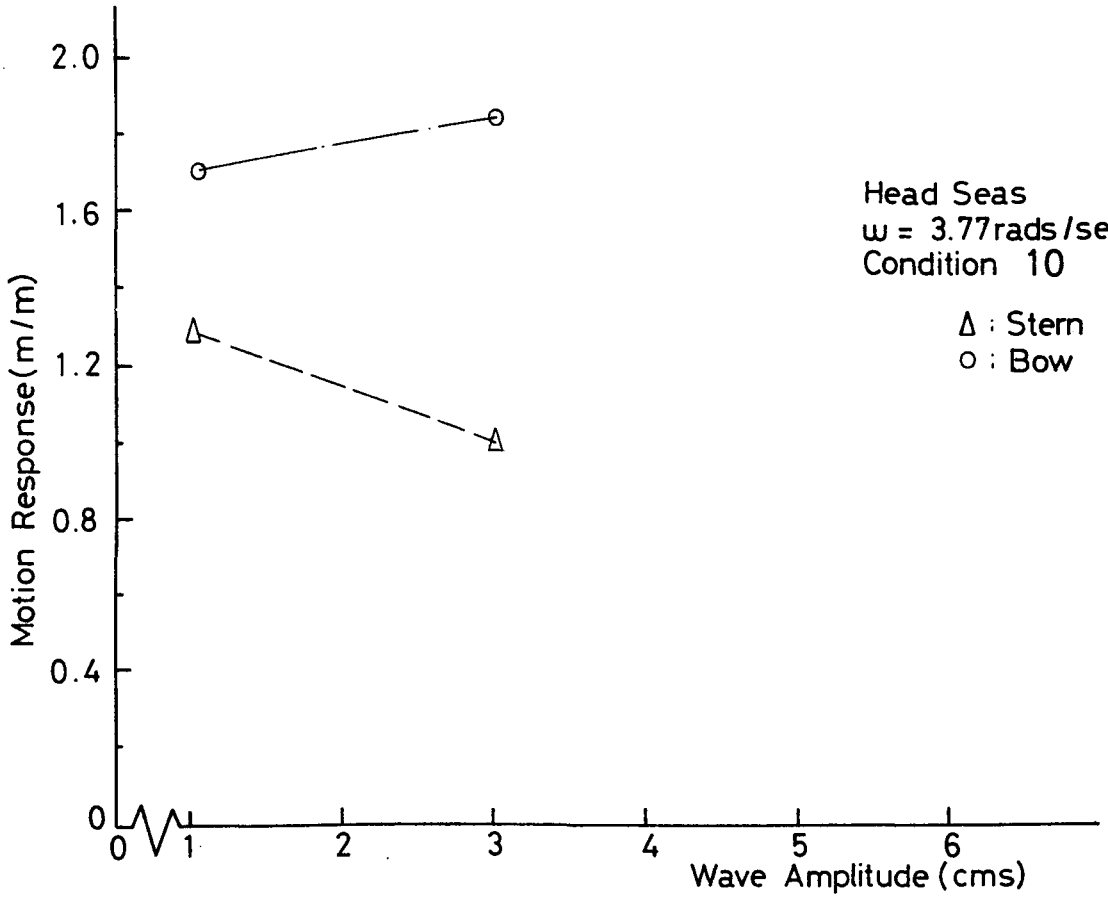

Fig. 8.3. Head Sea Motion Response.

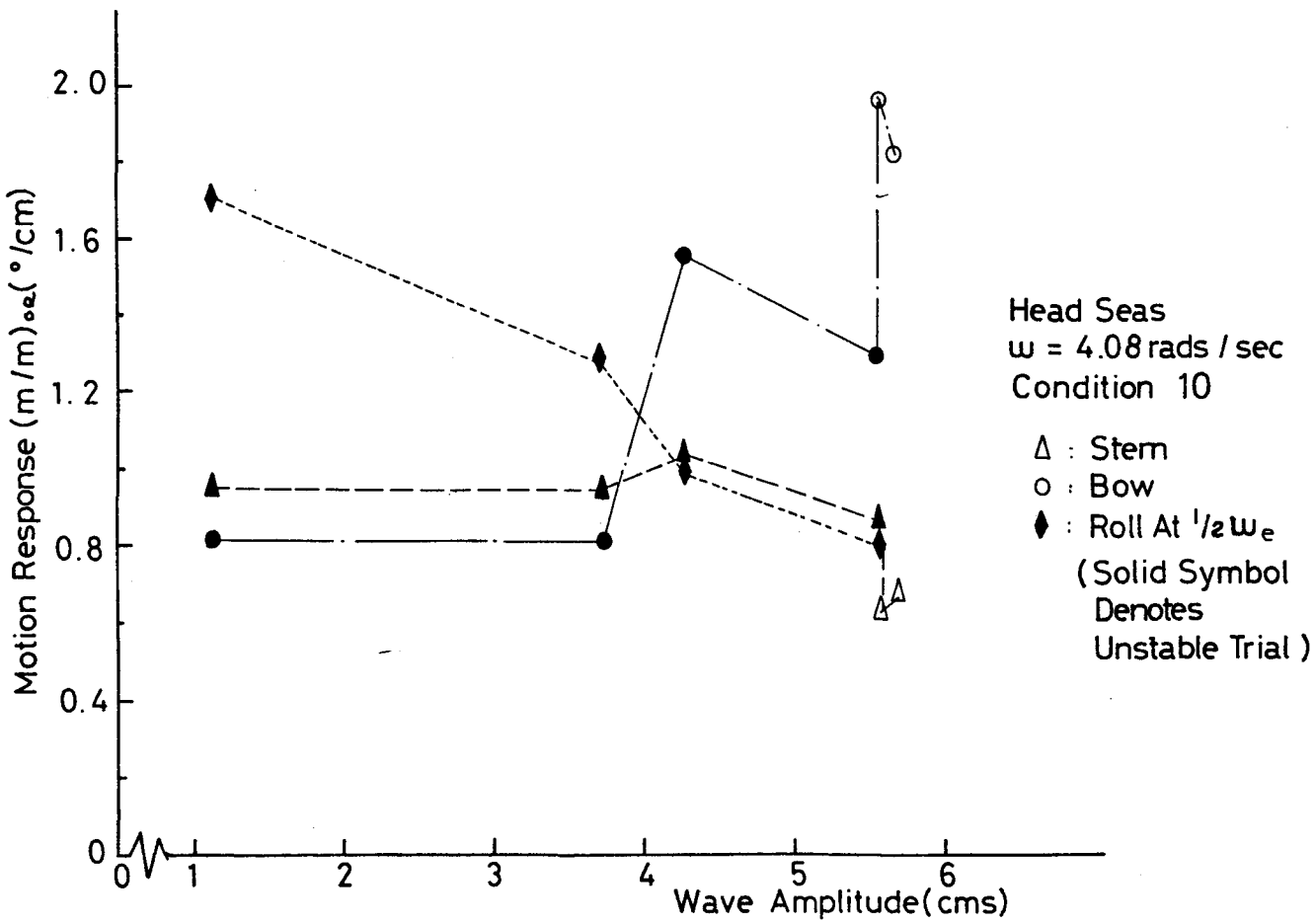

Fig. 8.4. Head Sea Motion Response.

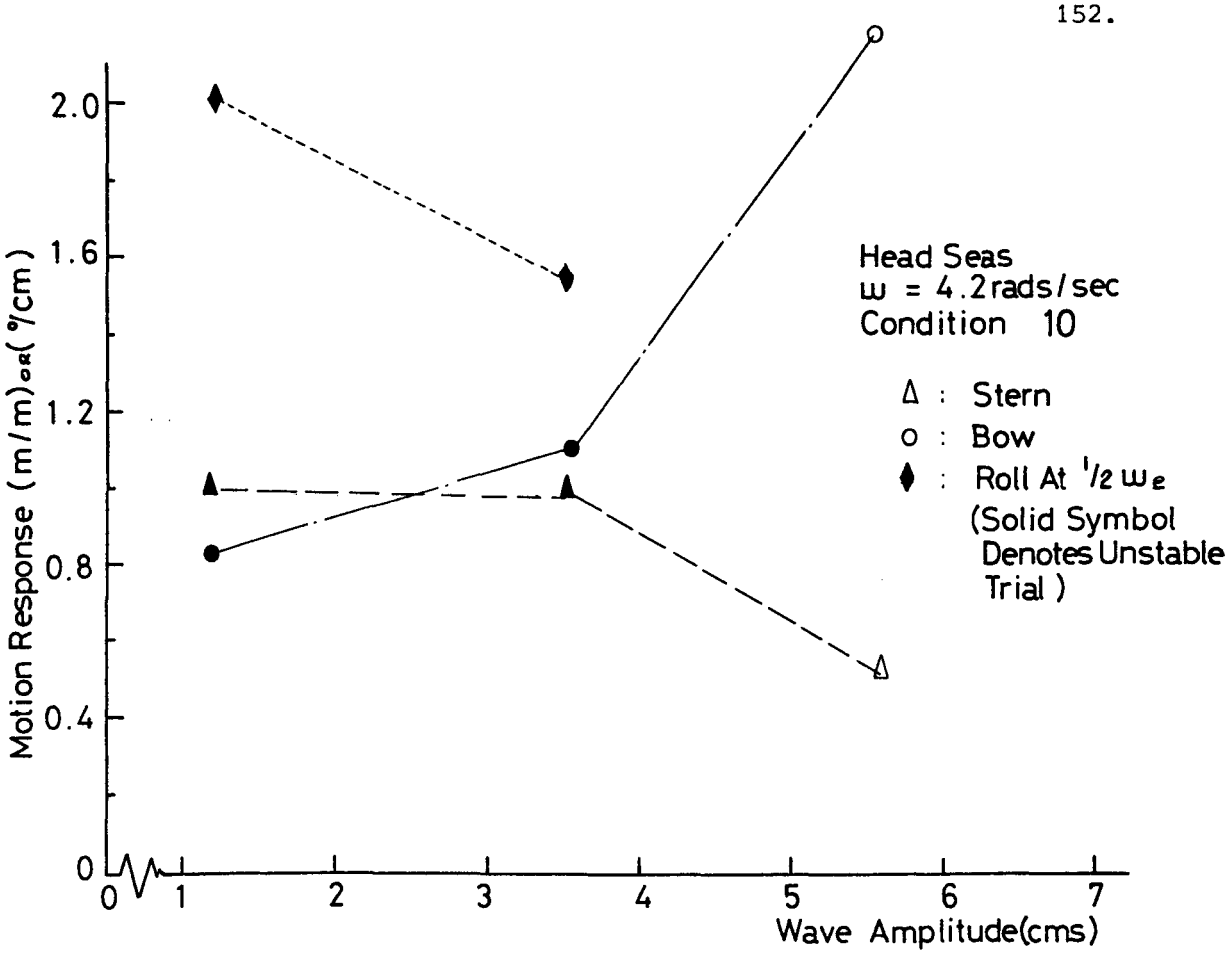

Fig. 8.5. Head Sea Motion Response.

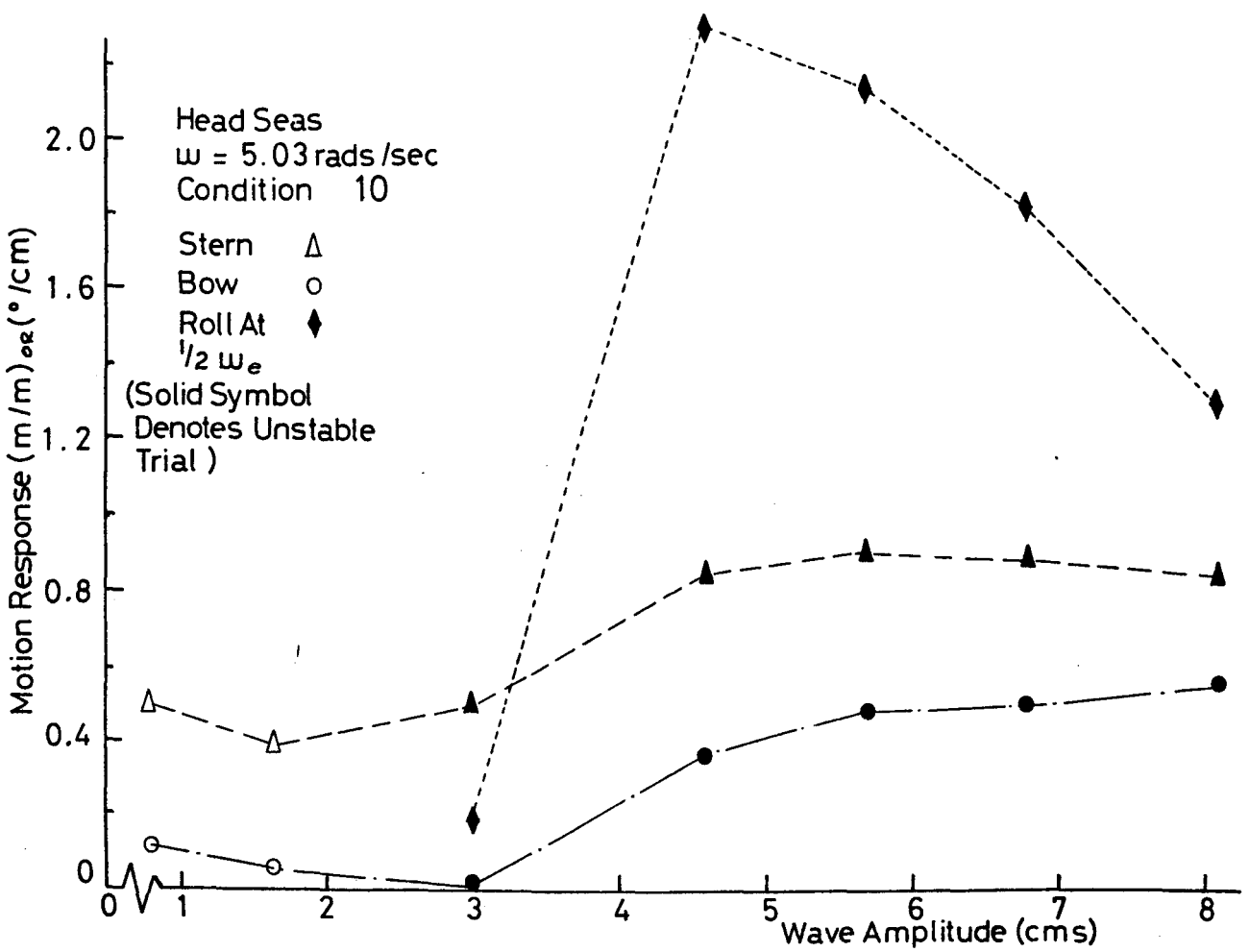

Fig. 8.6. Head Sea Motion Response.

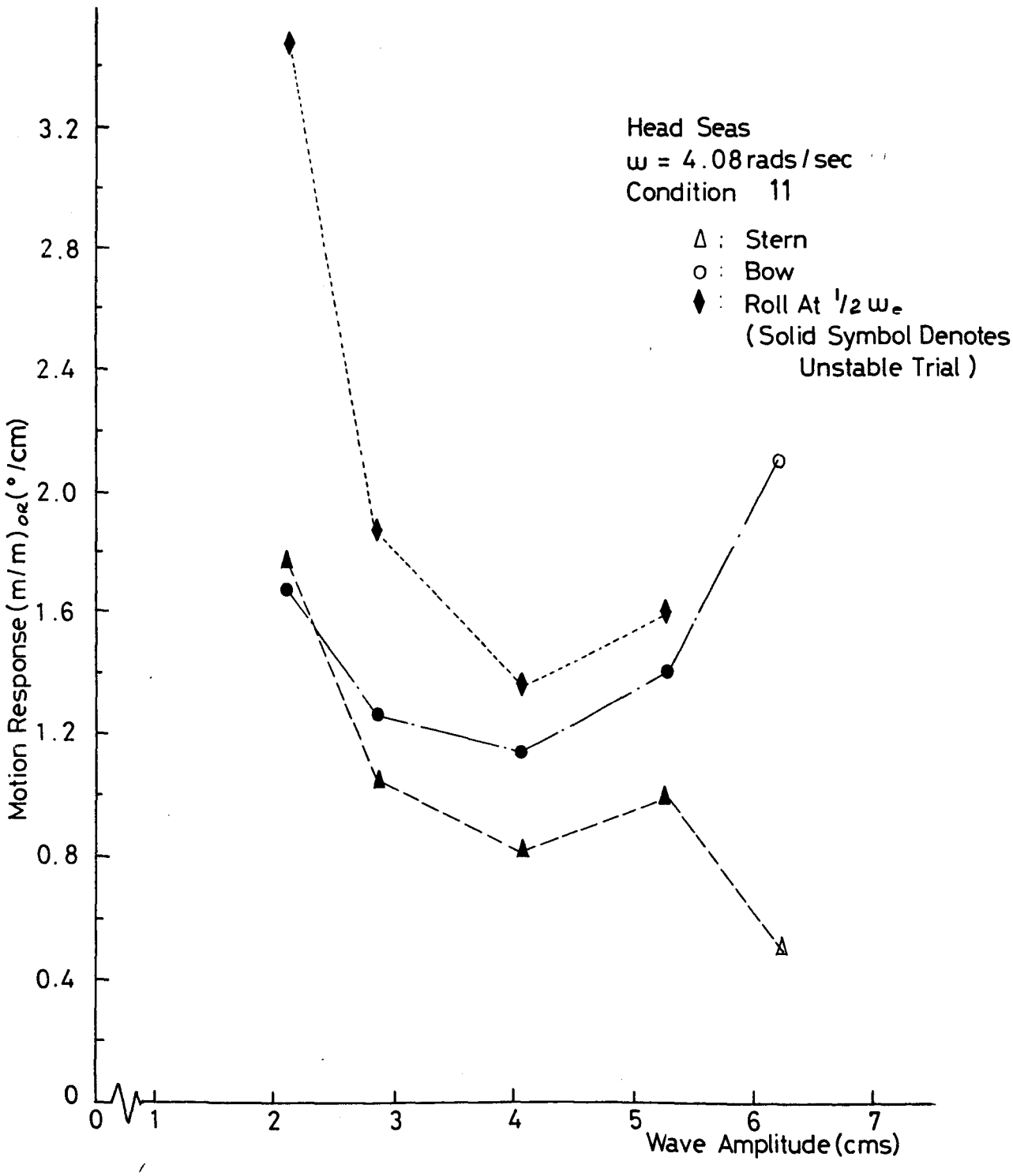

Fig. 8.7. Head Sea Motion Response.

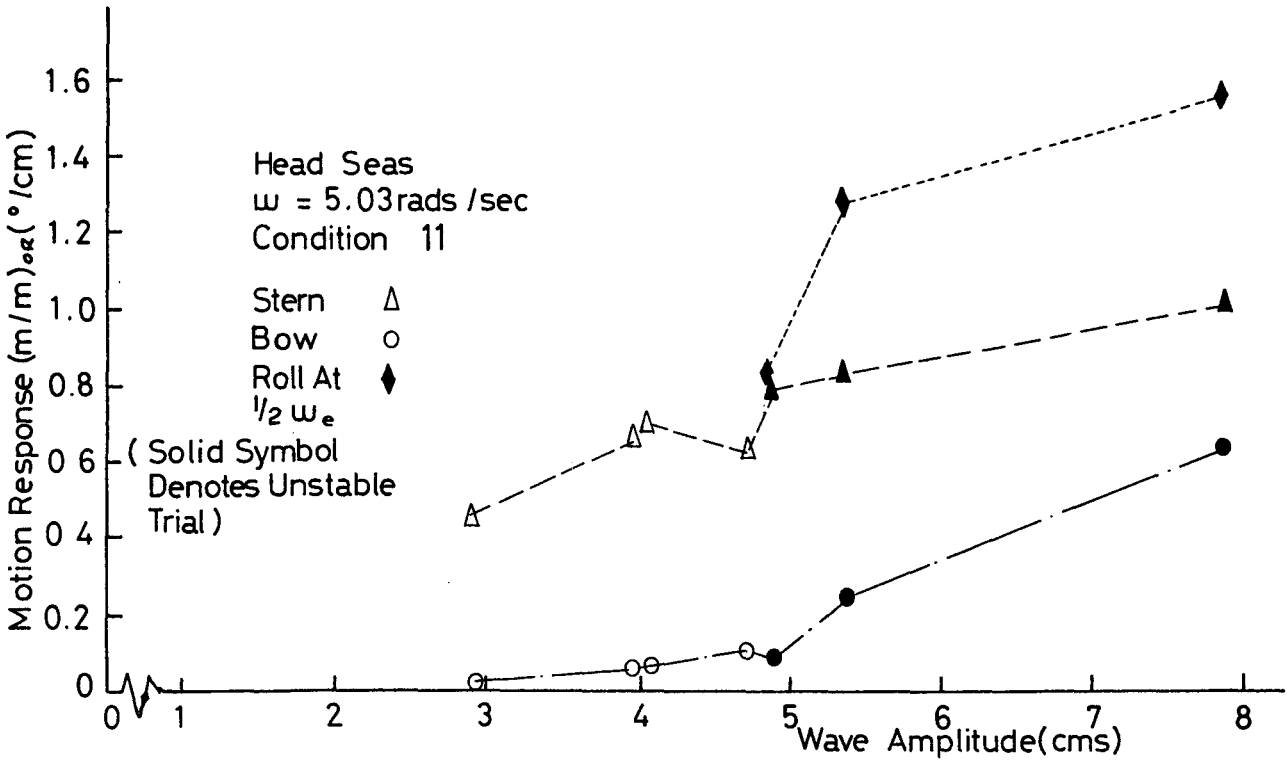

Fig. 8.8. Head Sea Motion Response.

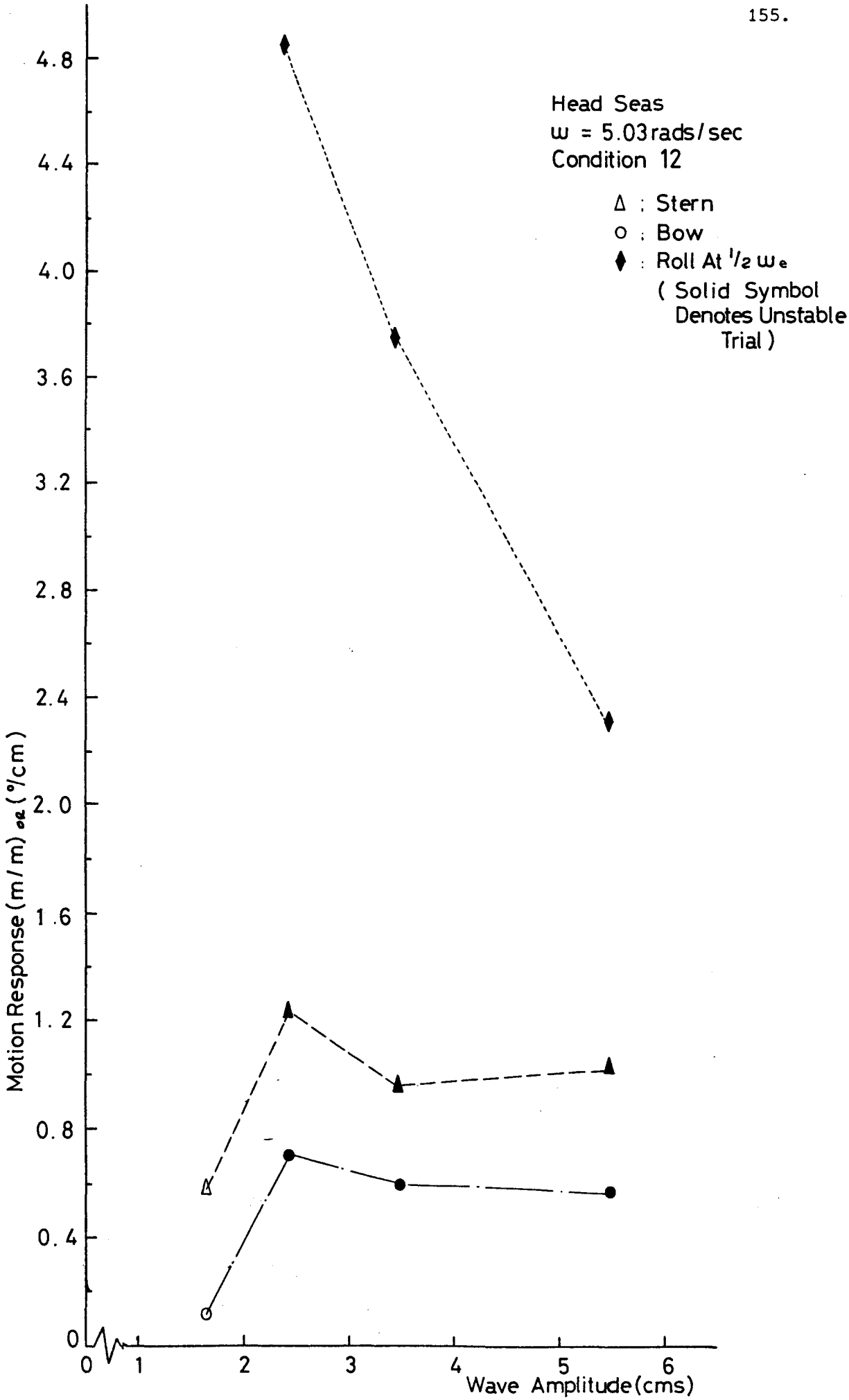

Fig. 8.9. Head Sea Motion Response.

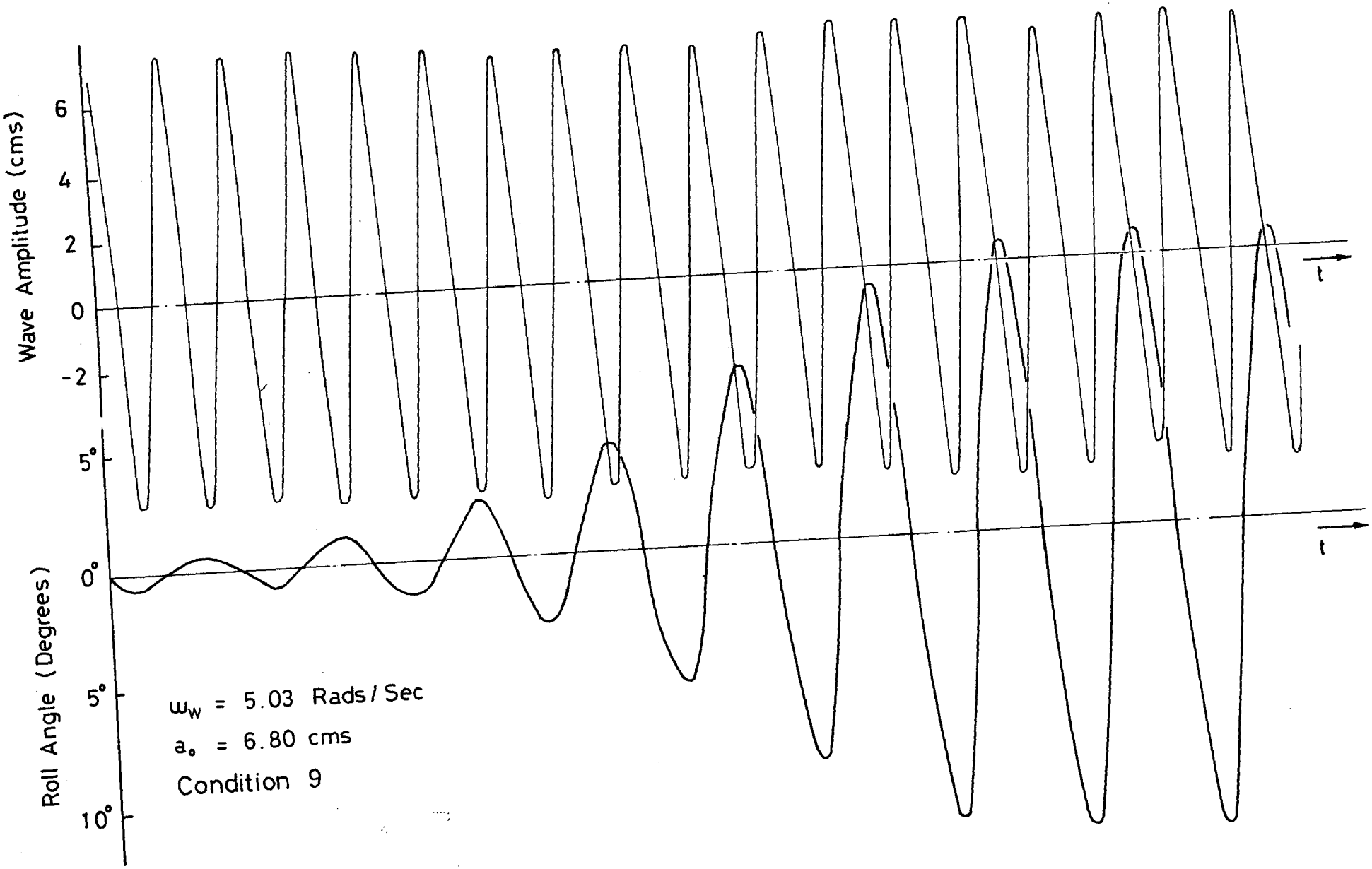

Fig. 8.10 Build-Up of Roll Motion in Regular Head-Seas

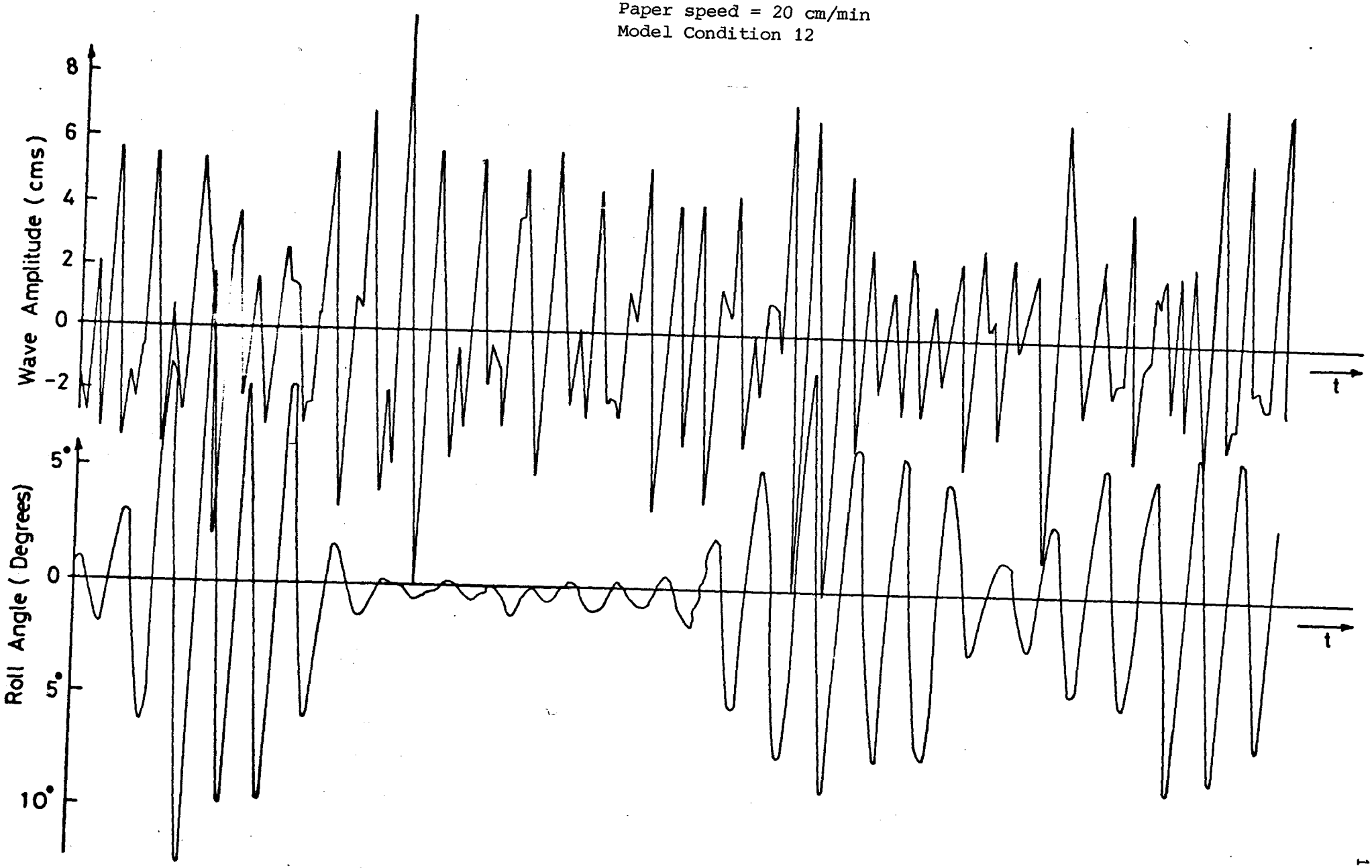

Fig. 8.11. Time History of Roll Motion in Irregular Head Seas.

CHAPTER 9

MOTION RESPONSE IN BEAM SEAS

9.1 Introduction

The motion response of the model was obtained for a range of wave frequencies and amplitudes and for a number of different conditions. As for head seas it was found that the response was generally linear with wave amplitude. However, subharmonic rolling occurred in the conditions for which unstable rolling was reported in head seas. A survival experiment was also conducted. The model was ballasted to give zero upright GM_T but it did not capsize under wave action.

9.2 Experimental Results

The experimental results for Condition 1 are shown in Figs. 9.1 - 9.8 inclusive. As in head seas, for Condition 1 the response is essentially linear with wave amplitude apart from at resonance when there is a decrease with increasing amplitude (Fig. 9.1) and in cases of low heave, Figs. 9.4 and 9.5, where there is a tendency for the RAO to increase with wave amplitude. The sharp rise in Fig. 9.6 is unexplained.

The ITTC recommend a wave height of $h=\lambda/40$ for seakeeping experiments. The results for the nearest experimental value to this are plotted in Fig. 9.9 from which it can be seen that the heave and roll responses are in fact very similar to the heave and pitch responses for Condition 1 in Figs. 6.4 and 6.5 respectively.

The GM was reduced to give Condition 13 with results plotted in Figs. 9.10 and 9.11. Comparing these with Figs. 9.1 and 9.5 indicates that this GM reduction had little effect on the response at either frequency. However, when the fin was removed but with standard GM, (Condition 5) Figs. 9.12 and 9.13, it can be seen that although the roll motion stayed about the same the heave motion was affected being generally greater in Fig. 9.12 than in 9.10 or 9.1 and less in Fig. 9.13 than in 9.11 or 9.5.

These heave results are exactly analogous to those for head seas. The main effect of removing the fin is reducing the damping or viscous forces, hence the resonant heave response increases while the near zero response becomes smaller. In these cases the wave frequency is sufficiently far from roll resonance for the damping to have little effect on roll motions.

9.3 Results with Column Flare

As for head seas (Chapters 6 and 7) the responses were found for varying degrees of column flare. Figures 9.14 to 9.18 inclusive give the results for Condition 8, and comparing results as before there seems to be no real benefit. Similarly, when the GM was reduced (Condition 14, Figs. 9.19 - 9.21) the effect was only small. Comparing Figs. 9.20 and 9.16 the roll RAO increases from about 0.3 to about 0.36 and the differences between Figs. 9.21 and 9.15 are even smaller.

9.4 Subharmonic Rolling

In head seas the occurrence of an unstable roll motion of half wave frequency was shown in Chapter 7 and similarly in beam seas a subharmonic rolling at half wave frequency can occur. (For conventional ships this has been investigated in regular and irregular seas in a number of papers such as Refs. 122, 126 - 129. The equation of roll motion is similar to Eq. 8.1 but in this case includes a roll exciting moment, i.e.

$$(I+I_{AM})\ddot{\theta} + B\dot{\theta} + C(t)\theta = M \cos \omega t \qquad \ldots\ldots \qquad 9.1$$

As in head seas the subharmonic roll motions did not occur until the column flare was increased to $A_W^* = 3A_W$, i.e. Condition 10. Various experimental results for this Condition are given in Figs. 9.22 - 9.27. In head seas the demarcation between rolling and not rolling was clear-cut but in beam seas the roll response for a number of trials exhibited a mixture of wave frequency and half wave frequency components (these are shown with a half-solid symbol). Generally, e.g. Figs. 9.22 and 9.24, normal rolling occurred for both low and high wave amplitudes. The cessation of subharmonic rolling at higher wave amplitudes may be attributable to small wave frequency pitching motions (caused by lack of fore-and-aft symmetry) which altered the

fluctuations in the restoring moment. However, for conventional ships Tasai[129] also notes that unstable rolling did not occur for waves of large steepness, but offers no explanation.

Results for a lower value of GM (Condition 11) are shown in Figs. 9.28 - 9.31. Little difference in magnitude is noticeable between Figs. 9.28 and 9.26 or 9.14 and between Figs. 9.31 and 9.27. However, near heave resonance, comparing Figs. 9.29 and 9.25 the sub-harmonic rolling seems to have a larger amplitude and extends to a higher range of wave amplitudes. This is more probably attributable to the variation in roll natural frequency than the lower value of GM_T *per se*, since the reduction in GM_T leads to the roll natural frequency, ω_θ, reducing to 1.85 rads/s for Condition 11. Therefore, at ω = 3.77 rads/s, ω/ω_θ is more nearly equal to 2 and $\omega \simeq \omega_H$ which combination tends to give the 'worst' result. Thus, as in head seas it is difficult to make a meaningful conclusion about the effect of GM in isolation.

9.5 Survival Experiment

The model was ballasted from Condition 10 to give zero upright GM_T at which the model took up a small angle of loll. An attempt was then made to capsize the model in large waves, Fig. 9.32. Because of the low GM the roll natural frequency was very low and the resulting roll motions were also very low and essentially at wave frequency. The model never seemed to be in danger from capsizing but with the large volumes of water sweeping the deck sinking due to added weight seemed a recurring possibility. It can be speculated that this would be particularly true if, due to damage say, the vessel had been at a deeper draught, and hence less freeboard, as well as having a very low GM.

9.6 Discussion of Unstable Motions

While the behaviour reported in Chapters 8 and 9 have been referred to as instabilities they should not be confused with the usual static or quasi-static roll-stability criterion. Although they have been identified as a possible capsize mechanism their occurrence is neither a necessary nor a sufficient condition for a capsize,

but of course that does not mean that their existence is desirable. Indeed the contrary is true and the knowledge that a small motion could build-up represents a dangerous situation. It would, therefore be desirable to have practical criteria for the avoidance of such motions. This has not yet been done but some very recent work on offshore structures, (September 1981) may be relevant[130]. (Another recent paper[131] reviews intact ship stability research and criteria which may also be applicable.) The basic difficulty is that changing an easily measurable parameter such as GM need not prevent unstable motions, it may only move them to a different frequency. It may transpire that setting a maximum permissible value of a parameter such as β in Eqs. 8.5 - 8.7 could be useful. Furthermore, if the GM is reduced to avoid subharmonic rolling it is possible, as evidenced by the survival experiment, to increase the wetness dramatically which is not desirable either. It should also be remembered that even for the trials in which the instabilities occurred there was never any capsizes and it seems reasonable to attribute this to having sufficient GM or area under the GZ curve. In other words, there was a sufficient reserve of stability in the conventional static sense. The effect of damping is also obviously important in limiting the motion amplitudes. In conclusion, it can be said that given the choice, the lesser of the two evils would be to have unstable motions and a large area under the GZ curve rather than unstable motion with small area under the GZ curve.

There is no reason to think that the above behaviour is a feature of the three-hulled design. The equations of motion are just as applicable to the twin-hull cases and the appropriate conditions could quite easily be designed into such a vessel unless care is exercised. Indeed from the literature it seems that both the *Kaimalino* and the *Marine.Ace* (twin struts) and also a 4000t design[132] have roll natural frequencies approximately half the heave natural frequency which are the conditions most likely to lead to parametric or subharmonic rolling. The fact that it has not been reported suggests that the column flare is not sufficiently great on these designs although it certainly would appear to be on other twin-hull designs[6].

As far as the three-hull design proposal is concerned the waterplane-area ratio is approximately as for Condition 8, which exhibited no parasitic motions, but the actual volume in the flared portion is slightly smaller so the motions would be even less likely.

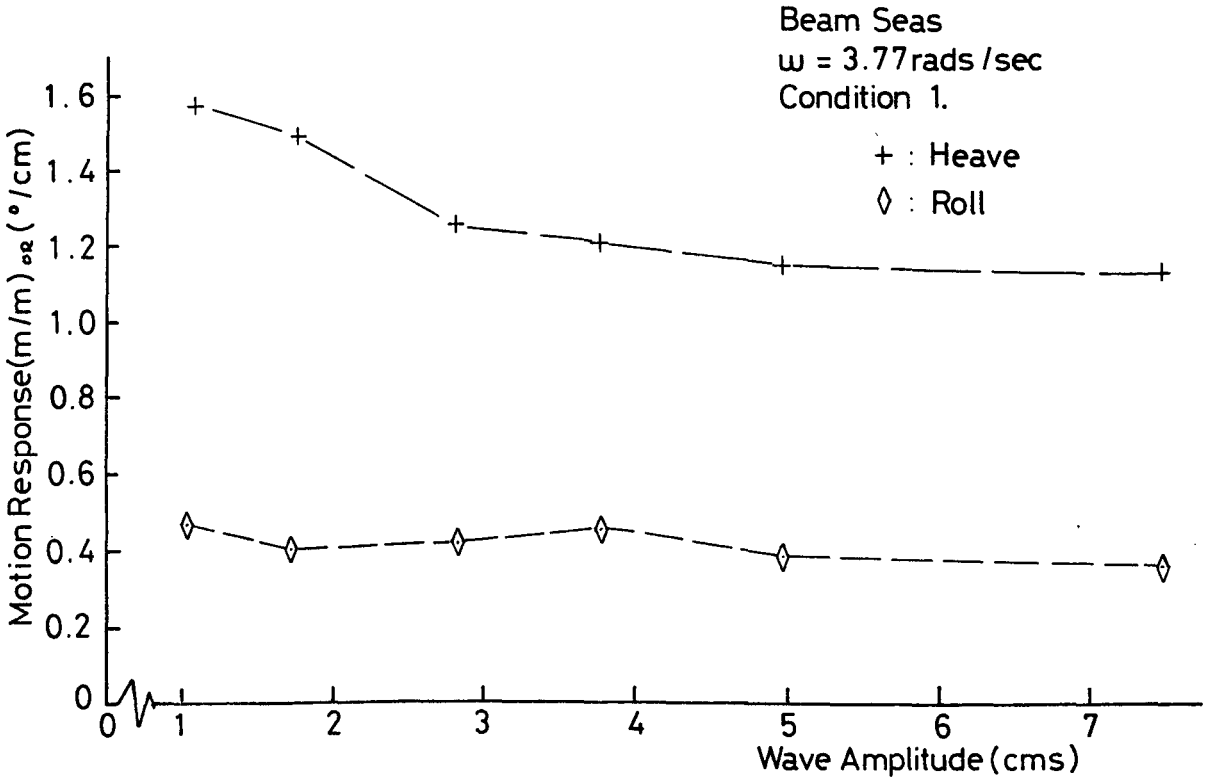

Fig. 9.1. Beam Sea Motion Response.

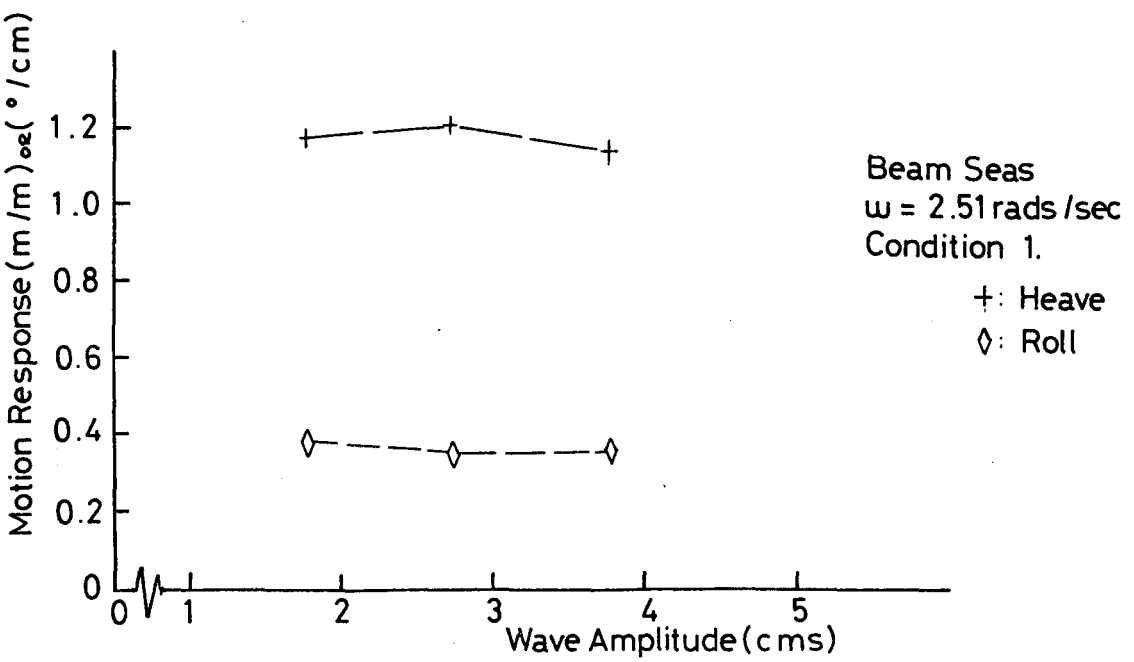

Fig. 9.2. Beam Sea Motion Response.

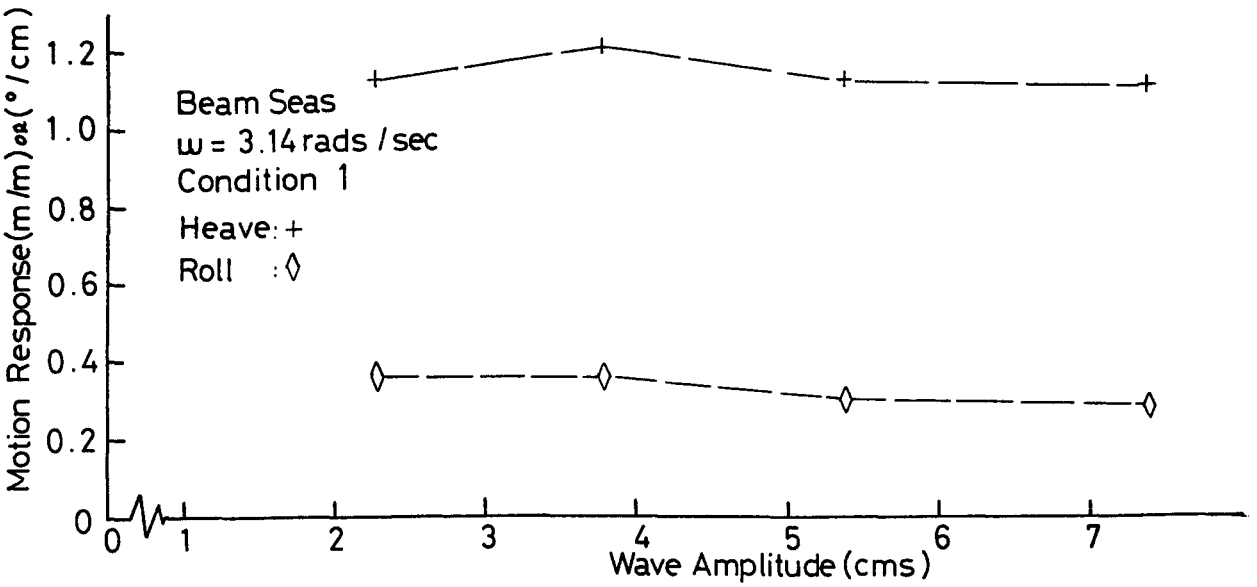

Fig. 9.3. Beam Sea Motion Response.

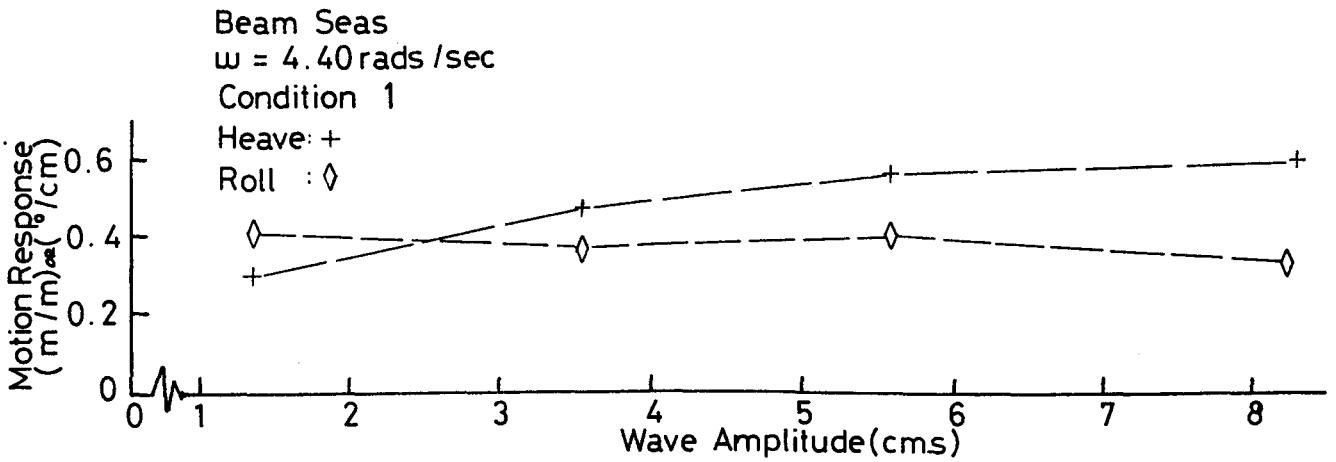

Fig. 9.4. Beam Sea Motion Response.

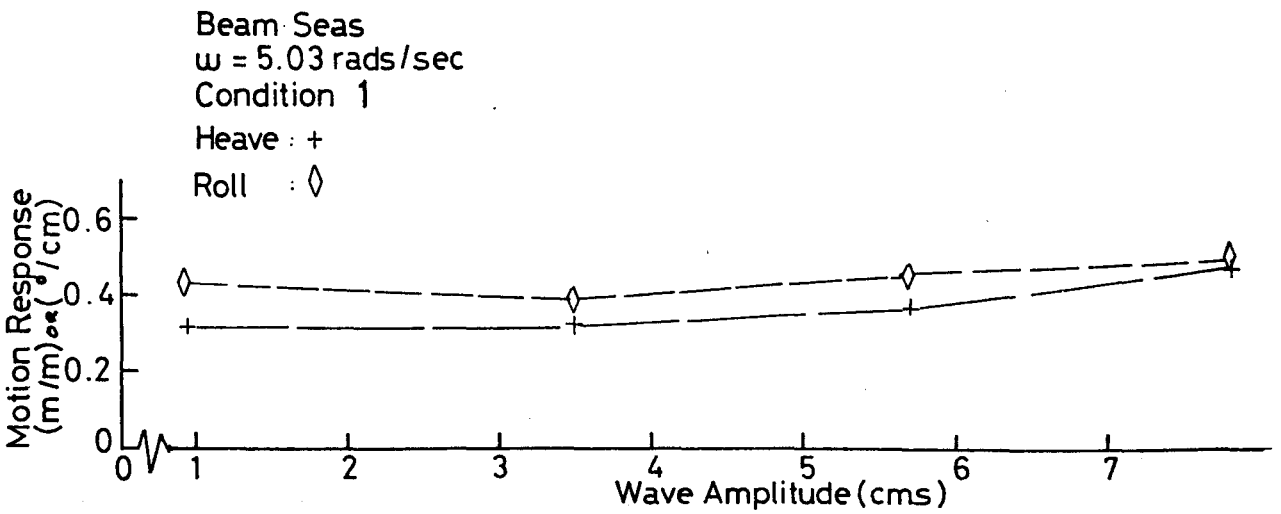

Fig. 9.5. Beam Sea Motion Response.

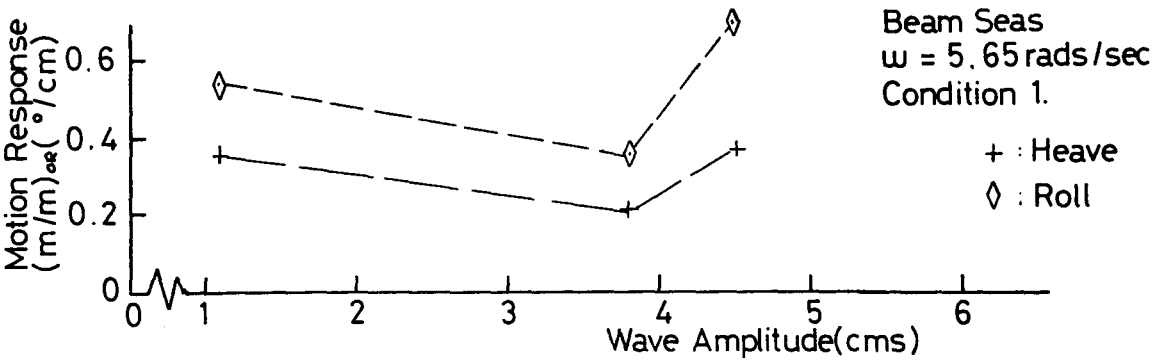

Fig. 9.6. Beam Sea Motion Response.

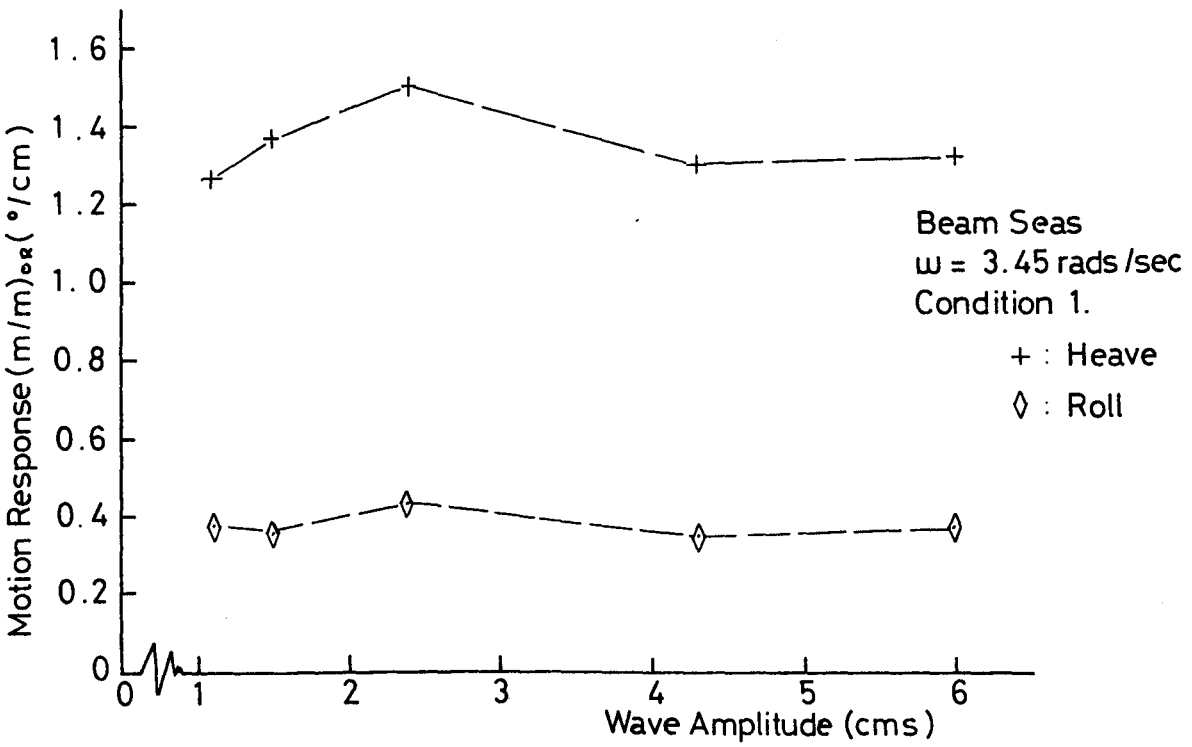

Fig. 9.7. Beam Sea Motion Response.

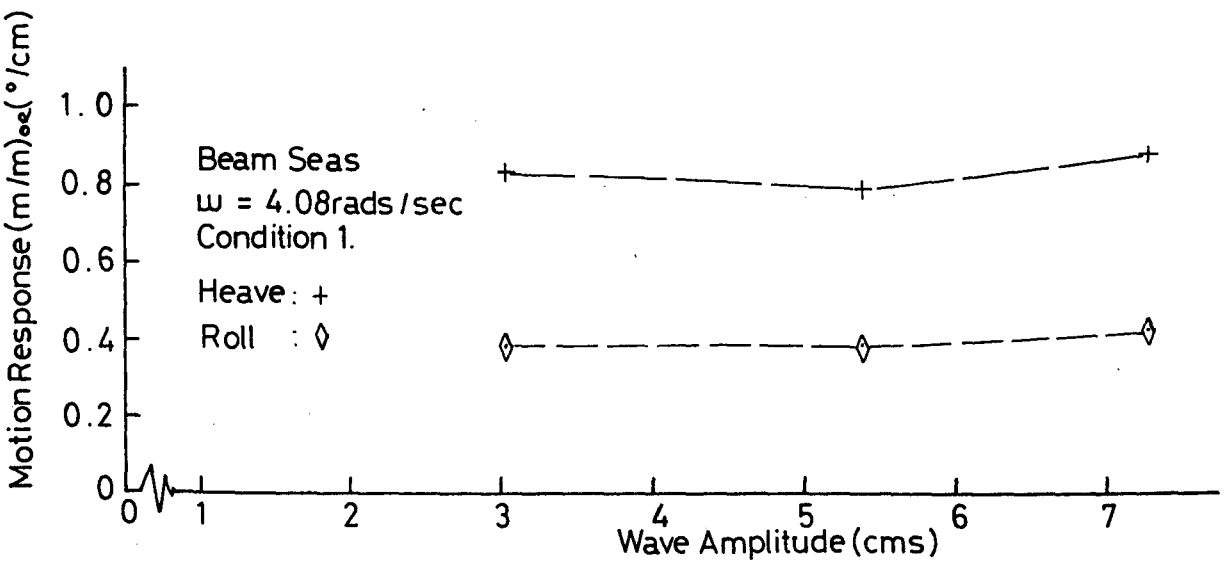

Fig. 9.8. Beam Sea Motion Response.

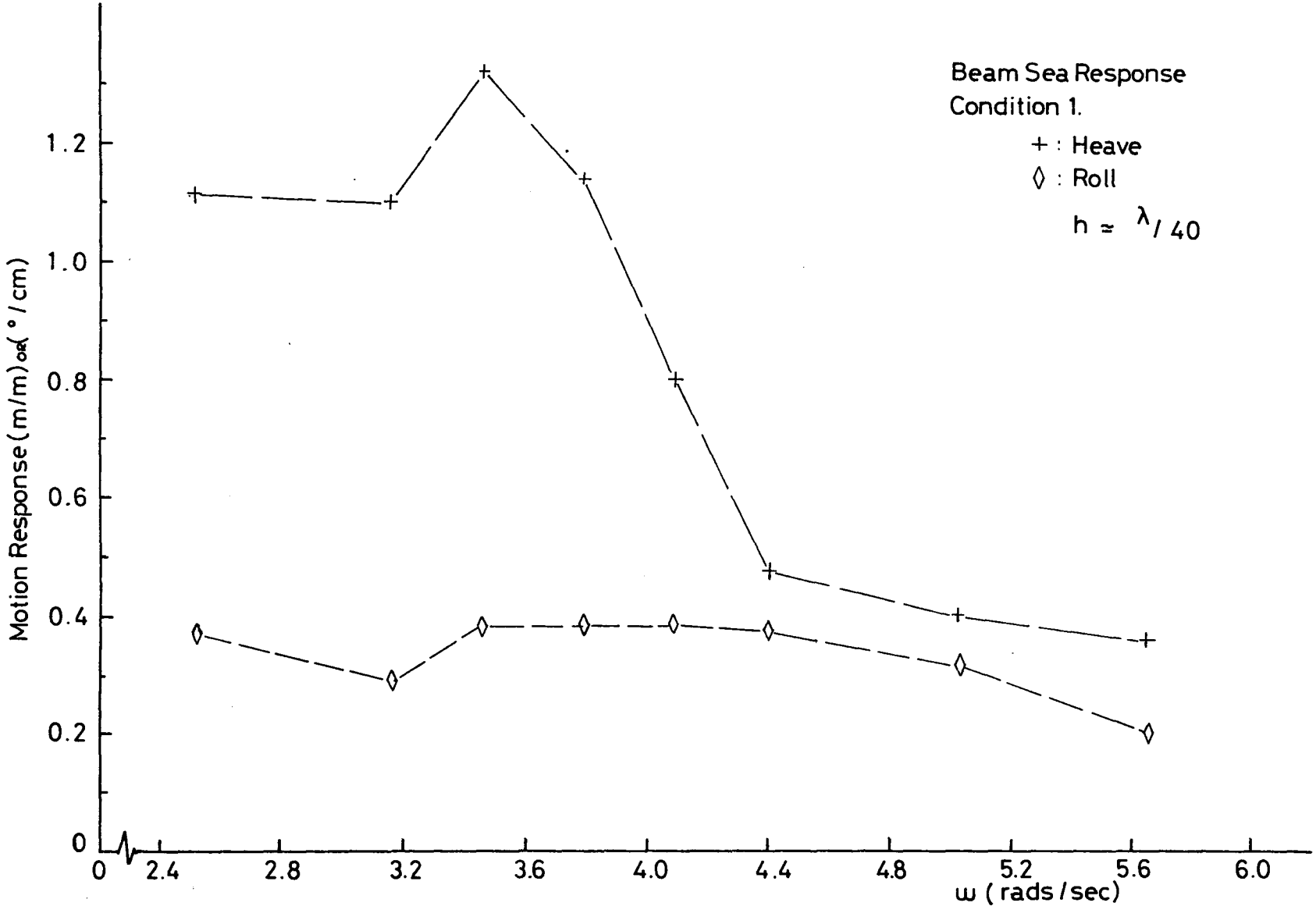

Fig. 9.9. Beam Sea Motion Response (Frequency Domain).

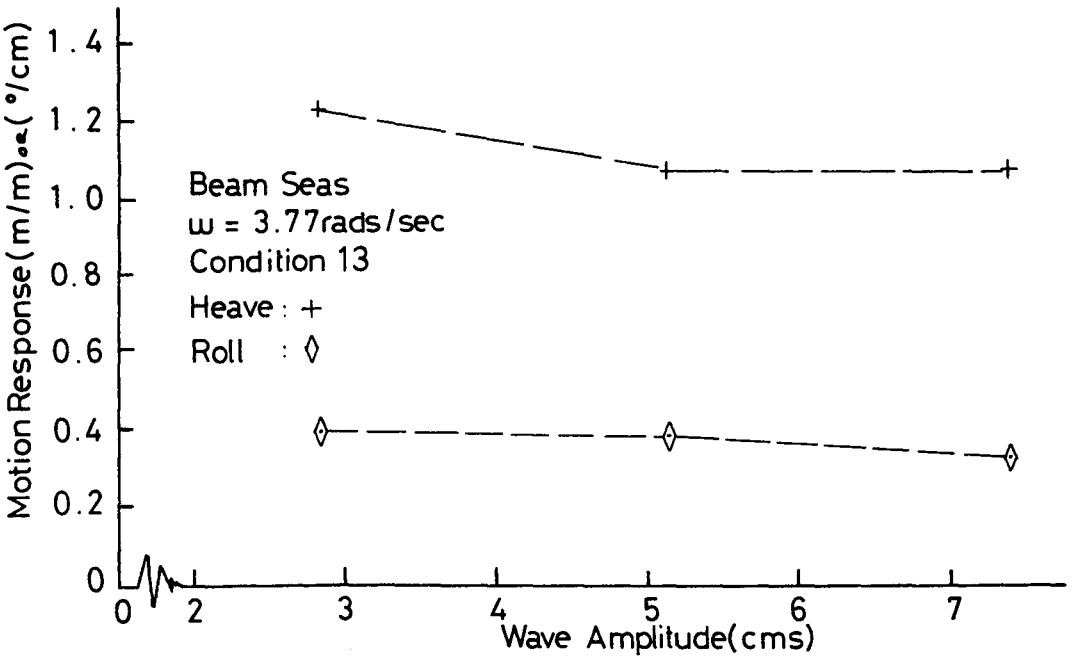

Fig. 9.10. Beam Sea Motion Response.

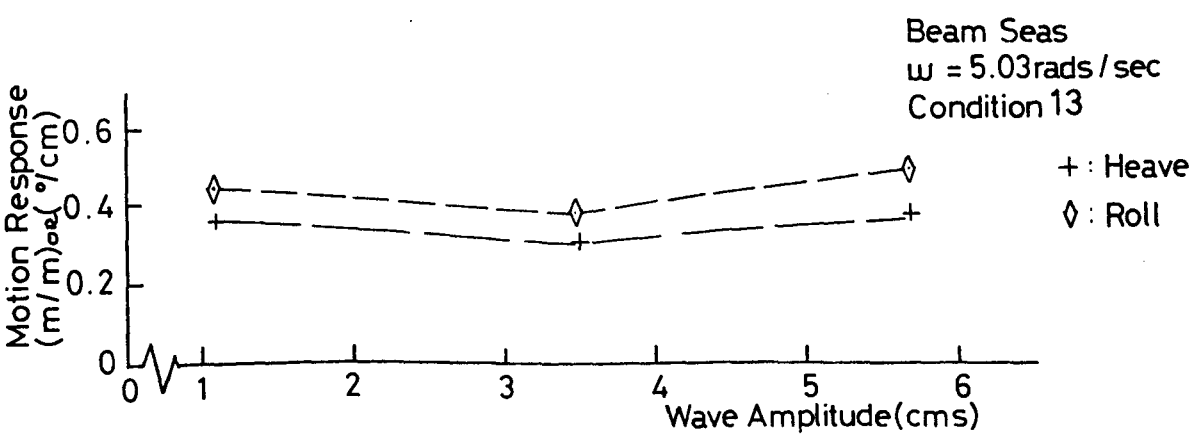

Fig. 9.11. Beam Sea Motion Response.

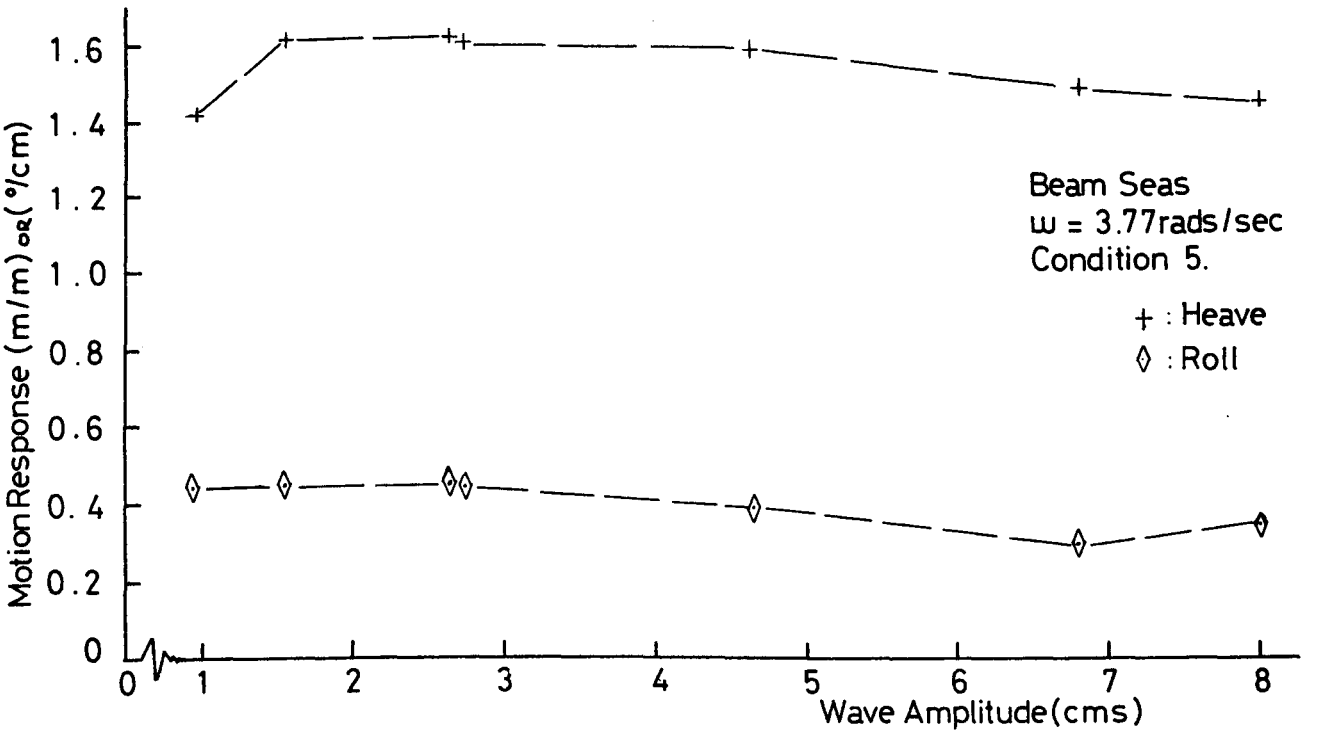

Fig. 9.12. Beam Sea Motion Response.

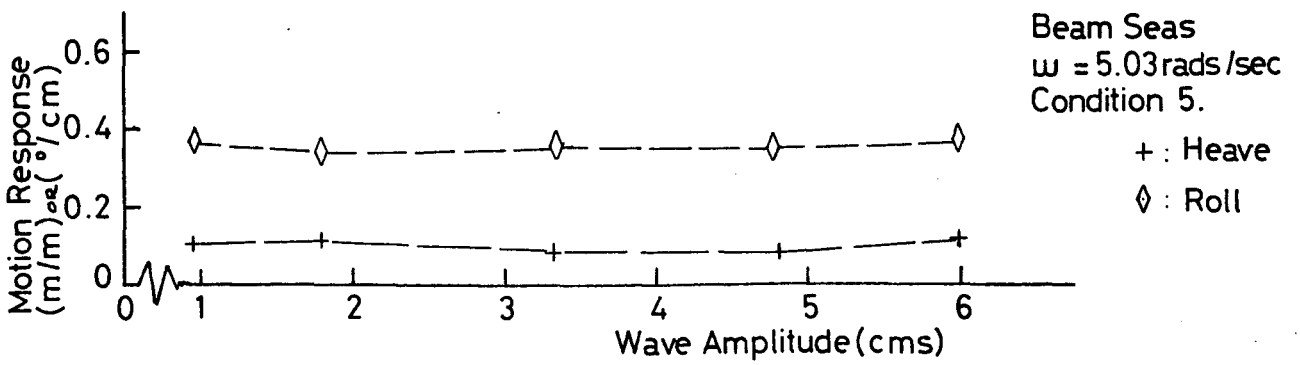

Fig. 9.13. Beam Sea Motion Response.

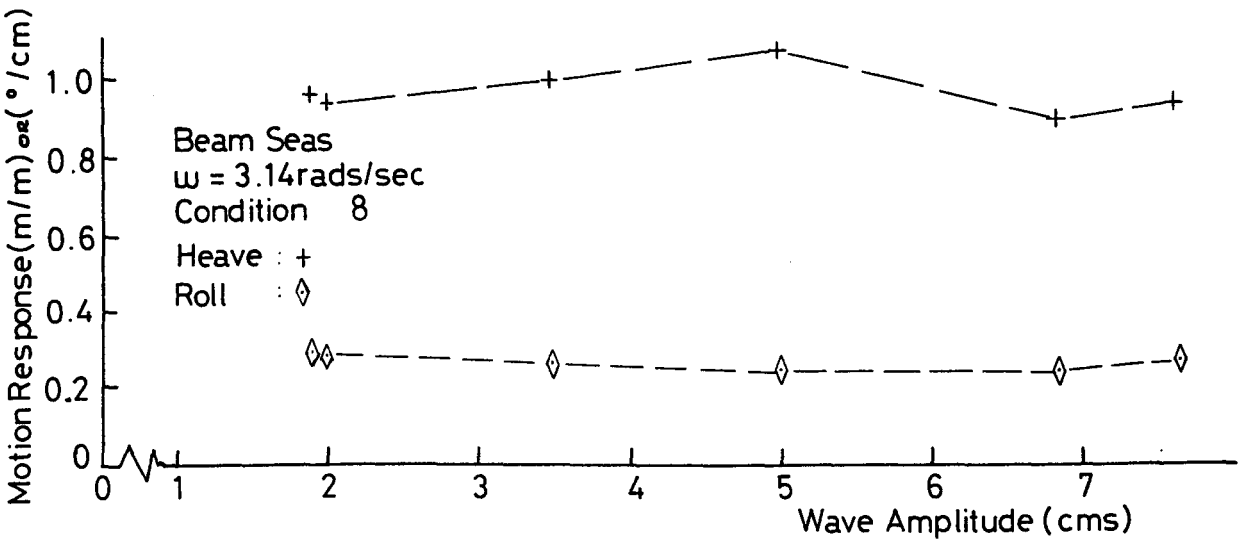

Fig. 9.14. Beam Sea Motion Response.

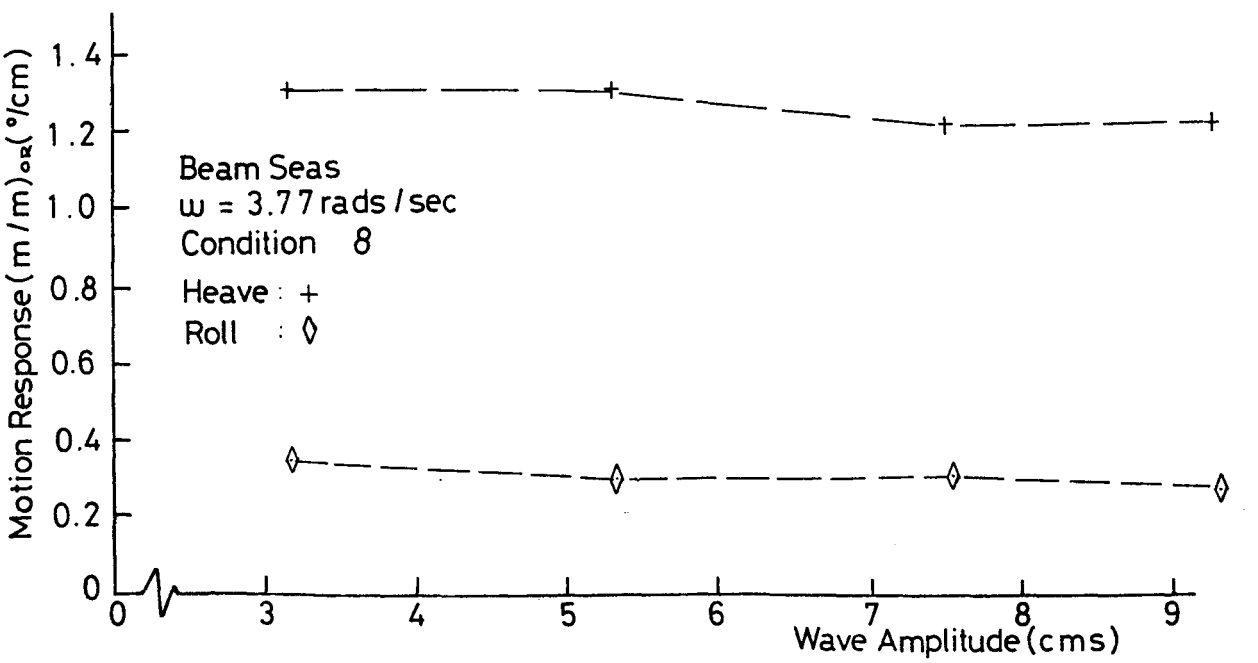

Fig. 9.15. Beam Sea Motion Response.

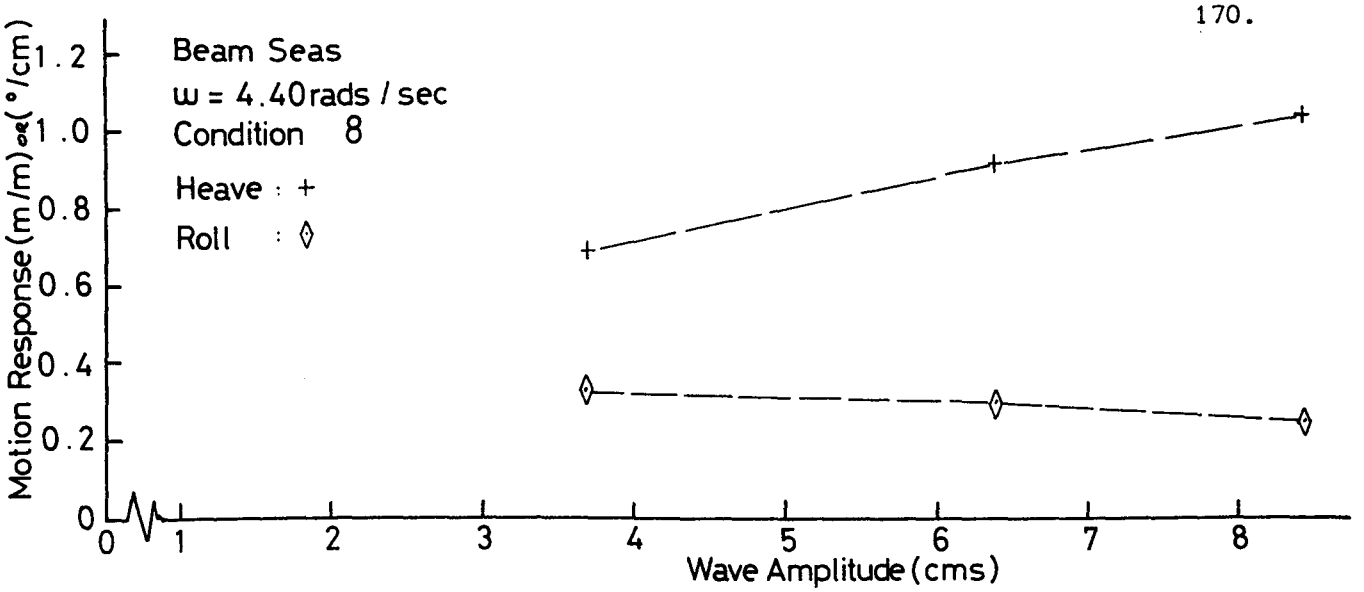

Fig. 9.16. Beam Sea Motion Response.

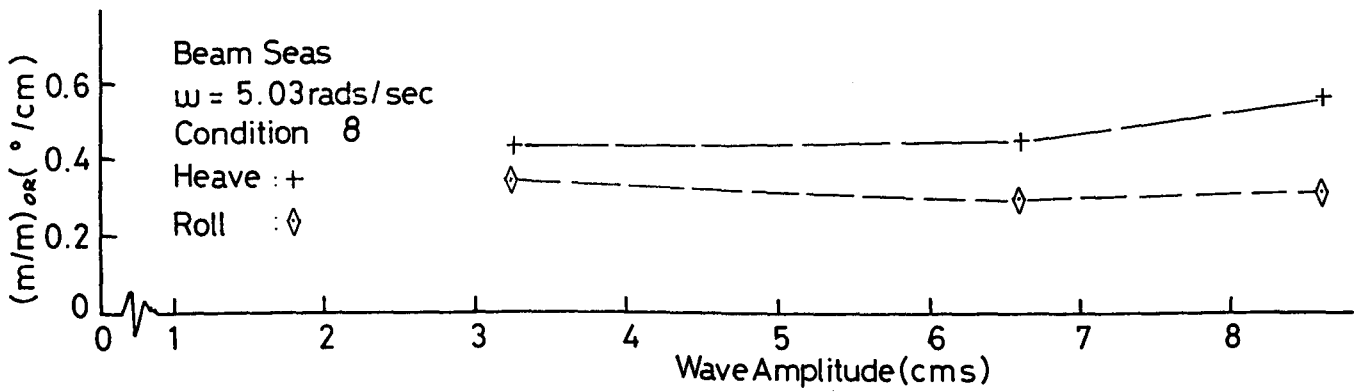

Fig. 9.17. Beam Sea Motion Response.

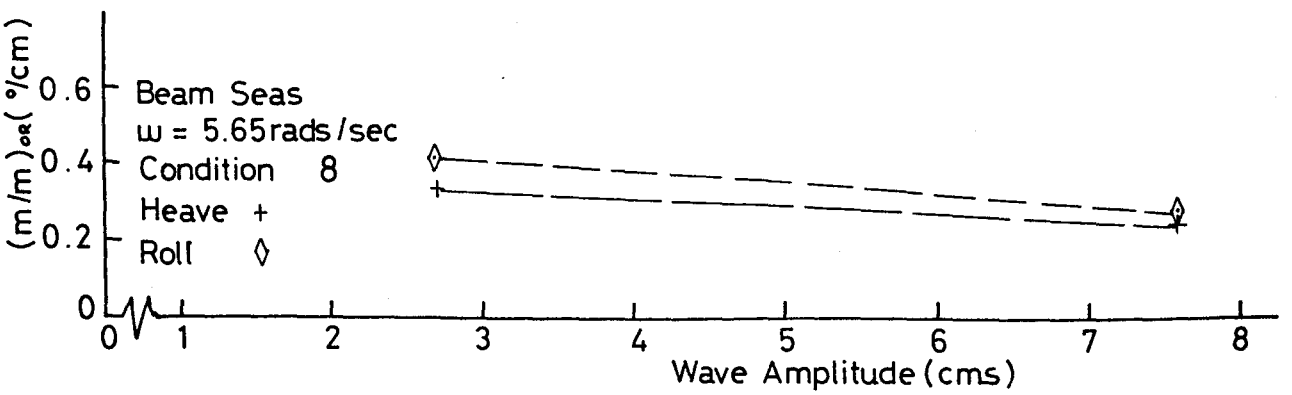

Fig. 9.18. Beam Sea Motion Response.

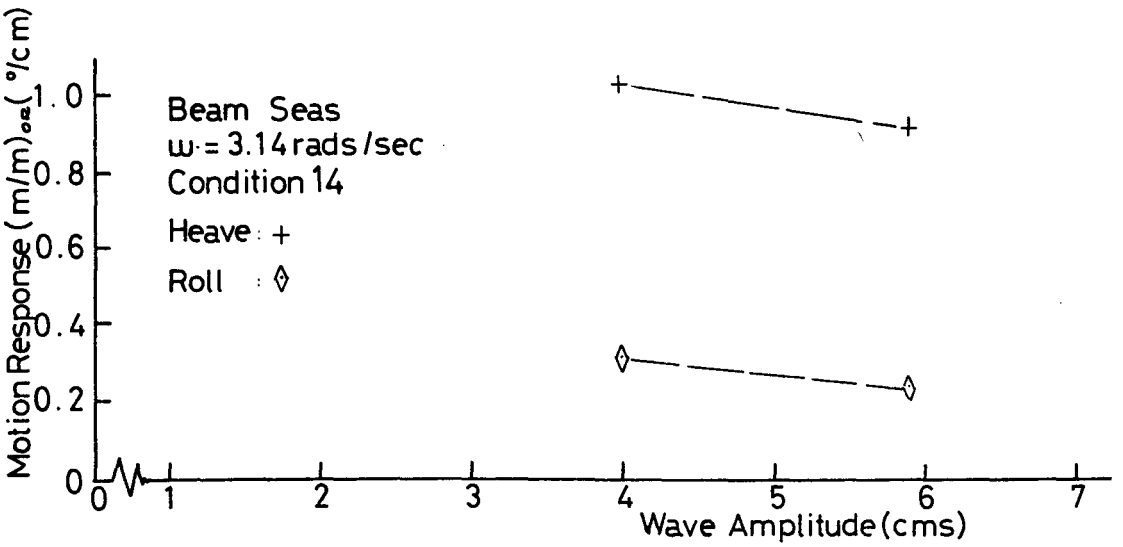

Fig. 9.19. Beam Sea Motion Response.

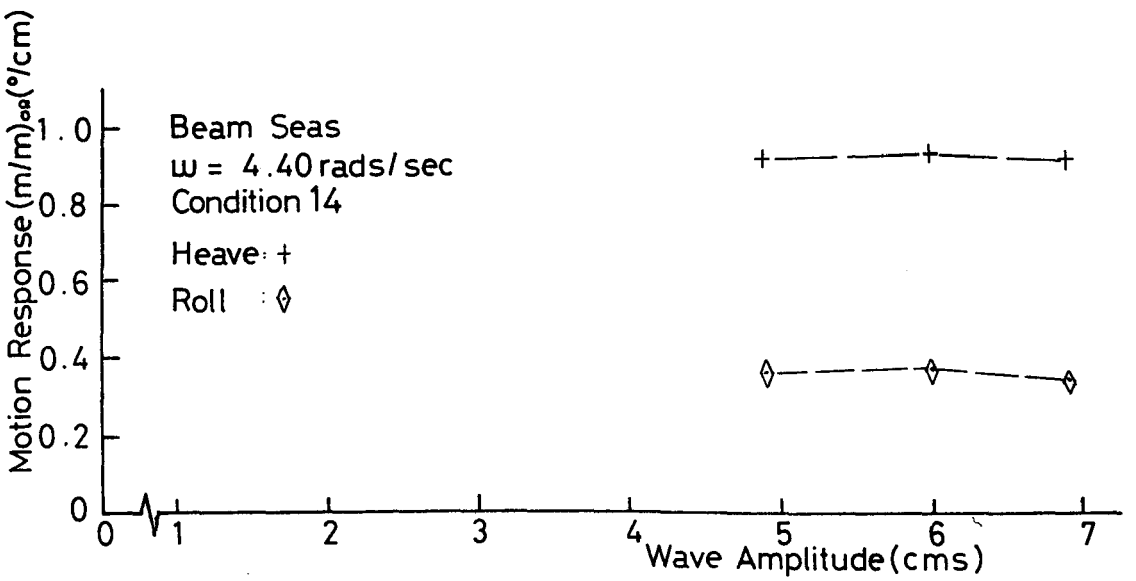

Fig. 9.20. Beam Sea Motion Response.

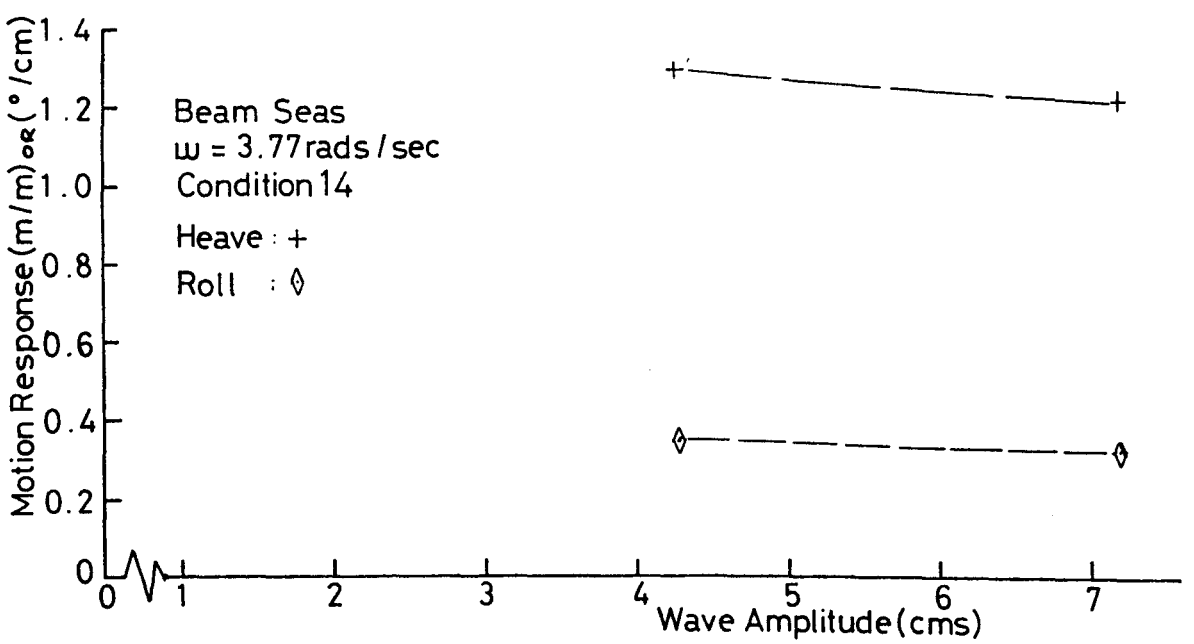

Fig. 9.21. Beam Sea Motion Response.

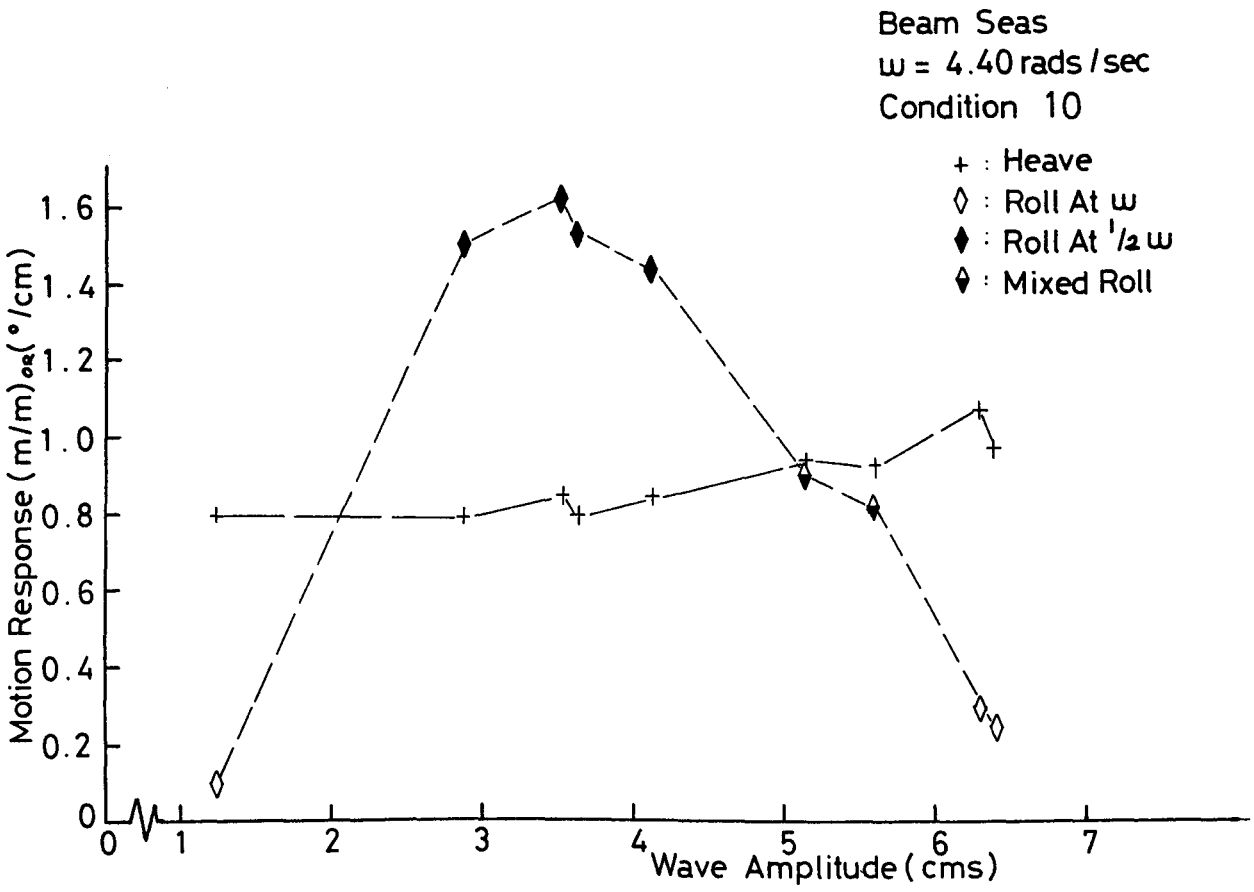

Fig. 9.22. Beam Sea Motion Response.

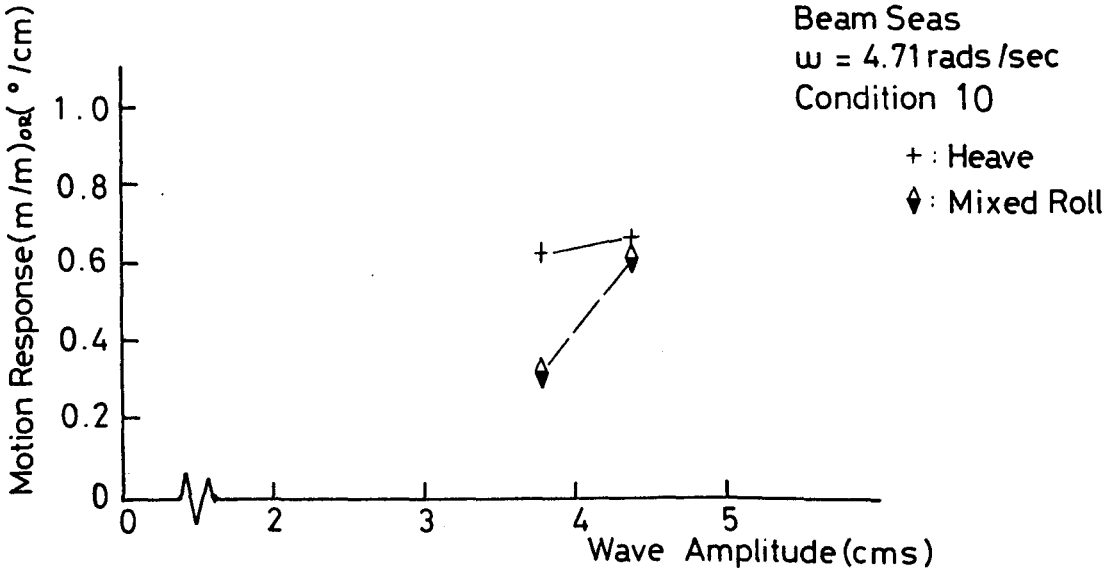

Fig. 9.23. Beam Sea Motion Response.

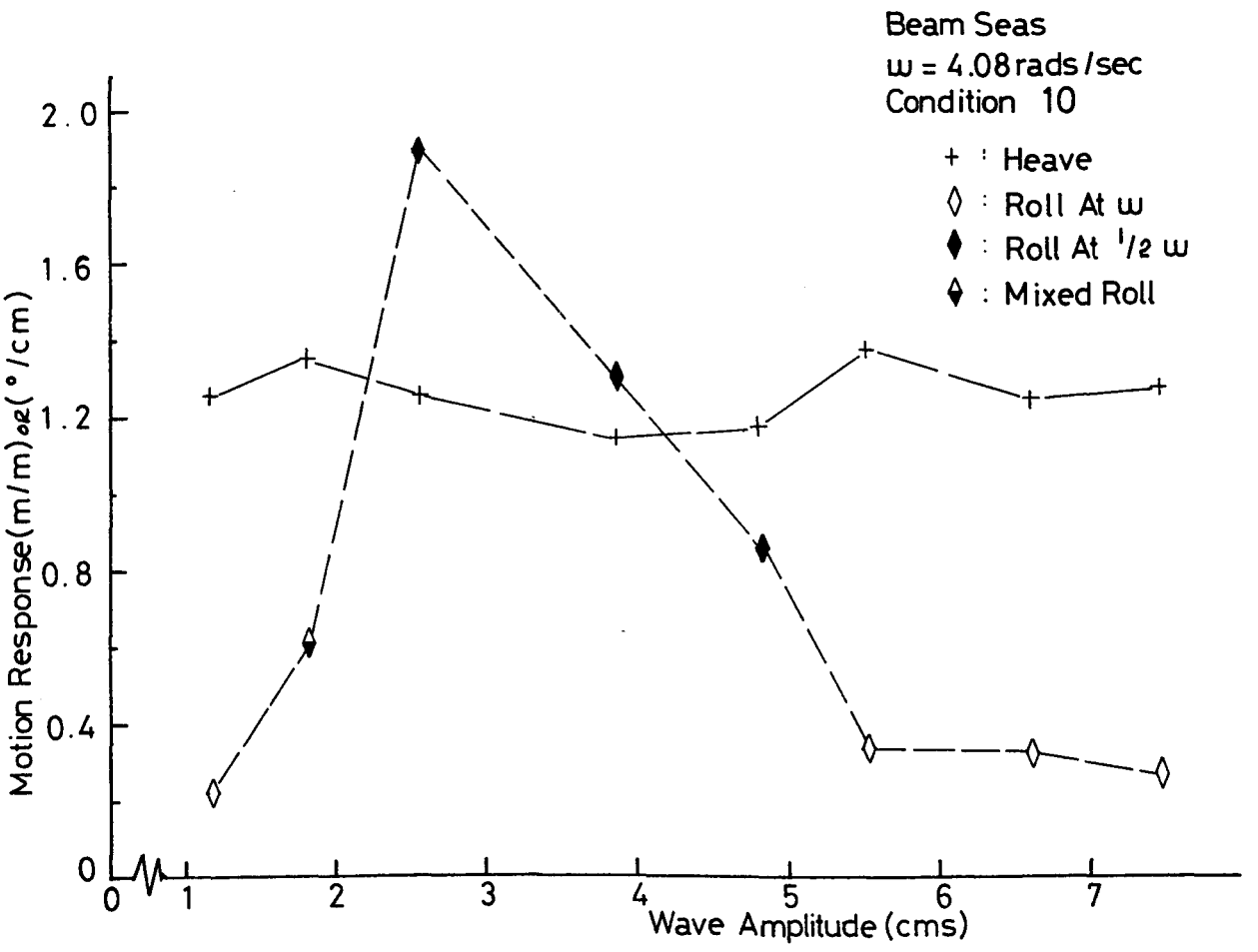

Fig. 9.24. Beam Sea Motion Response.

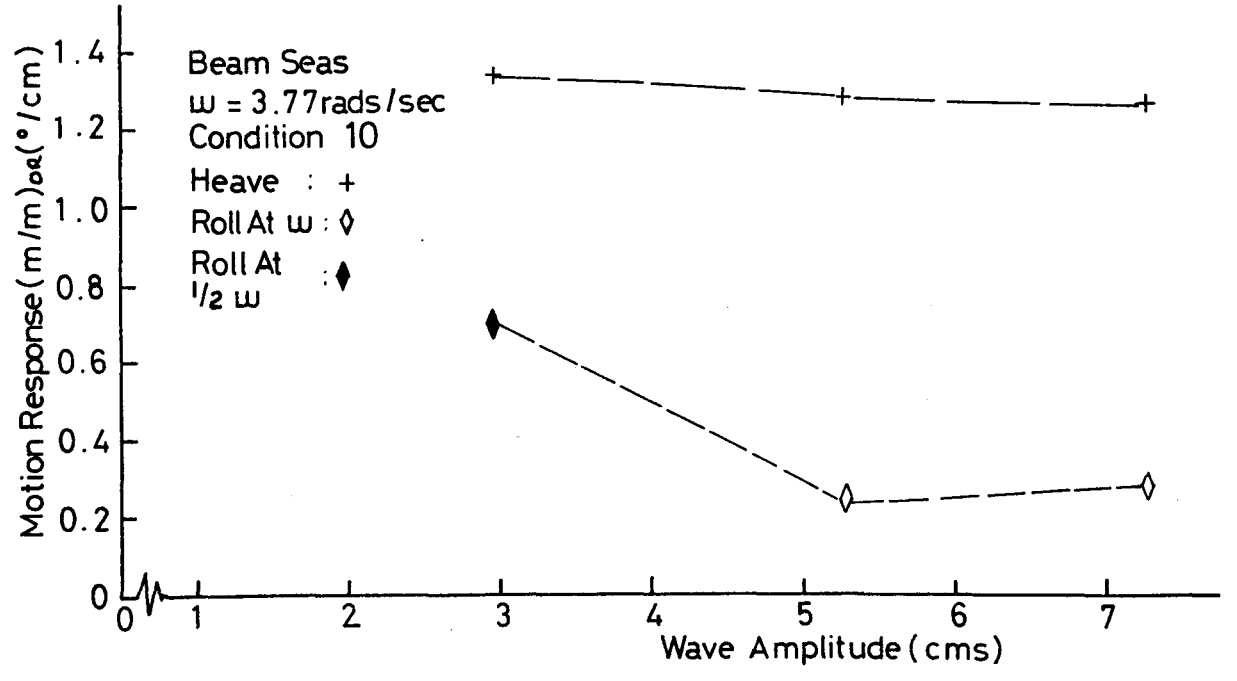

Fig. 9.25. Beam Sea Motion Response.

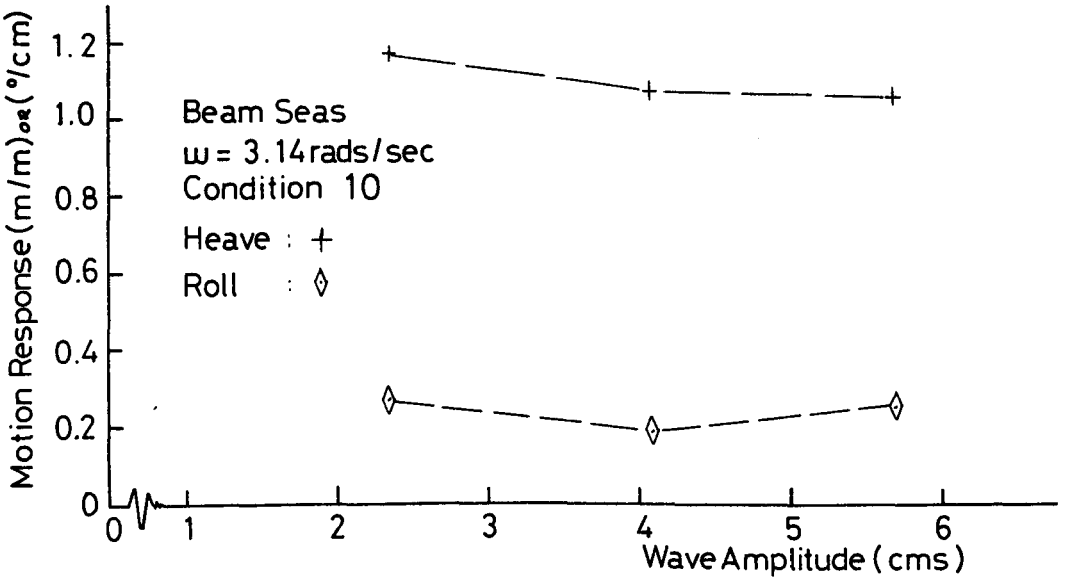

Fig. 9.26. Beam Sea Motion Response.

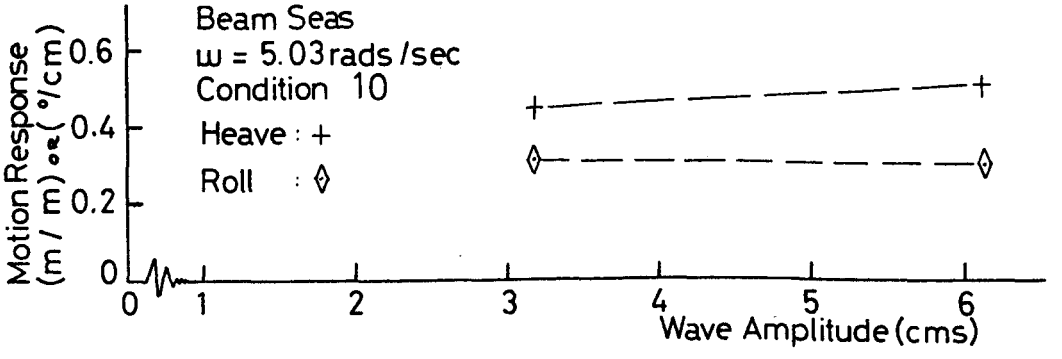

Fig. 9.27. Beam Sea Motion Response.

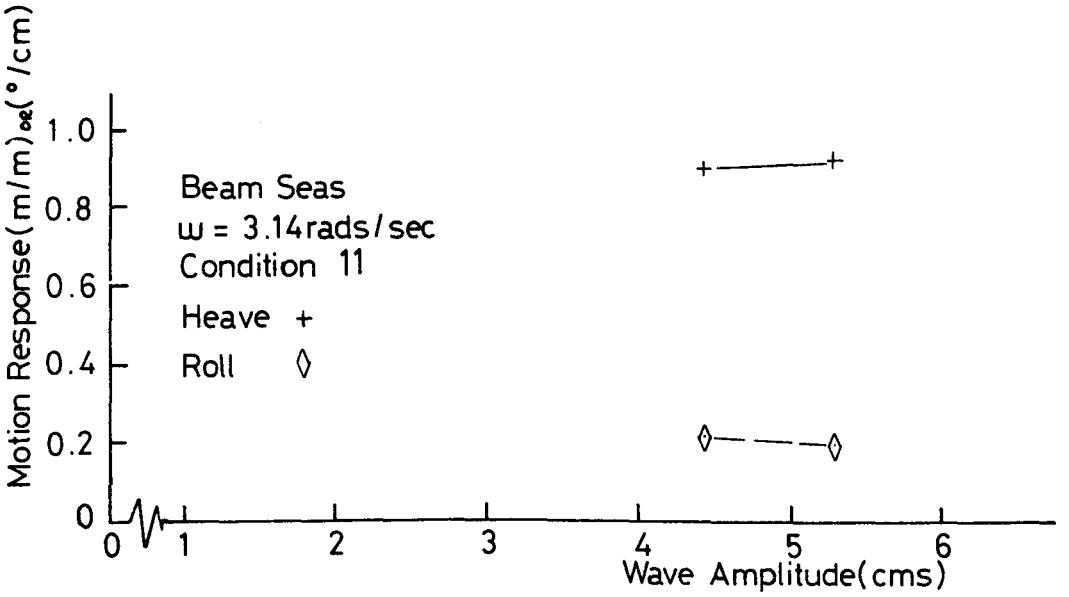

Fig. 9.28. Beam Sea Motion Response.

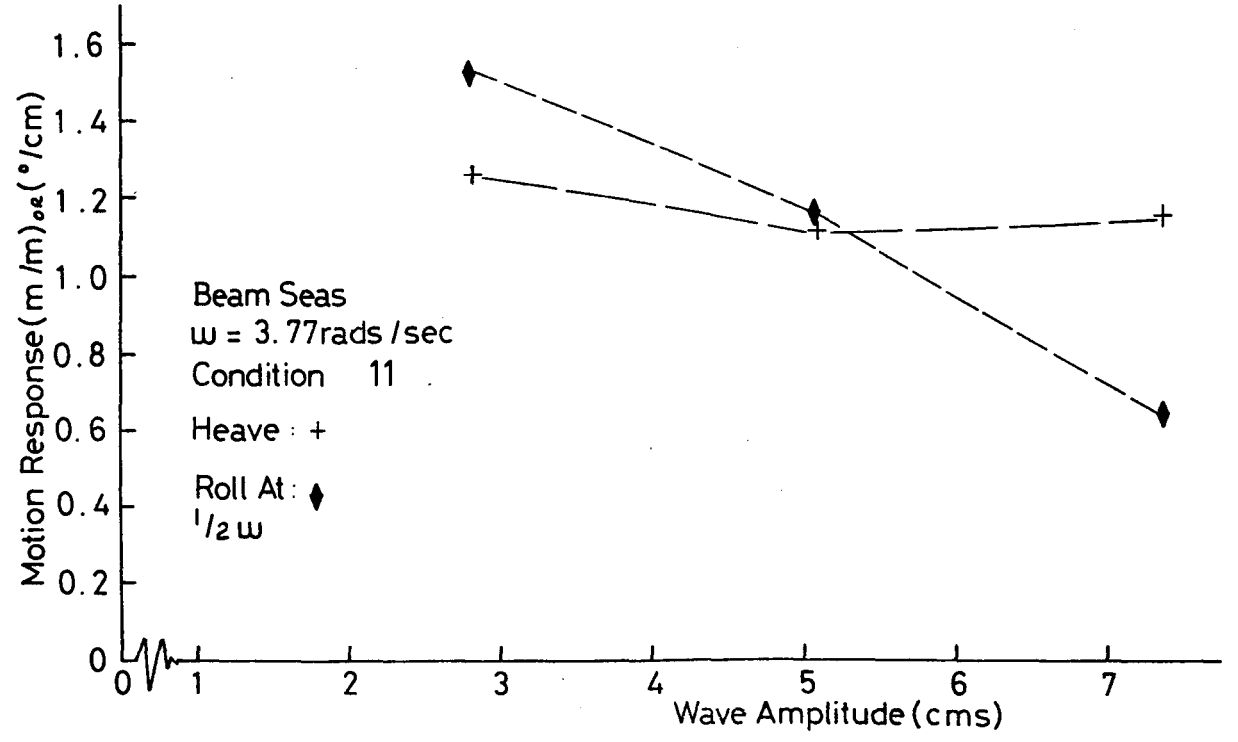

Fig. 9.29. Beam Sea Motion Response.

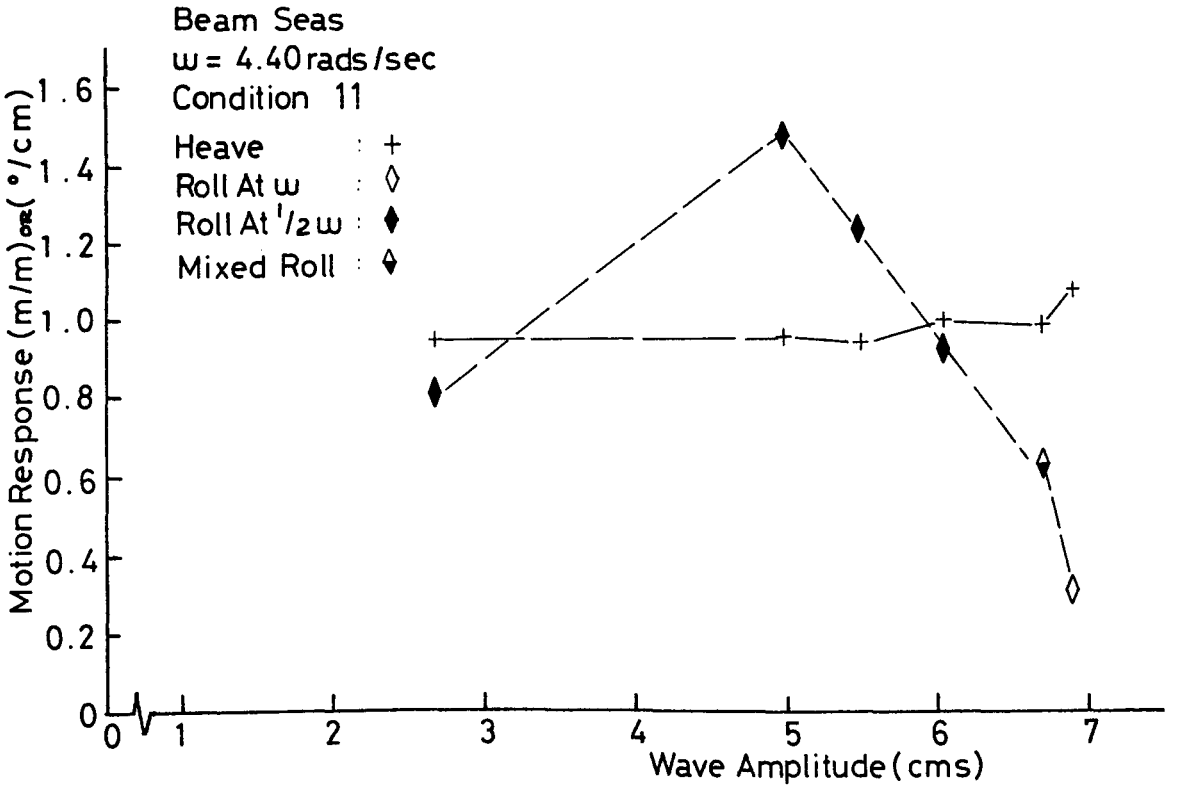

Fig. 9.30. Beam Sea Motion Response.

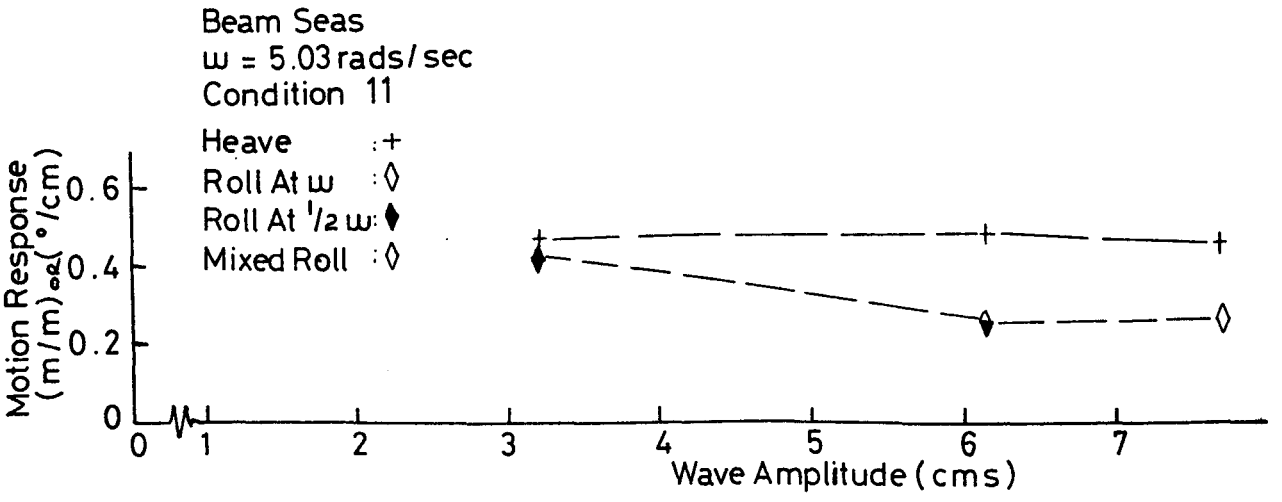

Fig. 9.31. Beam Sea Motion Response.

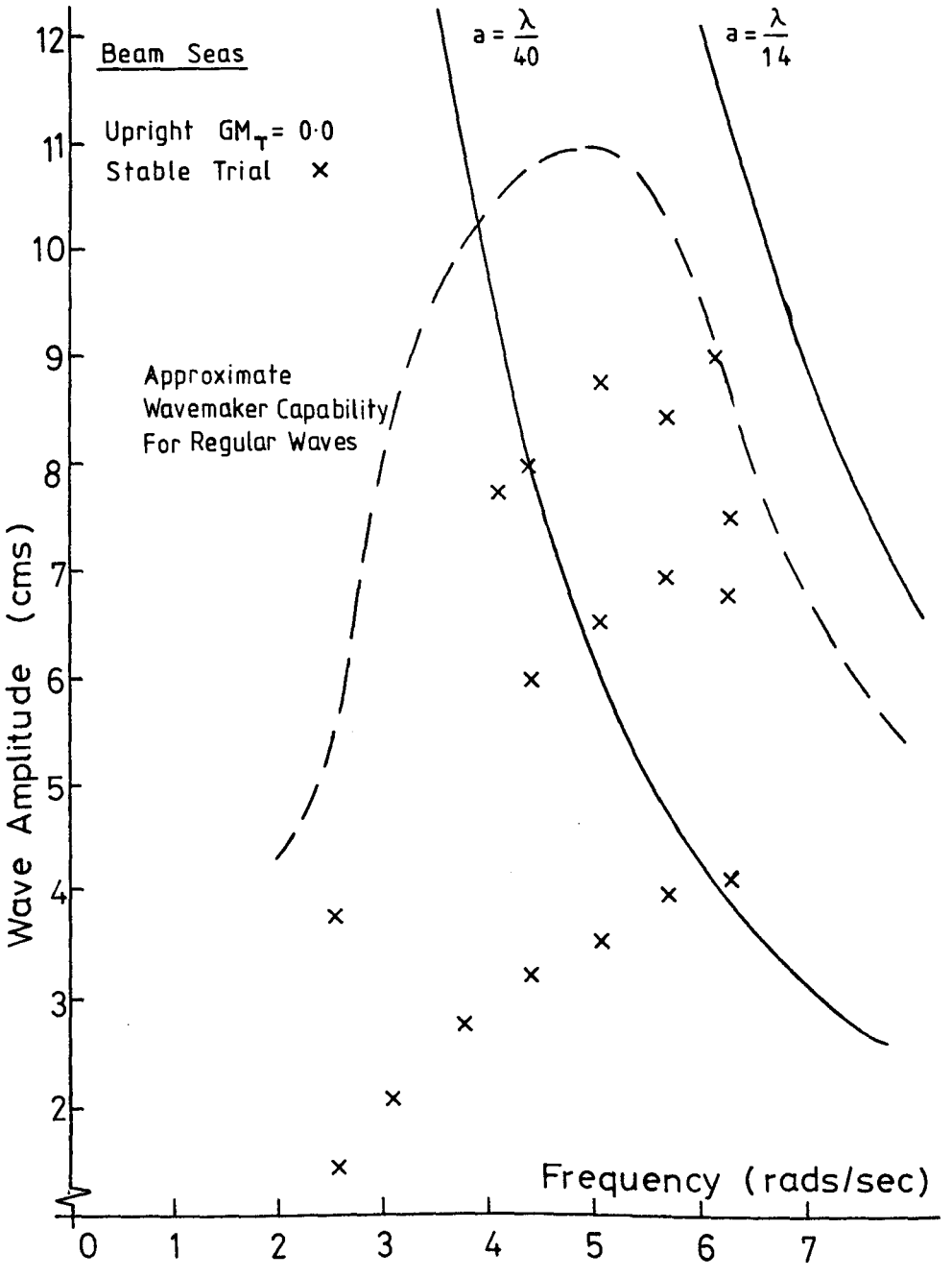

Fig. 9.32 Survival Experiment

CHAPTER 10

LARGE AMPLITUDE HEAVE MOTIONS

10.1 Introduction

The equation of motion for a floating vessel is frequently given as a second-order linear differential equation with a sinusoidal exciting force and frequency dependent coefficients as in Eq. 6.4. (Tick[133] has shown that such descriptions actually represent systems which are described in the time domain as integral equations, but this need only be borne in mind as an example of the possible inadequacy of the conventional approach.) Cummins[134] has commented on the usual representation and points out that for the actual system if the exciting force was suddenly doubled the response would not suddenly double despite being a linear representation. However, the usual approach is very convenient since it allows the use of spectral techniques by the methods of St. Denis and Pierson[86] and has been quite successful. Such an approach requires the sea to be represented by a sum of Fourier components and since we have frequency dependent coefficients there is an anomaly which does not receive much attention. The anomaly is that as we must assume all the Fourier components to be present at the same time we must have all the frequency dependent coefficients co-existing. Since each coefficient essentially represents a different flow or motion these must all exist at the same time which is not physically reasonable.

An alternative representation of the seaway is to consider it at any time instant as being composed of a series of single-cycle waves each characterised by their zero-crossing period and height. Such an approach is not without its difficulties since the examination of a wave record will show that, for instance, not all the visible 'waves' cross the zero-line and further a compact representation is not possible as with Fourier components. However, it is useful since, as will be shown, its combination with the complete solution to the equation of motion sheds some further light on the motion response problem.

In particular, this chapter proposes the use of design-wave-groups, which have some of the characteristics of an amplitude modulated wave system. Calculating the motion in the time-domain for such groups shows that the conventional use of steady-state transfer functions for the calculation of large motions is not necessarily justified. (The idea was originally developed in an internal report[94].) Linear theory will be adhered to, although it could be argued that investigating large amplitude motions with linear theory is anomalous in itself. However, some interesting results are arrived at, although in view of the above, they should be considered as representing a magnitude of uncertainty in the response rather than the actual response in a deterministic sense.

10.2 Equation of Motion

The equation of motion is exactly as in Chapter 6 except that the cosine term is replaced by a sine term for convenience in the simulation, i.e.

$$(\Delta+AM)\ddot{z} + C_1\dot{z} + K_z z = F \sin \omega t \qquad \ldots\ldots \qquad 10.1$$

The complete solution can be expressed analytically as in Eq. 6.5 but here it is solved in the time-domain by a step-by-step method, (the Runge-Kutta-Nystrom method, see Appendix E). The heave exciting force is calculated as in Chapter 6.

10.3 The Design-Wave-Group Concept

In ocean-engineering fairly heavy emphasis has been placed on spectral design techniques and the design-wave approach. Methods are available for estimating extreme wave heights and, more recently, since the responses are also frequency dependent the joint distribution of wave period and amplitude for the design-wave has been obtained[135]. It has also been shown how the conditional probability that the wave amplitude will exceed a certain range of values may be considered[136].

The designer now has a wave of given height and period, where the period is defined as the interval between successive up-crossings of the mean level. If he proceeds to calculate the response to this

extreme height on the basis of regular wave transfer functions, he will be in error. In reality the extreme response will depend on the preceeding conditions. This can be said with confidence because it is well-known that vibrations take time to build-up or decay, see for example Ref. 137 and Fig. 10.1. This has generally been ignored in vessel motion response calculations partly because of the Fourier representation and perhaps because ships tend to have higher damping than SWATHs or semi-submersibles. The time taken for the decay or build-up depends on the damping; the lower the damping the longer the time taken.

To investigate this behaviour the use of a group of design-waves is proposed. There has been considerable interest in wave-groups in the past four years and some of this is summarised in Appendix F. The group contains the single-frequency design-wave and also other sinusoidal waves of the same frequency, but lower amplitude, juxtaposed to give the general shape of an amplitude modulated wave system.

There is little mathematical justification for doing this since it introduces a discontinuity at the start and end of each cycle. If, alternatively, the envelope shape was preserved and the waves made continuous this would introduce other frequency components which is undesirable for the present purpose because of the frequency dependence of the coefficients in the equation of motion. (In a recent paper St. Denis[138] has set up a model by juxtaposition of third-order Stokes' waves to produce a statistical description of moderately severe seas. In this he treats the resulting discontinuity of orbital velocities with a fairing process.)

Having defined the group of design-waves the response is calculated in the time domain. The response to the n^{th} wave is calculated using the final value of motion velocity from the $(n-1)^{th}$ wave as the initial condition. (The displacement and acceleration at the first nodal point have been taken as zero.) This response is obtained digitally, rather than on the analogue, using the Runge-Kutta-Nystrom method (Appendix E) with, usually, a time step of $t = T/20$ where T is the wave period. (When the time step was taken as $t = T/40$ the same solution was achieved as for $t = T/20$.)

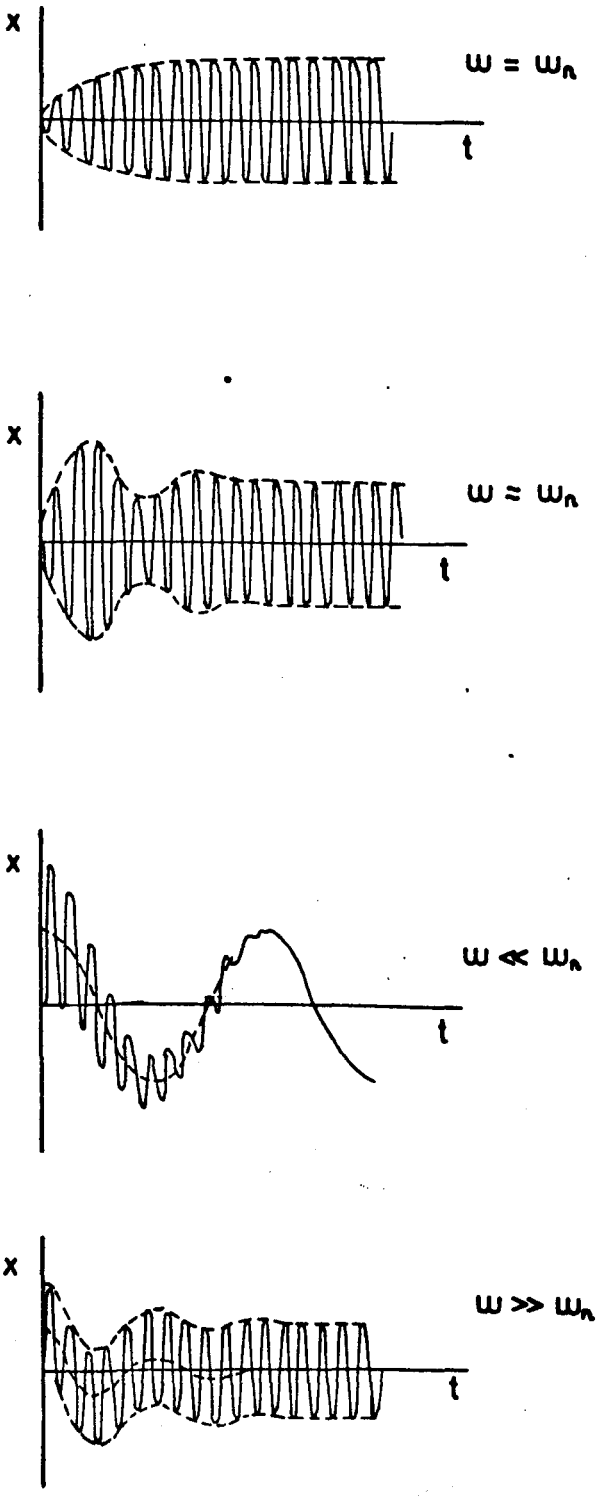

Build Up Of A Forced Vibration

Fig 10·1

10.4 Response in the Design-Wave-Group

In this section a relatively large design-wave-group with eleven-cycles is considered. The frequency of individual cycles is constant throughout the group and the wave amplitudes are given in Table XVI.

No. of Cycles in Group	Wave Amplitude (m)											Ratio $\frac{a_{ab}}{a_m}$
	a_1	a_2	a_3	a_4	a_5	a_6	a_7	a_8	a_9	a_{10}	a_{11}	
11	.025	.050	.075	.100	.125	.150	.125	.100	.075	.050	.025	0.8

Table XVI. Group Structure.

The resonant response is shown in Figs. 10.2 and 10.3 in the eleven-cycle wave-group for an assumed linear damping ratio of $\gamma = 0.1$ and 0.2 respectively. The steady-state response to the largest wave is also shown. In the former case the maximum response amplitude is some 15% less than the steady-state values. Assuming a doubling in the damping ratio to $\gamma = 0.2$ halves the steady-state response at resonance (hence illustrating the importance of obtaining the correct damping ratio) and also causes the transient to decay more quickly. Even so, the maximum response amplitude is some 12% less than the steady-state response to the highest wave.

Both diagrams show that, as expected for $\omega/\omega_H \simeq 1$, the motion lags the force by 90°, but it is interesting to note that in both cases the maximum response occurs during the cycle after the maximum force has occurred. This will obviously have implications for calculating the relative motions.

In Fig. 10.2 it can clearly be seen that the responses in the second half of the group are greater than those in the first half. In fact, if we look at the response to $a_o = 0.075$cms ($= a_3 = a_9$) then in the first half of the group the steady-state solution over-estimates the response by a certain error (denoted by ε_2), but in the second half of the group the steady-state solution under-estimates the response by ε_3. Since it can be seen that $\varepsilon_2 \simeq -\varepsilon_3$ then the average actual res-

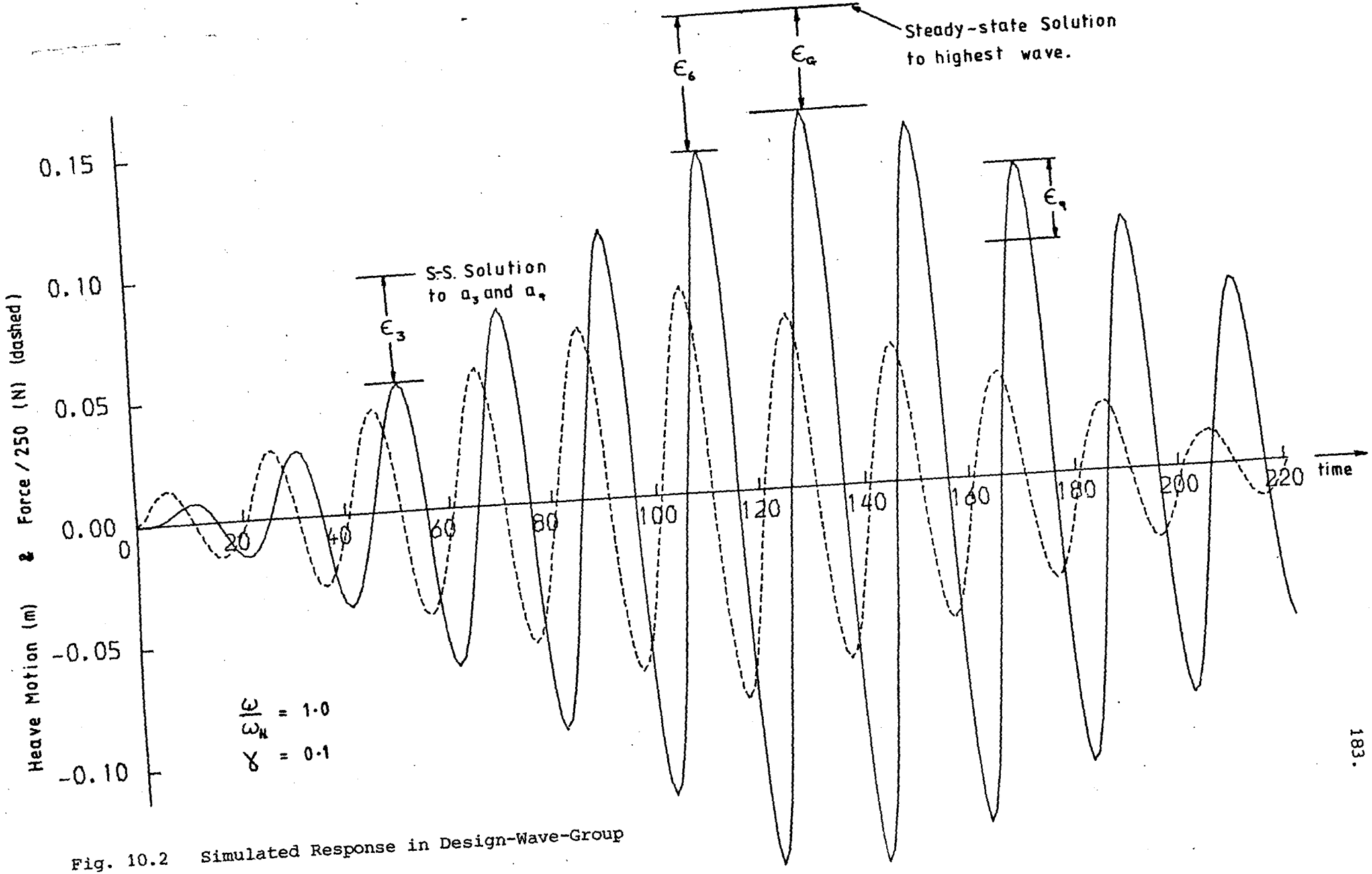

Fig. 10.2 Simulated Response in Design-Wave-Group

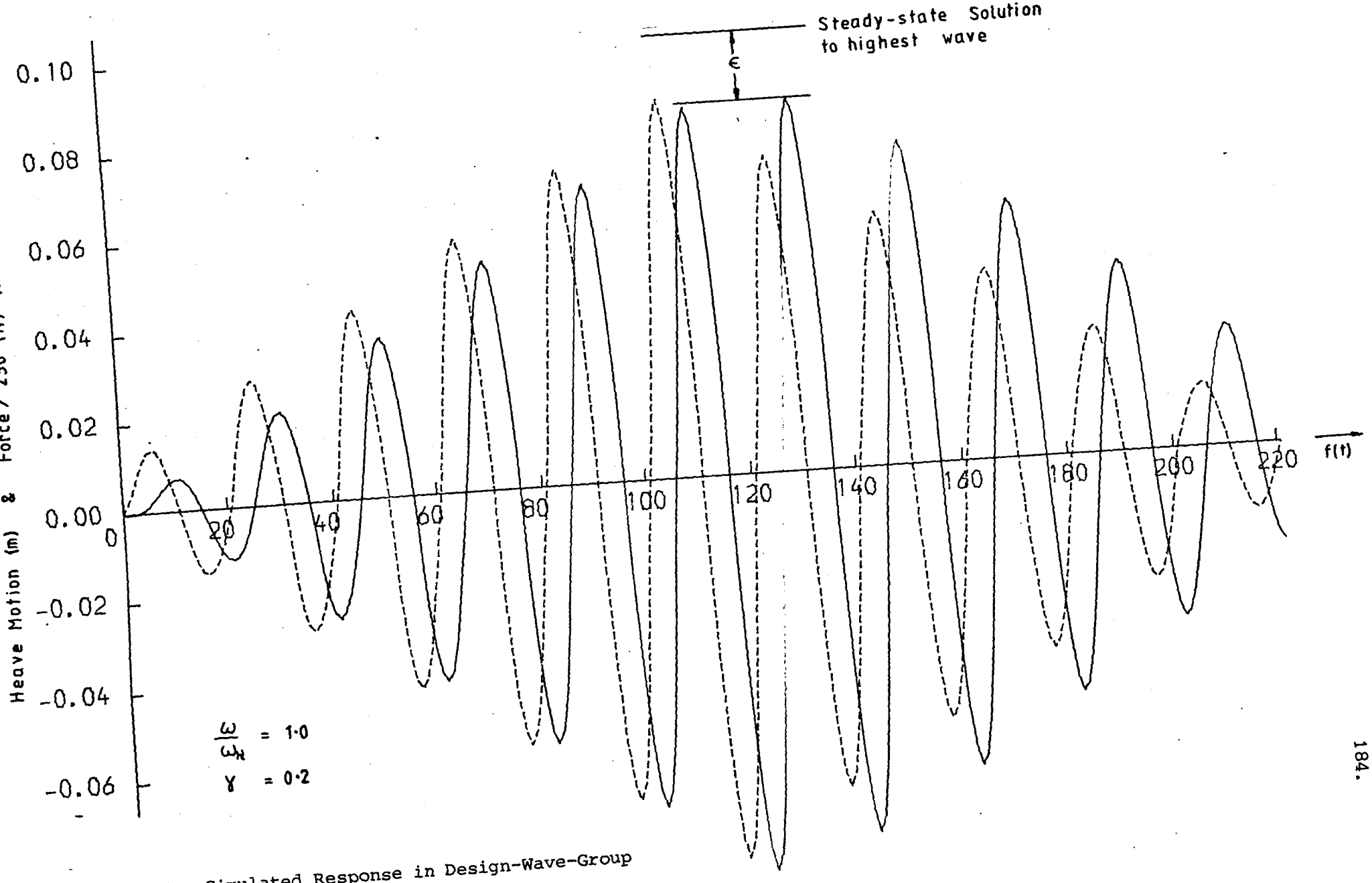

Fig. 10.3 Simulated Response in Design-Wave-Group

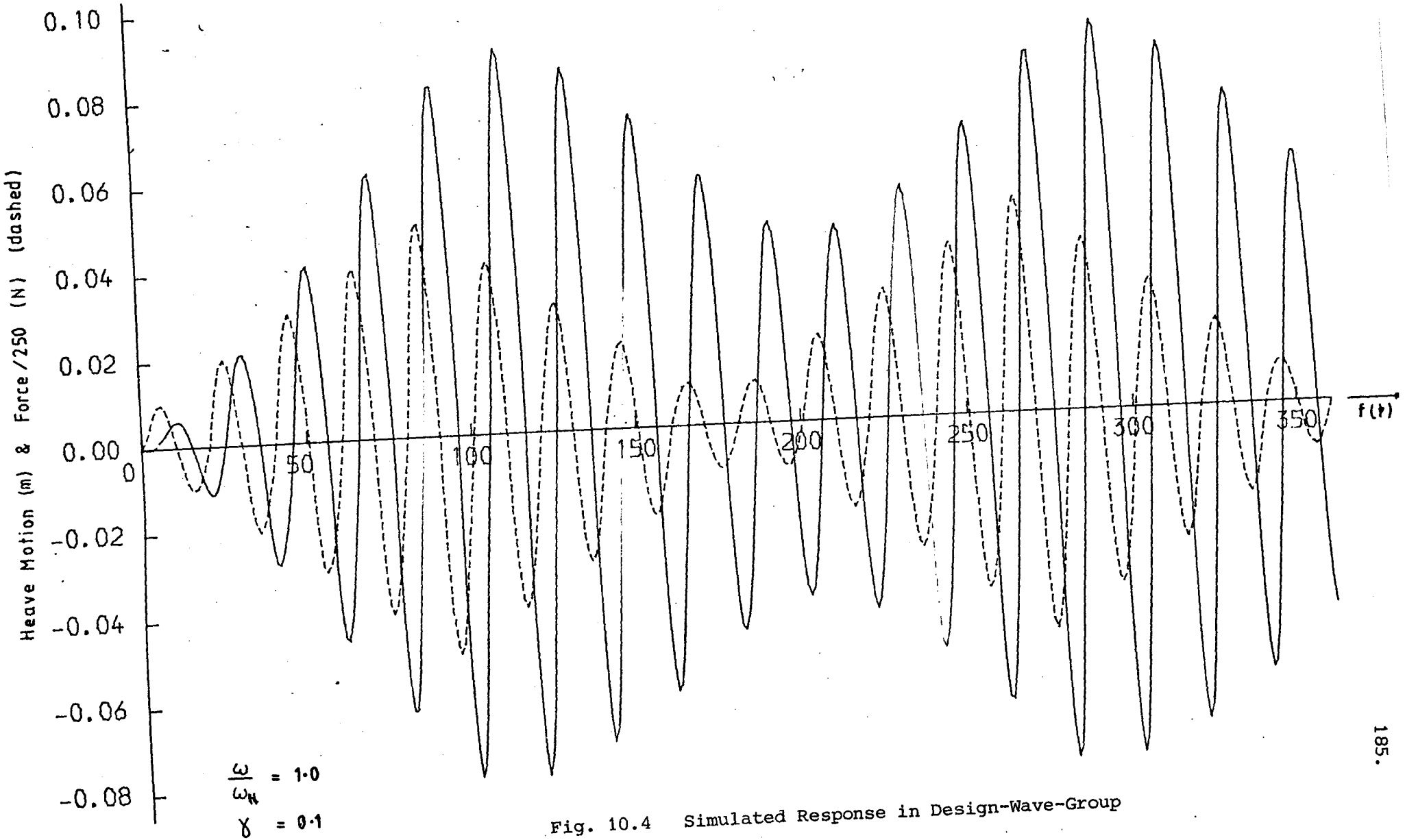

Fig. 10.4 Simulated Response in Design-Wave-Group

ponse will be similar to the average response predicted using steady-state solutions (or regular wave transfer function) see Table XVII.

	Steady-State Response	Simulated Response
Average	0.112 m	0.101 m
R.M.S.	0.124 m	0.114 m

Table XVII. Comparison of Average and R.M.S. Responses in an Eleven-Cycle Wave Group

All the above examples have started with the vessel stationary. If two groups of design-waves are considered as in Fig. 10.4, then it can be seen that the maximum response in the second group is no higher than in the first. The average response is, however, higher.

(In general this type of behaviour is attributable to what is referred to in the manoeuvring literature as 'memory effects'. The vessel is considered as having a 'memory' of its previous motions. The response at any time can then be calculated from the response to a unit impulse and the previous time history using the convolution integral. Such an approach for ship vertical motions has been advocated by Cummins[134].)

10.5 Discussion

The foregoing has shown discrepancies of 12 - 15% between the maximum resonant responses calculated by different methods. This is obviously quite significant but in the absence of experimental verification these results should be taken as representing some uncertainty in the maximum response rather than the 'correct' value in a deterministic sense. The larger the group becomes the smaller the discrepancy will be. The eleven-cycle group used here is by no means a severe one, since as shown in Appendix F there is data to suggest that the maximum wave height may be about 1.7 times the height of the previous wave. Thus the discrepancies could be larger than suggested above, although this will depend on factors such as damping and the height of the low waves in the groups. Further perspective is given if it is

borne in mind that for a sea with h_s = 7.5m the extreme wave height in 50 years may be only 8% higher than expected in 10 years[136]. This difference is about half the above discrepancies.

The examples illustrated here have all been at the resonant frequency and in accordance with Fig. 10.1 the steady-state response tends to over-estimate the simulated response. However, it should also be noticed that near resonance there can be a significant overshoot. In the present case, where resonant frequencies are also encountered, this is unlikely to result in the largest motions, but it could be very important for semi-submersibles because for typical modern rigs the 100-year storm design-wave can lie in this region. Thus, the maximum motions could be larger than hitherto anticipated with the possibility of severe consequences. It is recommended that this be investigated.

The design-wave-group concept could also be useful for semi-probabilistic methods which are likely to become more common in the design of marine structures[139]. Since motion-induced loads will need to be taken into account it will be necessary to estimate the uncertainty in motions and the above technique may therefore prove to be useful.

CHAPTER 11

CONCLUSIONS AND RECOMMENDATIONS

11.1 General

The background to the project, and the history of conventional research vessels and SWATH ships has been discussed from which it is shown that adopting a SWATH ship would fit into the historical context of research vessel and marine-science development.

The advantages of the three-hulled configuration have been presented and the overall conclusion is that there appears to be no technical reason why such a vessel could not be built and operated as a successful research vessel.

11.2 Costs

The increased 'research efficiency' for the SWATH should offset any increased operating costs. General considerations suggest that the first cost should not be appreciably greater than a conventional vessel, but this is not entirely borne out by the quotations which have been received based on the Specification. It is possible that the first cost will reduce as experience is gained in building this type of vessel.

11.3 Structure

High bending moments occur on the centreline of the deck-box and at the junction of the deck-box and columns. The use of the H.T.S. steel is beneficial in such areas to reduce the structural steelweight which is the largest single group-weight. (The deck-box is the largest fraction of steelweight.) The greatest loads appear to be induced at zero-speed in beam seas but the method used herein for calculating these loads is not completely satisfactory because of uncertainties due to diffraction effects. It is therefore recommended that appropriate theoretical means be adopted for determining these effects and that the answers be compared with model

experiments. These loads can then be used in an approach to the minimum-weight design of the deck-box which is particularly important because it is such a large proportion of the total steelweight. In this case if the deck-box weight could be reduced by 10% the weight of the scientific 'payload' could be increased by about 90%.

11.4 Stability and Flooding

SWATH ships can be designed with excellent water-tight subdivision and reserve buoyancy.

It has been suggested that the existing static stability criteria for SWATHs be revised to include the angle of down-flooding. Even with this revision it is shown that the criteria with respect to wind-loading can easily be met by SWATHs because of the large rise in GZ with the immersion of the column flare and the edge of the deck-box. The static stability requirements are more likely to be set by the need to limit the heel angle to, say, less than 15° when operating with large off-centre loads or following off-centre flooding.

11.5 Resistance

It is known that the resistance is generally higher than that of a monohull due, at least in part, to the SWATH having up to twice the wetted area. Developments at DTNSRDC appear to be succeeding in reducing the SWATH total resistance and, furthermore, the added resistance in a seaway for a SWATH is less than for a conventional ship.

The previously suggested C_D for the hull endings appears to be too high and it is recommended that to ease the problems of estimating the form drag and extrapolation to full-scale the model should be large enough for the Reynolds number based on hull diameter to be greater than about $Rn = 3 \times 10^5$ in the operating speed range. This may not, however, be compatible with the requirement for the model size to be such that for motion response tests it can be tested over the working range of frequencies at realistic wave amplitudes. The towing arrangement can greatly affect the trim during resistance tests, but the effect on measured resistance seems to be small.

The peak in the wave resistance curve is dependent on the column spacing, but in this case since the design speed range is below the peak the separation has little effect and it is more important to minimise the resistance of the individual components. Increases in column thickness cause a much greater change in wave resistance than increases in column chord and further calculations show that it would be quite feasible to reduce the total resistance for the case in question. There is considerable over-prediction in the total wave resistance calculation due mainly, it is thought, to the hull endings but also due to the canal width effect. It is recommended that the wave resistance calculated by the technique used herein and also by more sophisticated methods should be compared, both with each other, and with experimental wave resistance measured by a wave-cut or similar technique.

11.6 Motions

It has been shown that the motion response of the SWATH-type research vessel would generally be lower than an equivalent monohull. Even when the absolute motions are the same magnitude the SWATH would be more comfortable as measured by the subjective motion technique. Further benefits would accrue to the SWATH from the effects of forward speed raising the frequency of encounter and from the possibility of using an active control system.

The digital program gave good agreement with model experiment results at zero-speed in head seas for heave but not for pitch or relative motion of the bow. To achieve a low relative motion of the bow the heave and pitch natural frequencies should be well separated. It has been shown that the resonant motions are strongly dependent on viscous effects and the response dropped from about 1.8 to 1.2 m/m with increasing wave amplitude for conditions with the brace. Without the brace the resonant response was fairly linear with wave amplitude thus showing that the bracing made an important contribution to viscous effects. The theoretical approach used to investigate column flare was found to be over-simplified but experimental results showed that with small or moderate column flare the motions are essentially linear with wave amplitude. However, for large column flare non-

linearities and parasitic motions became important. It was concluded that the 'jump' phenomenon was caused by the relative motion of the forward column and the hardening-spring action of the flare.

The roll motions in head seas have been described in terms of the stable and unstable regions for the Mathieu equation. Although such motions have been identified as a capsize mechanism they did not, in this case, lead to capsizing and it is suggested that this is due to having a large area under the GZ curve. Removal of the transverse brace also indicated the importance of damping in limiting the roll motion amplitudes and in irregular seas it was only in the absence of bracing that rolling occurred. An interesting mechanism whereby the jump phenomenon precludes unstable rolling at large wave amplitudes has been identified.

It has been explained that these motions could just as easily happen for a twin-hull design as for a three-hull design. Further, at zero-speed in head seas for the design condition the motions are not expected.

In beam seas the responses and conclusions are generally as for head seas. The subharmonic rolling occurred for the same conditions as unstable rolling in head seas but was not observed when wave amplitudes were large. No explanation of this has been reached.

With zero upright GM_T the model did not capsize under beam-sea wave action but the passage of every wave resulted in 'green' water on deck.

For large amplitude motions a design-wave-group concept has been proposed. The use of this shows that the conventional use of steady-state transfer functions is not necessarily justified. It is suggested that the outcome be taken as a measure of the uncertainty of the response rather than the actual predicted response in a deterministic sense. There is a possibility of important consequences arising from this, particularly for conventional semi-submersibles and it is recommended that they be investigated. The approach may be useful in semi-probabilistic approaches to structural design.

11.7 Closure

Although a significant portion of this thesis has concentrated on undesirable motion behaviour it should be re-affirmed that there appears to be no technical reason why a three-hulled SWATH could not be built and operated as a successful research vessel.

Interest in SWATH ships continues to grow and it must be expected that more will be built. It is hoped that the work in this thesis will help in that trend.

REFERENCES

1. Eames, M.C.: 'Advances in Naval Architecture for Future Surface Warships', Trans. RINA, vol. 123, 1981.

2. Hightower, J.D. and Seiple, R.L.: 'Operational Experiences with the SWATH Ship *SSP Kaimalino*', AIAA/SNAME Advanced Marine Vehicles Conference, April 1978.

3. Oshima, M., Narita, H. and Kunitake, Y.: 'Experiences with 12m Long Semi-Submerged Catamaran (SSC) *Marine Ace* and Building of SSC Ferry for 446 Passengers', AIAA/SNAME Advanced Marine Vehicles Conference, 1979.

4. Olson, S.R.: 'The Military Utility of the Small Waterplane-Area Twin-Hull (SWATH) Concept', AIAA/SNAME Advanced Marine Vehicles Conference, April 1978.

5. Childers, K.C., Gloeckler, F.M. and Stevens, R.M.: 'SWATH - The VSTOL Aircraft Carrier for the Post-1990's', Naval Engineers Journal, February 1977.

6. Seidl, L.H., Wilkie, L.J. and Loui, S.C.H.: 'Application of SWATH/FPS Concept to a Passenger Excursion Vessel Design', Hawaii Section SNAME, 1980.

7. 'SWATH Ship for Safer Personnel Transport', The Naval Architect, January 1981.

8. '*Mesa 80*: Mitsui's Semi-Submersible Catamaran as a Fast Ferry', The Motor Ship, July 1980.

9. Lamb, G.R. and Fein, J.A.: 'The Developing Technology for SWATH Ships', AIAA/SNAME Advanced Marine Vehicles Conference, 1979.

10. Miller, N.S. and McGregor, R.C.: 'The Problem of Scale in Model Testing for Offshore Work', Society for Underwater Technology Seminar: Models and their use as Design Aids in Offshore Operations, May 1978.

11. Thompson, C.W.: 'The Depths of the Sea', Macmillan and Co., London, 1873.

12. Davis, R.A.: 'Principles of Oceanography', Addison-Wesley Publishing Co., 1972.

13. Cruise Report, *RRS Challenger*, Cruise 9B, 1980. Scottish Marine Biological Association, Dunstaffnage Marine Research Laboratory.

14. Trillo, R.L.: 'Janes Ocean Technology, 1979-80', Jane's Yearbooks, London.

15. Telfer, A.V.: Discussion of Oo and Miller, Ref. 93.

16. Payne, P.R.: 'The Performance Potential of Semi-Submerged Ships', Journal of Hydronautics, vol. 12, No. 4, October 1978.

17. Boericke, H.: 'Unusual Displacement Hull Forms for Higher Speeds', International Shipbuilding Progress, vol. 6, June 1959.

18. Lewis, E.V. and Breslin, J.P.: 'Semi-Submerged Ships for High-Speed Operation in Rough Seas', Third Symposium on Naval Hydrodynamics, 1960.

19. Mandel, P.: 'A Comparative Evaluation of Novel Ship Types', SNAME Spring Meeting, 1962.

20. Leopold, R.: 'A New Hull Form for High-Speed Volume Limited Displacement-Type Ships', SNAME Spring Meeting, 1969.

21. Van Sluiys, M.F.: 'Model and Full-Scale Motions of a Twin-Hull Vessel', Nederlands Scheepsstudiecentrum, TNO Report No. 131 S, August 1969.

22. Stenger, J.J.: 'The Trident Stabilised Vessel Concept for Offshore Drilling and Construction Operations', OTC (1969) No. 1138.

23. Fendall Marbury: 'Small Prototypes of Ships - Theory and a Practical Example', Naval Engineers Journal, October 1973.

24. Lang, T.G.: 'Hydrodynamic Design of an S^3 Semi-Submerged Ship', Ninth Symposium on Naval Hydrodynamics, 1972.

25. Lang, T.G. and Higdon, D.T.: 'S^3, Semi-Submerged Ship Concept and Dynamic Characteristics', AIAA/SNAME Advanced Marine Vehicles Meeting, 1972.

26. 'Navy Completes Semi-Submersible Ship', Ocean Industry, December 1973.

27. Oshima, M., Narita, H. and Kunitake, Y.: 'Development of the Semi-Submerged Catamaran (SSC)', AIAA/SNAME Advanced Marine Vehicles Conference, 1979.

28. '*Mesa 80* Undergoing Successful Trials', Zosen, January 1980.

29. 'World 1st. Commercial SSC Built by Mitsui', Zosen, vol. 24, 1979.

30. Smith, S.N.: 'Preliminary Design Study on Small Semi-Submersibles for Life Science, Oceanographic, and Engineering Research', University of Glasgow, Dept, of Naval Architecture and Ocean Engineering Report NAOE-HL-78-23, 1978.

31. Smith, S.N.: 'Design for a Small Three-Hulled Semi-Submersible Research Vessel', University of Glasgow, Dept, of Naval Architecture and Ocean Engineering Report NAOE-HL-79-14, September 1979.

32. Smith, S.N.: 'General Description and Background of Small Semi-Submersible Research Vessel', University of Glasgow, Dept. of Naval Architecture and Ocean Engineering Report NAOE-HL-80-11, January 1980.

33. Miller, N.S.: 'The use of a Small Semi-Submersible for Engineering Research', University of Glasgow, Dept. of Naval Architecture and Ocean Engineering Report NAOE-HL-78-30, Revised January 1980.

34. Andrews, D.: 'Creative Ship Design', Trans RINA, 1982.

35. Lang, T.G. and Higdon, D.T.: 'Hydrodynamics of the 190 ton Stable Semi-Submerged Platform (SSP)', AIAA/SNAME Advanced Marine Vehicles Conference, 1974.

36. Chapman, R.B.: 'Hydrodynamic Drag of Semi-Submerged Ships', Journal of Basic Engineering, December 1972.

37. McCreight, K.K. and Stahl, R.: 'Regular Wave Responses and Stability Characteristics of a Systematic Series of Unappended SWATH Designs', DTNSRDC/SPD 0886-01, February 1980.

38. Bishop, R.E.D., Price, W.G. and Tam, P.K.Y.: 'On the Dynamics of Slamming', Trans RINA, 1978.

39. Chapman, R.B.: 'Sinkage and Trim of SWATH Demihulls', AIAA/SNAME Advanced Marine Vehicles Conference, 1974.

40. Lee, C.M., and Curphy, R.M.: 'Prediction of Motion, Stability, and Wave Load of Small-Waterplane-Area, Twin-Hull Ships', Trans SNAME, vol. 85, 1977.

41. Bowes, J. and McNeill, D.: 'Machinery for Small Fast Warships', RINA Symposium on Small Fast Warships and Security Vessels, March 1978.

42. Rutherford, K.J. and Gibbons, D.J.: 'Machinery System Design for a Platform Emergency Support Vessel', Trans I.Mar.E., 1980.

43. Hammett, D.S.: 'The First Dynamically Stationed Semi-Submersible - *SEDCO 709*', Offshore Technology Conference, 1977, OTC 2972.

44. Everest, J.T.: 'Some Research on the Hydrodynamics of Catamarans and Multi-Hulled Vessels in Calm Water', Trans NECIES, 1967-68.

45. Narita, S.: 'Some Research on the Wave Resistance of a Trimaran', Int. Seminar on Wave Resistance, Japan, 1976.

46. Lackenby, H. and Slater, C.: 'The Case for Multi-Hull Ships with Particular Reference to Resistance Characteristics', SNAME Spring Meeting, 1968.

47. Craig, R.E.: 'Two Scottish Fishery Research Vessels', F.A.O. of the U.N. Research Craft Conference: 2, Seattle, Washington, 1968.

48. Gurtner, P.: 'Fisheries Exploratory and Training Vessels in United Nations Service', F.A.O. of the U.N. Research Craft Conference: 2, Seattle, Washington, 1968.

49. Sarchin, T.H. and Goldberg, L.L.: 'Stability and Buoyancy for U.S. Naval Surface Ships', Trans SNAME, 1962.

50. Goldberg, L.L. and Tucker, R.G.: 'Current Status of U.S. Navy Stability and Buoyancy Criteria for Advanced Marine Vehicles', AIAA/SNAME Advanced Marine Vehicles Conference, 1974.

51. Aronne, E.L., Lev, F.M. and Nappi, N.S.: 'Structural Weight Determination for SWATH Ships', AIAA/SNAME Advanced Marine Vehicles Conference, 1974.

52. Technical and Research Report R-21, 'Fundamentals of Cathodic Protection for Marine Service', SNAME, January 1976.

53. Faulkner, D. and Sadden, J.A.: 'Toward a Unified Approach to Ship Structural Safety', Trans RINA, 1979.

54. Nethercote, W.C.E. and Schmitke, R.T.: 'A Concept Exploration Model for SWATH Ships', Trans RINA, 1981.

55. Ward, G. and Hoyland, A.: 'Ship Design and Noise Levels', Trans NECIES, vol. 95, 1978-79.

56. Vatz, I.P. and Williams, R.F.: 'Development of Noise Control Specifications for the Woods Hole Oceanographic Research Vessel', Trans SNAME, vol. 71, 1963.

57. Yerges, L.F.: 'Sound, Noise and Vibration Control', Van Nostrand Reinhold Environmental Engineering Series, 1969.

58. Sandstrom, R.E. and Smith, N.P.: 'Eigenvalue Analysis as an Approach to the Prediction of Global Vibration of Deckhouse Structures', Marine Technology, October 1980.

59. Hirowatari, T. and Matsumoto, K.: 'On the Fore and Aft Vibration of Superstructure Located at Aftship' (Second Report), Journal of the Society of Naval Architects of Japan, vol. 125, June 1969.

60. Hawkins, S. and Sarchin, T.: 'The Small Waterplane-Area-Twin-Hull (SWATH) Program - a Status Report', AIAA/SNAME Advanced Marine Vehicles Conference, 1974.

61. Brown, D.K. and Andrews, D.: 'Warship Design to a Price', The Naval Architect, January 1981.

62. Scottish Marine Biological Association, Annual Reports, Dunstaffnage Marine Research Laboratory, Oban, Argyll.

63. University of Glasgow, Accounts for the Year 1979-80.

64. Meeke, M.: 'Operating Experiences of Large Containerships', Trans IESS, 1975, Paper No. 1389.

65. Gadd, G.E.: 'Scale Effect on Stern Separation and Resistance of a Full Hull Form', Trans RINA, 1977.

66. Grekoussis, C. and Miller, N.S.: 'The Resistance of Semi-Submersibles', IESS Paper No. 1413, Trans, 1978.

67. Hoerner, S.F.: 'Fluid-Dynamic Drag', published by the Author, 1965.

68. Zahm, A.F.: 'Flow and Drag Formulas for Simple Quadrics', Report No. 203, NACCA, 1926.

69. Fage, A. and Preston, J.H.: 'On Transition from Laminar to Turbulent Flow in the Boundary Layer', Proc. Royal Society of London, vol. 178, Series A, 1941.

70. Preston, J.H.: 'The Minimum Rn for a Turbulent Boundary Layer and the Selection of a Transition Device' JFM, vol. 3, Part 4, 1958.

71. Tani, I.: 'Boundary-Layer Transition', Annual Review of Fluid Mechanics (W.R. Sears and M. Van Dyke), vol. 1, 1969.

72 McCarthy, J.H., Power, J.L. and Huang, T.T.: 'The Roles of Transition, Laminar Separation, and Turbulence Stimulation in the Analysis of Axisymmetric Body Drag', 11th. Symposium on Naval Hydrodynamics, 1976.

73. Schlichting, H.: 'Boundary-Layer Theory', McGraw Hill, 1968.

74. Hughes, G. and Allan, J.F.: 'Turbulence Stimulation on Ship Models', Trans SNAME, vol. 59, 1951.

75. Yeh, H. and Neal, E.: 'Powering Characteristics of SWATH 6A in Calm Water and Head Seas', DTNSRDC Report SPD 396-20, January 1977.

76. Lin, W.C. and Day, W.G.: 'The Still-Water Resistance and Propulsion Characteristics of Small-Waterplane-Area Twin-Hull (SWATH) Ships', AIAA/SNAME Advanced Marine Vehicles Conference, 1974.

77. Chapman, R.B.: 'Spray Drag of Surface-Piercing Struts', AIAA/SNAME Advanced Marine Vehicles Meeting, 1972.

78. Lunde, J.K.: 'On the Linearised Theory of Wave Resistance for Displacement Ships in Steady and Accelerated Motion', Trans SNAME, vol. 59, 1951.

79. Srettensky, L.N.: 'On the Wave-Making Resistance of a Ship Moving along in a Canal', Philosophical Magazine, vol. 22, Series 7, 1936.

80. Sobolewski, A.D.: 'An Investigation of the Drag of Tandem Strut Configurations Applicable to Small Waterplane-Area Ships', DTNSRDC SPD-629-01.

81. Inui, T.: 'Wave-Making Resistance of Ships', Trans SNAME, vol. 60, 1972.

82. Amfilokhiev, W.B. and Conn, J.F.C.: 'Note on the Interaction between the Viscous and Wave-Making Component Resistances', Trans RINA, 1971.

83. Calisal, S.M.: 'An Attempt to Detect the Importance of Turbulent Boundary Layer in Ship Wave Resistance', Naval Academy, Annapolis, June 1979.

84. Saunders, H.E.: 'Hydrodynamics in Ship Design', SNAME Publication, 1957.

85. van der Meulen, J.H.J.: 'Incipient and Desinent Cavitation on Hemispherical Nosed Bodies', International Shipbuilding Progress, 19, 1972.

86. St. Denis, M. and Pierson, W.J.: 'On the Motions of Ships in Confused Seas', Trans SNAME, vol. 61, 1953.

87. Andrew, R.N. and Lloyd, A.R.J.M.: 'Full-Scale Comparative Measurements of the Behaviour of Two Frigates in Severe Head Seas', Trans RINA, 1981.

88. Dalzell, J.F.: 'A Note on the Form of Ship Roll Damping', J.S.R., vol. 22, No. 3, pp178-185, September 1978.

89. Faltinsen, O.M.: 'Theoretical Sea-Keeping, State-of-the-Art Survey', Int. Symp. on Advances in Marine Technology, 1979.

90. Salveson, N.: 'Ship Motions in Large Waves', Symposium on Applied Mathematics, Delft, 1978.

91. Borresen, R. and Tellsgard, F.: 'Time History Simulation of Vertical Motions and Loads on Ships in Regular, Head Waves of Large Amplitude', Norwegian Maritime Research, No. 2, 1980.

92. Dalzell, J.F.: 'A Simplified Evaluation Method for Vertical Plane, Zero-Speed, Sea-Keeping Characteristics of SWATH Vessels', Stevens Institute of Technology Report, SIT, DL-78-1970, July 1978.

93. Oo, K.M. and Miller, N.S.: 'Semi-Submersible Design: The Effect of Differing Geometries on Heaving Response and Stability', Trans RINA, 1977.

94. Smith, S.N.: 'Progress Report on the Simulation of Zero-Speed Heave Motions of a SWATH-Type Ship', University of Glasgow, Dept. of Naval Architecture and Ocean Engineering, NAOE-HL-81-04, March 1981.

95. Oakley, O.H., Paulling, J.R. and Wood, P.D.: 'Ship Motions and Capsizing in Astern Seas', Proc. of the Tenth Symposium on Naval Hydrodynamics, June 1974.

96. Bhattacharyya, R.: 'Dynamics of Marine Vehicles', John Wiley & Sons, 1978.

97. Rainey, R.C.T.: 'The Dynamics of Tethered Platforms', Trans RINA, 1978.

98. Rainey, R.C.T.: 'Parasitic Motions of Offshore Structures', Trans RINA, 1980.

99. Livingston, W. and Newman, D.L.: 'Advances in Implementing Ship Motion Predictors', AIAA/SNAME Advanced Marine Vehicles Conference, 1979.

100. Frank, W.: 'The Heave Damping Coefficients of Bulbous Cylinders, Partially Immersed in Deep Water', Journal of Ship Research, vol. 11, 1967.

101. Atlar, M.: Report in Preparation. University of Glasgow, Dept. of Naval Architecture and Ocean Engineering.

102. Lewis, F.M.: 'The Inertia of the Water Surrounding a Vibrating Ship', Trans. SNAME, vol. 37, 1929.

103. Saunders, H.E.: 'Hydrodynamics in Ship Design, Vol. II', SNAME Publication.

104. Hadler, J.B., Lee, C.M., Birmingham, J.T. and Jones, H.D.: 'Ocean Catamaran Seakeeping Design, Based on the Experiences of USNS Haynes', Trans. SNAME, 1964.

105. Ewing, J.A.: 'Some Results from the Joint North Sea Wave Project of Interest to Engineers', Int. Symp. on the Dynamics of Marine Vehicles and Structures in Waves. I. Mech. E., 1974.

106. Ochi, M.K.: 'A Series of JONSWAP Wave Spectra for Offshore Structure Design', BOSS '79, Paper 4.

107. Hasselman, K. et al.: 'Measurements of Wind-Wave Growth and Swell Decay during the Joint N. Sea Wave Project (JONSWAP)', Erganzungsheft zur Deutschen Hydrographischen Zeitsehrift Reike A (8') Nr. 12.

108. Shellard, H.C.: 'Tables of Surface Wind Speed and Direction over the United Kingdom', HMSO, London 1968.

109. Takagi, A. and Hirada, H.: 'Design of Oceanographic Research Vessel *Hakuho Maru*', Research Craft Conference: 2, Seattle, Washington 1968.

110. Shoenberger, R.W.: 'Subjective Response to Very Low-Frequency Vibration', Aviation Space and Environmental Medicine, 46(6), pp785-790, 1975.

111. Lloyd, A.R.J.M. and Andrew, R.N.: 'Criteria for Ship Speed in Rough Weather', Proc. 18th ATTC, vol. 2, 1977.

112. Brown, D.K. and Marshall, P.D.: 'Small Warships in the Royal Navy and the Fishery Protection Task', RINA Symposium on Small Fast Warships and Security Vessels, March 1978.

113. Heather, R.G., Nicholson, K., and Stevens, M.J.: 'Seakeeping and the Small Warship', RINA Symposium on Small Fast Warships and Security Vessels, March 1978.

114. Salvesen, N.: 'A Note on the Seakeeping Characteristics of Small-Waterplane-Area-Twin-Hull Ships', AIAA/SNAME Advanced Marine Vehicle Meeting, 1972.

115. Ewing, J.A.: 'The Effect of Speed, Forebody Shape and Weight Distribution on Ship Motions', Trans. RINA, 1967.

116. Sarpkaya, T.: 'The Hydrodynamic Resistance of Roughened Cylinders in Harmonic Flow', Trans. RINA, 1978.

117. Forsyth, D.W.G. and Miller, N.S.: 'The Effect of Bracing on the Dyanmic Performance of Semi-Submersibles', Symposium on the Mechanics of Wave-Induced Forces on Cylinders, Bristol, 1978. Ed. T.L. Shaw, Pitman Publishing Ltd.

118. Smith, S.N.: 'Progress Report on the Simulation of Zero-Speed Heave Motions of a SWATH-Type Ship', University of Glasgow, Dept. of Naval Architecture and Ocean Engineering, Report NAOE-HL-81-04.

119. Meirovitch, L.: 'Elements of vibration Analysis', McGraw-Hill, 1975.

120. Grim, O.: 'Rollschwingungen, Stabilität, und Sicherheit im Seegang', Schiffstechnick, vol. 1, 1952.

121. Paulling, J.R. and Rosenberg, R.M.: 'On Unstable Ship Motions Resulting from Non-Linear Coupling', Journal of Ship Research, June 1959.

122. Wellicome, J.: 'An Analytical Study of the Mechanisms of Capsizing', Proc. of Int. Conf. on Stability of Ships and Ocean Vehicles, Glasgow, 1975.

123. Rainey, R.C.T.: 'The Dynamics of Tethered Platforms', Trans. RINA, 1978.

124. Rainey, R.C.T.: 'Parasitic Motions of Offshore Structures', Trans. RINA, 1980.

125. Hooft, J.P.: 'Dynamic Behaviour of Moored Structures in Waves', 4th. Int. Ocean Development Conference, Tokyo, 1976.

126. Barr, R.A.: 'Dynamic Stability and Capsizing', Proceedings of the 18th. ATTC, vol. 2, 1977.

127. Price, W.G.: 'A Stability Analysis of the Roll Motion of a Ship in an Irregular Seaway', Int. Shipbuilding Progress, vol. 22, No. 247, 1975.

128. Haddara, M.R.: 'On the Parametric Excitation of Non-Linear Rolling Motion in Random Seas', Int. Shipbuilding Progress, vol. 27, No. 315, 1980.

129. Tasai, F.: 'Ship Motions in Beam Seas', Reports of Research Institute for Applied Mechanics (Japan), vol. XIII, No. 45, 1965.

130. Cash, D.G.F. and Rainey, R.C.T.: 'Design Rules for the Avoidance of Sub-harmonic Oscillations in Large Floating Offshore Structures', Atkins Research and Development Report OT-R-8142, September 1981.

131. Kuo, C. and Welaya, Y.: 'A Review of Intact Ship Stability Research and Criteria', Ocean Engineering, vol. 8, No. 1, 1981.

132. Warren, N.F.: 'What Future for the Semi-Submersible Twin-Hull Ship?', The Naval Architect, March 1977.

133. Tick, L.J.: 'Differential Equations with Frequency-Dependent Coefficients', Journal of Ship Research, October 1959.

134. Cummins, W.E.: 'The Impulse Response Function and Ship Motions', Schiffstechnik, Bd. 9, 1962, Heft 47.

135. Longuet-Higgins, M.S.: 'On the Joint Distribution of the Periods and Amplitudes of Sea Waves', Journal of Geophysical Research, vol. 80, No. 18, June 1975.

136. Ochi, M.K. and Whalen, J.E.: 'Estimation of Extreme Waves Critical for the Safety of Offshore Structures', Offshore Technology Conference, 1979, OTC 3596.

137. Van Santen, G.W.: 'Introduction to a Study of Mechanical Vibration', Philips Technical Library, 1958.

138. St. Denis, M.: 'On the Statistical Description of Seaways of Moderate Severity', Proceedings of SNAME STAR Symposium, 1980.

139. Faulkner, D.: 'Semi-Probabilistic Approach to Design of Marine Structures', SSC-SNAME Extreme Loads Response Symposium, Arlington Virginia, 1981.

140. Scott, J.R.: 'A Comparison of Two Ship Resistance Estimators', Trans. RINA, 1971.

141. Tamura, K.: 'Study on the Blockage Correction', Journal of Society of Naval Architects of Japan, vol. 131, June 1972.

142. Taniguchi, K. and Tamura, K.: 'On Blockage Effect', Mitsubishi Experimental Tank Report No. 307, 1958.

143. Emerson, A.: 'Ship Model Size and Tank Boundary Correction', Trans. NECIES, vol. 76, 1959/60.

144. Hughes, G.: 'Tank Boundary Effects on Model Resistance', Trans. RINA, 1961.

145. Conn, J.F.C., Lackenby, S. and Walker: 'BSRA Resistance Experiments on the Lucy Ashton', Trans. RINA, 1953.

146. Conn, J.F.C.: Discussion of Ref. 143.

147. Scott, J.R.: 'On Blockage Correction and Extrapolation to Smooth Ship Resistance', Trans. SNAME, 1970.

148. Lamb, H.: 'Hydrodynamics', Dover, New York, 1945.

149. Newman, J.N.: 'Marine Hydrodynamics', The MIT Press, Cambridge, Massachusetts, 1977.

150. Hamilton, J., Hui, W.H. and Dorelan, M.A.: 'A Statistical Model for Groupiness in Wind Waves', Journal of Geophysical Research, vol. 184, No. C8, August 20, 1979.

151. Johnson, R.R., Mansard, E.P.D. and Ploeg, J.: 'Effects of Wave Grouping on Breakwater Stability', 16th Coastal Engineering Conference, Hamburg, 1978.

152. Ghosh, S., Chou, F.S. and Huang, E.W.: 'A Rational Approach to the Design of a Pipelay/Derrick Semi-Submersible Barge', Trans. SNAME, 1979.

153. Spangenberg, S. and Kofoed Jacobsen, B.: 'The Effect of Wave Grouping on Slow Oscillations of an Offshore Structure', International Symposium on Ocean Engineering Ship Handling, 1980.

154. Goda, Y. 'On Wave Groups', BOSS '76.

155. Ewing, J.A.: 'Mean Length of Runs of High Waves', Journal of Geophysical Research, vol. 78, No. 12, April 20, 1973.

156. Mollo-Christensen, E. and Ramamonjiarsoa, A.: 'Modelling the Presence of Wave Groups in a Random Wave Field', Journal of Geophysical Research, vol. 83, No. C8, August 20, 1978.

157. Davidan, I.N., Kublanov, Y.M., Lopatukhin, L.I. and Rochkov, V.A.: 'The Results of Experimental Studies of the Probabilistic Characteristics of Wind Waves', International Symposium on the Dynamics of Marine Vehicles and Structures in Waves, I Mech E, 1974.

SELECTIVE BIBLIOGRAPHY FOR RESEARCH VESSELS

Baxter, B.: 'Oceanographic Survey Ships', Trans. RINA, 1967.

Baxter, B.: 'Hydrographic Survey on Research Ship', Trans. RINA, 1977.

Bennet, R.: 'Recent Developments in the Design and Operation of Fishing Vessels', Trans. RINA, 1972.

Cheesley, J.R. and Foster, J.F.: 'Principle UK Fishing Vessel Types', The Naval Architect, July 1979.

Dermody, J., Leiby, J. and Silverman, M.: 'An Evaluation of Recent Research Vessel Construction in the USA', Trans. SNAME, 1964.

'Janes Ocean Technology, 1979-80', Jane's Yearbooks, London.

Powel, A.L. and Stover, H.B.: 'Special Design Features, OSS 01 Oceanographer and OSS 02 Discoverer', Marine Technology, July 1968.

Research Craft Conference: 2, Ed. Jan Olaf Traung, Food and Agriculture Organisation of the United Nations, Seattle, Washington, 1968.

Vats, J.P. and Williams, R.F.: 'Development of Noise Control Specifications for the Woods Hole Oceanographic Research Vessel', Trans. SNAME, 1963.

APPENDIX A: LIST OF MEETINGS

	Name and Affiliation		Interests and Techniques
(1)	Mr. P. Meadows,	Zoology Dept. Glasgow University	General marine-science
(2)	Prof. A.D. Boney,	Botany Dept. Glasgow University	Phytoplankton
(3)	Dr. M.S. Baxter,	Chemistry Dept. Glasgow University	Sediment Layers, coring
(4)	Prof. A.S.G. Curtis,	Cell Biology Glasgow University	Diving, underwater photography
(5)	Dr. R. Gatten,	Inst. of Marine Bio-chemistry, Aberdeen	Bio-chemistry
(6)	Prof. R.I. Currie, Mr. C. Grier, Dr. Mauchlin, Dr. Gordon, Mr. Ellet,	Scottish Marine Biological Associates Dunstaffnage	Various
(7)	Prof. J.A. Allen, Dr. P.G. Moore, Dr. J.A. Atkinson,	Marine Biological Station Millport	Specimen collect-ion, Various
(8)	Dr. G. Farrow,	Geology Dept. Glasgow University	Sediment Layers, megaripples
(9)	Mr. Q. Wilson,	Dept. of Mechanical & Off-shore Engineering Robert Gordon Institute of Science & Technology	Anchors
(10)	Mr. J. Adams, Mr. Hyslop, Mr. R.E. Craig,	DAFS Marine Laboratory Aberdeen	Various
(11)	Dr. R. Ralph	Zoology Dept. Aberdeen University	Marine fouling of offshore structures Biological succession
(12)	Mr. Kalmin Mr. I. McDonald	MAFF Torry Research Station Aberdeen	Fisheries
(13)	Capt. B. Atkinson	Aberdeen Harbour Authority	Harbour Master
(14)	Prof. D. Blundell	Geology Dept. Chelsea College	Deep-ocean geo-physics
(15)	Dr. D. Cronan	Geology Dept. Imperial College of Science & Technology	Manganese nodules

(16) Dr. Emson,	Zoology Dept. King's College	Littoral and sub-littoral benthos
(17) Mr. J. Crease, Mr. J. Ewing,	Inst. of Oceanographics Sciences (Wormley)	Oceanography
(18) Prof. A.J. Smith,	Geology Dept. Bedford College	Geo-physics
(19) Mr. W. Halcrow,	Forth River Purification Board	Estuary monitoring
(20) Mr. T.W. Finlay,	Civil Engineering Dept. Glasgow University	Anchors
(21) Mr. McQuillan,	Marine Geo-physics Unit Inst. of Geological Sciences (Edinburgh)	Marine Geo-physics
(22) Dr. J. Cheshire, Dr. Evans,	Continental Shelf Unit Inst. of Geological Sciences (Edinburgh)	Seabed Sampling
(23) Mr. C. Adams, Mr. K. Robertson, Mr. I. Gilchrist,	NERC Research Vessel Base Barry	

APPENDIX B: INTACT STABILITY

Goldberg and Tucker[50] have presented intact stability criteria applicable to SWATH ships from consideration of the hazards due to:

(a) beam winds combined with rolling, and
(b) large off-centre loads.

It is suggested from a philosophical standpoint that, because of the danger of downflooding, the criteria should be modified to read as follows.

Beam Winds Combined with Rolling

When the heeling arms, due to wind heel, are superimposed on the plot of the ship's righting arm, as shown in Fig. B1, and an assumption is made for the angle of rolling into the wind, θ_R, the following must be satisfied:

(1) the heeling arm at the intersection of the heeling arm and righting arm curves (point C) must not exceed six-tenths of the maximum righting arm, and

(2) area A_1 is to be not less than 1.4 times area A_2 (A_2 extends θ_R degrees to windward from point C and A_1 extends from C to the angle of downflooding or the angle of second intercept of the curves (point D), whichever is the less.

θ_R is the roll angle associated with the storm wind and sea conditions. A value of 25° was used by Sarchin and Goldberg[49] but for SWATH ships (as for air-cushion vehicles in displacement mode[50]) a value of 15° seems more reasonable.

Large Off-Centre Loads

These can arise from lifting heavy weights over the side or over the stern or from the crowding of passengers to one side or end. The criteria are similar to the above except that the heeling arm is due to the off-centre load rather than the wind heeling moment, and are as follows:

(1) the angle of heel at the intersection of the curves (point C) must not exceed 15°,

(2) the heeling arm at point C must not exceed six-tenths of the maximum righting arm, and

(3) the reserve of dynamic stability (corresponding to area A_1) up to the angle of downflooding or the angle of second intercept, whichever is the less, must not be less than four-tenths of the total area under the righting arm curve up to the same angle.

Other Considerations

For certain SWATH applications high-speed turning and icing may need to be considered. Also, as discussed in Chapter 9, the value of GM_T has a bearing on the occurrence of parasitic motions and there may, therefore, be some further control on this value if criteria for the avoidance of such motions are developed. It may be more helpful to develop criteria for acceptable values of β in Eq. 8.6 but unfortunately the theoretical determination of β for a given vessel will never be simple.

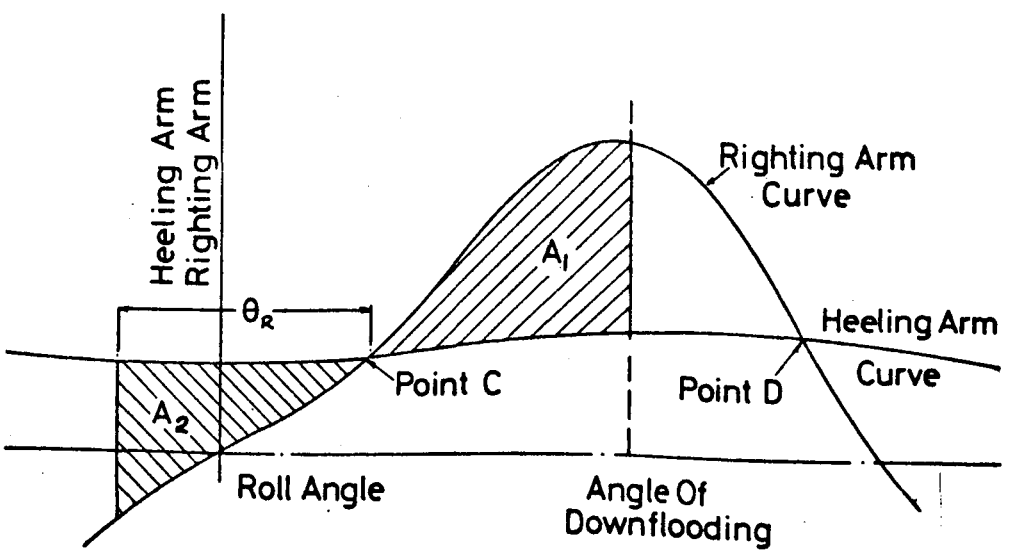

Fig. B1. Stability Curve.

APPENDIX C: BLOCKAGE CORRECTION

Various formulae exist for the blockage correction of speed for conventional ships. A selection of these as follows were programmed on the 'Apple' micro-computer.

Scott[140]: $$\frac{\delta V}{V} = K_1 \nabla A^{-3/2} + BL^2 K_2 A^{-3/2} \quad \ldots\ldots \quad C1$$

where K_1 is a function of Reynolds number and the non-dimensional number $C_B \nabla^{1/3}/L$, and

$K_2 = 2.4\ (Fn - 0.22)$ for $0.22 < Fn < 0.38$

$K_2 = 0$ for $Fn < 0.22$.

Tamura[141]: $$\frac{\delta V}{V} = 0.51 \times m_4^{1.05} \left(\frac{2L}{b}\right)^{0.8 - 4.76 m_4} \frac{1}{1 - Fn_h^2} \quad \ldots\ldots \quad C2$$

Simplified Tamura[141]: $$\frac{\delta V}{V} = 0.85 m_1 \left(\frac{L}{b}\right)^{3/4} \frac{1}{1 - Fn_h^2} \quad \ldots\ldots \quad C3$$

Taniguchi-Tamura[142]: $$\frac{\delta V}{V} = 1.1 \times m_1 \times \left(\frac{L}{b}\right)^{3/4} \quad \ldots\ldots \quad C4$$

Emerson[143]: $$\frac{\delta V}{V} = 1.65 \frac{m_3}{1 - m_3 - Fn_h^2} \quad \ldots\ldots \quad C5$$

Hughes[144]: $$\frac{\delta V}{V} \simeq \frac{0.77 \times Fn_h^{-1/2} \times m_2}{1 - m_2 - Fn_h^2} \quad \ldots\ldots \quad C6$$

Conn-Lackenby-Walker[145]: $$\frac{\delta V}{V} = \frac{m_2}{1 - m_2 - Fn_h^2} \quad \ldots\ldots \quad C7$$

Conn[146]: $$\left(\frac{V_1}{V}\right)^3 \frac{Fn_h^2}{2} - \left[1 - \frac{Am}{bh} + \frac{Fn_h^2}{2}\right] \frac{V_1}{V} + 1 = 0 \quad \ldots\ldots \quad C8$$

where $V_1 = V + \delta V$

In the above $m_1 = \frac{a_m}{A}$, $m_2 = \frac{\nabla}{LA}$, $m_3 = \frac{1}{2}(m_1 + m_2)$, $m_4 = \frac{4m_1}{\pi}$

and we take a_m = 3 × transverse mid-area of one hull-column

A = cross-sectional area of tank

∇ = model volume of displacement

L = model length.

The first seven equations can be solved directly. Conn's formula (Eq. C8) is solved by noting that it is a cubic in V_1/V. Although various solutions exist for this it can be demonstrated that the discriminant is less than zero and that the required solution is always given by the same root.

Note that for $Fn_h > 0.81$ and $m_1 \leq 0.02$ there may exist two valid solutions but that the chosen root always gives the lower of these.

There are, in addition, other formulations which correct the resistance, but these have not been considered.

The model particulars given in Table XVIII were used to evaluate the eight blockage correctors; the results being shown in Figure C1.

Item	Dimension
L_{BP}	1.1m
L_c	0.4m
C_B	(0.65 say)
∇	$0.0194m^3$
a_m	$0.049m^2$

Table XVIII. Particulars for Blockage Correction (Light Draught)

The Scott formula was derived from considering models between 3 and 9m long and at speeds up to Fn = 0.38, and is therefore inapplicable for the present case. Several variations of the formula are in use throughout the world, and it could be adapted for use with

SWATHs when some appropriate data becomes available. It may be that the Froude number considered should be based on column length since this affects the wave resistance.

Of the others, the Emerson and Conn formulae give an appreciably higher result. (Scott[147] rates these and the Hughes formula as being low in the order of merit.) The remainder suggest a correction of up to about 0.25% at the highest speeds. Since this is probably less than the experimental error, no correction for blockage was applied to the experimental results.

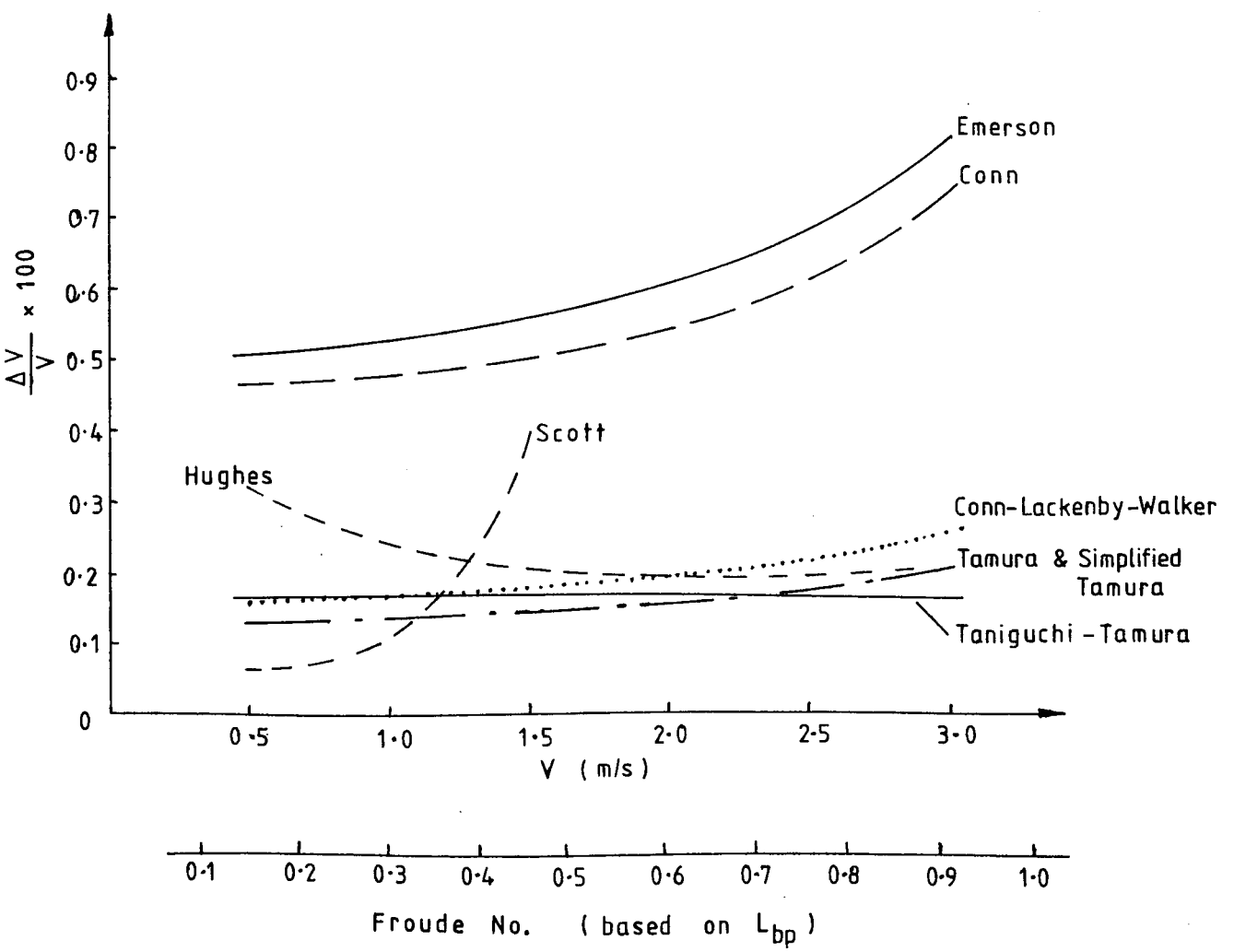

Fig. C1. Blockage Correction.

APPENDIX D: WAVE RESISTANCE THEORY

This Appendix is based on the paper by Chapman[36] which in turn is based on classical thin-ship theory[78,79]. However, the lack of fore-and-aft symmetry for the three-hulled SWATH requires that the contributions to the wave resistance from certain of the parts must be calculated in a slightly different manner including terms which cancelled through symmetry for the twin-hull case.

Equations are based on a co-ordinate system (x,y,z) moving with the ship, x positive in direction of motion, z positive upowards, with the origin at the intersection of the still waterline, the longitudinal centreline and the mid-chord point of the aft columns, Fig. D1.

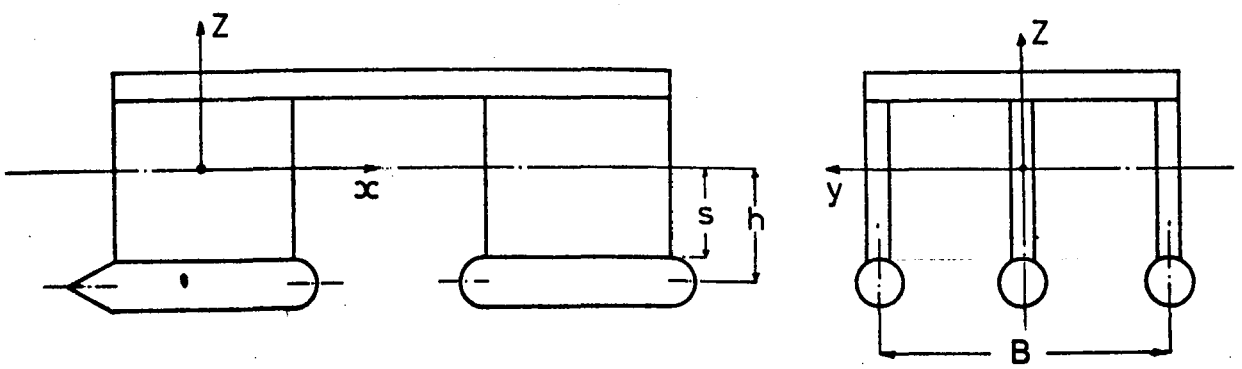

Fig. D1. Co-ordinate System for Wave Resistance.

Let the ship move with steady forward velocity c. This causes the perturbation velocities for the fluid u,v,w in the directions Ox,Oy, Oz, respectively. If F(x,y,z,t) = 0 is the equation of the bounding surface then from Lamb[148] (pp3-7)

$$\frac{DF}{Dt} = \frac{\partial F}{\partial t} + u\frac{\partial F}{\partial x} + v\frac{\partial F}{\partial y} + w\frac{\partial F}{\partial z} = 0 \qquad \text{.....} \qquad D1$$

If the underwater surface is then represented by an equation of the form

$$y = \pm \eta(x,z) \qquad \ldots\ldots \quad D2$$

i.e. $F = y - \eta(x,z)$

then for time invariant motion

$$\left| (c+u)\frac{\partial \eta}{\partial x} - v + w\frac{\partial \eta}{\partial z} \right|_{y=\eta} = 0 \qquad \ldots\ldots \quad D3$$

For thin-ships this condition may be approximated by

$$v = \pm c\frac{\partial \eta}{\partial x}, \quad y = 0 \qquad \ldots\ldots \quad D4$$

so that a single-hulled ship is represented by a source distribution on the plane y=0 with strength

$$\sigma = -\frac{c}{2\pi}\frac{\partial \eta}{\partial x} \qquad \ldots\ldots \quad D5$$

For three-hulls there will be three such source distributions.

For irrotational flow the perturbation velocities in Eq. D3 can be expressed in terms of the velocity potential, ϕ, giving

$$\left| c + \frac{\partial \phi}{\partial x}\cdot\frac{\partial \eta}{\partial x} + \frac{\partial \phi}{\partial z}\cdot\frac{\partial \eta}{\partial z} = \frac{\partial \phi}{\partial y} \right|_{y=\eta} \qquad \ldots\ldots \quad D6$$

The boundary condition at the free surface can then be derived, by also using Bernoulli's equation (see for example Newman[149]). The linearised free surface condition can then be written as

$$\frac{\partial^2 \phi}{\partial x^2} + K\frac{\partial \phi}{\partial z} = 0 \qquad \text{where } K = \frac{g}{c^2} \qquad \ldots\ldots \quad D7$$

For this condition Lunde[78] shows that the wave-making resistance of a source distribution $\sigma(x,y,z)$ is given by

$$R = 16\pi\rho K^2 \int_0^\infty (I^2+J^2)\cosh^2 u\, du \qquad \ldots\ldots \quad D8$$

and

$$I+iJ = \iint \sigma \exp(iK(x\cosh u + y\sinh u\cosh u) + Kz\cosh^2 u)\, dS \qquad \ldots\ldots \quad D9$$

In order to evaluate the integral in D8 it must be approximated by a sum. Chapman[36] shows that the expression derived by Srettensky[79] for the wave-resistance of a source distribution moving in a infinitely deep canal of width W can be used, i.e.

$$R = \frac{16\pi^2\rho K}{W}\left\{I_o^{\,2} + J_o^{\,2} + 2\sum_{n=1}^{\infty}(I_n^{\,2} + J_n^{\,2})\frac{\cosh^2 u_n}{\cosh 2u_n}\right\} \quad .. \quad D10$$

where $$\sinh 2u_n = \frac{4\pi n}{K\,W} \quad ..... \quad D11$$

so that $$\cosh 2u_n = \sqrt{\sinh^2 2u_n + 1}$$

$$\cosh^2 u_n = \tfrac{1}{2}(\cosh 2u_n + 1) \quad ..... \quad D12$$

Chapman shows that for a twin-hulled ship the integrand in D8 is a factor, P say, times that for a single-hulled ship where

$$P = 2(1 + \cos(K\,B \sinh u \cosh u)) \quad ..... \quad D13$$

and B is the transverse centreline spacing. Therefore, using subscript t to represent the twin-hulled ship

$$I_t^{\,2} + J_t^{\,2} = P(I^2 + J^2) \quad ..... \quad D14$$

so that

$$I_t = \sqrt{P}\,I\,, \quad J_t = \sqrt{P}\,J \quad ..... \quad D15$$

which will be used again later.

Contribution of Hulls

It is convenient to define

$$m = K \cosh u_n$$

then in the thin ship approximation Eq. D9 becomes

$$I_n + iJ_n = \iint \sigma \exp(imx + zm^2 K^{-1})\,dxdz \quad ..... \quad D16$$

Substituting Eq. D5 into this and replacing the integral over z by an approximation, Chapman derives the net contribution of the hull to wave-making as

$$I_n + iJ_n = -\left(\frac{c}{4\pi}\right) \exp\left(\frac{-hm^2}{K}\right) \int \frac{dA}{dx} \exp(imx)\, dx \quad \ldots\ldots \quad D17$$

where h is the mean depth of the hull and A(x) is the cross-sectional area. The only parts contributing to the wave-making are those with

$$\frac{dA}{dx} \neq 0$$

which in this case is only hull endings since the hulls themselves are cylindrical.

Conical Tail Section

Consider a cone with apex at x_A, radius b, length a

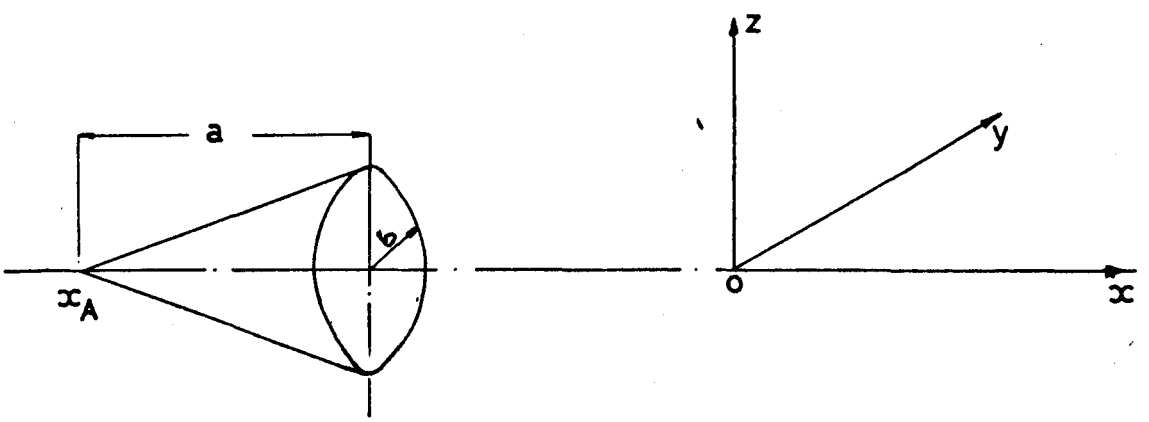

Fig. D2. Tail Section Geometry.

(In this case x_A will be negative, however a and b being lengths are positive.) The length from x_A to a general point x in the cone is $x-x_A$. Since at x the radius is

$$r_x = (x-x_A)\,\frac{b}{a}$$

therefore

$$A(x) = \pi(x-x_A)^2 \left(\frac{b}{a}\right)^2 \quad \ldots\ldots \quad D18$$

and

$$\frac{dA}{dx} = 2\pi(x-x_A)\left(\frac{b}{a}\right)^2 \quad \ldots\ldots \quad D19$$

Substituting into D17 (using subscript c to represent the contribution from the cone) gives

$$I_c+iJ_c = -\left(\frac{cb^2}{2a^2}\right) \exp\left(\frac{-hm^2}{K}\right) \int (x-x_A) \exp(imx)\, dx \quad \ldots \quad D20$$

Now let $x_{new} = x - x_A$, $dx_{new} = dx$

$$I_c+iJ_c = -\left(\frac{cb^2}{2a^2}\right) \exp\left(\frac{-hm^2}{K}\right) \int_0^a x \exp(imx + imx_A)\, dx$$

$$= -\frac{cb^2}{2a^2} \exp\left(imx_A - \frac{hm^2}{K}\right) \int_0^a x \exp(imx)\, dx$$

Integrating by parts yields

$$I_c+iJ_c = -\left(\frac{cb^2}{2a^2}\right) \exp\left(imx_A - \frac{hm^2}{K}\right) \{(1-ima) \exp(ima) - 1\}$$

..... D21

which is similar to Chapman's Eq. 20.

Expanding D21 and identifying real and imaginary parts gives

$$I_c = \frac{-cb^2}{2m^2a^2} \exp\left(\frac{-hm^2}{K}\right) \{\cos mx_A(\cos ma + ma \sin ma - 1) - \sin mx_A(\sin ma - ma \cos ma)\}$$

..... D22

$$J_c = \frac{-cb^2}{2m^2a^2} \exp\left(\frac{-hm^2}{K}\right) \{\cos mx_A (\sin ma - ma \cos ma) + \sin mx_A (\cos ma + ma \sin ma - 1)\}$$

..... D23

Spheroidal Tail Section

Consider a spheroidal tail section from $x=x_o-a$ to $x=x_o$ of the form

$$\frac{(x-x_o)^2}{a^2} + \frac{y^2+z^2}{b^2} = 1 \quad \ldots \quad D24$$

In which case

$$A(x) = \pi b^2 - \pi\left(\frac{b}{a}\right)^2 (x-x_o)^2 \quad \ldots \quad D25$$

$$\frac{dA}{dx} = -2\pi\left(\frac{b}{a}\right)^2 (x-x_o) \quad \ldots \quad D26$$

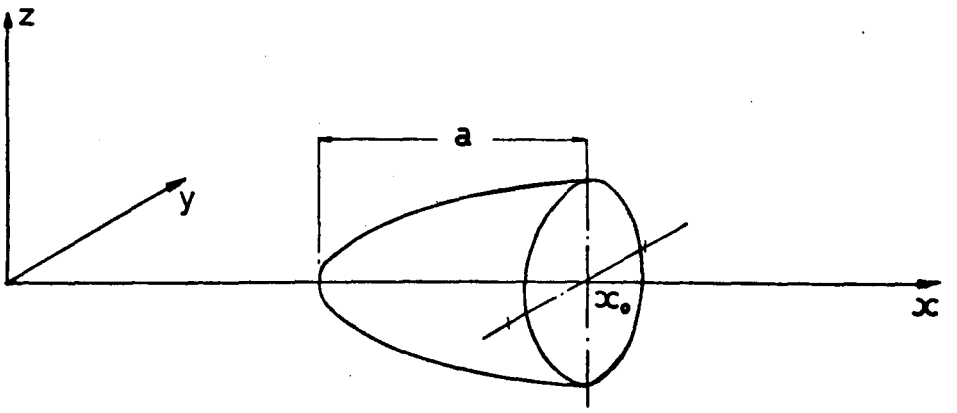

Fig. D3. Forward Hull, Aft Ending Geometry.

Using a subscript st for this case

$$I_{st}+iJ_{st} = \frac{cb^2}{2a^2}\exp\left(\frac{-hm^2}{K}\right)\int (x-x_o)\exp(imx)\,dx \quad \ldots\ldots \text{D27}$$

putting $x_{new} = x-x_o$

$$I_{st}+iJ_{st} = \frac{cb^2}{2a^2}\exp\left(\frac{-hm^2}{K}\right)\int_{-a}^{o} x\exp(im(x+x_o))\,dx \quad \ldots\ldots \text{D28}$$

$$= \frac{cb^2}{2a^2}\exp(imx_o - \frac{hm^2}{K})\int_{-a}^{o} x\exp imx\,dx$$

$$= \frac{cb^2}{2a^2}\exp(imx_o - \frac{hm^2}{K})\left[\exp(imx)\,\frac{x}{im} + \frac{1}{m^2}\right]_{-a}^{o}$$

$$= \frac{cb^2}{2m^2a^2}\exp\left(imx_o - \frac{hm^2}{K}\right)\{1 - (1+ima)\exp(-ima)\}$$

expanding and identifying real and imaginary parts gives

$$I_{st} = \frac{cb^2}{2m^2a^2}\exp\left(\frac{-hm^2}{K}\right)\{\cos mx_o\,(1 - \cos ma - ma\sin ma) - \sin mx_o\,(\sin ma - ma\cos ma)\} \quad \ldots\ldots \text{D29}$$

$$J_{st} = \frac{cb^2}{2m^2a^2}\exp\left(\frac{-hm^2}{K}\right)\{\cos mx_o\,(\sin ma - ma\cos ma) + \sin mx_o\,(1 - \cos ma - ma\sin ma)\} \quad \ldots\ldots \text{D30}$$

Spheroidal Nose Section

This case is considered by Chapman. Using subscript sn the contribution can be written

$$I_{sn}+iJ_{sn} = \frac{b^2c}{2m^2a^2} \exp\left(imx_o - \frac{hm^2}{K}\right) \{(1-ima)\ \exp(ima) - 1\} \quad \ldots\ldots \quad D31$$

where x_o is now the co-ordinate at the start of the nose. This is similar to Eq. D21 and yields

$$I_{sn} = \frac{b^2c}{2m^2a^2} \exp\left(\frac{-hm^2}{K}\right) \{\cos mx_o\ (\cos ma + ma \sin ma - 1) - \sin mx_o\ (\sin ma - ma \cos ma)\} \quad \ldots\ldots \quad D32$$

$$J_{sn} = \frac{b^2c}{2m^2a^2} \exp\left(\frac{-hm^2}{K}\right) \{\cos mx_o\ (\sin ma - ma \cos ma) + \sin mx_o\ (\cos ma + ma \sin ma - 1)\} \quad \ldots\ldots \quad D33$$

Combined Spheroidal Nose and Tail

If we consider a complete spheroidal body of revolution made up of a symmetrical spheroidal nose and tail section then for all values of $x_o = \pm k/2$ it can be seen that Eqs D32 and D29 summate to zero leaving only J terms. This is analogous to the parabolic strut (see below).

Contribution of Struts

For a strut with parabolic cross-section, maximum thickness t, chord length ℓ, and submerged span s, of the form

$$y = \frac{2t}{\ell^2}\left(\frac{\ell^2}{4} - (x-x_o)^2\right) \quad \ldots\ldots \quad D34$$

$$\frac{\partial y}{\partial x} = -\frac{4t}{\ell^2}(x-x_o) \quad \ldots\ldots \quad D35$$

the contribution to wave-making is

$$I_K+iJ_K = \frac{2tc}{\pi\ell^2} \exp(imx_o) \int_{-s}^{o} \int_{-\ell/2}^{\ell/2} x \exp\left(imx + \frac{m^2z}{K}\right) dxdz \quad \ldots\ldots \quad D36$$

Integrating by parts and simplifying gives

$$I_K+iJ_K = \frac{2tKc}{\pi m^2}\exp(imx_o)\left(1 - \exp\frac{-m^2s}{K}\right)\left\{\frac{2\ell}{(m\ell)^2}\sin\frac{m\ell}{2} - \frac{i}{m\ell}\cos\frac{m\ell}{2}\right\} \quad \ldots\ldots \quad D37$$

which is Chapman's Eq. 27 with an extra term in x_o still included.

Aft Strut

In this case the contribution from an aft strut is obtained by putting $x_o=0$, which gives

$$I_{as} = 0 \quad \ldots\ldots \quad D38$$

$$J_{as} = \frac{2tcK}{\pi m^2}\left(1 - \exp\frac{-sm^2}{K}\right)\left(\frac{2}{m^2\ell^2}\sin\frac{m\ell}{2} - \frac{1}{m\ell}\cos\frac{m\ell}{2}\right) \quad \ldots\ldots \quad D39$$

Forward Strut

For a forward strut Eq. B37 is expanded giving

$$I_{fs}+iJ_{fs} = \frac{2tcK}{\pi m^2}\left(1 - \exp\frac{-sm^2}{K}\right)(\cos mx_o + i\sin mx_o)\times i\left\{\frac{2}{m^2\ell^2}\sin\frac{m\ell}{2} - \frac{1}{m\ell}\cos\frac{m\ell}{2}\right\} \quad \ldots\ldots \quad D40$$

which simplifies to

$$I_{fs} = -\frac{2tcK}{\pi m^2}\left(1 - \exp\frac{-sm^2}{K}\right)\sin mx_o\left(\frac{2}{m^2\ell^2}\sin\frac{m\ell}{2} - \frac{1}{m\ell}\cos\frac{m\ell}{2}\right) \quad \ldots\ldots \quad D41$$

$$J_{fs} = \frac{2tcK}{\pi m^2}\left(1 - \exp\frac{-sm^2}{K}\right)\cos mx_o\left(\frac{2}{m^2\ell^2}\sin\frac{m\ell}{2} - \frac{1}{m\ell}\cos\frac{m\ell}{2}\right) \quad \ldots\ldots \quad D42$$

Complete Ship

The contributions from the aft parts have so far been derived neglecting the 'y' co-ordinate or the breadth of the vessel at the stern which is permissible because we know the parallel hull interference factor, P, from Eq. D13. However, summing over the

ship this has to be taken into account and for the total ship we get the contributions

$$I_t = (I_c+I_{sn})\sqrt{P} + I_{fs} + I_{sn} + I_{st} \quad \ldots\ldots \quad D43$$

$$J_t = (J_c+J_{sn}+J_{as})\sqrt{P} + I_{fs} + I_{sn} + I_{st} \quad \ldots\ldots \quad D44$$

where the I's and J's are obtained from the relevant equations. Equations D43 and D44 are then used in Eq. D10 giving the total wave resistance as

$$R_t = \frac{16\pi^2\rho K}{W}\left\{I_{to}^2 + J_{to}^2 + 2\sum_{n=1}^{\infty}(I_{tn}^2+J_{tn}^2)\ \frac{\cosh^2 u_n}{\cosh 2u_n}\right\} \quad \ldots\ldots \quad D45$$

APPENDIX E: THE RUNGE-KUTTA-NYSTROM METHOD

This fourth-order method is a generalisation of the Runge-Kutta method and is applicable to second-order differential equations of the form

$$y'' = f(x, y, y')$$

In the general step (the $(n+1)^{th}$ step) the following auxiliary quantities are first computed

$$A_n = \tfrac{1}{2}h\, f(x_n, y_n, y_n') \qquad h = \text{step size}$$

$$B_n = \tfrac{1}{2}h\, f(x_n + \tfrac{1}{2}h, y_n + \beta_n, y_n' + A_n) \qquad \beta_n = \tfrac{1}{2}h(y_n' + \tfrac{1}{2}A_n)$$

$$C_n = \tfrac{1}{2}h\, f(x_n + \tfrac{1}{2}h, y_n + \beta_n, y_n' + B_n)$$

$$D_n = \tfrac{1}{2}h\, f(x_n + h, y_n + \delta_n, y_n' + 2C_n) \qquad \delta_n = h(y_n' + C_n)$$

The new approximations are then

$$y_{n+1} = y_n + h(y_n' + K_n) \qquad \text{where} \quad K_n = \tfrac{1}{3}(A_n + B_n + C_n)$$

$$y_{n+1}' = y_n' + K_n^* \qquad \text{where} \quad K_n^* = \tfrac{1}{3}(A_n + 2B_n + 2C_n + D_n)$$

APPENDIX F: WAVES AND WAVE-GROUPS

In Chapter 10 vessel motions were calculated in the time-domain in certain synthesized wave-groups without particularly aiming to establish the likelihood of occurrence of these groups. In this appendix a previously used time-domain approach is summarised and a brief review is given of some pertinent wave-group literature.

The simplest continuous wave-group is the system formed by the addition of two sinusoids of slightly different frequencies, i.e. the wave profile is given by

$$\eta = \eta_1 + \eta_2 \qquad \ldots\ldots \quad F1$$

$$= a_1 \cos(K_1 x - \omega_1 t) + a_2 \cos(K_2 x - \omega_2 t) \qquad \ldots\ldots \quad F2$$

Putting $a_1 = a_2$ gives

$$\eta = 2a \cos\left\{(K_1 x - \omega_1 t) - \left(\frac{\Delta K}{2} x - \frac{\Delta\omega t}{2}\right)\right\} \cos\left\{\frac{\Delta K x}{2} - \frac{\Delta\omega t}{2}\right\} \qquad \ldots\ldots \quad F3$$

where $\Delta K = K_1 - K_2$ and $\Delta\omega = \omega_1 - \omega_2$.

If $x = 0$ and assuming $\omega_1 \simeq \omega_2 \simeq \omega$

$$\eta(t) = 2a\left\{\cos\left(-\omega_1 t - \frac{\Delta\omega t}{2}\right)\cos\left(\frac{\Delta\omega t}{2}\right)\right\} \qquad \ldots\ldots \quad F4$$

$$\simeq 2a \cos(\omega t) \cos\left(\frac{\Delta\omega}{2}\right) t \qquad \ldots\ldots \quad F5$$

This has the form shown in Fig. F1 below.

In general, but not exclusively, oceanographers and others have assumed that a sea-state is a continuous random process so that most treatments of statistical properties of wind waves start from the premise that the wave field consists of a super-position of uncorrelated frequency components[150]. In other words, when a Fourier transform is performed on a recorded wave train, only the amplitude portion of the spectrum is kept and the phase spectrum is ignored as containing no relevant information. However, the amplitude spectrum alone does not give a unique description of the wave record associated with it since a combination of the same amplitude spectrum with differ-

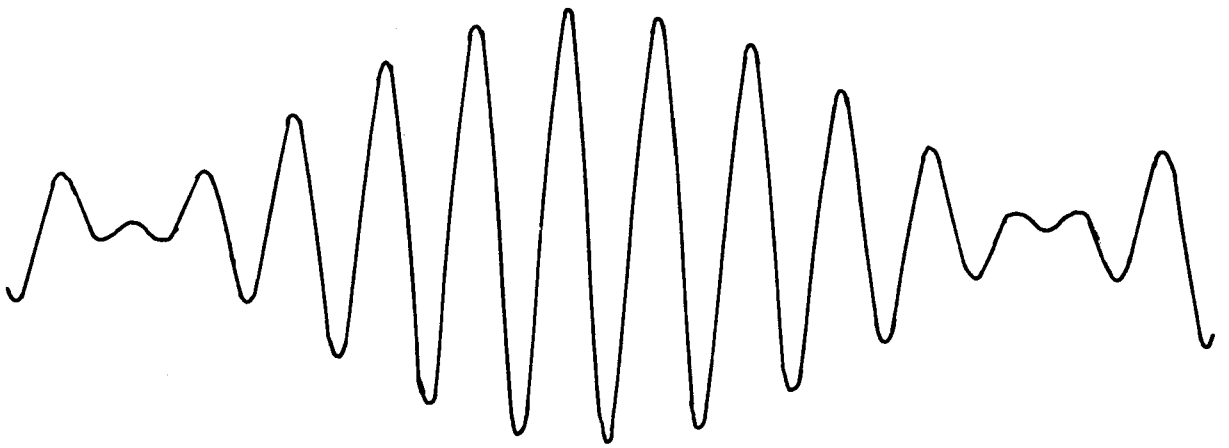

Fig. F1. Simple Wave-Group.

ent phase spectrum can result in entirely different wave trains (grouped or ungrouped) [151]. (Reference 151 also refers to work at the National Research Council of Canada on reproducing wave trains in the laboratory.)

For practical purposes it is sometimes desirable to reproduce a wave train from the spectrum. For instance, Ghosh et al. [152] used a time-domain approach to investigate the survival performance of a pipelay/derrick semi-submersible barge. For a given spectrum $S_s(\omega)$ they assume that the wave elevation in the time-domain can be approximated by

$$h(t) = \sum_{n=1}^{30} \cos\{\omega_p t + \varepsilon(\omega_p)\} \sqrt{2S_s(\omega_p)\ \delta\omega} \qquad \ldots\ldots \qquad F6$$

where $\varepsilon(\omega_p)$ is a random phase lag and a half amplitude spectrum is used.

They then assume that the system is linear and use regular wave motion responses to calculate the time-domain motion in this irregular sea. From Chapter 10 it seems unlikely that such an approach will

yield an accurate motion prediction for the large motions expected in the survival condition because of the inapplicability of the regular wave responses for large motions.

For the type of simulation developed in Chapter 10 it is necessary to define some of the characteristics of the wave-groups to be used.

Spangenberg and Jacobsen[153] starting from the equation for the surface elevation at a fixed position in terms of a sum of Fourier components reproduce time series which contain different wave-groups but have approximately the same energy spectrum. However, no attempt seems to have been made to see if these wave-groups have realistic parameters or not.

Goda[154] gives a review of various information concerning wave-groups from which some of the following remarks are drawn.

A run of waves is the occurrence of a number of waves above some preselected height and the run length is the number of consecutive waves above that height. If the independence of successive wave heights (or their randomness) is assumed, then the distribution of run lengths can be calculated with the probability of exceedance of wave height beyond a particular level, say H_c. If the distribution function of wave heights is P(H) and the probability of exceedance is p, then by definition

$$p = 1-q \qquad \ldots\ldots \quad F7$$

where $q = P(H_c)$.

Now, the run with length of j is the phenomenon that (j-1) consecutive wave heights exceed H_c, after the first exceedance and the $(j+1)^{th}$ one fails to exceed. The probability of the run with the length of j denoted by $P_1(j)$ is

$$P_1(j) = p^{j-1}q \qquad \ldots\ldots \quad F8$$

The mean and the standard deviation of run lengths are then

$$\bar{j}_1 = E\{j\} = \sum_{j=1}^{\infty} jP_1(j) = \frac{1}{q} \qquad \ldots\ldots \quad F9$$

$$\sigma(j_1) = \sqrt{E\{j^2\} - E\{j\}^2} = \frac{p}{q} \qquad \ldots\ldots \quad F10$$

If the distribution of wave heights, P(H) is approximated by the Rayleigh distribution

$$P(H_c) = P(H > H_c) = 1 - \exp\left\{\frac{-H_c}{8m_o}\right\} \quad \ldots\ldots \quad F11$$

and the exceedance level is taken as $H_c = H_{1/3}$ then the exceedance probability becomes

$$p = 0.1348, \qquad q = 0.8652 \quad \ldots\ldots \quad F12$$

The observed frequencies of long runs are larger than those calculated from the foregoing, thus suggesting the dependency of successive heights of ocean waves. In particular, the conditional run of wave heights containing the highest wave in a record exhibits a strong persistency. The mean length of such conditional runs is 2.4 for $H > H_{1/3}$. In other words, the highest wave does not appear singly, but is accompanied by several high, but smaller, waves.

The duration of wave-groups can also be calculated from envelope theory (e.g. Ewing[155]).

A paper by Mollo-Christensen and Ramamonjiarisoa[156] suggests that the wave field does not consist of independently propagating Fourier components, but wholly or in part of wave-groups of permanent type, (Stokes' wave packets). They show that it is possible to construct a random wave field from randomly spaced wave-groups and to produce a model field that has a continuous power spectral density and a dispersion similar to that of observed wave fields.

They suggest that theory and experiment confirm the existence of wave-group of permanent envelope shape, initiated by 'modulational instability', and that under certain circumstances such 'envelope solitons' will be left unchanged by collisions with other groups.

However, Hamilton et al.[150] question the validity of some of these findings. They propose a statistical model with de-coupled wave-groups which reproduce some of the characteristics of the time series of surface elevation at a point.

These studies do not, at the moment, provide a great deal of help for the purposes of the motion simulation. However, they certainly illustrate that wave-groups are a real phenomenon and that a significant amount of work is being done in studying them. Here

the environment of the high waves is of interest for calculating the response and it seems reasonable to use the design-wave-group concept or a group as in Fig. F1 to do this. Such groups can be formed using the data given by Goda[154] and others. In particular, Davidan et al.[157] suggest that the number of waves in a group varies from 2 to 15. For moderate and fully developed seas this number amounts, on the average, to 5 - 6 and in addition, the values of h_{ab}/h_m and T_{ab}/T_m are distributed in accordance with a law which is close to the normal law, with the mean values of $h_{ab}/h_m \simeq 0.6$ and $T_{ab}/T_m = 1$.

The height values can be compared with Table XVI and the period values suggest that using a single frequency group is in fact quite realistic.